

Bioanalysis

Series Editor: Tuan Vo-Dinh

Tuan Vo-Dinh *Editor*

Nanoparticle-Mediated Immunotherapy




Springer

Bioanalysis

Advanced Materials, Methods, and Devices

Volume 12

Series Editor

Tuan Vo-Dinh , Fitzpatrick Institute for Photonics, Duke University,
Durham, NC, USA

The book series on *BIOANALYSIS: Advanced Materials, Methods, and Devices* is intended to serve as an authoritative reference source for a broad, interdisciplinary audience involved in the research, teaching, learning, and practice of bioanalytical science and technology. Bioanalysis has experienced explosive growth due to the dramatic convergence of advanced technologies and molecular biology research, which has led to the development of entirely new analytical tools for chemistry, biochemistry, biology, pharmaceutical and clinical sciences, environmental, forensic and materials sciences. New approaches are developed to probe biomolecular and cellular processes as well as biological responses to implanted biomaterials and engineered tissues. Novel optical techniques using a wide variety of reporter gene assays, ion channel probes, and fluorescent probes have provided powerful bioanalytical tools for cell-based assays. The combination of molecular nanotechnology and various sensing modalities (optical, electrochemical, mass-based, etc.) opens the possibility of detecting and manipulating atoms and molecules using nano-devices, which have the potential for a wide variety of bioanalyses at the cellular level. This book series will present the most recent scientific and technological advances in materials, methods and instrumentation of interest to researchers, students, and manufacturers. The goal is to provide a comprehensive forum to integrate the contributions of chemists, physicists, biologists, engineers, materials scientists, and others involved in the analytical science and technology revolution that is reshaping molecular biology and medicine.

Examples of topics could include (but are not limited to):

- Molecular spectroscopy (luminescence, absorption, scattering Raman, photoacoustics, OCT)
- Non-linear spectroscopic techniques (CARS, CSRS, ISRS, photon echo, etc.)
- Super-resolution techniques (STED, SIM, STORM, etc.)
- Ultrafast spectroscopies (pico-, atto-, zepto-second regimes)
- Nanosystems and technologies for bioanalysis (plasmonics nanosystems, quantum dots, etc.)
- Near-field, far-field, and remote sensing techniques
- Single-molecule and single-cell analysis
- Biosensors and biochips
- Quantum sensing and imaging
- Robotics-guided biosensing, bioimaging, diagnostics and therapy
- Isothermal sample amplification techniques (LAMP, SDA, NASBA, etc.)
- Genomic and proteomic analysis, enzymatic assays, ligand binding assays
- Genomics-enabled techniques (optogenetics, CRISPER, etc.)
- Next-generation sequencing technologies
- Bioanalytical sample preparation, micro-extraction and hyphenated separation techniques
- Bioanalytical method validation
- Data treatment methods in bioanalysis (artificial intelligence, machine learning, data fusion)

Contact for further information:

tuan.vodinh@duke.edu

loyola.dsilva@springer.com

More information about this series at <http://www.springer.com/series/8091>

Tuan Vo-Dinh
Editor

Nanoparticle-Mediated Immunotherapy

 Springer

Editor

Tuan Vo-Dinh 
Fitzpatrick Institute of Photonics
Duke University
Durham, NC, USA

ISSN 2364-1118

ISSN 2364-1126 (electronic)

Bioanalysis

ISBN 978-3-030-78337-2

ISBN 978-3-030-78338-9 (eBook)

<https://doi.org/10.1007/978-3-030-78338-9>

© Springer Nature Switzerland AG 2021

This work is subject to copyright. All rights are reserved by the Publisher, whether the whole or part of the material is concerned, specifically the rights of translation, reprinting, reuse of illustrations, recitation, broadcasting, reproduction on microfilms or in any other physical way, and transmission or information storage and retrieval, electronic adaptation, computer software, or by similar or dissimilar methodology now known or hereafter developed.

The use of general descriptive names, registered names, trademarks, service marks, etc. in this publication does not imply, even in the absence of a specific statement, that such names are exempt from the relevant protective laws and regulations and therefore free for general use.

The publisher, the authors, and the editors are safe to assume that the advice and information in this book are believed to be true and accurate at the date of publication. Neither the publisher nor the authors or the editors give a warranty, expressed or implied, with respect to the material contained herein or for any errors or omissions that may have been made. The publisher remains neutral with regard to jurisdictional claims in published maps and institutional affiliations.

Cover art: Life Fields, oil painting by Kim-Chi Le Vo-Dinh. Reproduced with permission of the artist

This Springer imprint is published by the registered company Springer Nature Switzerland AG
The registered company address is: Gewerbestrasse 11, 6330 Cham, Switzerland

Preface

The book *Nanoparticle-Mediated Immunotherapy* is intended to present recent scientific and technological advances in disease treatment at the intersection of nanotechnology and immunology. The book includes chapters grouped in two parts.

Part I contains chapters on basic principles and methods, including fundamental optical properties of nanoparticles and their effects on the immune system, strategies for immunotherapy from discovery to bedside, basic analysis, and imaging methods such as intravital microscopy to monitor anti-tumor immunological response, and theoretical studies of nanoparticle-mediated photothermal treatment for photoimmunotherapy.

Part II contains chapters describing various applications of nanoparticle-mediated immunotherapy. For instance, cancer immunotherapy uses the host's inherent immune system to treat cancer and imparts a memory effect on the immune system that can inhibit cancer relapse. However, tumor cells often form their own immune mechanisms to interact with tumor microenvironments in order to escape from cancer immunotherapy. To enhance the therapeutic efficacy of cancer immunotherapy, various nanostructured materials have been developed to modulate such immune suppressive factors in the tumor microenvironments. Engineered nanoparticles have also been developed and used as immune-stimulating adjuvants to strengthen the immunogenicity of antigens. Immunotherapies could synergistically benefit from targeted thermal nanotherapies, especially when hyperthermia around the tumor bed is combined with precise thermal ablation of cancer cells. Photothermal therapy combined with adjuvant immunotherapy has been developed to produce synergistic outcomes. Copper sulfide nanoparticles as well as bacterium-mimicking liposomes have been designed as adjuvant delivery systems. Various inorganic nano-agents such as gold nanostructures, carbon nanotubes, graphene oxide, CuS nanoparticles, and MoS₂ nanosheets with strong near-infrared (NIR) absorbance have been explored for in situ photoimmunotherapy. Other types of nanomaterials, including liposomes, polymeric nanoparticles, quantum dots, magnetic nanoparticles, mesoporous silica nanoparticles, and carbon-based nanomaterials have been utilized to deliver photosensitizers, aiming at enhancing their tumor accumulation and therapeutic efficacy. Upconversion

nanoparticles, which can emit visible light under NIR light excitation, have been developed to allow NIR-mediated photodynamic therapy with improved tissue penetration. Plasmonic nanoparticles such as gold nanostars (GNS) have unique properties that allow them to amplify the optical properties of the excitation light and thus increase the effectiveness of light-based photothermal tumor ablation. The combination of GNS-mediated photothermal therapy with checkpoint blockade immunotherapy has shown great promise to address one of the most challenging problems in the treatment of metastatic cancer, i.e., achieve complete eradication of primary treated tumors as well as distant untreated tumors in murine models. Furthermore, GNS-mediated photoimmunotherapy has shown to elicit a long-term immunologic memory, ultimately inducing an anticancer vaccine effect.

The goal of this book is to provide a forum that integrates interdisciplinary research and development of interest to scientists, engineers, manufacturers, teachers, students, and clinical providers. As nanotechnology is rapidly becoming an important tool and a powerful weapon in the armory of the modern physician, it is our hope that this book will stimulate a greater appreciation of the usefulness, efficiency, and potential of the synergistic combination of nanotechnology and immunotherapy in modern medicine.

Durham, NC, USA

Tuan Vo-Dinh

Contents

Part I Basic Principles and Methods

The New Frontier in Medicine at the Convergence of Nanotechnology and Immunotherapy	3
Tuan Vo-Dinh	
Cancer Immunotherapy Strategies: Basic Principles	29
Pakawat Chongsathidkiet, Jessica Waibl Polania, Selena J. Lorrey, Matthew M. Grabowski, Eric W. Sankey, Daniel S. Wilkinson, and Peter E. Fecci	
Immunotherapy: From Discovery to Bedside	51
Ankeet Shah, Dominic Grimberg, and Brant A. Inman	
Intravital Optical Imaging to Monitor Anti-Tumor Immunological Response in Preclinical Models	67
Gregory M. Palmer, Yuxiang Wang, and Antoine Mansourati	
Nanoparticle-Mediated Heating: A Theoretical Study for Photothermal Treatment and Photo Immunotherapy	89
Stephen J. Norton and Tuan Vo-Dinh	

Part II Nanosystems for Biomedical Applications

Nanoparticle Systems Applied for Immunotherapy in Various Treatment Modalities	117
Vanessa Cupil-Garcia, Bridget M. Crawford, and Tuan Vo-Dinh	
Design of Nanostructure Materials to Modulate Immunosuppressive Tumour Microenvironments and Enhance Cancer Immunotherapy	143
Seung Mo Jin, Sang Nam Lee, Hong Sik Shin, and Yong Taik Lim	

Plasmonic Gold Nanostars for Immuno Photothermal Nanotherapy to Treat Cancers and Induce Long-Term Immunity	173
Tuan Vo-Dinh, Brant A. Inman, Paolo Maccarini, Gregory M. Palmer, Yang Liu, and Wiguins Etienne	
Nanotechnologies for Photothermal and Immuno Cancer Therapy: Advanced Strategies Using Copper Sulfide Nanoparticles and Bacterium-Mimicking Liposomes for Enhanced Efficacy	191
Binbin Zheng and Wei Lu	
Nanoparticle-Based Phototherapy in Combination with Checkpoint Blockade for Cancer Immunotherapy	209
Qian Chen and Zhuang Liu	
Development of Nanoparticles as a Vaccine Platform	223
Kenichi Niikura	
Multifunctional Gold Nanostars for Sensitive Detection, Photothermal Treatment and Immunotherapy of Brain Tumor	235
Yang Liu, Pakawat Chongsathidkiet, Ren Odion, Peter E. Fecci, and Tuan Vo-Dinh	
Index	257

About the Editor



Tuan Vo-Dinh is *R. Eugene and Susie E. Goodson* Distinguished Professor of Biomedical Engineering, Professor of Chemistry, and Director of the Fitzpatrick Institute for Photonics at Duke University. Dr. Vo-Dinh completed high school education in Saigon (now Ho Chi Minh City) and pursued studies in Europe where he received a B.S. in physics in 1970 from EPFL (École Polytechnique Fédérale de Lausanne), Lausanne and a Ph.D. in physical chemistry in 1975 from ETH (Swiss Federal Institute of Technology), Zurich, Switzerland. Before joining Duke University in 2006, Dr. Vo-Dinh was Director of the Center for Advanced Biomedical Photonics, Group Leader of Advanced Biomedical Science and Technology Group, and a Corporate Fellow, one of the highest honors for distinguished scientists at Oak Ridge National Laboratory (ORNL). His research has focused on the development of advanced technologies for the protection of the environment and the improvement of human health. His research activities involve nano-biophotonics, nanosensors, laser spectroscopy, molecular imaging, medical theranostics, and photoimmunotherapy.

Dr. Vo-Dinh has authored over 500 publications in peer-reviewed scientific journals. He is the author of a textbook on spectroscopy and editor of 8 books. Elected Fellow of the National Academy of Inventors (NAI), he holds over 59 US and international patents. Dr. Vo-Dinh has received seven *R&D 100 Awards* for Most Technologically Significant Advance in Research and Development for his pioneering research and inventions of inno-

vative technologies. He has received the *Gold Medal Award*, Society for Applied Spectroscopy (1988); the *Languedoc-Roussillon Award* (France) (1989); the *Scientist of the Year Award*, ORNL (1992); the *Thomas Jefferson Award*, Martin Marietta Corporation (1992); two *Awards for Excellence in Technology Transfer*, Federal Laboratory Consortium (1995, 1986); the *Inventor of the Year Award*, Tennessee Inventors Association (1996); the Lockheed Martin *Technology Commercialization Award* (1998); the *Distinguished Inventors Award*, UT-Battelle (2003); and the *Distinguished Scientist of the Year Award*, ORNL (2003). In 1997, Dr. Vo-Dinh was presented the *Exceptional Services Award* for distinguished contribution to a Healthy Citizenry from the U.S. Department of Energy. Dr. Vo-Dinh received the 2017 *Award for Spectrochemical Analysis* from the American Chemical Society (ACS), and the 2019 *Sir George Stokes Award* from the Royal Society of Chemistry (United Kingdom).

Part I
Basic Principles and Methods

The New Frontier in Medicine at the Convergence of Nanotechnology and Immunotherapy



Tuan Vo-Dinh 

1 Nanoparticles and the Immune System

1.1 *Stepping into the Nanoworld*

Thousands of years ago, the Greek philosophers Leucippus and Democritus have suggested that all matter was made from tiny particles like atoms. The advent of nanotechnology in the modern era has triggered the development of a new generation of imaging instruments capable of revealing the structure of these tiny particles conceived since the Hellenic Ages. For scale appreciation, let us look up in the dimension scale, from the cell up to the outer edges of our “local universe”, the Milky Way, a galaxy of 100–400 billion stars. This universe revealed to us has the dimension of 50,000 light-years from the outer edges to its center. A light-year is the distance that light travels in 1 year at the speed of approximately 300 million (300,000,000) meters per second, which corresponds to approximately 10,000,000,000,000,000 (sixteen zeros) or 10^{16} m. The meter, a dimension unit closest to every-day human experience, is often considered as the basic dimension of reference for human beings. Therefore, the distance from the center to the outer edge of the Milky Way is 500,000,000,000,000,000,000 or 5×10^{20} m. Let’s now look down in the other direction of the dimensional scale, down to a nanometer, which is a billion (1,000,000,000) times smaller than a meter (i.e., 10^{-9} m). The word *nano* is derived from the Greek word meaning “dwarf.” In dimensional scaling

T. Vo-Dinh (✉)

Fitzpatrick Institute for Photonics, Duke University, Durham, NC, USA

Department of Biomedical Engineering, Duke University, Durham, NC, USA

Department of Chemistry, Duke University, Durham, NC, USA

e-mail: tuan.vodinh@duke.edu

© Springer Nature Switzerland AG 2021

T. Vo-Dinh (ed.), *Nanoparticle-Mediated Immunotherapy*, Bioanalysis 12,

https://doi.org/10.1007/978-3-030-78338-9_1

nano refers to 10^{-9} —i.e., one billionth of a unit. Diameters of atoms are on the order of tenths of (10^{-1}) nanometers whereas the diameter of a DNA strand is about a few nanometers. Thus, *nanotechnology* allows us to enter, explore and interact with the innerworld of a cell within the dimensional scale at the level of atoms and molecules.

It is now generally accepted that nanotechnology involves research and development on materials and species at length scales from 1 to 100 nm. The average animal cell size is approximately 10–20 microns, which is 10–20 thousand nanometers. Due to their small sizes, nanoparticles (NPs) can enter and/or be absorbed deep inside cells, where they can interact with and affect many biological species contained in the cell, which have molecular structures at the nanoscale levels. These species comprise a wide variety of basic structures such as proteins (e.g., antibodies), polymers, carbohydrates (e.g., sugars), and lipids, which have a great variety of chemical, physical, and functional properties affecting the immune system. By evolutionary modification over trillions of generations, the immune system of living organisms have perfected an armory of molecular machines, structures, and processes to defend against invaders and eradicate illnesses. The immune system of the living cell, with its myriad of biological components, may be considered the ultimate “nano machinery”. It is conceivable that nanoparticle systems could interact with affect and actually “manipulate” individual atoms and molecules in the immune system in very specific ways, thus inducing new properties and triggering new functions in the immune system. Upon entering the body, NPs can be taken up by phagocytes, which are an important component of both immunosuppression and immunostimulation. The ability to produce NPs can be designed to be in the range of chemical ligands, bioreceptors, proteins and equipped with appropriate biochemical entities in order to achieve new therapeutic possibilities for a variety of illnesses. For instance, NPs could be designed to carry payloads such as antigens and/or immunomodulatory agents including cytokines, ligands for immunostimulatory receptors or antagonists for immunosuppressive receptor to have improved therapeutic effectiveness. Nanotechnology is of great importance to molecular biology and medicine because immunological processes are maintained by the action of a series of biological molecular nanomachines in the cell machinery.

1.2 The Immune System

Figure 1 shows a schematic diagram of the possible effects of nanoparticles on the body’s immune system. Upon entering the body, NPs interact with cells and proteins and could stimulate or suppress the innate immune response, and similarly activate or avoid the complement system. Their physicochemical properties of NPs, including size, shape, hydrophobicity and surface modification, are the factors that could influence the interactions between NPs and the innate immune system

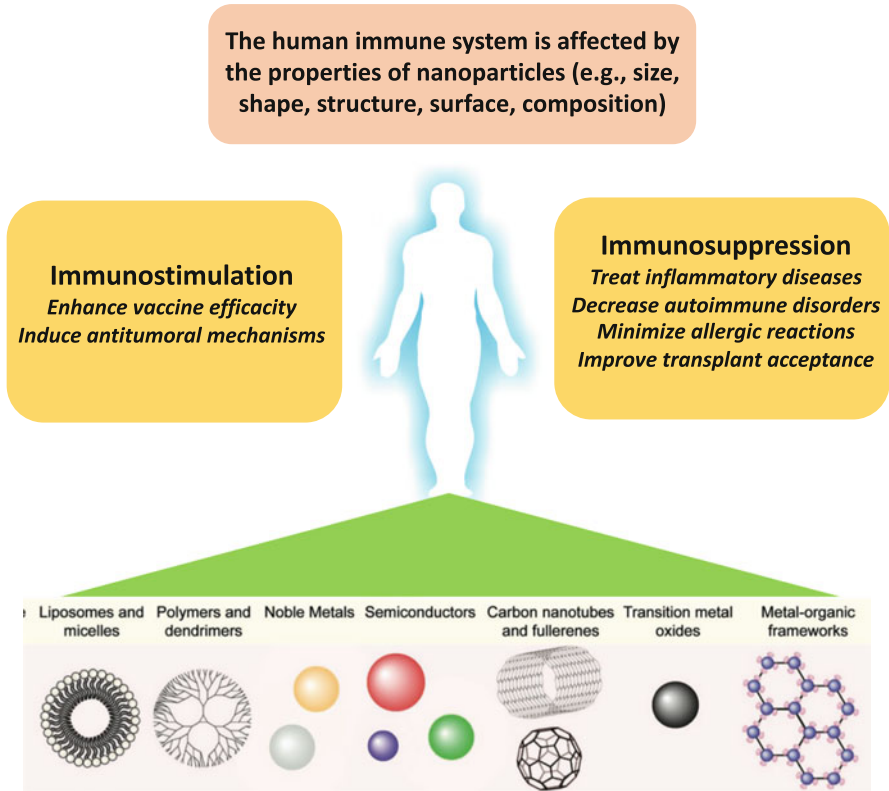


Fig. 1 Effect of Nanoparticles on the Immune System. Inside the body, nanoparticles could stimulate or suppress the innate immune response. The properties of nanoparticles, such as chemical composition, structure, size, shape, hydrophobicity and surface modification, are the factors that could influence the interactions between them and the innate immune system

[1].The immune system is designed to react to foreign threats and entities entering the body in order to protect the host and maintain homeostasis [2]. Two basic subsystems control the immune response: the innate immunity and the adaptive immunity. The innate immunity is the first line of defense, producing a non-specific inflammatory response upon the detection of conserved biological motifs; in general these motifs are often associated with bacteria and viruses. On the other hand, the adaptive immune system responds with a more specific defense mechanism by which antibodies that are highly-specific to detected antigens are produced; the initial antigen production is often followed by creation of memory cells for future immunological protection [3]. The acquired immune system is activated by mechanisms whereby antigen presenting cells (APCs) present acquired antigens to T cells.

As they enter the body, NPs usually interact with the innate immune system first; this interaction could generate an immunomodulatory response based on their

physicochemical properties [4]. Therefore, knowledge of the interactions NPs with the innate immune system could provide useful insight into developing immune-compatible, immune-modulating, or immune-stimulating NP platforms for specific medical applications of interest. The innate immune system is a broad-based, non-specific defense mechanism, which involves molecular (complement system, cytokines) and cellular (phagocytes and leukocytes) components that recognize classes of molecules such as frequently encountered pathogens. The innate immune system recognizes pathogens mainly via pattern-recognition receptors (PRPs). Also there is a highly organized complement system, which involves a set of serum proteins that are usually in an inactive state; however, these proteins can be converted into an active state to damage and clear pathogenic organisms. Activation of the complement system induces the formation of potent proteins that elicit physiological responses such as chemoattraction (attract phagocytes to sites of injury or inflammation) and enhanced vascular permeability [5]. Several circulating and tissue-specific cell types, such as natural killer (NK) cells, granulocytes (neutrophils, basophils, eosinophils, mast cells) and antigen-presenting cells (macrophage and dendritic cells (DC)) are part of the innate immune system.

In the innate immune response, APCs and neutrophils can recognize pathogens via pattern recognition receptors (PRRs) PRRs, which identify pathogen-associated molecular patterns (PAMPs), which can identify two classes of molecules: pathogen-associated molecular patterns (PAMPs), which are associated with microbial pathogens, and damage-associated molecular patterns (DAMPs), which are associated with components of host's cells that are released during cell damage or death. Upon identification, the cells uptake and digest the pathogens and induce an inflammatory response [6]. Activation of the innate immune system induce changes that can cause cytokine secretion (e.g. interleukins (ILs), tumor necrosis factor (TNF- α) [6]. It is noteworthy that activation of PRRs is process of the inflammatory immune response that allows the host cell to distinguish "self" from "non-self". PRRs are expressed on either the cell membrane (such as Toll-like receptors (TLRs) and C-type lectin receptors (CLRs)) or in the cytosol (such as NOD-like receptors (NLRs) and RIG-I-like receptors (RLRs) [7]. Physicochemical properties of NPs are important factors affecting the contact of NPs with the innate immune system and the resulting immune response.

1.3 Nanoparticle Size Effect

An important factor that has a significant impact on the uptake of these materials by cells, the initiation of innate immune response, and their overall bio-distribution in vivo if the size of NPs [4, 8]. The interactions with the innate immune system is affected by the surface to volume ratio of NPs. Endocytosis, the general process by which cells engulf external substances, gathering them into special membrane-bound vesicles contained within the cell. The endocytotic uptake of NPs involve several endocytic uptake mechanisms: pinocytosis, macropinocytosis, phagocytosis

and clathrin/caveolar-mediated endocytosis. Pinocytosis and micropinocytosis, are non-specific processes by which NPs in liquid droplets are ingested by living cells. Phagocytosis is a process by which particles, microbes or fragments of dead cells are engulfed and internalized, usually by specific membrane receptors. Clathrin-mediated endocytosis, also called receptor-mediated endocytosis (RME) is a process that absorb particles, metabolites, proteins, etc. by the inward budding of the plasma membrane (invagination) and forms vesicles containing the absorbed substances; RME is strictly mediated by receptors on the surface of the cell as only the receptor-specific substances can enter the cell through this process.

Various studies have shown that uptake of NPs into cells could involve a combination of several processes. For example, 600-nm polystyrene NPs were engulfed by phagocytosis/macropinocytosis, while 40-nm NPs were internalized by both clathrin-mediated endocytosis as well as phagocytosis or macropinocytosis by macrophages [9]. Smaller 10-nm gold NPs per cell were uptaken in greater amounts than larger 50-nm gold NPs into cells via a clathrin/dynamin-dependent mechanism by DCs [10]. Nanoparticle size, surface charge and composition have been demonstrated to be important for immunostimulatory activity. For example, NPs with small sizes ranging from <40 to 50 nm have been shown to be very effective in stimulating both humoral immunity and MHC-I restricted CD8+ T cell immunity [11–13]. The effect of NPs of different sizes on the immune systems were investigated. Most NPs accumulate in the liver (Kupffer cells), the amount increasing with the size of NPs and smaller NPs exhibiting higher retention than larger NPs [14, 15]. Smaller NPs (<200 nm) are rapidly drained to the lymph nodes, where they were taken up by resident DC, whereas larger NPs (>500 nm) depended on cellular transport by DC, immigrating from the injection site to the lymph nodes [16]. These results indicated that larger NPs prefer interacting with tissue-resident APCs, while smaller NPs (<200 nm) could circulate through vein and lymphatic drainage, providing better antigen presentation.

Nanoparticle sizes can be controlled so that they passively accumulate in tumors due to the enhanced permeability and retention (EPR) effect of tumor vasculature. The EPR effect is a result of the inherent leakiness of the tumor vasculature, which is underdeveloped and allows nanoparticles to escape the circulation and accumulate passively in tumors. In addition, retention of nanoparticles in the tumor is enhanced by the lack of an efficient lymphatic system which would normally carry extravasated fluid back to the circulation. To take advantage of the EPR effect nanoparticles can be engineered to have a narrow size range between approximately 10 and 100 nm. For example, gold nanostars can take advantage of the EPR effect because they can be synthesized to have hydrodynamic sizes that fit well in the 10–100 nm size ranges. Figure 2 shows results of a study of gold nanostars' biodistribution and intratumoral uptake using radiolabeling, as well as X-ray computed tomography (CT) and optical imaging in a sarcomas mouse model. The data show that the 30-nm GNSs exhibit the most optimal tumor uptake, compared to the smaller 12-nm and the larger 60-nm GNSs [17].

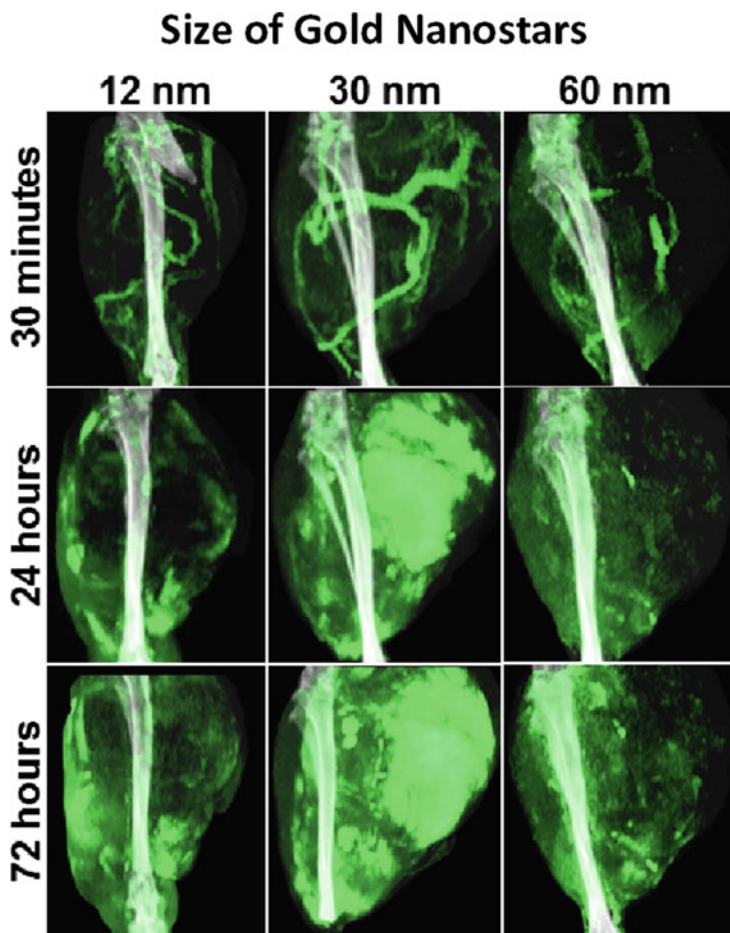


Fig. 2 Effect of the Size of Gold Nanostars on Accumulation into Tumors. Depending on their sizes, nanoparticles have a natural propensity to accumulate in and around cancer cells due to the enhanced permeability and retention effect. Computed tomography images of hind leg primary sarcomas following injection gold nanostars with different sizes (12-nm, 30-nm and 60-nm diameter) at 30 minutes, 24 hours, and 72 hours. The 30-nm GNSs exhibit optimal tumor uptake, compared to the smaller 12-nm and the larger 60-nm GNS (Adapted from Ref [17])

1.4 Nanoparticle Shape, Structure, and Surface Effect

The shape of NPs has also been demonstrated to affect interactions with the innate immune system [6, 18]. Figure 3 shows some examples of metal (gold, silver) nanoparticles that can be engineered to have different shapes (prism, cube, rod, pyramid, dumbbell, star). Gold nanoparticles (GNPs) have received great interest for biomedical applications because they offer several advantages, including

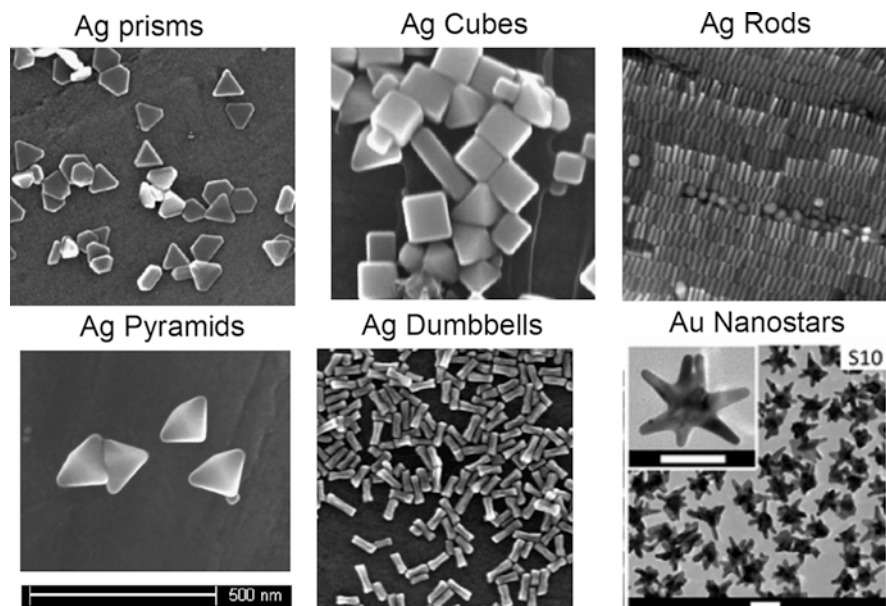


Fig. 3 Examples of Different Shapes of Engineered Metallic Nanoparticles

biocompatibility, the ease of adding functional ligands, efficiency in penetrating cells, and the possibility to heat them using near-infrared light. The effect of size and shape on the biodistribution of a set of gold nanoparticles (GNPs) after intravenous administration in mice has been investigated [17]. The efficiency of cellular uptake of the gold nanoparticles with different shapes was found to rank in the following order from lowest to highest: stars, rods, and triangles [19]. Different shapes tended to use the various endocytosis pathways in different proportions. The results indicated that (a) the size and the shape greatly influence the kinetics of accumulation and excretion of GNPs in filter organs; (b) spherical and star-like GNPs showed the same percentage of accumulation, but a different localization in liver; (c) only star-like GNPs are able to accumulate in lung; (d) changes in the geometry did not improve the passage of the blood brain barrier [20]. Gold nanostars have shown to be an effective theranostic nanoprobe for brain tumor delivery, and spatially controlled blood-brain-barrier permeation in a mouse study [21]. Systemically administered ^{124}I -labeled GNSs via iv tail vein injection were shown to cross the blood-brain barrier in glioblastoma mouse model and permeate the neoplastic vasculature and accumulated in brain tumor intracellular vesicles [22]. The uptake of gold nanorods by macrophages was found to be more efficient than that of nanospheres [23]. Blocking experiments and electron microscopic studies indicated macropinocytosis as the major uptake mechanism.

The effect of surface modifications on cellular uptake of gold nanorods in human primary cells and established cell lines was investigated [24]. The results indicated

that the surface properties of gold nanorods affected their cellular uptake, and the cationic surface tended to be advantageous for uptake, but it depended on the cell types. The size and shape of various nanostructures can also affect the immunological response in biological systems. GNPs of varied shapes coated with West Nile virus envelope (E) protein can induce different cytokine secretion behaviors in dendritic cells: rod-shaped GNPs induced the secretion of the inflammasome-related cytokines, interleukin 1 β and interleukin 18, while cubic AuNPs induce the secretion of the pro-inflammatory cytokines 18 at high levels [25]. A study of the shape effect of glyco-nanoparticles on macrophage cellular uptake and immune response showed that spherical GNPs were internalized to a much greater extent than cylindrical GNPs [26]. This phenomenon was attributed to different endocytosis pathways, spherical GNPs being internalized based on clathrin- and caveolin-mediated endocytosis while cylindrical GNPs mainly involving clathrin-mediated endocytosis.

Grafting of poly(ethylene oxide) (PEO) onto the nanorods was found to significantly delay their internalization for several hours. It was also observed that neutrophil granulocytes did not fully internalize the particles but trapped them in their extracellular structures. Human cytokine-induced killer cells loaded with gold nanoprisms have been used as a theranostic platform for targeted photoacoustic imaging and enhanced immuno-photothermal combined therapy [27]. Titanium dioxide NPs of different shapes could raise levels of proinflammatory cytokines, increase maturation, and increase expression of costimulatory molecules on DCs [28]. A study of various sizes and shapes of polystyrene NPs showed that particles possessing the longest dimension exhibited maximum tendency to attach to macrophages as these size particles exhibit the strongest binding to the membrane ruffles of the macrophage surface [29].

Chitosan-coated hollow CuS nanoparticles that assemble the immunoadjuvants oligodeoxynucleotides containing the cytosine-guanine (CpG) motifs have been developed for combined NIR laser-induced photothermal ablation and immunotherapy [30]. In this method, photothermal ablation-induced tumor cell death reduces tumor growth and releases tumor antigens into the surrounding milieu, while the immunoadjuvants potentiate host antitumor immunity. These hollow CuS nanoparticles are biodegradable and can be eliminated from the body after laser excitation.

Before interacting with the immune system, NPs must first enter the cell. Therefore, it is important to engineer NPs for effective delivery systems that could offer various advantages: (1) effective accumulation into cellular systems of interest; (2) site-specific delivery of drugs, peptides, and genes for specific applications; (3) improved *in vitro* and *in vivo* stability; and (4) minimum side effect profile. Two-dimensional Raman imaging was used to investigate nanoprobe uptake in single cells by monitoring spatial and temporal tracking via Raman-labeling and modulation of surface charge [31]. To study the efficiency of cellular uptake, silver nanoparticles functionalized with three different positive, negative-, and neutrally-charged Raman labels [4-mercaptobenzoic acid (4-MBA), 4-aminothiophenol (4-ATP), and 4-thiocresol (4-TC)] were co-incubated with cell cultures, and allowed to be taken up via normal cellular processes. The results showed that the 4-ATP

particles are taken up into the cells more efficiently than particles functionalized with 4-MBA (Fig. 4a). The surface charge on the nanoparticles was observed to modulate their uptake efficiency during co-incubation, demonstrating a dual function of the surface modifications as tracking labels and as modulators of cell uptake. Uptake of nanoparticles in the nucleus of a cell was demonstrated with a

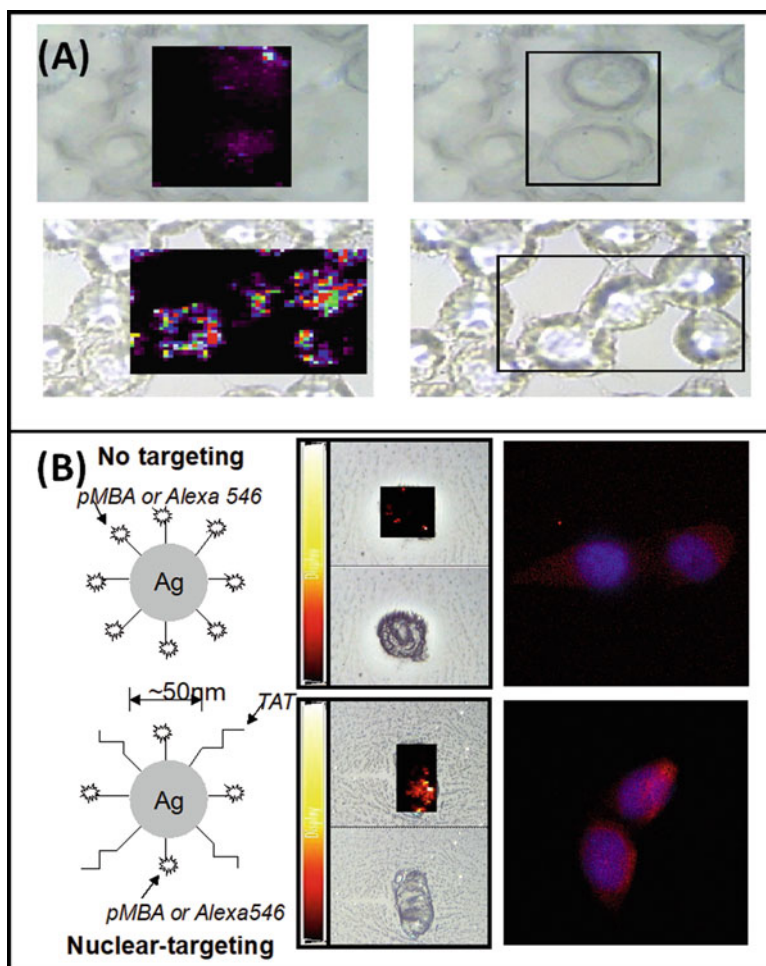


Fig. 4 Effect of Chemical Ligands on Cellular Uptake. (a) Two-dimensional surface-enhanced Raman scattering (SERS) map showing cellular distribution of with 4-ATP-labeled silver nanoparticle labeled with 4-MBA dye (top) and 4-AT dye (bottom) in J774 cells; the 4-ATP particles are taken up into the cells more efficiently than particles functionalized with 4-MBA (Adapted from Ref. [31]); (b) Two-dimensional SERS mapping was used to track the spatial and temporal progress of cell uptake and localization of nanoparticles. Silver nanoparticles co-functionalized with the TAT peptide (bottom) showed greatly enhanced uptake into the nucleus over the nanoparticles without the targeting moiety (top). (Adapted from Ref. [32])

co-functionalized nanosensing/biodelivery platform combining a nuclear targeting peptide (NTP) for improved cellular uptake and intracellular targeting, and p-mercaptobenzoic acid (pMBA) as a surface-enhanced Raman scattering (SERS) reporter (Fig. 4b) [32]. The nuclear targeting peptide, an HIV-1 protein-derived TAT sequence, has been previously shown to aid entry of cargo through the cell membrane via normal cellular processes and, furthermore, to localize small cargo to the nucleus of the cell. Silver nanoparticles co-functionalized with the TAT peptide showed greatly enhanced cellular uptake over the control nanoparticles lacking the targeting moiety.

The size, chemical structure and composition of NPs could play an important role in their interaction with the immune system. For example, some NPs could trigger immunostimulatory responses mediated by the production of inflammatory cytokines. Secretion of inflammatory cytokines has been shown for a variety of nanomaterials themselves including gold colloids, dendrimers, polymers, and lipid NPs [12, 33–37]. Cationic liposomes facilitate secretion of inflammatory cytokines such as TNF- α , IL-12, and IFN- γ , and increase the expression of CD80/CD86 activation markers on the surface of DCs than anionic or neutral NPs [38, 39]. Therefore, great care should be taken with therapies that use NPs and their safety should be well evaluated before clinical use.

2 Nanoparticles, Antitumor Immunity and Cancer Immunotherapy

2.1 Nanoparticle and Cancer Immunosurveillance and Tumor Microenvironment

Nanoparticles have great potential to produce novel therapeutic strategies that target malignant cells through the ability of nanoparticles to get access to and be ingested preferentially by tumors due to the EPR effect. The accumulation of NPs in tumors and specific effects on the immune system are topics of extensive research. Nanoparticles have been reported to exhibit properties capable of stimulating antitumor immunity [40]. In cancer research, it has been observed that while the immune system can recognize and potentially attack tumors, the tumor could develop immunosuppressive systems that affect the immune system and protect it against anti-tumor immunity [41, 42]. Extensive research effort have been devoted to cancer immunosurveillance and to the so-called concept of ‘cancer immunoediting’. Cancer immunoediting consists of three phases: elimination (i.e., cancer immunosurveillance), equilibrium, and escape. Cytotoxic lymphocytes, which are major protagonists of immunosurveillance and immunotherapy of cancer, are capable of eradicating malignant cells. The selective killing of transformed cells requires a precise molecular recognition of “malignant self” [42]. Better understanding of the

immunobiology of cancer immunosurveillance and immunoediting could lead to the development of more effective immunotherapeutic approaches to eradicate human cancers.

The therapeutic efficacy of cancer immunotherapy for many patients is mainly limited by the immunosuppressive tumor microenvironment (TME). The key to current immunotherapy strategies is modifying the tumor microenvironment such that the tumor-mediated immunosuppression is reduced, immune recognition of the tumor is supported and the immune system effectively attacks the tumor. There is increasing interest in developing strategies based on NPs to change and modulate the tumor microenvironment (TMI) in order to stimulate innate and adaptive immune systems and achieve effective anti-tumor immune responses. The ultimate goal is to trigger, modulate and expand the capabilities of the patient's immune system to attack and eradicate tumors. Immunomodulation of immunosuppressive factors and therapeutic immune cells (e.g., T cells and antigen-presenting cells) could be designed to reprogram the immunosuppressive TME. Nano-biomaterials can be rationally designed to modulate the immunosuppressive TME in a spatiotemporal manner for enhanced cancer immunotherapy [43]. A syringeable immunomodulatory multidomain nanogel (iGel) that overcomes the limitation by reprogramming of the pro-tumoral TME to antitumoral immune niches [44]. Local and extended release of immunomodulatory drugs from iGel deplete immunosuppressive cells, while inducing immunogenic cell death and increased immunogenicity. The iGel approach has the potential to offer an immunotherapeutic platform that can reshape immunosuppressive TMEs and synergize cancer immunotherapy with checkpoint therapies, with minimized systemic toxicity.

Figure 5 depicts a schematic diagram of molecular processes in anti-tumor immunity, depicting the three different phases of immunization, T-cell activation, and immunosuppression in the tumor microenvironment [45]. In the immune system, tumor-associated antigens are captured by dendritic cells (DCs). The DCs process the captured antigens and expose them onto the major histocompatibility complexes (MHC) I or II and migrate to draining lymph nodes. In the lymph node, antigen presentation to T cells will elicit responses depending on the type of DC maturation stimulus received and on the interaction of T-cell costimulatory molecules with their surface receptors on DCs. For instance, interaction of CTLA4 with CD80/86 or PD-1 with PD-L1/PD-L2 will suppress T cell responses. Antigen-educated T cells (along with B cells and NK cells) will exit the lymph node and enter the tumor bed, where a host of immunosuppressive defense mechanisms can be produced by tumors [45].

2.2 Nanosystems with Tumor Antigens

Tumors often produce antigenic species that could induce immunogenic responses from the patient's body; however, these immune responses are usually not sufficiently strong or are suppressed by various mechanisms. Processes that suppress

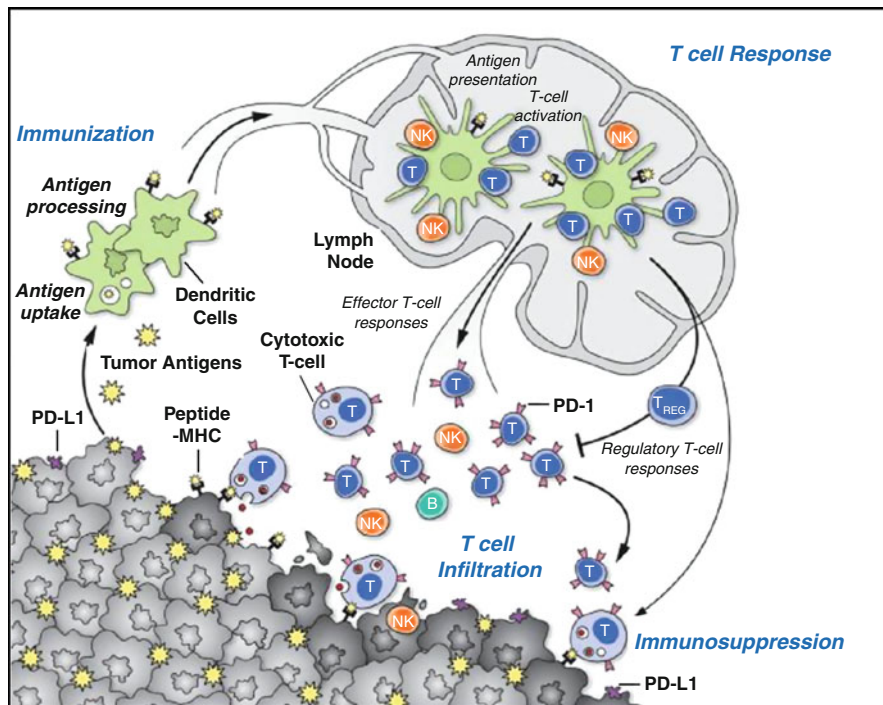


Fig. 5 Schematic Diagram of Molecular Processes and Biological Species Involved in Anti-Tumor Immunity. The three different phases of immunization, T-cell activation, and immunosuppression in the tumor microenvironment are depicted (Adapted from Ref [45])

anti-tumor responses of the immune system could involve recruitment of immunosuppressive leukocytes. A possible strategy for effective delivery system tumor antigens is to use NPs that are loaded with tumor antigens; phagocytes will then take up these NPs, become stimulated and present antigens to T cell, the main cell type in anti-tumor immune responses. Also tumor-associated immunosuppressive phagocytes, which are present in the tumor microenvironment of solid tumors, and cells that are critical for tumor progression, are constantly recruited to the tumor, and therefore could carry NPs to tumors. In this case the antigen-loaded NPs stimulate phagocytic cells to become activated immunostimulatory antigen-presenting cells (APC), resulting in a more effective adaptive immune response. In line of this strategy, various nanoplateforms loaded with tumor antigens have been developed to enhance the response of the immune system against tumors [46–48]. Cancer vaccines loaded with tumor-associated antigens are able to induce antigen-specific immunities against tumors, rather than non-specific immunological responses triggered by other methods such as the checkpoint-blockade therapy. Also, cancer vaccines may offer a long-term immune-memory effect that could be helpful to prevent cancer recurrence.

2.3 Nanoparticles Having Adjuvant Activity

As discussed previously, the process of tumor antigen presentation is important in activating and enhancing the adaptive immune system. However, tumor antigen presentation by APCs is often an ineffective process. A method to achieve this enhancement effect involves addition of an adjuvant to NP payloads in order to modulate immunosuppressive APCs, such as dendritic cells (DCs), into immunostimulatory phenotypes in the tumor microenvironment. DCs are important regulators of the immune system, with the ability to induce and maintain primary immune responses as well as tolerance. It has been shown that phagocytic APCs tend to ingest NPs preferentially as compared to other cells [49]. Toll-like receptors (TLRs), an important type of receptors that recognize pathogen-associated constituents, are expressed in APCs [50]. Activation of these receptors is an effective strategy to activate APCs and stimulate an effective adaptive immune response [51]. It is noteworthy that some vaccines used adjuvant substances that activate TLRs or other “danger” signal receptors in order to stimulate the innate immune response, leading to a more effective adaptive immune response.

Nanoparticle-delivered adjuvants have been used to ‘precondition’ or alter the vascular and immunological biology of the tumor to enhance its susceptibility to thermal therapy [52]. The ‘preconditioning’ process involves the use of a bioactive agent (e.g., TNF-alpha, arsenic trioxide, and interleukins) to modify the vascular and/ or immunological components of the tumor microenvironment in order to make the tumor tissue more susceptible to a secondary treatment, such as thermal therapy. A gold nanoparticle tagged with a vascular targeting agent (i.e., TNF-alpha) demonstrated the possibility of preconditioning through reduction in tumor blood flow and induction of vascular damage, which recruits a strong and sustained inflammatory infiltrate in the tumor.

Some ligands are used to induce an immunostimulatory effect in NPs. Polyethyleneimine (PEI) is a positively charged polymer that has shown to induce anti-tumor immune effect. PEI-based nanoparticles encapsulating siRNA were preferentially and engulfed by regulatory DCs expressing CD11c and programmed cell death 1–ligand 1 (PD-L1) [53]. PEI-siRNA uptake transformed these DCs from immunosuppressive cells to efficient antigen-presenting cells that activated tumor-reactive lymphocytes and exerted direct tumoricidal activity, both in vivo and in situ. In particular siRNA-PEI nanoparticles were shown to stimulate TLR5 and TLR7 stimulation of siRNA-PEI nanoparticles and synergize with the gene-specific silencing activity of siRNA; this process transform tumor-infiltrating regulatory DCs into DCs capable of promoting therapeutic antitumor immunity. PEI-based nanoparticles have been developed for use as vaccine adjuvants. Other types of NP generating polymer were also shown capable of stimulating TLRs. For instance, polymethyl vinyl ether-co-maleic anhydride (PVMA)-coated NPs were also successfully used as an adjuvant to activate DCs by stimulating TLR2/4 stimulation. These findings indicate that NPs engineered to include adjuvant activity have considerable potential for cancer immunotherapy. Gold NPs have been shown

to be effective vaccine adjuvants and enhance the immune response via different cytokine pathways depending on their sizes and shapes [54].

2.4 Virus-like Nanoparticles and Cancer Immunotherapy

Virus-like particles (VLPs) are multiprotein structures that mimic the organization and conformation of authentic native viruses but are non-infectious by lacking the viral genome. The FDA has approved several VLP-based vaccines to prevent infection by viruses that cause cancer. Examples of these VLP vaccines include the one against human papilloma virus (HPV) that causes human cervical cancer, and a VLP vaccine that protects against hepatitis B virus (HBV) infection, which is associated to liver cancer. The main idea behind the use of VLP vaccine technology against infectious disease or tumors is based on the facts that the VLPs can carry a payload but also can be recognizable by the immune system as a pathogen and can activate APCs [54, 55]. Like other NPs, VLPs also can be engineered to incorporate exogenous molecules, such as antigens, giving them potential value for immunotherapy, and as vaccines for a range of cancers and other diseases. Virus-based cancer vaccines have received increasing interest in the field of cancer immunotherapy; it has been observed that most of the immune responses they elicit are against the virus and not against the tumor. On the other hand, targeting tumor-associated antigens is effective, however the identification of these antigens remains challenging. To address this challenge a multi-vaccination strategy focused on an oncolytic virus artificially wrapped with tumor cancer membranes carrying tumor antigens has been developed. This nanoparticle platform can control the growth of aggressive melanoma and lung tumors *in vivo* both in preventive and therapeutic setting, creating a highly specific anti-cancer immune response [56].

A VLN was developed as a nanoplatform to co-deliver CRISPR/Cas9 [Clustered Regularly Interspaced Short Palindromic Repeats (CRISPR)-associated protein 9 (Cas9)] system and small molecule drugs for effective malignant cancer immunotherapy [57]. VLN has a core-shell structure, in which small molecule drugs and CRISPR/Cas9 system are loaded in the mesoporous silica nanoparticle (MSN)-based core, which is further encapsulated with a lipid shell. Upon reaching tumors, VLN releases the CRISPR/Cas9 system and small molecule drugs in response to the reductive microenvironment, resulting in the synergistic regulation of multiple cancer-associated pathways.

3 Nanoparticle-Mediated Hyperthermia and the Immune System

3.1 Hyperthermia Effect on the Immune System

Another area of increasing interest for immune-mediated anti-tumor nanotechnology in hyperthermia is the use of NPs that are dormant by themselves but can be activated using external energy sources. As one of the first effective systemic cancer treatments, hyperthermia (HT) aims to increase tumor temperature above the normal value ($\sim 36^\circ\text{C}$) to trigger local and systemic antitumor effects and/or ablate cancer cells. HT at high temperature ($>55^\circ\text{C}$) can actually induce immediate thermal death (ablation) to targeted tumors. On the other hand, HT at mild fever-range can be used to improve drug delivery to tumors, improve cancer cell sensitivity to other therapies, and trigger potent systemic anti-cancer immune responses [58–61]. Fever-range thermal stress was shown to increase tumor cell susceptibility to NK cells via increased expression of NK target molecule [62]. Upon hyperthermia treatment, cancer cells experience stress and induce heat shock proteins (HSPs) as a part of the defense mechanisms. HSPs released after heat-induced necrosis can activate APCs through TLR signaling pathways and exhibit immunostimulatory properties [63]. Increased production of inflammatory cytokines, such as TNF- α , IL-1 β , and IL-12 was observed following the binding of HSP70 to TLR2 and TLR4 on DCs [64, 65]. Several studies demonstrated that HSPs can enhance the adaptive anti-tumor immune response by inducing cross-presentation of cancer antigen to prime cytotoxic CD8+ T cells [66–68].

Traditional HT modalities such as microwaves, radiofrequency and ultrasound can control macroscopic heating around the tumor region, but cannot precisely target or ablate cancer cells in a timely manner. Cancer treatment using photothermal therapy (PTT), which exploits high temperature transduced from photon energy is a promising method offering high efficiency and specificity because cancer cells are more sensitive to elevated temperature ($>42^\circ\text{C}$) than normal cells.

3.2 Nanoparticle-Mediated Hyperthermia

Nanoparticle (NP)-mediated thermal therapy has demonstrated the potential to combine the advantages of precise cancer cell ablation. NPs have a natural propensity to extravasate from the tumor vascular network and accumulate in and around cancer cells due to the enhanced permeability and retention (EPR) effect. Selective absorption of NPs into the tumors using external energy sources can induce nanoparticle-mediated local hyperthermia. The NP-mediated thermal techniques are, in general, minimally invasive and achieve superior localized heating of the entire tumor mass while sparing surrounding normal tissues. This

feature greatly minimizes the amount of laser energy needed to induce local damage of the diseased cells, making the therapy method less invasive.

Nanoparticles have been employed in methods for in situ delivery of thermal energy to tumors [69]. These approaches utilize the unique properties of nanoparticles inherent to their size and composition, such as optical and dielectric properties, magnetic susceptibility, thermal or electrical conductivity. Nanoparticles such as gold nanoparticles and have been often used as platform for nanoparticle-mediated-PTT. In particular, the use of plasmonics-enhanced photothermal properties of metal nanoparticles including nanoshells, nanorods and nanostars for PTT has been reported [70–76]. Gold nanoshells have been used for targeted bimodal or trimodal cancer therapy because they can be tuned to absorb NIR light which can penetrate tissue and can be designed to be specifically targeted and delivered to cancer cells.. The promising role of nanoshells in photothermal therapy of tumors has been demonstrated [70]. Among various types of nanoparticles, gold nanostars (GNS) whose sharp branches create a “lightning rod” effect that enhances the local electromagnetic (EM) field dramatically, are the most effective in converting light into heat for photothermal therapy (PTT) [73, 74]. The unique tip-enhanced plasmonics property of GNS can be optimally tuned in the near infrared (NIR) ‘therapeutic’ optical window, where photons can travel further in healthy tissue to be ‘captured’ and converted into heat by GNS taken up in cancer cells [17, 21, 72, 76].

External energy sources, such as near infrared photons, alternating magnetic field, radiofrequency electromagnetic field, can be used to excite metallic nanoparticles (silver, gold, iron) as well as non-metallic polymer-based NPs such as carbon nanotubes [77]. The use of tumor-associated peritoneal phagocytes to ingest and carry iron oxide nanoparticles (IONPs) specifically to tumors has been demonstrated [78]. These specifically delivered nanoparticles can damage tumor cells after IONP-mediated hyperthermia generated by AMF an alternating magnetic field (AMF).

4 Synergistic Combination Nano Immunotherapies

These observations that elevated temperatures can increase anti-cancer immune responses in cells suggest that developing novel cancer treatment based on NP-mediated hyperthermia in combination with immunotherapy has potential to enhance anti-tumor immunity. Developing effective therapeutic strategies with high specificities and low toxicities to eradicate tumors, particularly post their metastases, and further prevent their recurrence, is the ultimate goal in the battle against cancer. Traditional treatment approaches, such as surgery chemotherapy and radiotherapy, cannot achieve this goal. With the increased knowledge on molecular biology of cancers and their interactions with immune systems, cancer immunotherapy has received increasing interest as the next generation treatment modality by involving or stimulating the patient’s immunological system to attack tumor cells. There are different strategies of cancer immunotherapies including

cytokine therapy, checkpoint-blockade therapy, adoptive T-cell transfer especially the emerging chimeric antigen receptor T (CAR-T) cell therapy, as well as cancer vaccines.

4.1 Immunotherapy Using Checkpoint Inhibitors

In 2007, a T cell co-stimulation (immune checkpoint) molecule called programmed death ligand 1 (PD-L1) was associated with bacillus Calmette-Guérin (BCG) immunotherapy failure and stage progression in BC was reported [79]. It was subsequently confirmed this finding and showed associations with worse survival [80–82]. The PD-L1 immune checkpoint is commonly expressed by many cancers as a method of immune evasion [83, 84]. PD-L1 binds to the PD-1 receptor found on activated T cells and inhibits cytotoxic T-cell function, thus escaping the immune response from T-cell. Using animal models of cancer [83, 85], it was shown that that PD-L1 blockade might represent a therapeutic possibility. It was found that a soluble form of PD-L1 exists in cancer patients and retains its immunosuppressive activity [84, 86]. To reverse tumor-mediated immunosuppression, therapeutic anti-PD-1/PD-L1 antibodies have been designed to block PD-L1/PD-1 interaction. By suppressing this tumor defense, the tumor cells are now vulnerable to the killing action of immune system cells that have been primed against the tumor by the nanoparticle phototherapy. Immune checkpoint drugs targeting PD-L1 and its receptor (PD-1) have been developed; phase I and II trials showed that atezolizumab (Tecentriq), a PD-L1 blocking antibody, leads to significant anti-tumor responses in BC patients who have failed conventional chemotherapy [86, 87].

4.2 Synergistic Dual-Modality Immunotherapies

The combination of immune checkpoint inhibitor-based immunotherapy with GNS-mediated photothermal therapy has produced an effective two-pronged treatment modality referred to as Synergistic Immuno Photo Nanotherapy (SYMPHONY), which is designed to treat both primary and secondary tumor cells [76, 88–90]. This two-pronged treatment modality aimed at achieving three main goals: (1) GNS-mediated photothermal heating and ablation of the primary tumour, (2) induction of a strong immunogenic cell lethality, and (3) reversal of factors contributing to immune suppression. One therapeutic arm uses laser light to irradiate the primary tumor area where GNS have accumulated, resulting in generation of heat, which kills the primary tumor cells. Not only is there an immediate killing effect at the site treated with light, but this treatment also results in a general activation of the immune system, as evidenced by the fact that distant tumors that are not treated with light also show cancer cell killing. The second therapeutic arm involves administration of PD-L1 immune checkpoint blockade to disable cancer resistance.

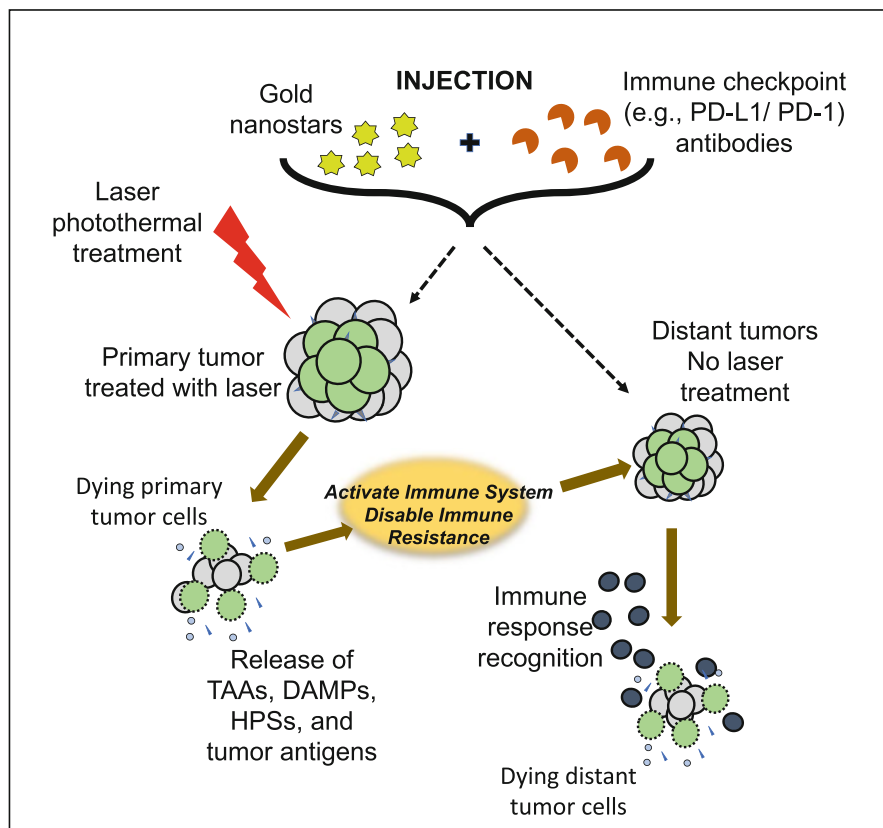


Fig. 6 Principle of two-pronged modality combining nanoparticle-mediated photothermal treatment (PTT) and checkpoint immunotherapy to treat both primary and secondary tumor cells. Following laser PTT of the primary tumor, tumor cells incubated with gold nanostars are selectively destroyed and subsequently trigger an immune response to eradicate distant untreated tumors. An abscopal effect occurs when distant untreated tumors regress during treatment of a primary tumor. Abscopal effects are thought to be due to immune activation and generally indicate the induction of effective immunity; Inset: Dual-tumor mouse model (Adapted from Ref. [88])

The efficacy of SYMPHONY is based on several synergistic processes (Fig. 6). First, localized PTT with GNS and NIR irradiation is used to kill primary tumor cells. Upon GNS-PTT treatment, dying tumor cells after thermal ablation could release tumor associated antigens (TAAs), damage-associated molecular pattern molecules (DAMPs), heat shock proteins (HSPs), etc. In live cells DAMPs are intracellular molecules that are normally hidden. When cells are damaged or dying, DAMPs are released and acquire immunostimulatory properties. DAMPs have been shown to exert various effects on antigen-presenting cells (APCs), such as maturation, activation and antigen processing/presentation [91, 92]. APCs, which are present in the tissue or in local draining lymph nodes, process the tumor antigens

and present tumor-derived peptides to T cells. Combining anti-PD-L1 treatment with tumor antigen presentation will activate tumor-specific T cells that will attack both in the primary and distant/metastatic cancer cells. This is particularly important in the primary tumor bed, hypoxic-oxygenated boundary, where it is believed metastatic/ differentiating/proliferating potential is maximum. Mouse studies have revealed that the two-pronged therapeutic approach, combining immune-checkpoint inhibition and GNS-mediated photothermal therapy, was effective in destroying primary treated tumors as well as untreated distant tumors in mice implanted with the bladder cancer cell line [88]. The effect of the combination of plasmonic GNS-enabled photothermal ablation and PD-L1 immunomodulation was demonstrated to be synergistic and not just additive. Furthermore, the delayed rechallenge with repeated tumor injections into cured mice did not lead to new tumor formation, indicating that the combined treatment induced effective long-lasting immunity, i.e. an anticancer ‘vaccine’ effect [88–90].

Another therapeutic strategy involves the combination of adjuvant nanoparticle-based photothermal therapy with a different checkpoint-blockade immunotherapy, anti-cytotoxic T-lymphocyte antigen-4 (CTLA4) [91, 92]. Indocyanine green (ICG), a photothermal agent, and imiquimod (R837), a Toll-like-receptor-7 agonist, are co-encapsulated by poly(lactic-co-glycolic) acid (PLGA). The formed PLGA-ICG-R837 nanoparticles composed purely by three clinically approved components can be used for near-infrared laser-triggered photothermal ablation of primary tumors, generating tumor-associated antigens, which in the presence of R837-containing nanoparticles as the adjuvant can show vaccine-like functions. The generated immunological responses were able to attack remaining tumor cells in mice. Furthermore, such strategy offers a strong immunological memory effect, which can provide protection against tumor rechallenging post elimination of their initial tumors.

5 Conclusion: The Next Frontier in Medicine

The development and application of nanotechnology will be important to the future of biological research and medical science. Applications of nanomaterials could revolutionize biology and medicine in much the same way that materials science changed health care three decades ago with the introduction of synthetic heart valves, nylon arteries, and artificial joints. The nanotechnology-enabled biomedical applications discussed previously are just some examples of a new generation of treatments that have the potential to modulate the inner power of the human body’s immune system; these nanotools could provide fundamental information that drastically change our fundamental understanding of the health process itself. With the recent advances in nanotechnology, the development of sophisticated nanotools and the ever increasing knowledge on the immune system, the convergence of nanotechnology and immunology will propel this area into the forefront of the most advanced strategies for the treatment of many diseases such as cancer.

Modern medicine is witnessing the emergence of are many different nanotechnology-enabled immunotherapy strategies that are being developed and tested in preclinical and clinical models. As the new field at the convergence of nanotechnology and immunology matures, it is expected that the clinical strategies will combine multiple immunotherapy approaches, along with the traditional treatment modalities of surgery, chemotherapy and radiation, in multi-modal strategies to overcome the complex challenges of medical treatment of disease.

Acknowledgements This work was supported by National Institutes of Health (1R01EB028078-01A1).

References

1. Liu, Y., Hardie, J., Zhang, X., Rotello, V.M.: Effects of engineered nanoparticles on the innate immune system. *Semin. Immunol.* **34**, 25–32 (2017)
2. Dobrovolskaia, M.A., Shurin, M., Shvedova, A.A.: Current understanding of interactions between nanoparticles and the immune system. *Toxicol. Appl. Pharmacol.* **299**, 78–89 (2016)
3. Vivier, E., Malissen, B.: Innate and adaptive immunity: specificities and signaling hierarchies revisited. *Nat. Immunol.* **6**, 17–22 (2005)
4. Kononenko, V., Narat, M., Drobne, D.: Nanoparticle interaction with the immune system. *Arch. Ind. Hyg. Toxicol.* **66**, 97–108 (2015)
5. Sarma, J.V., Ward, P.A.: The complement system. *Cell Tissue Res.* **343**, 227–235 (2011)
6. Najafi-Hajivar, S., Zakeri-Milani, P., Mohammadi, H., Niazi, M., Soleymani-Goloujeh, M., Baradaran, B., Valizadeh, H.: Overview on experimental models of interactions between nanoparticles and the immune system. *Biomed. Pharmacother.* **83**, 1365–1378 (2016)
7. Coyne, C.B., Zeh, H.J., Lotze, M.T.: PAMPs and DAMPs: signal 0s that spur autophagy and immunity. *Immunol. Rev.* **249**, 158–175 (2012)
8. Petrarca, C., Clemente, E., Amato, V., Pedata, P., Sabbioni, E., Bernardini, G., Iavicoli, I., Cortese, S., Niu, Q., Otsuki, T., Paganelli, R., Di Gioacchino, M.: Engineered metal based nanoparticles and innate immunity. *Clin. Mol. Allergy.* **13**, 13 (2015)
9. Kuhn, D.A., Vanhecke, D., Michen, B., Blank, F., Gehr, P., Petri-Fink, A., Rothen-Rutishauser, B.: Different endocytotic uptake mechanisms for nanoparticles in epithelial cells and macrophages. *Beilstein. J. Nanotechnol.* **5**, 1625–1636 (2014)
10. Tomić, S., Dokić, J., Vasilijić, S., Ogrinc, N., Rudolf, R., Pelicon, P., Vučević, D., Milosavljević, P., Janković, S., Anžel, I., Rajković, J., Rupnik, M.S., Friedrich, B., Čolić, M.: Size-dependent effects of gold nanoparticles uptake on maturation and antitumor functions of human dendritic cells in vitro. *PLoS One.* **9**, 1–13 (2014)
11. Fifis, T., Gamvrellis, A., Crimeen-Irwin, B., Pietersz, G.A., Li, J., Mottram, P.L., McKenzie, I.F., Plebanski, M.: Size-dependent immunogenicity: therapeutic and protective properties of nano-vaccines against tumors. *J. Immunol.* **173**, 3148–3154 (2004)
12. Mottram, P.L., Leong, D., Crimeen-Irwin, B., Gloster, S., Xiang, S.D., Meanger, J., Ghildyal, R., Vardaxis, N., Plebanski, M.: Type 1 and 2 immunity following vaccination is influenced by nanoparticle size: formulation of a model vaccine for respiratory syncytial virus. *Mol. Pharm.* **4**, 73–84 (2007)
13. Scholer, N., Hahn, H., Muller, R.H., Liesenfeld, O.: Effect of lipid matrix and size of solid lipid nanoparticles (SLN) on the viability and cytokine production of macrophages. *Int. J. Pharm.* **231**, 167–176 (2002)
14. Hirn, Semmler-Behnke, M., Schleh, C., Wenk, A., Lipka, J., Schäffler, M., Takenaka, S., Möller, W., Schmid, G., Simon, U., Kreyling, W.G.: Particle size-dependent and surface

- charge-dependent biodistribution of gold nanoparticles after intravenous administration. *Eur. J. Pharm. Biopharm.* **77**, 407–416 (2011)
15. Sonavane, G., Tomoda, K., Makino, K.: Biodistribution of colloidal gold nanoparticles after intravenous administration: effect of particle size. *Colloids Surfaces B Biointerfaces.* **66**, 274–280 (2008)
 16. Manolova, V., Flace, A., Bauer, M., Schwarz, K., Saudan, P., Bachmann, M.F.: Nanoparticles target distinct dendritic cell populations according to their size. *Eur. J. Immunol.* **38**, 1404–1141 (2008)
 17. Liu, Y., Ashton, J.R., Moding, E.J., Yuan, H., Register, K., Choi, J., Whitley, M., Zhao, X., Qi, Y., Ma, Y., Vaidyanathan, G., Zalutsky, M.R., Kirsch, D.G., Badea, C.T., Vo-Dinh, T.: A plasmonic gold Nanostar Theranostic probe for *in vivo* tumor imaging and photothermal therapy. *Theranostics.* **5**(9), 946–960 (2015)
 18. Getts, D.R., Shea, L.D., Miller, S.D., King, N.J.C.: Harnessing nanoparticles for immune modulation. *Trends Immunol.* **36**, 419–427 (2015)
 19. Xie, X., Liao, J., Shao, X., Li, Q., Lin, Y.: The effect of shape on cellular uptake of gold nanoparticles in the forms of stars, rods, and triangles. *Sci. Rep.* **7**, 3827 (2017)
 20. Talamini, L., Violatto, M.B., Cai, Q., Monopoli, M.P., Kantner, K., Krpetic, Z., Perez-potti, A., Cookman, J., Garry, D., Silveira, C.P., Boselli, L., Pelaz, B., Serchi, T., Gutleb, A.C., Feliu, N., Yan, Y., Salmona, M., Parak, W.J., Dawson, K.A., Bigini, P.: Influence of size and shape on the anatomical distribution of endotoxin-free gold nanoparticles. *ACS Nano.* **11**, 5519–5529 (2017)
 21. Yuan, H., Wilson, C.M., Xia, J., Doyle, S.L., Li, S., Fales, A.M., Liu, Y., Ozaki, E., Mulfaul, K., Hanna, G., Palmer, G.M., Wang, L.V., Grant, G.A., Vo-Dinh, T.: Plasmonics-enhanced and optically modulated delivery of gold nanostars into brain tumor. *Nanoscale.* **6**(8), 4078–4082 (2014)
 22. Liu, Y., Carpenter, A.B., Pirozzi, C., Yuan, H., Waitkus, M., Zhou, Z., Hansen, L., Seywald, M., Odion, R., Greer, P.K., Hawk, T., Chin, B.B., Vaidyanathan, G., Zalutsky, M.R., Yan, H., Vo-Dinh, T.: Non-invasive sensitive brain tumor detection using dual-modality bioimaging nanoprobe. *Nanotechnology.* **30**, 27 (2019)
 23. Bartneck, M., Keul, H.A., Singh, S., Czaja, K., Bockstaller, M., Moeller, M., Zwadlow-klarwasser, G.: Rapid uptake of gold Nanorods by primary human blood phagocytes and chemistry. *ACS Nano.* **4**, 3073–3086 (2010)
 24. Xiao, Y., Xu, W., Komohara, Y., Fujiwara, Y., Hirose, H., Futaki, S., Niidome, T.: Effect of surface modifications on cellular uptake of gold Nanorods in Human primary cells and established cell lines. *ACS Omega.* **5**(50), 32744–32752 (2020)
 25. Niikura, K., Matsunaga, T., Suzuki, T., Kobayashi, S., Yamaguchi, H., Orba, Y., Kawaguchi, A., Hasegawa, H., Kajino, K., Ninomiya, T., Ijio, K., Sawa, H.: Gold nanoparticles as a vaccine platform: influence of size and shape on immunological responses *in vitro* and *in vivo*. *ACS Nano.* **7**, 3926–2938 (2013)
 26. Li, Z., Sun, L., Zhang, Y., Dove, A.P., O'Reilly, R.K., Chen, G.: Shape effect of glyco-nanoparticles on macrophage cellular uptake and immune response. *ACS Macro Lett.* **5**(9), 1059–1064 (2016)
 27. Yang, Y., Zhang, J., Xia, F., Zhang, C., Qian, Q., Zhi, X., Yue, C., Sun, R., Cheng, S., Fang, S., Jin, W., Yang, Y., Cui, D., Human, C.I.K.: Cells loaded with au Nanorods as a theranostic platform for targeted photoacoustic imaging and enhanced immunotherapy and photothermal therapy. *Nanoscale Res. Lett.* **11**, 285 (2016)
 28. Schanen, B.C., Karakoti, A.S., Seal, S.D.R.D., Warren, W.L.: Exposure to titanium dioxide nanomaterials provokes inflammation of an *in vitro* human immune construct. *ACS Nano.* **3**, 2523–2532 (2009)
 29. Doshi, N., Mitragotri, S.: Macrophages recognize size and shape of their targets. *PLoS One.* **5**, 1–6 (2010)
 30. Guo, L., Yan, D.D., Yang, D., Li, Y., Wan, X., Zalewski, O., Yan, B., Lu, W.: Combinatorial photothermal and immuno cancer therapy using chitosan-coated hollow sulfide nanoparticles. *ACS Nano.* **8**(6), 5670–5681 (2014)

31. Gregas, M.K., Scaffidi, J.P., Lauly, B., Vo-Dinh, T.: Characterization of nanoprobe uptake in single cells: spatial and temporal tracking via SERS labeling and modulation of surface charge. *Nanomedicine*. **7**, 115–122 (2011)
32. Gregas, M.K., Scaffidi, J.P., Lauly, B., Vo-Dinh, T.: Surface-enhanced Raman scattering detection and tracking of nanoprobes: enhanced uptake and nuclear targeting in single cells. *Appl. Spectrosc.* **64**, 858–866 (2010)
33. Scholer, N., Hahn, H., Muller, R.H., Liesenfeld, O.: Effect of lipid matrix and size of solid lipid nanoparticles (SLN) on the viability and cytokine production of macrophages. *Int. J. Pharm.* **231**, 167–176 (2002)
34. Fifis, T., Gamvrellis, A., Crimeen-Irwin, B., Pietersz, G.A., Li, J., Mottram, P.L., McKenzie, I.F.: Plebanski tumors. *J. Immunol.* **173**, 3148–3154 (2004)
35. Shvedova, A.A., Kisin, E.R., Mercer, R., Murray, A.R., Johnson, V.J., Potapovich, A.I., Tyurina, Y.Y., Gorelik, O., Arepalli, S., Schwegler-Berry, D., et al.: Unusual inflammatory and fibrogenic pulmonary responses to single-walled carbon nanotubes in mice. *Am. J. Physiol. Lung Cell. Mol. Physiol.* **289**, L698–L708 (2005)
36. Vallhov, H., Qin, J., Johansson, S.M., Ahlborg, N., Muhammed, M.A., Scheynius, A., Gabriellson, S.: The importance of an endotoxin-free environment during the production of nanoparticles used in medical applications. *Nano Lett.* **6**, 1682–1686 (2006)
37. Zolnik, B.S., Gonzalez-Fernandez, A., Sadrieh, N., Dobrovolskaia, M.A.: Nanoparticles and the immune system. *Endocrinology*. **151**, 458–465 (2010)
38. Tan, Y., Li, S., Pitt, B.R., Huang, L.: The inhibitory role of CpG immunostimulatory motifs in cationic lipid vector-mediated transgene expression in vivo. *Hum. Gene Ther.* **10**, 2153–2161 (1999)
39. Carlson, C., Hussain, S.M., Schrand, A.M., Braydich-Stolle, L.K., Hess, K.L., Jones, R.L., Schlager, J.J.: Unique cellular interaction of silver nanoparticles: size-dependent generation of reactive oxygen species. *J. Phys. Chem. B*. **12**, 13608–13619 (2008)
40. Sheen, M.R., Lizotte, P.H., Toraya-Brown, S., Fiering, S.: Stimulating antitumor immunity with nanoparticles. *Wiley Interdiscip. Rev. Nanomed. Nanobiotechnol.* **6**(5), 496–505 (2014)
41. Dunn, G.P., Old, L.J., Schreiber, R.D.: The immunobiology of cancer immunosurveillance and immunoeediting. *Immunity*. **21**, 137–148 (2004)
42. Ullrich, E., Koch, J., Cerwenka, A., Steinle, A.: New prospects on the NKG2D/NKG2DL system for oncology. *Onco. Targets. Ther.* **2**, e26097 (2013)
43. Phuengkham, H., Ren, L., Shin, I.W., Lim, Y.T.: Nanoengineered immune niches for reprogramming the immunosuppressive tumor microenvironment and enhancing cancer immunotherapy. *Adv. Mater.* **31**(34), e1803322 (2019)
44. Song, C., Phuengkham, H., Kim, Y.S., Dinh, V.V., Lee, I., Shin, I.W., Shin, H.S., Jin, S.M., Um, S.H., Lee, H., Hong, K.S., Jin, S.M., Lee, E., Kang, T.H., Park, Y.M., Lim, Y.T.: Syringeable immunotherapeutic nanogel reshapes tumor microenvironment and prevents tumor metastasis and recurrence, nature. *Communications*. **10**, 3745 (2019)
45. Roth, A., Rohrbach, F., Weth, R., Frisch, B., Schubert, F., Wels, W.S.: Induction of effective and antigen-specific antitumor immunity by a liposomal ErbB2/HER2 peptide-based vaccination construct. *Br. J. Cancer*. **92**, 1421–1429 (2005)
46. Un, K., Kawakami, S., Suzuki, R., Maruyama, K., Yamashita, F., Hashida, M.: Suppression of melanoma growth and metastasis by DNA vaccination using an ultrasound-responsive and mannose-modified gene carrier. *Mol. Pharm.* **8**, 543–554 (2011)
47. Wegmann, F., Gartlan, K.H., Harandi, A.M., Brinckmann, S.A., Coccia, M., Hillson, W.R., Kok, W.L., Cole, S., Ho, L.P., Lambe, T.: Polyethyleneimine is a potent mucosal adjuvant for viral glycoprotein antigens. *Nat. Biotechnol.* **30**, 883–888 (2012)
48. Ma, W., Chen, M., Kaushal, S., McElroy, M., Zhang, Y., Ozkan, C., Bouvet, M., Kruse, C., Grotjahn, D., Ichim, T., Mineev, B.: PLGA nanoparticle-mediated delivery of tumor antigenic peptides elicits effective immune responses. *Int. J. Nanomedicine*. **7**, 1475–1487 (2012)
49. Toraya-Brown, S., Sheen, M.R., Baird, J.R., Barry, S., Demidenko, E., Turk, M.J., Hoopes, P.J., Conejo-Garcia, J.R., Fiering, S.: Phagocytes mediate targeting of iron oxide nanoparticles to tumors for cancer therapy. *Integr. Biol. (Camb)*. **5**, 159–171 (2012)

50. Nie, L., Cai, S.Y., Shao, J.Z., Chen, J.: Toll-like receptors, associated biological roles, and signaling networks in non-mammals. *Front. Immunol.* **9**, 1523 (2018)
51. Beck, B., Dorfel, D., Lichtenegger, F.S., Geiger, C., Lindner, L., Merk, M., Schendel, D.J., Subklewe, M.: Effects of TLR agonists on maturation and function of 3-day dendritic cells from AML patients in complete remission. *J. Transl. Med.* **9**, 151 (2011)
52. Sheno, M.M., Shah, N.B., Griffin, R.J., Vercellotti, G.M., Bischof, J.C.: Nanoparticle pre-conditioning for enhanced thermal therapies in cancer. *Nanomedicine (Lond.)*. **6**(3), 545–563 (2011)
53. Cubillos-Ruiz, J.R., Engle, X., Scarlett, U.K., Martinez, D., Barber, A., Elgueta, R., Wang, L., Nesbeth, Y., Durant, Y., Gewirtz, A.T., et al.: Polyethylenimine-based siRNA nanocomplexes reprogram tumor-associated dendritic cells via TLR5 to elicit therapeutic antitumor immunity. *J. Clin. Invest.* **119**, 2231–2244 (2009)
54. Niikura, K., Matsunaga, T., Suzuki, T., SKobayashi, S., HYamaguchi, H., Orba, Y., AKawaguchi, A., Hasegawa, H., Kajino, K., Ninomiya, T., Ijiro, K., HSawa, H.: Gold nanoparticles as a vaccine platform: influence of size and shape on immunological responses in vitro and in vivo. *ACS Nano*. **7**(5), 3926–3938 (2013)
55. Roldão, A., Mellado, M.C.M., Castilho, L.R., Carrondo, M.J.T., Alves, P.M.: Virus-like particles in vaccine development. *Expert Rev. Vaccines*. **9**(10), 1149–1176 (2010)
56. Fusciello, M., Fontana, F., Tähtinen, S., Capasso, C., Feola, S., Martins, B., Chiaro, J., Peltonen, K., Ylösmäki, L., Ylösmäki, E., Hamdan, F., Kari, O.K., Ndika, J., Alenius, H., Urtti, A., Hirvonen, J.T., Santos, H.A., Cerullo, V.: Artificially cloaked viral nanovaccine for cancer immunotherapy. *Nat. Commun.* **10**, 5747 (2019)
57. Liu, Q., Wang, C., Zheng, Y., Zhao, Y., Wang, Y., Hao, J., Zhao, X., Yi, K., Shi, L., Kang, C., Liu, Y.: Virus-like nanoparticle as a co-delivery system to enhance efficacy of CRISPR/Cas9-based cancer immunotherapy. *Biomaterials*. **258**, 120275 (2020)
58. Hildebrandt, B., Wust, P., Ahlers, O., et al.: The cellular and molecular basis of hyperthermia. *Crit. Rev. Oncol. Hematol.* **43**(1), 33–56 (2002)
59. Frey, B., Weiss, E.M., Rubner, Y., et al.: Old and new facts about hyperthermia-induced modulations of the immune system. *Int. J. Hyperth.* **28**(6), 528–542 (2012)
60. Schildkopf, P., Ott, O.J., Frey, B., et al.: Biological rationales and clinical applications of temperature controlled hyperthermia—implications for multimodal cancer treatments. *Curr. Med. Chem.* **17**(27), 3045–3057 (2010)
61. Wust, P., Hildebrandt, B., Sreenivasa, G., et al.: Hyperthermia in combined treatment of cancer. *Lancet Oncol.* **3**(8), 487–497 (2002)
62. Ostberg, J.R., Dayanc, B.E., Yuan, M., Oflazoglu, E., Repasky, E.A.: Enhancement of natural killer (NK) cell cytotoxicity by fever-range thermal stress is dependent on NKG2D function and is associated with plasma membrane NKG2D clustering and increased expression of MICA on target cells. *J. Leukoc. Biol.* **82**, 1322–1331 (2007)
63. Todryk, S.M., Melcher, A.A., Dalglish, A.G., Vile, R.G.: Heat shock proteins refine the danger theory. *Immunology*. **99**, 334–337 (2000)
64. Asea, A., Rehli, M., Kablingu, E., Boch, J.A., Bare, O., Auron, P.E., Stevenson, M.A., Calderwood, S.K.: Novel signal transduction pathway utilized by extracellular HSP70: role of toll-like receptor (TLR) 2 and TLR4. *J. Biol. Chem.* **277**, 15028–15034 (2002)
65. Vabulas, R.M., Ahmad-Nejad, P., Ghose, S., Kirschning, C.J., Issels, R.D., Wagner, H.: HSP70 as endogenous stimulus of the toll/interleukin-1 receptor signal pathway. *J. Biol. Chem.* **277**, 15107–15112 (2002)
66. Suzue, K., Zhou, X., Eisen, H.N., Young, R.A.: Heat shock fusion proteins as vehicles for antigen delivery into the major histocompatibility complex class I presentation pathway. *Proc. Natl. Acad. Sci. U. S. A.* **94**, 13146–13151 (1997)
67. Moroi, Y., Mayhew, M., Trcka, J., Hoe, M.H., Takechi, Y., Hartl, F.U., Rothman, J.E., Houghton, A.N.: Induction of cellular immunity by immunization with novel hybrid peptides complexed to heat shock protein 70. *Proc. Natl. Acad. Sci. U. S. A.* **97**, 3485–3490 (2000)
68. Noessner, E., Gastpar, R., Milani, V., Brandl, A., Hutzler, P.J., Kupfner, M.C., Roos, M., Kremmer, E., Asea, A., Calderwood, S.K., Issels, R.D.: Tumor-derived heat shock protein 70

- peptide complexes are cross-presented by human dendritic cells. *J. Immunol.* **169**, 5424–5432 (2002)
69. Day, E.S., Morton, J.G., West, J.L.: Nanoparticles for thermal cancer therapy. *J. Biomech. Eng.* **131**(7), 074001 (2009)
 70. Hirsch, L.R., Stafford, R.J., Bankson, J.A., Sershen, S.R., Rivera, B., Price, R.E., et al.: Nanoshell-mediated near-infrared thermal therapy of tumors under magnetic resonance guidance. *PNAS.* **100**, 13549–13554 (2003)
 71. Huang, X., Jain, P.K., El-Sayed, I.H., El-Sayed, M.A.: Plasmonic photothermal therapy (PPTT) using gold nanoparticles. *Lasers Med. Sci.* **23**(3), 217–228 (2008)
 72. Yuan, H., Khoury, C.G., Wilson, C.M., Grant, G.A., Bennett, A.J., Vo-Dinh, T.: In vivo particle tracking and photothermal ablation using plasmon resonant gold Nanostars. *Nanomedicine.* **8**, 1255–1363 (2012)
 73. Yuan, H., Fales, A.M., Vo-Dinh, T.: TAT peptide-functionalized gold Nanostars: enhanced intracellular delivery and efficient NIR photothermal therapy using ultralow irradiance. *J. Am. Chem. Soc.* **134**, 11358–11361 (2012)
 74. Yuan, H., Khoury, C.G., Hwang, H., Wilson, C.M., Grant, G.A., Vo-Dinh, T.: Gold nanostars: surfactant-free synthesis, 3D modelling, and two-photon photoluminescence imaging. *Nanotechnology.* **23**(7), 075102 (2012)
 75. Vo-Dinh, T., Fales, A.M., Griffin, G.D., Khoury, C.G., Liu, Y., Ngo, H., Norton, S.J., Register, J.K., Wang, H.N., Yuan, H.: Plasmonic nanoprobe: from chemical sensing to medical diagnostics and therapy. *Nanoscale.* **5**, 10127–10140 (2013)
 76. Vo-Dinh, T., Liu, Y., Crawford, B.M., Wang, H.N., Yuan, H., Register, J.K., Khoury, C.G.: Shining gold nanostars: from cancer diagnostics to photothermal treatment and immunotherapy. *J. Immunological Sci.* **2**(1), 1–8 (2018)
 77. Gannon, C.J., Cherukuri, P., Yakobson, B.I., Cognet, L., Kanzius, J.S., Kittrell, C., Weisman, R.B., Pasquali, M., Schmidt, H.K., Smalley, R.E., Curley, S.A.: Carbon nanotube-enhanced thermal destruction of cancer cells in a noninvasive radiofrequency field. *Cancer.* **110**, 2654–2665 (2007).
 78. Toraya-Brown, S., Sheen, M.R., Baird, J.R., Barry, S., Demidenko, E., Tur, M.J.P.J., Conejo-Garcia, J.R., Fiering, S.: Phagocytes mediate targeting of iron oxide nanoparticles to tumors for cancer therapy. *Integr. Biol. (Camb).* **5**(1), 159–171 (2013)
 79. Inman, B.A., Sebo, T.J., Frigola, X., et al.: PD-L1 (B7-H1) expression by urothelial carcinoma of the bladder and BCG-induced granulomata: associations with localized stage progression. *Cancer.* **09**(8), 1499–1505 (2007)
 80. Bellmunt, J., Mullane, S.A., Werner, L., et al.: Association of PD-L1 expression on tumor-infiltrating mononuclear cells and overall survival in patients with urothelial carcinoma. *Ann. Oncol.* **26**(4), 812–817 (2015)
 81. Xylinas, E., Robinson, B.D., Kluth, L.A., et al.: Association of T-cell co-regulatory protein expression with clinical outcomes following radical cystectomy for urothelial carcinoma of the bladder. *Eur. J. Surg. Oncol.* **40**(1), 121–127 (2014)
 82. Boorjian, S.A., Sheinin, Y., Crispen, P.L., et al.: T-cell coregulatory molecule expression in urothelial cell carcinoma: clinicopathologic correlations and association with survival. *Clin. Cancer Res.* **14**(15), 4800–4808 (2008)
 83. Inman, B.A., Frigola, X., Dong, H., Kwon, E.D.: Costimulation, coinhibition and cancer. *Curr. Cancer Drug Targets.* **7**(1), 15–30 (2007)
 84. Dong, H., Strome, S.E., Salomao, D.R., et al.: Tumor-associated B7-H1 promotes T-cell apoptosis: a potential mechanism of immune evasion. *Nat. Med.* **8**(8), 793–800 (2002)
 85. Webster, W.S., Thompson, R.H., Harris, K.J., et al.: Targeting molecular and cellular inhibitory mechanisms for improvement of antitumor memory responses reactivated by tumor cell vaccine. *J. Immunol.* **179**(5), 2860–2869 (2007)
 86. Rosenberg, J.E., Hoffman-Censits, J., Powles, T., et al.: Atezolizumab in patients with locally advanced and metastatic urothelial carcinoma who have progressed following treatment with platinum-based chemotherapy: a single-arm, multicentre, phase 2 trial. *Lancet.* **387**(10031), 1909–1920 (2016)

87. Powles, T., Eder, J.P., Fine, G.D., et al.: MPDL3280A (anti-PD-L1) treatment leads to clinical activity in metastatic bladder cancer. *Nature*. **515**(7528), 558–562 (2014)
88. Liu, Y., Maccarini, P., Palmer, G.M., Etienne, W., Zhao, Y., Lee, C., Ma, X., Inman, B.A., Vo-Dinh, T.: Synergistic Immuno Photothermal Nanotherapy (SYMPHONY) for the Treatment of Unresectable and Metastatic Cancers. *Scientific Reports*. **7**, 8606 (2017)
89. Liu, Y., Chongsathidkiet, P., Crawford, B.M., Odion, R., Dechant, C.A., Kemeny, H.R., Cui, X., Maccarini, P.F., Lascola, C.D., Fecci, P., Vo-Dinh, T.: Plasmonic gold nanostar-mediated photothermal immunotherapy for brain tumor ablation and immunologic memory. *Immunotherapy*. **11**, 1293–1302 (2019)
90. Vo-Dinh, T., Inman, B.A.: What potential does plasmonics-amplified synergistic immuno photothermal nanotherapy have for treatment of cancer. *Nanomedicine*. **13**(2), 139–144 (2018)
91. Garg, A.D., Nowis, D., Golab, J., Vandenabeele, P., Krysko, D.V., Agostinis, P.: Immunogenic cell death, DAMPs and anticancer therapeutics: an emerging amalgamation. *Biochim. Biophys. Acta*. **1805**(1), 53–71 (2010)
92. Chen, Q., Xu, L., Liang, C., Wang, C., Peng, R., Liu, Z.: Photothermal therapy with immune-adjuvant nanoparticles together with checkpoint blockade for effective cancer immunotherapy. *Nat. Commun.* **7**, 13193 (2016)

Cancer Immunotherapy Strategies: Basic Principles



Pakawat Chongsathidkiet, Jessica Waibl Polania, Selena J. Lorrey, Matthew M. Grabowski, Eric W. Sankey, Daniel S. Wilkinson, and Peter E. Fecci

1 Introduction and the Current State-of-the-Art Strategies for Immunotherapy

Cancer immunotherapy has advanced significantly over the last decade, showing efficacy in many cancer types. Several FDA-approved immunotherapeutics, such as cancer vaccines and chimeric antigen receptor (CAR) T cells, are still gaining clinical momentum. Others, such as immune checkpoint blockade, have already become standard of care in certain tumor types, such as metastatic melanoma [1]. In this chapter, we summarize the most recent therapeutic advances within cancer immunotherapy and introduce the roles that nanotechnology might play in

P. Chongsathidkiet · M. M. Grabowski · E. W. Sankey · D. S. Wilkinson
Department of Neurosurgery, Duke University School of Medicine, Durham, NC, USA

Brain Tumor Immunotherapy Program, Duke University Medical Center, Durham, NC, USA

J. Waibl Polania

Brain Tumor Immunotherapy Program, Duke University Medical Center, Durham, NC, USA

Department of Pathology, Duke University Graduate School, Durham, NC, USA

S. J. Lorrey

Brain Tumor Immunotherapy Program, Duke University Medical Center, Durham, NC, USA

Department of Immunology, Duke University Graduate School, Durham, NC, USA

P. E. Fecci (✉)

Department of Neurosurgery, Duke University School of Medicine, Durham, NC, USA

Brain Tumor Immunotherapy Program, Duke University Medical Center, Durham, NC, USA

Department of Pathology, Duke University Graduate School, Durham, NC, USA

Department of Immunology, Duke University Graduate School, Durham, NC, USA

e-mail: peter.fecci@duke.edu

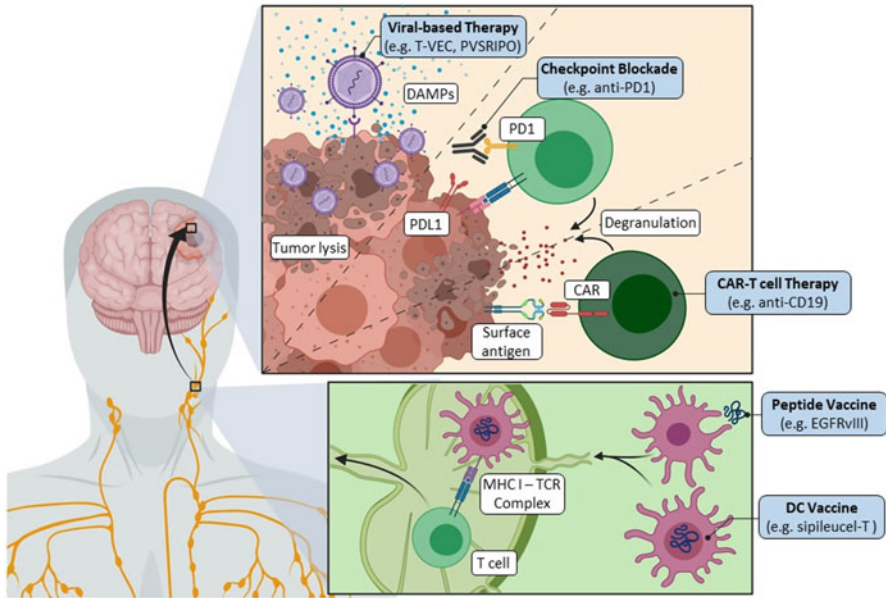


Fig. 1 Current Strategies for Cancer Immunotherapy. Cancer immunotherapy employs various techniques to stimulate a robust immune response either systemically or at the site of the tumor. Areas under investigation include vaccine-based strategies such as dendritic cell (DC) vaccines and peptide/antigenic vaccines, adoptive lymphocyte transfer such as CAR T cell therapy, viral-based therapies such as oncolytic viruses, and immune checkpoint blockade to license effector T-cells. Figure created with Biorender.com

enhancing these treatment modalities. Figure 1 shows an overview of the various immunotherapeutic modalities described in this chapter.

1.1 Cancer Vaccines

Cancer vaccines aim to stimulate patient immunity against tumor cells or tumor cell components. Such stimulation is designed to augment the endogenous immune response, which will have already failed in its cancer surveillance task. The goal of a vaccine (as an active form of immunotherapy) is to elicit and amplify the host's immune response, often by the introduction of foreign antigens or antigen-presenting cells (APCs). Cancer vaccines are typically combined with other adjuvant therapies to strengthen the response and aid in the breaking of tolerance. Among the most common forms of cancer vaccines are dendritic cell (DC) and peptide vaccines. Together, these strategies aim to redirect, reinvigorate and expand tumor and antigen-specific adaptive immune responses, specifically cytolytic T cell responses. The ultimate goal is T cell-mediated tumor cell lysis.

1.1.1 DC Vaccines

DCs are professional APCs responsible for antigen uptake, processing, and presentation for subsequent priming of naïve T cells [2]. During infection, foreign antigens encountered in the context of various danger signals activate DCs and enable their migration to lymph nodes for interaction with T cells. In contrast, tumors often consist predominantly of mis-expressed self-antigens and do not engender the same degree of danger. Tumors, then, frequently do not elicit the same robust inflammatory state as an infection [3]. Immunotherapy is designed to address this lack of immunogenicity and permit mounting of a sufficient adaptive immune response against cancer. In the case of DC vaccines, DCs are dramatically expanded, loaded with tumor antigen, and activated *ex vivo*. Activation induces morphological changes in DCs, which enhance their ability to activate naïve T cells, including upregulation of MHC I and II, as well as, co-stimulatory molecules on their cell surface [4]. After successful activation, and antigen-loading, DCs are administered to the patient. DC vaccines are associated with little chance of severe treatment-related adverse effects, in contrast to immune checkpoint blockade and other immunotherapies which can be associated with off-target autoimmune effects [5].

Early clinical trials investigating DC vaccines in prostate cancer [6, 7], renal cell carcinoma [8, 9], non-small cell lung carcinoma [10], and colon cancer [11] showed some promising immunologically-relevant responses, prompting further study. Before eventual FDA approval of the first cell-based cancer vaccine, optimization of several steps in the preparation process was required. In early trial, DCs were pulsed with tumor-lysate or specific peptide antigens. Later trials aimed to optimize antigen loading, methods of activation, and routes of administration. The first FDA approved DC vaccine was sipileucel-T in 2010 for treatment of castrate-resistant prostate cancer. Approval was second to three pivotal phase 3 clinical trials [12]. The largest of these three trials, called Immunotherapy for Prostate Adenocarcinoma Treatment (IMPACT) was the largest, enrolling 512 men. In all three trials, patients were randomized to placebo or vaccine groups, and each time, the vaccine treatment group demonstrated increased overall survival. Importantly, following normalization for baseline prognostic factors, chemotherapy use, and non-prostate cancer-related deaths, the treatment effect remained significant. Leukapheresis was used to harvest autologous peripheral blood mononuclear cells (PBMCs) which were subsequently activated using granulocyte-macrophage colony-stimulating factor (GM-CSF) and loaded with prostate cancer antigen. Three doses of vaccine were given over the course of 2 weeks intravenously.

1.1.2 Peptide/Antigenic Vaccines

In line with DC vaccines, peptide vaccines focus on endogenous T cell recognition of tumor-specific or -associated antigens, derived from mutations or overexpression of gene products, respectively (e.g. EGFRvIII in malignant glioma [13]). Tumor-

specific antigens (TSA) are found only in tumor cells, not healthy tissue, whereas tumor-associated antigens (TAA) are upregulated on tumor cells but also found in lower abundance in healthy tissue. The goal of infusing these peptide antigens into patients in conjunction with an adjuvant is to elicit their uptake by APCs at the site of injection. APC subsequently migrate to lymph nodes and present the antigen(s) to T cells (reviewed in [14]). Peptide sequences can often be developed through *in silico* analysis of immunogenic antigens. Sequences are chosen that are likely to bind major histocompatibility complex (MHC) I and/or MHC II to stimulate a cytotoxic T cell-mediated response and CD4⁺ T cell help, respectively [15]. The benefits of this form of immunotherapy lie in the ability to select both surface and intracellular antigens, as well as in its cost-effectiveness. Using specific peptide epitopes relies on the assumption that there is a T cell receptor (TCR) within the endogenous repertoire that binds with high enough affinity to generate a response. In some cases, however, focusing on specific peptide epitopes versus whole protein can limit the breadth of response and allow for immune escape. An example of this is found in the reports of Sampson et al. regarding their phase II experience with peptide vaccination for malignant glioma, during which 82% of recurrent tumors proved to be antigen-loss variants [16]. This is a depiction of Schreiber's immunoeediting process, whereby the immune system controls tumor outgrowth while simultaneously shaping tumor immunogenicity [17, 18].

1.2 Adoptive Lymphocyte Transfer

Adoptive lymphocyte transfer (ALT) has also emerged as a common form of immunotherapy. ALT utilizes a patient's own T cells, manipulated and expanded *ex vivo*, to mediate anti-tumor activity [19]. ALT involves the isolation of T cells from cancer patients for *ex vivo* expansion following identification of anti-tumor clones. Alternatively, T cells can be expanded against unidentified tumor antigens isolated from tumor cells. T cells are then infused back into the patient, often accompanied by cytokines and/or adjuvant, to enhance their proliferation and survival [20]. This strategy overcomes the limitations of cancer vaccines that require *in vivo* expansion of tumor-specific T cells in patients who are commonly immunocompromised.

ALT has enjoyed some marked successes as an approach. Dudley et al. observed tumor regression in patients with metastatic melanoma following adoptive transfer of *in vitro* activated T cells, sparking excitement for treatment of advanced stage cancer patients. Inclusion of host lymphodepletion prior to ALT has allowed greater efficacy with this treatment and was first described in 1988 [21]. Although ALT proved successful in melanoma patients with high levels of tumor-infiltrating lymphocytes (TILs), many cancers do not exhibit the same wealth of TILs that might predict a therapeutic response. The number of TILs frequently correlates with tumor mutational burden (TMB) and tumor immunogenicity. Tumor immune responses typically arise from recognition of tumor-specific neo-antigens that reflect nonsynonymous somatic mutations in cancer genomes [22–24]. Cancers that exhibit

high neo-antigen burdens include melanoma [25] and non-small cell lung carcinoma (NSCLC) [26]. Both have high numbers of mutations, likely owing to carcinogen-provoked origins [27]. A higher TMB increases the probability of generating immunogenic neo-antigens, which may in turn permit robust T cell responses [28, 29]. While ALT has indeed offered some promise as an immunotherapeutic modality, the labor-intensive nature of T cell isolation and expansion make ALT difficult to scale and use across cancers. Still, ALT has provided a foundation for T cell-based therapies, as well as encouragement for the continued development of immunotherapies.

1.2.1 CAR T Cell Therapy

More recently, chimeric antigen receptor (CAR) T cell therapy, an alternative type of ALT, has gained increasing levels of attention with its success in the treatment of hematological malignancies [30, 31]. This strategy genetically redirects T cells to target tumor surface antigens, rather than those presented in the context of MHC. A CAR is composed of the single chain variable fragment (scFv) of an antibody, which sits on the T cell surface, combined with the intracellular TCR CD3z signaling chain with or without co-stimulatory signaling domains [32]. These engineered receptors combine the protein recognition capacities of an antibody with the activating signaling effects of a TCR [33, 34]. The CAR T cell approach has a number of theoretical advantages: the scFv has much higher target affinity than a TCR, can recognize intact proteins unlike endogenous T cells (which obviates the need for antigen processing and presentation by APCs), and functions independent of MHC I (limiting tumor escape via downregulation of MHC I by tumor cells).

Despite these advantages, initial clinical studies of CAR T cell therapy in solid tumors such as metastatic ovarian and renal cell cancer were disappointing. In these phase I studies, CAR T cells failed to accumulate at the tumor site despite high initial concentrations in the circulation. Likewise, they failed to persist long-term, becoming undetectable after 1 month [35, 36]. These limitations were addressed with the generation of second and third generation CARs, which added a co-stimulatory signaling domain to the intracellular component of the CAR. Second generation CARs employed co-stimulatory domains, the most common of which were CD28 or 4-1BB, which enabled prolonged persistence of CAR T cells *in vivo* by mimicking physiologic co-stimulation [37, 38]. Clinical trials of 4-1BB/CD3z CAR T cells showed unprecedented on-target efficacy in patients with chronic lymphocytic leukemia (CLL) [39, 40]. Third generation CARs encompassing two co-stimulatory molecules have also been designed. Stringent comparisons of second and third generation CARs have not been made but should provide better insight into the ideal CAR constitution.

To date, the greatest success in CAR T therapy has been seen in the treatment of hematologic B cell malignancies expressing the CD19 target. Expressed on B cell malignancies as well as on healthy B cells, CD19 is absent on hematopoietic stem cells and early B precursor cells, limiting on-target toxic effects to B cell aplasia,

which can be supported with intravenous immunoglobulin replacement. While the CD19-CAR constructs used in the respective trials differ in the scFvs against CD19, the type of costimulatory domain(s) used, as well as the use of lentiviral versus γ -retroviral transduction regimens, the therapeutic promise of CD19-CAR T cells has been demonstrated by several independent groups [41, 42]. Porter et al. reported on three patients with CLL treated with chemotherapy followed by split infusion of a CD19-41BB-zCAR [40], whereby two patients achieved a complete and one patient a partial remission. Whereas *in vivo* persistence of CAR T cells beyond a few weeks was problematic in many of the early CAR T cell trials, this group demonstrated not only persistence of CAR T cells in the blood and bone marrow exceeding 6 months, but also *in vivo* expansion of infused CAR T cells by >3 log steps.

Despite the tremendous success of CAR T therapy in B cell leukemias and lymphomas, efficacy has not been observed in other cancers, especially solid tumors. Perhaps the most prominent obstacle in solid tumors is marked intratumoral heterogeneity, which can limit the impact of targeting one or a few antigens and lead to subsequent tumor immune escape. Unlike B cell malignancies, which ubiquitously express CD19, solid tumors seldom demonstrate clonal expansion. GBM is a notorious example, and researchers have identified different GBM subtypes co-existing within the same tumor [43, 44]. CAR targeting of a single antigen will provide a selective advantage for non-expressing clone outgrowth [45].

Additionally, CAR T cells are equally susceptible to the immunosuppressive microenvironment as their non-engineered counterparts. Treg- and TGF-B-induced immunosuppression has been well documented in CAR T cells, although this issue has been partially resolved with the development of second and third generation constructs [46, 47]. Combining multiple immunotherapeutic strategies has also emerged for enhanced CAR T cell therapeutic efficacy. Development of a bi-specific T cell antibody (BiTE)-secreting CAR T has recently shown pre-clinical promise [48], as well as combining immune checkpoint blockade strategies [49]. Significant progress has been made in overcoming obstacles to CAR T cell therapy across cancer, continued efforts and new technologies will be essential to reach this goal.

1.3 Viral-Based Strategies for Immunotherapy

Oncolytic viruses (OVs) have been used as a cancer therapeutic against many different types of tumors. The mechanism of action for oncolytic viruses is two-fold: first, these viruses can selectively infect and lyse tumor cells upon replication; second, infection or subsequent lysis can initiate an endogenous immune response. OVs, as a whole, are quite malleable and can be genetically manipulated to reduce pathogenicity of the virus, redirect the virus to have a tropism for cancer cells, or to arm the virus with additional therapeutics. In the latter case, OVs can be viewed as a type of nanotherapeutic, selectively delivering a treatment to the tumor site.

Tumor cells infected with an oncolytic virus can stimulate the immune system in a number of ways, including production of reactive oxygen species (ROS),

release of anti-viral cytokines, and release of Type I interferons. Additionally, lysed tumor cells can further stimulate APCs in the tumor microenvironment (TME) to take up tumor antigen (important for subsequent presentation to T cells in the draining lymph node) by releasing pathogen-associated molecular patterns (PAMPs) and damage-associated molecular patterns (DAMPs) that bind and stimulate APCs through toll-like receptors (TLRs) [50, 51].

Although there are numerous OV's in clinical trials, the first, and to-date the only, OV to receive FDA approval is *Talimogene Laherparepvec* (T-VEC) for the treatment of advanced melanoma. This OV is a version of the herpes simplex virus (HSV) that has been genetically modified to attenuate neurovirulence and enhance immunogenicity through the insertion of genes encoding GM-CSF. Pre-clinical work showed that this engineered version of the HSV selectively replicated in tumor cells. The efficacy of this OV was attributed to decreased levels of suppressor cells (including regulatory T cells [Tregs] and myeloid-derived suppressor cells [MDSCs]) in the TME, as well as an increase in tumor-specific CD8⁺ effector T cells [52].

OV therapy has also enjoyed some success in classically difficult-to-treat tumors such as glioblastoma (GBM). In the context of GBM, an extension of survival is frequently considered a success. PVSRIPO is a recombinant, nonpathogenic poliovirus chimera that selectively infects cells through the poliovirus receptor (CD155), which is upregulated on GBM cells. In a clinical trial of patients with recurrent GBM, the overall survival rate of PVSRIPO-treated patients was higher at both 24 and 36 months post-treatment, when compared to historical controls [53].

1.4 Immune Checkpoint Blockade

Immune checkpoint blockade has garnered attention for recent successes and has FDA-approval in numerous cancer types. The overall goal of immune checkpoint therapy is to overcome tumor-mediated T cell dysfunction, and permit / perpetuate T cell activation and effector function. 'Immune checkpoints' are co-inhibitory molecules located on the T cell surface that, along with co-stimulatory molecules like CD28, function to regulate T cell activation. It is the balance of these two types of molecules that guides a sufficient T cell response to a given pathogen. Without the presence of co-inhibitory molecules, a sustained T cell response in a setting such as infection could result in tissue damage and autoimmunity. However, on the other hand, disproportionate co-inhibitory signals can result in an inadequate T cell response. Within tumors, the balance frequently favors co-inhibition. Tumor cells and APCs within the TME often express co-inhibitory ligands that bind co-inhibitory immune checkpoints on T-cells, leading to suppression of T cell activity. As T cells within the TME are frequently exhausted, they characteristically express high levels of checkpoint molecules on their surface, compounding the problem [54].

The two most well recognized co-inhibitory checkpoints are programmed cell death protein 1 (PD-1) and cytotoxic T lymphocyte-associated antigen 4 (CTLA-4). The 2018 Nobel Prize was awarded to Tasuku Honjo and James Allison for discovering and harnessing the therapeutic potential of antibodies targeting PD-1 and CTLA-4, respectively. Checkpoint blockade therapy refers to a group of monoclonal antibodies that bind the relevant checkpoint molecule on T cells and block binding of their cognate ligand on tumor cells or APCs. CTLA-4 binds B7 (CD80/CD86) on APCs with higher affinity than CD28 (its competing co-stimulatory molecule) and can lead to T cell tolerance [55]. PD-1 binds its cognate ligands PD-L1 or PD-L2 on APCs or tumor cells, resulting in suppressed TCR signaling [56].

There are now several FDA-approved immune checkpoint blockade therapies, including ipilimumab, nivolumab and pembrolizumab. Ipilimumab targets CTLA-4, while the latter therapies target PD-1. Ipilimumab was the first FDA-approved checkpoint blockade therapy, specifically for use in patients with metastatic melanoma [57]. Nivolumab and pembrolizumab have been FDA-approved for metastatic melanoma, NSCLC, head and neck cancers, and Hodgkin's Lymphoma, among other tumor types. Checkpoint blockade therapies also can target the relevant ligands, such as PD-L1. Anti-PD-L1 therapies that have been FDA approved include atezolizumab, avelumab and durvalumab [58].

2 Challenges of Immunotherapy: Limitations of Access and Immune Suppression

As mentioned above, immunotherapy can take many forms, from monoclonal antibodies used in checkpoint blockade therapy, to oncolytic viruses, adoptive cell transfer and vaccine-based therapies. Although mechanistically independent, the common goal of these therapies is to initiate an endogenous immune response and make tumor cells recognizable to the immune system. In order for immunotherapy to be effective against a given tumor, there are two main requirements: (1) T cells must be able to infiltrate and recognize the tumor, and (2) T cells must effectively function within the tumor microenvironment. Factors contributing to or limiting T cell tumor access and function are addressed below:

2.1 Immune Access

Many immunotherapies work to activate T cell effector function against a tumor. If immune cells, specifically effector T cells, cannot infiltrate a tumor, however, their successful activation becomes moot. Different types of cancers exhibit varying degrees of immune infiltration [59]. As previously noted, for instance, melanoma

is a particularly “hot” tumor, and is often heavily infiltrated by T cells, facilitating immunotherapeutic responses. On the other hand, GBM is one example of a “cold” tumor, and is often relatively devoid of T cell infiltrates. Those T cells that do successfully arrive at tumor are likewise subject to GBM-imposed immunosuppression and are largely dysfunctional [60]. One means for bypassing limits to tumor immune access is to simply inject therapies directly into the tumor itself, or a resection cavity. An example is the FDA-approved melanoma treatment, T-VEC, which is injected directly into advanced lesions [61].

2.2 Immune Suppression

The tumor microenvironment of many cancers can often be markedly immunosuppressive, inhibiting the effector function of those immune cells that are able to infiltrate the tumor. T cells, for instance, often become exhausted or otherwise dysfunctional upon tumor infiltration [62]. The source of such suppression can be the tumor itself or components of the TME, the latter of which can contribute suppressive myeloid cells or Tregs.

Tumors may directly inhibit or thwart immune responses via expression of inhibitory ligands and/or soluble inhibitory cytokines, or by limiting their own antigen presentation. Most notably, tumors can express PD-L1 and PD-L2, which can bind PD-1 on T-cells or other immune cells to inhibit activation and suppress effector function. Tumor-elaborated immunosuppressive cytokines can include TGF β , which is upregulated in the serum of many cancer patients including those with glioblastoma, lung, breast, gastric and ovarian cancers [63, 64]. TGF β is a potent inhibitor of IFN γ secretion and stimulates counterproductive Th-17 and Treg cells [65]. Tumor cells can also downregulate MHC I on their surface and may have non-functional or impaired antigen processing machinery, such that proper antigen presentation is impossible [65]. Either of these scenarios effectively hide tumor antigens and cells from T cells, evading their detection.

As noted, the TME also often serves to restrict anti-tumor immunity in a variety of cancers. Myeloid cells are a large constituent of the TME in many cancers and include MDSCs, monocyte-derived macrophages, DCs, and granulocyte infiltrates. These myeloid cells often remain immature within the TME, limiting their capacity to generate effective immunity. Despite their plasticity, these cells are often found biased toward a pro-tumor phenotype within the TME and can promote resistance to therapy [66]. As a result, tumors are prone to secrete cytokines such as granulocyte-colony stimulating factor (G-CSF), GM-CSF and vascular endothelial growth factor (VEGF), which serve to recruit myeloid cell infiltration and function [66]. In nearly all cancers, the TME also contains Tregs that have the ability to suppress both cytotoxic T cells and natural killer (NK) cells. Treg activity likewise begets the generation of further Tregs, thus perpetuating the immunosuppressive state [67].

3 Nanotechnologies to Enhance Cancer Immunotherapy

Although cancer immunotherapy has achieved significant efficacy, its widespread, successful application in various clinical settings is still hindered by the aforementioned obstacles, deeper discussion of which is beyond the scope of this chapter. Regardless, novel means of strengthening immune responses and/or countering tumors' immune-restrictive mechanisms are needed. Recent advances to nanotechnologies may proffer new and synergistic strategies for improving immunotherapeutic approaches. For the remainder of this chapter, we will explore how various nanotechnologies may be able to augment and potentiate responses to cancer immunotherapy.

3.1 Nanotechnologies to Improve ALT

As mentioned previously, adoptive lymphocyte transfer (ALT) has shown success in a number of tumor types, such as melanoma. Limitations, however, have been found in the poor expansion and *in vivo* survival of the transferred cells [20, 68]. To counter this, some have begun to employ nanotechnologies in efforts to enhance T cell stimulation *ex vivo*, improve T cell targeting, increase T cell proliferative potential, reduce immunosuppressive signals, or even deliver genome-editing vehicles to generate CAR-Ts *in vivo*.

The process of *ex vivo* training, expansion, and activation of T cells has been improved by a number nano- or microtechnologies. For example, Fadel et al. were able to create a carbon nanotube-polymer nanoparticle complex that mimics the function of APCs to stimulate T cells, including the secretion of stimulatory cytokines. Peptide-loaded (p)MHC and anti-CD28 were inserted onto the carbon nanotubes and IL-2 was loaded on polylactic-co-glycolic acid (PLGA) polymers. When combined, the complex was successful at expanding clinically useful cytotoxic T cells that inhibited tumor growth in a melanoma model, while using only 1/1000th the amount of soluble IL-2 [69]. Additionally, magnetite was co-loaded onto PLGA nanoparticles to permit magnetic separation from T cells after culturing was complete.

Another study utilized mesoporous silica microrods with adsorbed IL-2, anti-CD3, and anti-CD28 to complex with cultured T cells, and by varying the density of the complexed molecules, were able to achieve a polyclonal expansion of primary mouse and human T cells 2-10x greater than commercial expansion beads [70]. This system also allowed for antigen-specific expansion of T cells with substitution of pMHC for CD3 on the construct, as well as expansion of CD19 CAR-T cells that were efficacious in a xenograft lymphoma model. Additional constructs to achieve similar functions have been published, and as a whole, these methods allow for high local concentration of tumor-specific antigens and cytokines for robust T

cell stimulation and expansion that may reduce costs and time compared to current techniques [71, 72].

By targeting ALT T cells with various nanosystems, one can increase proliferative signaling and reduce immunosuppressive signaling in the setting of ALT therapy. Guasch et al. exploited cyclic Arg-Gly-Asp (cRGD), an integrin-binding ligand, cross-linked to a hydrogel with gold nanoparticles that were functionalized with anti-CD3. This complex was able to induce T cell activation and proliferation with memory [73]. Alternatively, Wayteck et al. were able to limit immunosuppressive signaling by attaching gold nanoparticles to the surface of cytotoxic T cells, and through pulsed laser illumination, created transient membrane pores that allowed for transfection of siRNA that targeted immunosuppressive pathways [74]. Zheng et al. created a liposome that contains an inhibitor of the immunosuppressive cytokine TGF- β and targets ALT T cells through either the internalizing receptor CD90 or a non-internalizing receptor CD45 [75]. Depending on the receptor chosen, this complex was utilized in an *ex vivo* or *in vivo* manner to improve T cell activity and promote tumor regression in a murine melanoma model.

These nano-systems can also target tumor cells. Utilizing the modified iRGD peptide to target liposomes containing a PI3K inhibitor and an alpha-Galactosylceramide agonist to the tumor, Zhang et al. were able to modify the tumor microenvironment to improve the immunostimulation/immunosuppression ratio in a murine glioma model. This created a therapeutic window of 2 weeks, during which the administration of tumor-specific CAR T cells was able to double the survival time compared to conventional CAR T treatment [76].

While CAR T therapy overcomes some of the limitations of traditional ALT therapy, there remain safety issues during the T cell harvesting and CAR T manufacturing process. Nanotechnology can help eliminate difficult steps by transporting genome-editing tools to host T cells *in vivo* to achieve *in situ* CAR T production. Smith et al. created a targeted nanoparticle to deliver a plasmid DNA encoding leukemia-specific 19/4-1BBz CAR and a hyperactive form of transposase to circulating T cells. The percentage of CAR-transfected T cells increased to nearly 20% on day 12, and these cells remained in circulation until day 24, with off-target binding limited to 5.9%. They were able to show comparable efficacy to traditionally-generated CAR-Ts in a mouse model of B-cell acute lymphoblastic leukemia [77]. Similar techniques have been developed to deliver mRNA [78].

Nano-constructs can enhance or streamline many aspects of the development, administration, and monitoring of ALT therapies. As ALT therapies continue to be developed and make their way into human trials, various nanotechnologies will likely be an indispensable component of their successful translation.

3.2 Nanotechnologies to Improve Cancer Vaccines

In order to instigate an effective anti-tumor immune response, vaccines must effectively deliver the relevant tumor-specific or -associated antigens to naïve T

cells to elicit and amplify the host's immunity. This can frequently be an inefficient and rate-limiting step that hinders vaccine efficacy. To overcome these limitations, various types of nanoparticles have been employed to date. These nanoparticles are often used to deliver a variety of antigens, including peptides, proteins, and nucleic acids, into APC or other relevant locales. Uses have been flexible, and the technologies have been applied creatively and variably to perform functions ranging from antigen delivery to transport of other molecules (including contrast agents or heat sensitizers) to even disguising themselves in tumor cell membranes to permit their uptake.

Some of the most common forms of cancer vaccines administer peptide antigens, with the goal of their uptake by APCs and subsequent presentation to T cells. Such strategies often suffer from inefficient peptide localization to APC or lymph nodes, and the peptides fall victim to enzymatic degradation. Nanoparticles have been designed to improve the delivery of these peptides to APCs. They can be engineered to protect the antigen from degradation or clearance and possess an ideal size distribution to spread throughout a region and be taken up by APCs. Likewise, they can be designed to co-deliver a variety of immunostimulatory molecules with the antigens to induced a robust response [79].

Zhu et al. were able to create a nanovaccine that binds to albumin *in vivo* and is transported to lymph nodes where presentation of its peptide antigen(s) occurs. Their nanovaccine increased the frequency of peripheral antigen-specific memory T cells approximately ten-fold over traditional approaches, and it was effective in a variety of murine cancer models [80]. In a separate example, Kuai et al. utilized high-density lipoprotein-mimicking nanodiscs coupled with peptide neoantigens and TLR-agonist CpG to improve antigen delivery to lymph nodes. The result was sustained antigen presentation by DCs [81]. The group reported 47-fold greater frequencies of neoantigen-specific cytotoxic T cells than that achieved with soluble vaccines. When combined with anti-PD1- and anti-CTLA-4 therapy, they were able to achieve complete response rates of 88% and 90% in colon adenocarcinoma and melanoma models, respectively. The vaccines were also able to deliver doxorubicin to tumor cells with the nanodiscs, eliciting immunogenic cell death of cancer cells and causing significant antitumor cytotoxic T cell responses [82].

In addition to peptides, researchers have also focused on the delivery of nucleic acid-based tumor antigens to APC via nanoparticles. For this purpose, nanoparticle-based methods have a number of advantages, including nucleic acid protection from degradation by nucleases, increased drainage to lymph nodes, and reduced off-target effects via APC-targeted transfection [79]. For example, Liu et al. utilized nanoparticles modified with mannose to successfully deliver an mRNA vaccine encoding the tumor antigen MUC1 into the cytosol of host DCs. The vaccine activated and expanded tumor-specific T cells against triple negative breast cancer in a murine model and significantly inhibited tumor growth when combined with anti-CTLA-4 therapy [83]. DCs can also be targeted effectively by nucleic acid-containing nanoparticles *in vivo* by adjusting the charge of the nanoparticles. In a widely cited manuscript, Kranz et al. employed RNA-loaded liposomes to deliver viral or mutant neoantigens and trigger IFN α release by DCs and macrophages

[84]. This methodology facilitated potent IFN α -dependent rejection of a variety of tumors in animal models, and in a phase 1 trial of 3 melanoma patients, was able to demonstrate strong antigen-specific T cell responses. Such nanoparticle-based approaches are promising as any polypeptide-based antigen can be encoded as RNA.

Nanoparticle-based techniques can also be utilized to deliver larger molecules, such as tumor-derived proteins. These techniques can employ various surface chemistry characteristics to bind proteins through noncovalent hydrophobic-hydrophobic interactions, ionic interactions, or covalent interactions [85]. Min et al. have developed a variety of nanoparticles to capture different antigens and deliver them to APCs. Once delivered, the vaccines expanded the cytotoxic T cell compartment, increasing the CD4⁺/Treg and CD8⁺/Treg ratios. This approach attained a 20% cure rate in a murine melanoma model when co-administered with anti-PD-1 therapy (compared to 0% without the nanoparticles) [85]. Like the other types of nanoparticle-based vaccines, protein presentation can be enhanced by codelivery with immunostimulatory molecules, such as CpG, as has been demonstrated recently [86, 87].

Nanoparticles can be designed to do more than deliver antigens and immunoadjuvants. For example, contrast for various imaging modalities can be delivered through effective design of inorganic nanoparticles. Gold nanoparticles have been conjugated with anti-PD-L1 to be used to treat a mouse model of colon cancer. As gold is visible on CT imaging, researchers were able to perform a noninvasive measurement of nanoparticle accumulation levels within the tumors and predict treatment response as early as 48 hours after therapy initiation. Their system also required only 20% of the standard dose in order to prevent tumor growth [88].

Nanoparticles comprised of iron oxide–zinc oxide are able to bind certain peptide motifs with high affinity, as well as provide MR imaging contrast due to the properties of iron oxide [89]. Other inorganic nanoparticles can be employed to generate heat-induced or reactive oxygen species-induced immunogenic cell death, in which dying tumor cells express and release tumor antigens and immunostimulatory molecules that activate APCs and downstream effector cells. Xu et al. loaded nanoparticles with a photosensitizer and a Toll-like-receptor-7 (TLR7) agonist to employ near-infrared irradiation with high tissue penetration depth. This led to photodynamic destruction of murine colon carcinoma tumors and generated a pool of tumor-associated antigens. With the aid of TLR7, in combination with anti-CLTA-4 therapy, this then created strong anti-tumor immune responses that likewise inhibited the growth of distant tumors [90].

Instead of simply attaching antigen to the nanoparticle surface, researchers now also have the ability to directly apply natural cell membranes onto a synthetic nanoparticulate core [79]. While membranes of normal cells can be utilized, tumor cell membranes have particularly promising potential to improve cancer vaccine therapies. Kroll et al. were able to coat nanoparticles in tumor cell membranes from the B16 murine melanoma line, and with vaccination, were able to prevent tumor occurrence in 86% of mice 150 days after challenge with tumor cells [91]. The known membrane-bound tumor-associated antigens, such as MART-1, TRP-2, and gp100, were confirmed to be present on their nanoparticles, which also contained

stimulatory CpG. Nanoparticles can also be created to coat the surface of tumor cells *in vivo* to mimic immunogenic cell death and promote immune responses. Fan et al. generated dying tumor cells undergoing immunogenic cell death and modified their surface with CpG-loaded nanoparticles. This effectively promoted antigen-specific CD8 α^+ T cells *in vivo*, and in combination with immune checkpoint blockade, was able to produce complete tumor regression in approximately 78% of tumor-bearing mice in a colon carcinoma model [92].

Nanoparticles, in their various forms, have a unique set of properties that can improve the delivery of antigens to APCs, as well as create other opportunities, such as the incorporation of immunoadjuvants or molecules to enable theranostics. With further advances, the utilization of nanoparticles in the development of cancer vaccines has marked potential to increase the effectiveness and utility of these therapies.

3.3 Nanotechnologies to Improve Viral-Based Immunotherapy

With recent advances to OV engineering and development for clinical use, intratumoral delivery becomes the most important obstacle to overcome for furthering therapeutic efficacy. Several novel strategies to enhance OV delivery are under investigation, including use of nanoparticles, immunomodulatory agents, and complex viral-particle ligands, along with modulations of patient immunity and the TME [93]. Modes of OV delivery have evolved quickly over time. One recent example includes the engineering of virus-containing complex nanoparticles that can be deposited within the tumor using minimally invasive imaging, such as ultrasound-guided delivery [94]. Furthermore, to improve the penetration of OVs into tumor, novel approaches to manipulate the TME and to decrease extracellular matrix deposition have been utilized [95, 96]. Some approaches involve modification of the viral genome to enhance their ability to penetrate tumors. Concomitant use of several different viral strains has been associated with better tumor penetration [97]. Simultaneous delivery of multiple therapeutic viral vectors using biomaterials to bypass neutralization by the host immune system has the potential for delivery of complementary viruses to achieve maximal synergy [97]. From the active propagation perspective, nano-filaments can be used to augment viral propagation, in a manner comparable to the spontaneously formed tunneling nanotubes in cancer cells [98]. Likewise, improvements to real-time monitoring methods for viral delivery and to viral particle labeling for better *in vivo* tracking are also gaining interest. Such strategies include the production of magnetic viral complexes that are detectable by MRI [99].

3.4 *Nanotechnologies to Improve Immune Checkpoint Blockade*

Since the FDA approval of immune checkpoint blockade therapies for use in several cancers, continuous efforts have been made to improve their efficacy. Applications of nanotechnology in this arena focus on strategies to better deliver checkpoint inhibitors [100, 101]. Luo et al. co-encapsulated anti-PD-1 peptide (APP) and hollow gold nanoshell (HAuNS) into biodegradable PLGA nanoparticles (APP- and HAuNS-loaded PLGA nanoparticles, AA@PN) [102]. The AA@PN platform was administered in combination with tumor photothermal ablation. Slow and sustained release of APP from AA@PN occurred over more than 40 days. Peptide release could be accelerated by firing of a near-infrared (NIR) laser. Effective concentration of intratumoral APP was maintained by continuous release over the study period. Furthermore, co-culturing of cancer cells and PBMCs with AA@PN followed by NIR treatment revealed a killing effect on distant cancer cells. This result suggests immune response activation in this combined therapeutic platform [102]. In a similar fashion, Wang et al. developed a CpG oligodeoxynucleotide (CpG ODN)-based nanocarrier for PD-1 blockade delivery. The controlled release of PD-1 blockade antibodies and CpG ODN by a CpG DNA-based “nano-cocoon” showed a significant survival prolongation, with a 40% complete response rate in mice that underwent incomplete tumor resection. This strategy was also shown to reduce the risk tumor relapse and metastasis when compared with free PD-1 blockade and CpG treatment [103].

From a different perspective, Zhang et al. developed cellular nanovesicles (NVs) with stable PD-1 expression on their membranes through the membrane extrusion method. Administered NVs demonstrated prolonged circulation time in the blood when compared with free antibodies [104]. These engineered NVs were shown to bind to the PD-L1 domains on melanoma cells. The NVs, therefore, prevent the inhibitory interaction between PD-1 on T cells and PD-L1 on tumor cells. In addition, 1-methyl-tryptophan, an inhibitor of indoleamine 2,3-dioxygenase (IDO) can be added to the NVs to simultaneously target another immunosuppressive pathway in the microenvironment. This therapeutic strategy resulted in increased density of tumor infiltrating-CD8+ T cells [104].

An additional study employed a microneedle patch for locally sustained delivery of checkpoint blockade antibody. The microneedle was composed of self-degradable hyaluronic acid and was incorporated with pH-sensitive dextran nanoparticles containing anti-PD-1 and glucose oxidase. The oxidase converts blood glucose into gluconic acid. The generation of a low-pH environment induces self-dissociation of the dextran nanoparticles, leading to anti-PD1 release. This approach showed superior efficacy to the microneedle patch without glucose oxidase or direct intratumoral free anti-PD-1 injection in a mouse melanoma model. Furthermore, this strategy can be applied to other checkpoint blockade strategies, including anti-CTLA-4, to enhance their efficacy [105].

As immune checkpoint monotherapy has yet to show satisfactory outcomes in some cancers, co-delivery of checkpoint inhibitors with antibodies that in turn stimulate immunity has gained significant interest within the nanotechnology field [106]. Wang et al. developed a dual immunotherapy nanoparticle (DINP) that co-delivers anti-PD-1 (antagonistic antibody) and anti-OX40 (CD134) (agonistic antibody). This strategy increases the chance of simultaneous T cell exposure to both types of antibody. This multi-pronged approach elicited a higher number of IFN- γ secreting T cells with greater overall cytokine producing activity, a higher number of tumor infiltrating T cells, a higher ratio of cytotoxic T cells to Tregs, and a higher ratio of effector memory to central memory T cells when compared with a mixture of free anti-PD1 and OX40 agonist treatment. The superior efficacy was shown in both B16F10 melanoma and 4 T1 breast cancer murine models. Importantly, re-challenge with tumor revealed significant resistance to tumor recurrence, suggesting a long-lasting anti-tumor immunological memory [107]. In addition to OX40, 4-1BB (CD137) is another co-stimulatory target of interest. Administration of nanoparticles containing both anti-PD-L1 and a 4-1BB agonist was likewise shown to delay tumor growth in colon cancer and melanoma models [108].

4 Summary and Future Directions

Cancer immunotherapy is a promising anti-cancer platform that has made rapid progress over the past decade. Various cancer immunotherapy modalities have been translated into the clinic. With increasing momentum, nanotechnologies have begun to be employed to better enable these cancer immunotherapy platforms. Often, these technologies are designed to overcome the challenges to current immunotherapies such as improving delivery and increasing access of various immunotherapeutic modalities to the tumor site. While cancer-induced immune suppression remains one of the most challenging issue for delivering successful immunotherapy, novel nanotechnologies start to show that they can be helpful in the immunosuppressive TME. It is anticipated that many of these immunotherapy-coupled nanotechnologies will be under clinical investigation in the near future. Although the goal remains strengthened immune responses, it is unclear whether the increased immune activation from nanotechnology will also increase autoimmune side effects. If so, strategies need to be established to mitigate the adverse effects. The field of nanotechnology-enabled cancer immunotherapy is still in the early phase of evolution. As the understanding in cancer biology and immunology mature, we expect the integration of nanotechnology and cancer immunotherapy to create novel therapeutic modalities with high efficacy and safety for patients with cancer.

References

1. Queirolo, P., et al.: Immune-checkpoint inhibitors for the treatment of metastatic melanoma: a model of cancer immunotherapy. *Semin. Cancer Biol.* **59**, 290 (2019)
2. Steinman, R.M.: The dendritic cell system and its role in immunogenicity. *Annu. Rev. Immunol.* **9**, 271–296 (1991)
3. Reis e Sousa, C.: Dendritic cells as sensors of infection. *Immunity.* **14**(5), 495–498 (2001)
4. Dhodapkar, M.V., et al.: Antigen-specific inhibition of effector T cell function in humans after injection of immature dendritic cells. *J. Exp. Med.* **193**(2), 233–238 (2001)
5. Sabado, R.L., Balan, S., Bhardwaj, N.: Dendritic cell-based immunotherapy. *Cell Res.* **27**(1), 74–95 (2017)
6. Murphy, G.P., et al.: Phase II prostate cancer vaccine trial: report of a study involving 37 patients with disease recurrence following primary treatment. *Prostate.* **39**(1), 54–59 (1999)
7. Fong, L., et al.: Dendritic cells injected via different routes induce immunity in cancer patients. *J. Immunol.* **166**(6), 4254–4259 (2001)
8. Holtl, L., et al.: Cellular and humoral immune responses in patients with metastatic renal cell carcinoma after vaccination with antigen pulsed dendritic cells. *J. Urol.* **161**(3), 777–782 (1999)
9. Kugler, A., et al.: Regression of human metastatic renal cell carcinoma after vaccination with tumor cell-dendritic cell hybrids. *Nat. Med.* **6**(3), 332–336 (2000)
10. Fong, L., et al.: Altered peptide ligand vaccination with Flt3 ligand expanded dendritic cells for tumor immunotherapy. *Proc. Natl. Acad. Sci. U. S. A.* **98**(15), 8809–8814 (2001)
11. Morse, M.A., et al.: Preoperative mobilization of circulating dendritic cells by Flt3 ligand administration to patients with metastatic colon cancer. *J. Clin. Oncol.* **18**(23), 3883–3893 (2000)
12. Anassi, E., Ndefo, U.A.: Sipuleucel-T (provenge) injection: the first immunotherapy agent (vaccine) for hormone-refractory prostate cancer. *P T.* **36**(4), 197–202 (2011)
13. Sugawa, N., et al.: Identical splicing of aberrant epidermal growth factor receptor transcripts from amplified rearranged genes in human glioblastomas. *Proc. Natl. Acad. Sci. U. S. A.* **87**(21), 8602–8606 (1990)
14. Kumai, T., et al.: Peptide vaccines in cancer-old concept revisited. *Curr. Opin. Immunol.* **45**, 1–7 (2017)
15. Bijker, M.S., et al.: CD8+ CTL priming by exact peptide epitopes in incomplete Freund’s adjuvant induces a vanishing CTL response, whereas long peptides induce sustained CTL reactivity. *J. Immunol.* **179**(8), 5033–5040 (2007)
16. Sampson, J.H., et al.: Immunologic escape after prolonged progression-free survival with epidermal growth factor receptor variant III peptide vaccination in patients with newly diagnosed glioblastoma. *J. Clin. Oncol.* **28**(31), 4722–4729 (2010)
17. Dunn, G.P., et al.: Cancer immunoeediting: from immunosurveillance to tumor escape. *Nat. Immunol.* **3**(11), 991–998 (2002)
18. Matsushita, H., et al.: Cancer exome analysis reveals a T-cell-dependent mechanism of cancer immunoeediting. *Nature.* **482**(7385), 400–404 (2012)
19. Dudley, M.E., et al.: Cancer regression and autoimmunity in patients after clonal repopulation with antitumor lymphocytes. *Science.* **298**(5594), 850–854 (2002)
20. Rosenberg, S.A., et al.: Adoptive cell transfer: a clinical path to effective cancer immunotherapy. *Nat. Rev. Cancer.* **8**(4), 299–308 (2008)
21. Rosenberg, S.A., et al.: Use of tumor-infiltrating lymphocytes and interleukin-2 in the immunotherapy of patients with metastatic melanoma. A preliminary report. *N. Engl. J. Med.* **319**(25), 1676–1680 (1988)
22. Gubin, M.M., et al.: Checkpoint blockade cancer immunotherapy targets tumour-specific mutant antigens. *Nature.* **515**(7528), 577–581 (2014)
23. Lennerz, V., et al.: The response of autologous T cells to a human melanoma is dominated by mutated neoantigens. *Proc. Natl. Acad. Sci. U. S. A.* **102**(44), 16013–16018 (2005)

24. Dubey, P., et al.: The immunodominant antigen of an ultraviolet-induced regressor tumor is generated by a somatic point mutation in the DEAD box helicase p68. *J. Exp. Med.* **185**(4), 695–705 (1997)
25. Snyder, A., et al.: Genetic basis for clinical response to CTLA-4 blockade in melanoma. *N. Engl. J. Med.* **371**(23), 2189–2199 (2014)
26. Rizvi, N.A., et al.: Cancer immunology. Mutational landscape determines sensitivity to PD-1 blockade in non-small cell lung cancer. *Science*. **348**(6230), 124–128 (2015)
27. Alexandrov, L.B., et al.: Signatures of mutational processes in human cancer. *Nature*. **500**(7463), 415–421 (2013)
28. Schumacher, T.N., Schreiber, R.D.: Neoantigens in cancer immunotherapy. *Science*. **348**(6230), 69–74 (2015)
29. Champiat, S., et al.: Exomics and immunogenics: bridging mutational load and immune checkpoints efficacy. *Oncotargets Ther.* **3**(1), e27817 (2014)
30. US Food & Drug Administration. FDA Approves CAR-T Cell Therapy to Treat Adults with Certain Types of Large B Cell Lymphoma. 2017.; Available from: <https://www.fda.gov/newsevents/newsroom/pressannouncements/ucm581216.htm>
31. US Food & Drug Administration. FDA Approves Tisagenlecleucel for Adults with Relapsed or Refractory Large B Cell Lymphoma. 2018.; Available from: <https://www.fda.gov/Drugs/InformationOnDrugs/ApprovedDrugs/ucm606540.htm>
32. Feins, S., et al.: An introduction to chimeric antigen receptor (CAR) T-cell immunotherapy for human cancer. *Am. J. Hematol.* **94**(S1), S3–S9 (2019)
33. Kuwana, Y., et al.: Expression of chimeric receptor composed of immunoglobulin-derived V regions and T-cell receptor-derived C regions. *Biochem. Biophys. Res. Commun.* **149**(3), 960–968 (1987)
34. Gross, G., Waks, T., Eshhar, Z.: Expression of immunoglobulin-T-cell receptor chimeric molecules as functional receptors with antibody-type specificity. *Proc. Natl. Acad. Sci. U. S. A.* **86**(24), 10024–10028 (1989)
35. Kershaw, M.H., et al.: A phase I study on adoptive immunotherapy using gene-modified T cells for ovarian cancer. *Clin. Cancer Res.* **12**(20 Pt 1), 6106–6115 (2006)
36. Lamers, C.H., et al.: Treatment of metastatic renal cell carcinoma with autologous T-lymphocytes genetically retargeted against carbonic anhydrase IX: first clinical experience. *J. Clin. Oncol.* **24**(13), e20–e22 (2006)
37. Finney, H.M., et al.: Chimeric receptors providing both primary and costimulatory signaling in T cells from a single gene product. *J. Immunol.* **161**(6), 2791–2797 (1998)
38. Imai, C., et al.: Chimeric receptors with 4-1BB signaling capacity provoke potent cytotoxicity against acute lymphoblastic leukemia. *Leukemia*. **18**(4), 676–684 (2004)
39. Kalos, M., et al.: T cells with chimeric antigen receptors have potent antitumor effects and can establish memory in patients with advanced leukemia. *Sci. Transl. Med.* **3**(95), 95ra73 (2011)
40. Porter, D.L., et al.: Chimeric antigen receptor-modified T cells in chronic lymphoid leukemia. *N. Engl. J. Med.* **365**(8), 725–733 (2011)
41. Brentjens, R.J., et al.: Safety and persistence of adoptively transferred autologous CD19-targeted T cells in patients with relapsed or chemotherapy refractory B-cell leukemias. *Blood*. **118**(18), 4817–4828 (2011)
42. Kochenderfer, J.N., et al.: Eradication of B-lineage cells and regression of lymphoma in a patient treated with autologous T cells genetically engineered to recognize CD19. *Blood*. **116**(20), 4099–4102 (2010)
43. Patel, A.P., et al.: Single-cell RNA-seq highlights intratumoral heterogeneity in primary glioblastoma. *Science*. **344**(6190), 1396–1401 (2014)
44. Qazi, M.A., et al.: Intratumoral heterogeneity: pathways to treatment resistance and relapse in human glioblastoma. *Ann. Oncol.* **28**(7), 1448–1456 (2017)
45. O'Rourke, D.M., et al.: A single dose of peripherally infused EGFRvIII-directed CAR T cells mediates antigen loss and induces adaptive resistance in patients with recurrent glioblastoma. *Sci. Transl. Med.* **9**, 399 (2017)

46. Loskog, A., et al.: Addition of the CD28 signaling domain to chimeric T-cell receptors enhances chimeric T-cell resistance to T regulatory cells. *Leukemia*. **20**(10), 1819–1828 (2006)
47. Koehler, H., et al.: CD28 costimulation overcomes transforming growth factor-beta-mediated repression of proliferation of redirected human CD4+ and CD8+ T cells in an antitumor cell attack. *Cancer Res.* **67**(5), 2265–2273 (2007)
48. Choi, B.D., et al.: CAR-T cells secreting BiTEs circumvent antigen escape without detectable toxicity. *Nat. Biotechnol.* **37**, 1049 (2019)
49. Avanzi, M.P., et al.: Engineered tumor-targeted T cells mediate enhanced anti-tumor efficacy both directly and through activation of the endogenous immune system. *Cell Rep.* **23**(7), 2130–2141 (2018)
50. Sobol, P.T., et al.: Adaptive antiviral immunity is a determinant of the therapeutic success of oncolytic virotherapy. *Mol. Ther.* **19**(2), 335–344 (2011)
51. Workenhe, S.T., Mossman, K.L.: Oncolytic virotherapy and immunogenic cancer cell death: sharpening the sword for improved cancer treatment strategies. *Mol. Ther.* **22**(2), 251–256 (2014)
52. Kaufman, H.L., et al.: Local and distant immunity induced by intralesional vaccination with an oncolytic herpes virus encoding GM-CSF in patients with stage IIIc and IV melanoma. *Ann. Surg. Oncol.* **17**(3), 718–730 (2010)
53. Desjardins, A., et al.: Recurrent glioblastoma treated with recombinant poliovirus. *N. Engl. J. Med.* **379**(2), 150–161 (2018)
54. Woroniecka, K., et al.: T-cell exhaustion signatures vary with tumor type and are severe in glioblastoma. *Clin. Cancer Res.* **24**(17), 4175–4186 (2018)
55. Greenwald, R.J., et al.: CTLA-4 regulates induction of anergy in vivo. *Immunity*. **14**(2), 145–155 (2001)
56. Barber, D.L., et al.: Restoring function in exhausted CD8 T cells during chronic viral infection. *Nature*. **439**(7077), 682–687 (2006)
57. Hodi, F.S., et al.: Improved survival with ipilimumab in patients with metastatic melanoma. *N. Engl. J. Med.* **363**(8), 711–723 (2010)
58. Hargadon, K.M., Johnson, C.E., Williams, C.J.: Immune checkpoint blockade therapy for cancer: an overview of FDA-approved immune checkpoint inhibitors. *Int. Immunopharmacol.* **62**, 29–39 (2018)
59. Kather, J.N., et al.: Topography of cancer-associated immune cells in human solid tumors. *elife*. **7** (2018)
60. Salmon, H., et al.: Host tissue determinants of tumour immunity. *Nat. Rev. Cancer.* **19**(4), 215–227 (2019)
61. Andtbacka, R.H., et al.: Talimogene Laherparepvec improves durable response rate in patients with advanced melanoma. *J. Clin. Oncol.* **33**(25), 2780–2788 (2015)
62. Sanchez-Perez, L., Chandramohan, V., Yu, Y.A., Bigner, D.D., Giles, A., Healy, P., Dranoff, G., Weinhold, K.J., Dunn, G.P., Fecci, P.E., W.K.C.P.R.K.K.H.D.C.F.S.E.A.C.X.K.S.J.C.H.L.J.T: T-cell exhaustion signatures vary with tumor type and are severe in glioblastoma. *Clin. Cancer Res.* **24**, 4175 (2018)
63. Haque, S., Morris, J.C.: Transforming growth factor-beta: a therapeutic target for cancer. *Hum. Vaccin. Immunother.* **13**(8), 1741–1750 (2017)
64. Seystahl, K., et al.: Biological role and therapeutic targeting of TGF-beta3 in glioblastoma. *Mol. Cancer Ther.* **16**(6), 1177–1186 (2017)
65. Schlosser, H.A., et al.: Overcoming tumor-mediated immunosuppression. *Immunotherapy*. **6**(9), 973–988 (2014)
66. Awad, R.M., et al.: Turn back the TIME: targeting tumor infiltrating myeloid cells to revert cancer progression. *Front. Immunol.* **9**, 1977 (2018)
67. Najafi, M., Farhood, B., Mortezaee, K.: Contribution of regulatory T cells to cancer: a review. *J. Cell. Physiol.* **234**(6), 7983–7993 (2019)
68. Kalos, M., June, C.H.: Adoptive T cell transfer for cancer immunotherapy in the era of synthetic biology. *Immunity*. **39**(1), 49–60 (2013)

69. Fadel, T.R., et al.: A carbon nanotube-polymer composite for T-cell therapy. *Nat. Nanotechnol.* **9**(8), 639–647 (2014)
70. Cheung, A.S., et al.: Scaffolds that mimic antigen-presenting cells enable ex vivo expansion of primary T cells. *Nat. Biotechnol.* **36**(2), 160–169 (2018)
71. Steenblock, E.R., Fahmy, T.M.: A comprehensive platform for ex vivo T-cell expansion based on biodegradable polymeric artificial antigen-presenting cells. *Mol. Ther.* **16**(4), 765–772 (2008)
72. Perica, K., et al.: Enrichment and expansion with nanoscale artificial antigen presenting cells for adoptive immunotherapy. *ACS Nano.* **9**(7), 6861–6871 (2015)
73. Guasch, J., et al.: Integrin-assisted T-cell activation on nanostructured hydrogels. *Nano Lett.* **17**(10), 6110–6116 (2017)
74. Wayteck, L., et al.: Comparing photoporation and nucleofection for delivery of small interfering RNA to cytotoxic T cells. *J. Control. Release.* **267**, 154–162 (2017)
75. Zheng, Y., et al.: Enhancing adoptive cell therapy of cancer through targeted delivery of small-molecule Immunomodulators to internalizing or noninternalizing receptors. *ACS Nano.* **11**(3), 3089–3100 (2017)
76. Zhang, F., et al.: Nanoparticles that reshape the tumor milieu create a therapeutic window for effective T-cell therapy in solid malignancies. *Cancer Res.* **78**(13), 3718–3730 (2018)
77. Smith, T.T., et al.: In situ programming of leukaemia-specific T cells using synthetic DNA nanocarriers. *Nat. Nanotechnol.* **12**(8), 813–820 (2017)
78. Moffett, H.F., et al.: Hit-and-run programming of therapeutic cytoreagents using mRNA nanocarriers. *Nat. Commun.* **8**(1), 389 (2017)
79. Mi, Y., et al.: Emerging nano-/microapproaches for cancer immunotherapy. *Adv. Sci. (Weinh).* **6**(6), 1801847 (2019)
80. Zhu, G., et al.: Albumin/vaccine nanocomplexes that assemble in vivo for combination cancer immunotherapy. *Nat. Commun.* **8**(1), 1954 (2017)
81. Kuai, R., et al.: Designer vaccine nanodiscs for personalized cancer immunotherapy. *Nat. Mater.* **16**(4), 489–496 (2017)
82. Kuai, R., et al.: Elimination of established tumors with nanodisc-based combination chemioimmunotherapy. *Sci. Adv.* **4**(4), eaao1736 (2018)
83. Liu, L., et al.: Combination immunotherapy of MUC1 mRNA Nano-vaccine and CTLA-4 blockade effectively inhibits growth of triple negative breast cancer. *Mol. Ther.* **26**(1), 45–55 (2018)
84. Kranz, L.M., et al.: Systemic RNA delivery to dendritic cells exploits antiviral defence for cancer immunotherapy. *Nature.* **534**(7607), 396–401 (2016)
85. Min, Y., et al.: Antigen-capturing nanoparticles improve the abscopal effect and cancer immunotherapy. *Nat. Nanotechnol.* **12**(9), 877–882 (2017)
86. Chao, Y., et al.: Combined local immunostimulatory radioisotope therapy and systemic immune checkpoint blockade imparts potent antitumour responses. *Nat. Biomed. Eng.* **2**(8), 611–621 (2018)
87. Zupancic, E., et al.: Rational design of nanoparticles towards targeting antigen-presenting cells and improved T cell priming. *J. Control. Release.* **258**, 182–195 (2017)
88. Meir, R., et al.: Fast image-guided stratification using anti-programmed death ligand 1 gold nanoparticles for cancer immunotherapy. *ACS Nano.* **11**(11), 11127–11134 (2017)
89. Cho, N.H., et al.: A multifunctional core-shell nanoparticle for dendritic cell-based cancer immunotherapy. *Nat. Nanotechnol.* **6**(10), 675–682 (2011)
90. Xu, J., et al.: Near-infrared-triggered photodynamic therapy with multitasking Upconversion nanoparticles in combination with checkpoint blockade for immunotherapy of colorectal cancer. *ACS Nano.* **11**(5), 4463–4474 (2017)
91. Kroll, A.V., et al.: Nanoparticulate delivery of cancer cell membrane elicits multiantigenic antitumor immunity. *Adv. Mater.* **29**, 47 (2017)
92. Fan, Y., et al.: Immunogenic cell death amplified by co-localized adjuvant delivery for cancer immunotherapy. *Nano Lett.* **17**(12), 7387–7393 (2017)

93. Yokoda, R., et al.: Oncolytic virus delivery: from nano-pharmacodynamics to enhanced oncolytic effect. *Oncolytic. Virother.* **6**, 39–49 (2017)
94. Bazan-Peregrino, M., et al.: Ultrasound-induced cavitation enhances the delivery and therapeutic efficacy of an oncolytic virus in an in vitro model. *J. Control. Release.* **157**(2), 235–242 (2012)
95. Choi, I.K., et al.: Effect of decorin on overcoming the extracellular matrix barrier for oncolytic virotherapy. *Gene Ther.* **17**(2), 190–201 (2010)
96. Jain, R.K.: Normalizing tumor microenvironment to treat cancer: bench to bedside to biomarkers. *J. Clin. Oncol.* **31**(17), 2205–2218 (2013)
97. Le Boeuf, F., et al.: Synergistic interaction between oncolytic viruses augments tumor killing. *Mol. Ther.* **18**(5), 888–895 (2010)
98. Ady, J., et al.: Tunneling nanotubes: an alternate route for propagation of the bystander effect following oncolytic viral infection. *Mol. Ther. Oncolytics.* **3**, 16029 (2016)
99. Almstatter, I., et al.: Characterization of magnetic viral complexes for targeted delivery in oncology. *Theranostics.* **5**(7), 667–685 (2015)
100. Li, S.Y., et al.: Restoring anti-tumor functions of T cells via nanoparticle-mediated immune checkpoint modulation. *J. Control. Release.* **231**, 17–28 (2016)
101. Chen, Q., et al.: Delivery strategies for immune checkpoint blockade. *Adv. Healthc. Mater.* **7**(20), e1800424 (2018)
102. Luo, L., et al.: Sustained release of anti-PD-1 peptide for perdurable immunotherapy together with photothermal ablation against primary and distant tumors. *J. Control. Release.* **278**, 87–99 (2018)
103. Wang, C., et al.: Inflammation-triggered cancer immunotherapy by programmed delivery of CpG and anti-PD1 antibody. *Adv. Mater.* **28**(40), 8912–8920 (2016)
104. Zhang, X., et al.: PD-1 blockade cellular vesicles for cancer immunotherapy. *Adv. Mater.* **30**(22), e1707112 (2018)
105. Wang, C., et al.: Enhanced cancer immunotherapy by microneedle patch-assisted delivery of anti-PD1 antibody. *Nano Lett.* **16**(4), 2334–2340 (2016)
106. Mahoney, K.M., Rennert, P.D., Freeman, G.J.: Combination cancer immunotherapy and new immunomodulatory targets. *Nat. Rev. Drug Discov.* **14**(8), 561–584 (2015)
107. Mi, Y., et al.: A dual immunotherapy nanoparticle improves T-cell activation and cancer immunotherapy. *Adv. Mater.* **30**(25), e1706098 (2018)
108. Kosmides, A.K., et al.: Dual targeting nanoparticle stimulates the immune system to inhibit tumor growth. *ACS Nano.* **11**(6), 5417–5429 (2017)

Immunotherapy: From Discovery to Bedside



Ankeet Shah, Dominic Grimberg, and Brant A. Inman

1 Immunotherapy: From Discovery to Bedside

Immunotherapy has been widely regarded for the hope that it brings to our goals of effectively treating cancer with more discrimination and less side effects compared to conventional treatments. However, immunotherapy has not been able to cure most cancers and challenges with this class raise many more questions about the interplay among the immune system, tumor cells, and their surrounding microenvironment. Improving our understanding of these relationships has yielded innumerable targets for new treatments in the immune-oncology space. In this chapter, we will review the broad categories of immunotherapy, as well as discuss the pathway(s) for bringing promising treatments to the clinic. Challenges posed by immune-oncology therapies have led to shifts in approaches to clinical trials which we will discuss.

1.1 Overview of Immunotherapy

The role of the immune system in detecting and eliminating non-self or danger signals from the body is a significant one, and immune responses have been implicated in both progression and inhibition/destruction of tumors. Understanding the interplay of the different elements of the immune system is critical for developing therapies to harness this system in treating tumors. The most simplistic view of the immune system in the context of a tumor is that tumor cells display some type

A. Shah · D. Grimberg · B. A. Inman (✉)
Division of Urology, Duke Cancer Institute, Durham, NC, USA

Duke University Medical Center, Durham, NC, USA
e-mail: ankeet.shah@duke.edu; dominic.grimberg@duke.edu; brant.inman@duke.edu

of antigen on their surface and generate signals which, in certain settings, drive innate immune cells to target those tumor cells. CD4 (helper) T-cells play a large role in facilitating this process by detecting the antigen on or around tumor cells and, depending on the nature of the inflammatory reaction at the time, consequently releasing a milieu of cytokines to drive a certain type of inflammatory response. The innate immune system also stimulates antigen-presenting cells (APCs) to capture tumor antigens and display them on cell surface MHC molecules to facilitate activation of the adaptive immune system, which effects a concerted attack on the tumor based on the information gained from the APCs [1–3]. In reviewing the overarching types of immunotherapy, we will provide a broad overview of the field from the perspective of specific (i.e., directly targeting tumor cells) and nonspecific immune mediators.

1.1.1 Nonspecific Immunity

Cytokines

Cytokines and chemokines are signaling molecules that coordinate immune response. Typical among these are interleukins and interferons, various glycoproteins with varying effects on the trajectory of immune response. For example, higher levels of interleukin-2 (IL-2) are associated with activation of CD8 (cytotoxic) T-cells and a more successful anti-tumor effect (Th1 response). On the other hand, higher levels of IL-4 are associated with more chronic inflammation phenotypes (Th2 response). The cytokines and chemokines may be released by tumor cells, cells from the surrounding tumor microenvironment (TME), or other local epithelial cells. In addition to driving a certain type of T-cell response, cytokine signaling recruits other leukocytes such as macrophages, neutrophils, natural killer (NK) cells, which help start the adaptive immune response in concert with dendritic cells [3, 4]. Administration of IL-2 and various interferons have been used to treat malignancies such as kidney and bladder cancer. Unfortunately, these treatments are notable in that they have been associated with significant side effects due to the consequences of high systemic cytokine levels (i.e. cytokine storm) [5, 6].

Immune Adjuvants

Stimulation of the host immune system against a tumor can also be achieved using immune adjuvants. These are typically thought of as substances that potentiate the effects of vaccines, but in the immune-oncology space, immune adjuvants have found a role in treating tumors as single agents. Immune adjuvants can be categorized by mechanism. Delivery systems such as mineral salts and microparticles act as carriers for antigens and can independently drive local proinflammatory responses to recruit the innate immune system, while immune potentiators recruit the innate immune system through detection by immune cell receptors. Mucosal

adjuvants combine the two approaches [7]. Imiquimod is one example of an immune potentiator, used to treat penile squamous cell carcinoma in situ as well as a variety of skin lesions and cancer (actinic keratoses, genital warts, basal cell carcinoma, etc.) [8, 7]. Bacillus Calmette-Guerin, on the other hand, is a live-attenuated mycobacterium that is instilled in the urinary bladder for treatment of high grade, non-muscle invasive cancer and carcinoma in situ, and functions more similarly to a mucosal adjuvant [9].

Checkpoint Inhibitors

When tumor cells are detected by T-cells, the antigen detection and consequent reaction is dependent on co-stimulation by a secondary ligand-receptor pair. These secondary ligand-receptor pairs are also known as immune checkpoints because they can steer the immune response to activity or anergy, depending on the situation (Fig. 1) [10]. Certain types of receptor-ligand pairings are stimulatory and drive T-cells towards anti-tumor activity while others are inhibitory and lead to anergy of the T-cells. These inhibitory responses normally play a role in self-recognition to prevent autoimmunity. However, tumor cells can develop the ability to express inhibitory costimulatory molecules and blocking these inhibitory receptor-ligand pairs can theoretically re-awaken a sleeping anti-tumor immune response. Well known among checkpoint inhibitors are anti-PD1/PD-L1 and CTLA-4 therapies (e.g., pembrolizumab and ipilimumab, respectively) [5, 11].

1.1.2 Specific Immunity

Adoptive Cell Transfer

In the interest of mounting a targeted antitumor response towards a tumor, a strategy known as adoptive cell transfer (ACT) has been developed and used with multiple different immune mediators. In this approach, immune mediator cells are extracted from a biospecimen and manipulated for a targeted effect prior to reinfusion [12]. For example, Sipuleucel-T is a treatment for castration resistant prostate cancer, and involves extraction of dendritic cells (a type of antigen presenting cell) followed by *in vitro* exposure to a fusion protein containing Prostatic Acid Phosphatase (PAP) and an immune stimulating factor. After an exposure period, the dendritic cells are reinfused back into a patient with prostate cancer and consequently drive a T-cell mediated antitumor response [13]. Adoptive cell transfer strategies have also been studied using T-cells directly, or after modification with a chimeric antigen receptor (CAR) which does not depend on co-stimulation and specific antigen presentation restrictions, in order facilitate a T-cell mediated response to tumor cell surface antigens [12]. Currently, CAR-T cell based therapies are approved for use in certain hematologic malignancies [14].

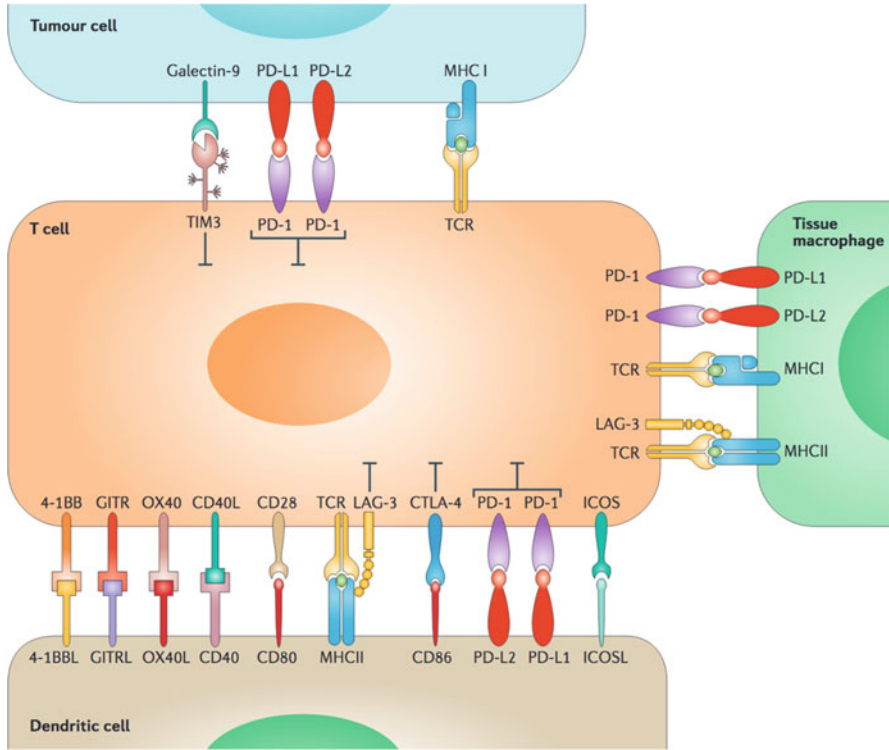


Fig. 1 Representative relationships between tumor and immune cells in the tumor microenvironment, with overview of numerous ligand-receptor interactions involved in immune-checkpoints. From Nishino [10]

Vaccines

Use of vaccines to prevent or treat cancer has gained attention as well. Prevention has largely centered around managing viral exposures that are pro-tumorigenic (e.g. human papilloma virus), while therapeutic cancer vaccines have centered around identification of neoantigens, generated from a tumor-specific mutation, or aberrantly-expressed but non-mutated, normal self-antigens. However, the development of vaccines has been hampered in part by the effect of a local inhibition of immune cells at the tumor (e.g., inhibitory co-stimulation of CD4 T-cells). Neoantigen based vaccines are thought to drive stronger T-cell responses that overcome the issue of local inhibition, but even with this technique early studies have shown that there is some effect that can be ameliorated by concurrent or sequential treatment with checkpoint inhibitors [2, 6, 15]. However, concern remains that resource intensive nature of personalized vaccines based on individual patient neoantigens will limit the development of cost-effective therapies, especially in a

competitive space with other promising immunologic therapies and an increasing number of combination therapy clinical trials [16].

Oncolytic Viruses

Viral replication inherently involves a destructive, “cytolytic” process and attempts over many years to use this property to facilitate tumor destruction have been met with limited success until more recently. Newer generations of oncolytic viruses are modified with a transgene designed to drive inflammation and immune recruitment to the site of disease. Talimogene laherparepvec (T-VEC, Imlygic®), constructed from attenuated herpes simplex virus, was approved in 2015 for intralesional use in melanoma on the basis of promising Phase III efficacy and safety data. In Phase I/II trials, combination with a checkpoint inhibitor has demonstrated improved response rates by more than double that seen with checkpoint inhibitor therapy, alone [6].

Antibodies and Antibody-Drug Conjugates

Antibodies play a role in humoral immunity, distinct from the cellular immunity discussed earlier. Typically released by cells involved in acquired immunity, antibodies target specific antigens and effectively label a cell for targeted phagocytosis, or activate a biochemical cascade of proteins which cooperatively disrupt the plasma membrane of the target cell leading to cytolysis [4]. However, the actual role played in immunologic control of cancer depends on the target of the antibody. Among other drugs, checkpoint inhibitors, are composed of antibodies, leveraging the very specific targeting to minimize collateral damage. Any number of cellular targets could be affected by antibodies. Conjugating targeted or cytotoxic drugs to antibodies for cell-specific anti-tumor effect with potentially significantly less side effects holds promise in early studies in a number of cancers [17, 18].

1.2 Drug Development

1.2.1 Overview

Conventionally, therapeutic development and approval by the US Food and Drug Administration (FDA) are broken into three phases (Fig. 1). First, the preclinical phase is comprised of the discovery of a potential therapeutic. Dosing parameters are optimally refined in animal models during this phase, while also generating data to support the expected safety and efficacy of the therapeutic. Such data is used to file an Investigational New Drug (IND) application with the FDA. The second phase, clinical trials, starts once the IND is approved. This is the start of human testing of a drug; trials are subcategorized into Phase I, II and III trials, with varying

scopes and goals of evaluating safety, efficacy, and comparative effectiveness [19–21]. With favorable results, a manufacturer may file a New Drug Application (NDA) with the FDA and begin marketing their drug. The postmarketing phase begins and may entail certain studies (Phase IV trials) requested by the FDA as a part of NDA approval. Traditionally, this whole process could take from 10–15 years, at an estimated cost of nearly \$1.3–1.7B to develop a new drug [22].

The attrition rate between phases of development is a source of concern, especially in the context of investment that does not bear returns for funding organizations. In 2012, the FDA Safety and Innovation Act (FDASIA) was signed into law, and as a part of that law, a new designation was created to facilitate innovation. The “breakthrough therapy” designation is given to those candidate therapies intended to treat a “serious or life-threatening condition and has preliminary clinical evidence to support a substantial improvement over existing therapies on one or more clinically significant endpoints over available therapies.” Once a therapy receives this designation, the FDA will provide resources to accelerate the development process and review of that therapy. It currently features as one of four pathways for expedited review from the FDA. Immuno-oncologic therapies have benefited from such expedited approval. Pembrolizumab, an immune checkpoint inhibitor, was approved for treatment of melanoma 3 months after publication of Phase I data with the condition that Merck was required to establish the superiority of pembrolizumab over other available therapies in a multicenter, randomized trial, as well as verify and describe the clinical benefits of the treatment [19, 22, 23]. However, in an analysis of the effect of expedited programs on drug development timelines from 1998–2014, multivariate models demonstrated that type of therapy was the only predictive factor for total time of clinical development, with targeted therapies having a median timeline of 5.4 years compared to 9.4 years for cytotoxic therapies. Certainly, the status of expedited approval pathway is no guarantee of faster FDA approval [11].

1.2.2 Preclinical Phase

As the least standardized phase, preclinical studies drive towards an end goal of an IND submission to the FDA and thus require adequate data surrounding preliminary efficacy, pharmacology, toxicology, planned clinical studies and parameters, as well as manufacturing information to ensure that the therapy can be consistently made and delivered. Once a target for therapy and the therapeutic candidate are identified, *in vitro* and *in vivo* studies commence to characterize the performance the candidate. Animal models largely drive the validation of a therapeutic candidate in this phase and facilitate acquisition of the data required for an IND application [20, 24, 25].

However, selection of a valid animal model requires careful consideration. Such models can come in the form of different types of animals (e.g. mice, dogs, pigs, etc.) whose size and biology influence cost, time of testing, and translatability to humans to a varying degree. In the oncology space, animal models also range from simplistic models of subcutaneous tumor implants (either xenografts from

human tumor lines or syngenic, animal-specific tumor lines) to more complex models involving humanized immune systems in animals with xenografted tumors, or even genetically engineered models with targeted expression of mutations that drive tumor formation. Increasingly sophisticated oncologic animal models derive the benefit of more specific analysis of the tumor cell lineage in question, without artifact of absent tumor microenvironment as seen in subcutaneous xenografts, and possibly with more complete recapitulation of disease progression. The more accurate representation of the biology at this phase, the more predictive the model will be for drug performance in clinical trials. However, advanced animal models are also associated with increased time for developing those models and/or higher cost [24, 25].

1.2.3 Clinical Phase

Phase I

Once an IND is approved, Phase I trials are implemented. The maximum tolerated dose (MTD) is the maximum dose that still meets a certain safety threshold, and is thought to be the most promising dose for planning Phase II trials. On the other hand, toxicity is defined largely by the dose-limiting toxicity (DLT) experienced by a pre-defined proportion of patients. Understanding the relationship between MTD and DLT is an important goal of Phase I trials, to facilitate appropriate dosing in humans, while also evaluating for toxicity and pharmacokinetic/pharmacodynamic parameters. Conventionally, the population size of such trials was in the range of 20–100 patients and the time required for this phase ranged from 6 to 18 months [19, 20, 26]. The average cost of running such trials ranged from \$1.4 M to 6.6 M (across disease spaces) between 2004 and 2012.

Phase II

Phase II trials represent a larger cohort of patients with the targeted disease (traditionally 100–300 patients) and further define the efficacy and toxicities of a drug. The trials may be conducted as placebo-controlled, randomized trials in a “proof-of-concept” framework, but are usually limited to the specific number of patients dictated by pre-trial calculations of statistical power to assess a specific clinical endpoint. Such trials typically are completed in 6 months to 2 years. Approximately 70% of candidate therapies make it to Phase II trials but less than half will proceed to larger, and more costly, Phase III trials [20, 21].

Phase III

With favorable Phase II results, Phase III trials involving large, randomized, placebo-controlled trials often with comparison to the available market standard treatment, are initiated prior to application for NDA. Conventional drugs typically recruit approximately 300 to 3000 patients for such studies, which are completed over the course of 1–5 years (FDA) [20]. The criteria to reach Phase III trials are targeted to minimize the risk of a negative trial given the high costs associated with this phase (ranging from \$11 M to \$53 M between 2004–2012 across all disease spaces) [22]. Nevertheless, approximately 10% of Phase III trials fail to proceed to NDA [27].

Phase IV

After approval of an NDA, or as a stipulation of NDA from the FDA, further study may be pursued either to assess response in a select, high risk population, or to evaluate for rare side effects not seen in the smaller sample sizes of earlier trials. This phase is often unstructured in that post-marketing surveillance continues throughout the market presence of the drug, without specific trial parameters [20].

1.2.4 Challenges of Immunotherapy Trials

Immunotherapy as a class presents a variety of challenges to the conventional drug development process, especially when compared to cytotoxic drugs in the oncology space. This is in part due to their biologic nature, and in part due to the growing proclivity for multimodal therapy regimens to optimize response to treatment. As more candidate immune-oncologic therapies are identified, alternative strategies are being developed to address these challenges.

Dosing

One way in which immunotherapy differs from cytotoxic therapy is that the relationship between MTDs and DLTs is not likely to be elicited early during Phase I trials. In cytotoxic therapy trials, acute DLTs were typically identified in the first cycle of treatment at this stage. Immunotherapy is typically associated with more variable and later onset, immune-related adverse events (irAEs). The example of the checkpoint inhibitor, nivolumab, bears this out. In 576 patients with advanced melanoma, median time to onset of any grade irAEs was 5 weeks for skin toxicities, while renal toxicities occurred at a median of 15 weeks [28]. Or, in the example of pembrolizumab, median onset of hepatitis was 1.3 months while that of diarrhea was 3.5 months [29].

In order to address this challenge, one strategy is to extend the timeline over which the DLT is identified, thus altering the intent of what would be considered Phase I trials [19]. A structured format for dose-identification in the setting of late-onset irAEs is the time-to-event continual reassessment method (TITE-CRM). Using this method, enrollment is not staggered and subjects are evaluated throughout the trial for a DLT. Dose-toxicity modeling is continuously updated with each patient's data to guide dosing for subsequent patients. Such trial design facilitates faster identification of the MTD at an acceptable rate of toxicity, with less risk of underdosing patients. The statistical and computational complexity of TITE-CRM trials are notable, and may be addressed with an alternative design which incorporates Bayesian Optimal Interval Design (TITE-BOIN) wherein algorithmic dose adjustment rules are pre-determined, facilitating easy adjustment based on continuously available patient data in lieu of updated dose-toxicity modeling [30, 31].

Endpoints

The presumption for dosing drugs is the premise that more medication leads to better efficacy (more therapeutic effect) until a certain limit is reached due to increasing toxicity. This concept is referred to as monotonicity, and is applicable to cytotoxic chemotherapy, but may not be applicable to immune-oncology therapies. Instead of focusing on using toxicity to guide dosing, an alternative approach is to identify the minimum effective dose required to treat a disease. However, this approach requires practical endpoints. In the space of oncology, it is not realistic to combine traditional clinical endpoints of overall survival and disease-free survival, which may take months to years to assess, for identifying the optimal dosing of a candidate therapeutic in the conventional trial design structure. The endpoints thus far have focused on early measures of efficacy as well as pharmacokinetic and pharmacodynamic data. Measuring efficacy of treatments in immunotherapy is an area of development, in particular in biomarkers as well as imaging-based metrics [19, 24, 32].

Imaging

How a cancer responds to chemotherapy has traditionally been measured by imaging criteria, most widely in the form of the Response Evaluation Criteria in Solid Tumors (RECIST) criteria. These criteria standardize the axis and method of measuring a tumor site, with particular rules for the organ affected and minimum size of an imaging feature to be classified as disease. Using these measurements and standardized interpretations of progressive disease (i.e., appearance of new lesions on successive imaging studies or increase by 20% in size of the sum of the target lesions), clinicians are able to track response to therapy and counsel patients on next lines of therapy, if needed [33]. In the case of immunotherapy, however, experience has shown that size alone is not consistently predictive of immune

response or tumor response. This has been seen in Sipuleucel-T therapy, as well as with immune checkpoint inhibitors. A phenomenon known as pseudoprogression has been identified, wherein imaging metrics of tumors seem to be worsening (i.e., the tumor is larger on imaging), but the actual effect seen on biopsy of such a lesion reflects significant infiltration of the tumor with immune cells and very little or no residual cancer [34]. Although biopsy is a definitive means of reconciling the pathologic effects of immunotherapy, it is invasive, time consuming, and may not be an option based on the clinical status of certain patients.

To manage the challenge of monitoring response to immunotherapy, a new form of RECIST criteria called Immune RECIST (iRECIST) have been introduced. For example, one measure involves confirmation of tumor growth at least 4 weeks after initial imaging, no later than 8 weeks later. Prior to re-evaluation, growth in target lesions is termed “unconfirmed progressive disease” (iUCD), while persistent growth after re-evaluation is termed “confirmed progressive disease” (iCPD) [35]. Early experience with functional imaging such as positron-emission tomography (PET) shows that comparison of the functional volume of a tumor and the morphological volume as measured by CT can be used to reconcile pseudoprogression [36]. Interest in monoclonal antibody-labeled PET and MRI imaging has led to animal modeling but adoption for clinical management in humans is pending [34, 37, 38].

Biomarkers

Identifying optimal patient cohorts for treatment with immunotherapy is an important area of work in the field of biomarker development, especially in the context of cost and limited response rates to immunotherapy. In the case of immune checkpoint inhibitors, PD-L1 (programmed death-ligand 1) expression would be reasonably expected to correlate with response to a therapy targeting that association with immune cells. However, PD-L1 expression may vary within a particular tumor and thus be undersampled by biopsies. It may also vary from primary site to metastasis. Importantly, PD-L1 expression may be influenced by prior treatments, thus raising the importance of a recent tumor sample. DNA mutations are another biomarker that may predict response to immunotherapy. For example, mismatch repair gene mutations are correlated with improved response and duration of response to immune checkpoint inhibitors across a variety of malignancies [39].

The imprecision of imaging in immunotherapy as well as the concerns of cost and resource utilization lend additional support for the need to develop biomarkers to monitor response to immunotherapy. A small case series of melanoma patients describes characterization of circulating tumor DNA profiles at baseline and at subsequent time points during and after treatment with checkpoint inhibitors. This study found that the absence of detectable circulating tumor DNA or a greater than ten-fold decrease in levels by 12 weeks correlated with pseudoprogression [40]. As our understanding of immunology and immune-oncology expands and generates additional targets for therapy (Fig. 2), companion biomarker development is likely to develop and facilitate prediction and monitoring of response to such therapies.

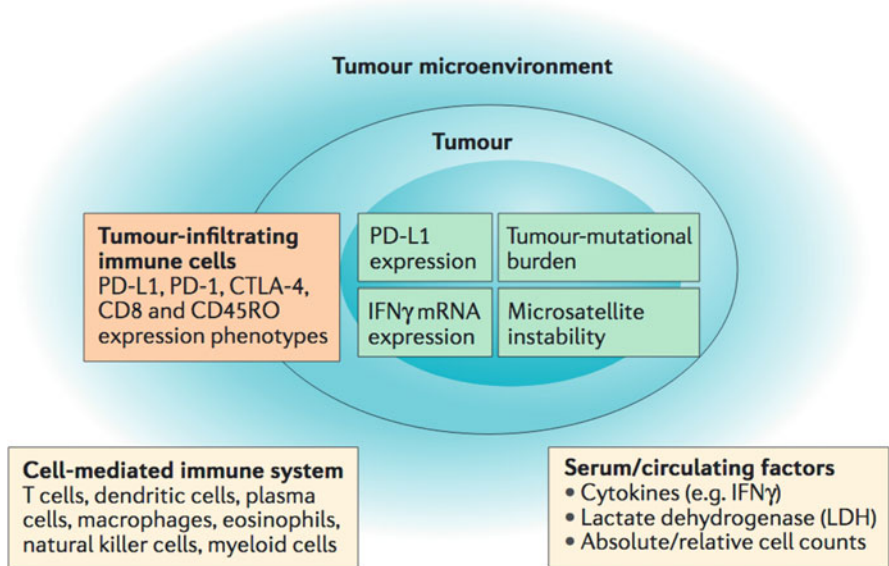


Fig. 2 Biomarker targets for immune-checkpoint inhibitor therapy. From Nishino [10]

Combinations

Improved understanding of the molecular mechanisms driving development, growth, and spread of cancer has led to a focus on multimodal treatment regimens. In the 1950s, select patients with multiple sites of cancer were treated with radiation, but disease regression was seen in untreated sites. This phenomenon was termed the abscopal effect, and was thought to represent an immunologic response to antigens released at the time of a cytotoxic treatment such as radiation [41, 42]. Since then, great interest remains in harnessing this effect. With the advent of immunotherapy, there is interest in combination of cytotoxic chemotherapy (with known activity in a particular cancer) to drive antigen release and immunotherapy to drive a systemic response with more targeted effect on cancer cells [43, 44].

However, trials of combination therapies raise their own challenges. For example, in planning dose adjustments in early phase trials, additional drugs in the combination regimen increases the possible dose combinations exponentially. Meanwhile, ascribing a toxicity to one specific medication becomes increasingly difficult. In order to avoid biased results, and to achieve appropriate statistical power, enlarging sizes of patient cohorts may be required [44–46].

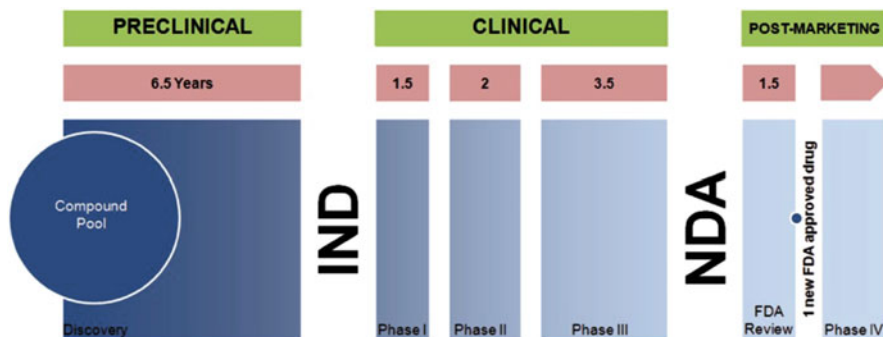


Fig. 3 Conventional framework for phases of FDA approval process. From Eifler [20]

Trends in Trial Design

These challenges prompt reassessment of the importance of strictly adhering to conventional trial design. Alternative trial designs are being formulated to capture the role of immunotherapy in manipulating a systemic function that has potential application to a broad range of disease. Expansion cohorts have garnered more attention as a means to expedite the transition to Phase II trials, wherein additional cohorts are recruited during so-called Phase I trials albeit with distinct objectives. Such objectives can range widely, from assessment of activity in a disease-specific setting, to evaluation of combination therapy with another medication, or even consideration of the predictive value of a biomarker. The concern with such an approach, however, is that it leads to larger populations of patients exposed to a medication which has an uncertain efficacy and toxicity profile [11]. The ideal manner in which to balance the benefits and risks of such a design will likely take further experience, although the FDA has drafted guidance around use of expansion cohorts [47]. Logically, expansion cohorts would still be restricted to patients with no other curative options (i.e., the usual population of conventional early phase trials). Each expansion cohort would have a specific justification for their involvement in the broader study along with a plan for analysis and termination of that cohort's participation [11, 48] (Fig. 3).

Incorporation of the above strategies for dosing, endpoints, combinations and expansion cohorts fits under the broad heading of seamless trial design. In addition to achieving greater efficiency, these strategies aim toward a more expeditious clinical trial phase with faster time to market. This could be significantly helpful to patients who have no other available treatment options [48]. However, it is important to maintain a sense of caution around implementing these trials in immunotherapy for a number of reasons. As discussed earlier, there is the potential for larger populations being exposed to an incompletely understood drug with expansion cohorts and seamless trial design, and potential for harm grows with larger Phase I cohorts. Outside of patient advocacy, there is also a concern of the complexity required to correctly execute such trials. Every change in protocol would

require updating disclosures and consents for trial participants, and consequently the administrative burden of the trial would be significant. Expansion cohorts and statistical analysis requires appropriate planning prior to the start of the trial. Given the nature of seamless trial design, omitting the typical pauses between phases effectively loses natural points of review by a regulatory agency such as the FDA. To avoid costly missteps, larger seamless trials require regular communication between the stakeholders. However, it is possible to imagine a point at which the FDA's capacity for such engagement will be exceeded. Also, pharmaceutical manufacturers are mindful that a seamless trial approved by the FDA may not generate adequate data to achieve approval in other markets. Thus, seamless trial design should involve the FDA (and other relevant regulatory agencies) early in planning and throughout the trial itself [11, 48–50].

1.3 Summary

Development of novel immunotherapy agents is a complex process, in part due to the complexity of the relationship between tumor cells the TME, and the numerous components of the immune system. A rapidly shifting clinical trial and regulatory landscape will play a role in the efficiency with which immunotherapy agents can be brought to market, but these challenges can be mitigated with appropriate planning and regular communication with the regulatory agency involved.

References

1. Silvestri, I., Cattarino, S., Giantulli, S., Nazzari, C., Collalti, G., Sciarra, A.: A perspective of immunotherapy for prostate cancer. *Cancers (Basel)*. **8**, 7 (2016). <https://doi.org/10.3390/cancers8070064>
2. Murphy, J.F.: Frontiers in cancer immunotherapy. In: Rezaei, N. (ed.) *Cancer Immunology: Bench to Bedside Immunotherapy of Cancers*, pp. 1–17. Springer-Verlag Berlin Heidelberg, New York (2015)
3. Pathogens, Infection, and Innate Immunity: In: Alberts, B.J.A., Lewis, J., Raff, M., Roberts, K., Walter, P. (eds.) *Molecular Biology of the Cell*, 4th edn. Garland Science, New York (2002)
4. The Adaptive Immune System: In: JA, A.B., Lewis, J., Raff, M., Roberts, K., Walter, P. (eds.) *Molecular Biology of the Cell*, 4th edn. Garland Science, New York (2002)
5. Yu, S.S., Ballas, L.K., Skinner, E.C., Dorff, T.B., Sadeghi, S., Quinn, D.I.: Immunotherapy in urothelial cancer, part 2: adjuvant, neoadjuvant, and adjunctive treatment. *Clin. Adv. Hematol. Oncol.* **15**(7), 543–551 (2017)
6. Guo, Q., Huang, F., Goncalves, C., Del Rincon, S.V., Miller Jr., W.H.: Translation of cancer immunotherapy from the bench to the bedside. *Adv. Cancer Res.* **143**, 1–62 (2019). <https://doi.org/10.1016/bs.acr.2019.03.001>
7. Apostolico Jde, S., Lunardelli, V.A., Coirada, F.C., Boscardin, S.B., Rosa, D.S.: Adjuvants: classification, modus operandi, and licensing. *J Immunol Res.* **2016**, 1459394 (2016). <https://doi.org/10.1155/2016/1459394>

8. Manjunath, A., Brenton, T., Wylie, S., Corbishley, C.M., Watkin, N.A.: Topical therapy for non-invasive penile cancer (Tis)-updated results and toxicity. *Transl. Androl. Urol.* **6**(5), 803–808 (2017). <https://doi.org/10.21037/tau.2017.06.24>
9. Redelman-Sidi, G., Glickman, M.S., Bochner, B.H.: The mechanism of action of BCG therapy for bladder cancer—a current perspective. *Nat. Rev. Urol.* **11**(3), 153–162 (2014). <https://doi.org/10.1038/nrurol.2014.15>
10. Nishino, M., Ramaiya, N.H., Hatabu, H., Hodi, F.S.: Monitoring immune-checkpoint blockade: response evaluation and biomarker development. *Nat. Rev. Clin. Oncol.* **14**(11), 655–668 (2017). <https://doi.org/10.1038/nrclinonc.2017.88>
11. Hobbs, B.P., Barata, P.C., Kanjanapan, Y., Paller, C.J., Perlmutter, J., Pond, G.R., et al.: Seamless designs: current practice and considerations for early-phase drug development in oncology. *J. Natl. Cancer Inst.* **111**(2), 118–128 (2019). <https://doi.org/10.1093/jnci/djy196>
12. Restifo, N.P., Dudley, M.E., Rosenberg, S.A.: Adoptive immunotherapy for cancer: harnessing the T cell response. *Nat. Rev. Immunol.* **12**(4), 269–281 (2012). <https://doi.org/10.1038/nri3191>
13. Handy, C.E., Antonarakis, E.S.: Sipuleucel-T for the treatment of prostate cancer: novel insights and future directions. *Future Oncol.* **14**(10), 907–917 (2018). <https://doi.org/10.2217/fon-2017-0531>
14. Beavis, P.A., Darcy, P.K.: CAR T cells take Centre stage. *Clin. Transl. Immunol.* **8**(7), e01068.-e. (2019). <https://doi.org/10.1002/cti2.1068>
15. Grivas, P., Koshkin, V.S., Pal, S.K.: Cancer vaccines at the age of immune checkpoint inhibitors: reasonable approach as combination therapy in advanced urothelial carcinoma? *Ann. Oncol.* **28**(4), 680–682 (2017). <https://doi.org/10.1093/annonc/mdx063>
16. Pal, S.K., Agarwal, N., Dizman, N., Sonpavde, G.: Vaccine therapy in renal cell carcinoma: attempting to leap over a rising bar. *Lancet Oncol.* **17**(11), 1477–1478 (2016). [https://doi.org/10.1016/s1470-2045\(16\)30493-4](https://doi.org/10.1016/s1470-2045(16)30493-4)
17. Passariello, M., Camorani, S., Vetrei, C., Cerchia, L., De Lorenzo, C.: Novel human bispecific aptamer-antibody conjugates for efficient cancer cell killing. *Cancers (Basel)*. **11**, 9 (2019). <https://doi.org/10.3390/cancers11091268>
18. Vlachostergios, P.J., Jakubowski, C.D., Niaz, M.J., Lee, A., Thomas, C., Hackett, A.L., et al.: Antibody-drug conjugates in bladder cancer. *Bladder Cancer*. **4**(3), 247–259 (2018). <https://doi.org/10.3233/blc-180169>
19. Wages, N.A., Chiuzan, C., Panageas, K.S.: Design considerations for early-phase clinical trials of immune-oncology agents. *J. Immunother. Cancer*. **6**(1), 81 (2018). <https://doi.org/10.1186/s40425-018-0389-8>
20. Eifler, A.C., Thaxton, C.S.: Nanoparticle therapeutics: FDA approval, clinical trials, regulatory pathways, and case study. *Methods Mol. Biol.* 2011/03/23 ed., 325–338 (2011)
21. Artaud C, Kara L, Launay O. Vaccine development: from preclinical studies to phase 1/2 clinical trials. In: Arieu F, Gay F, Ménard R (eds). *Malaria Control and Elimination*. 2019/07/04 ed. *Methods Mol. Biol.* 165–176 (2013)
22. Sertkaya, A., Wong, H.H., Jessup, A., Beleche, T.: Key cost drivers of pharmaceutical clinical trials in the United States. *Clin. Trials*. **13**(2), 117–126 (2016). <https://doi.org/10.1177/1740774515625964>
23. FDA. Guidance for industry: expedited programs for serious conditions—drugs and biologics. In: Services USDoHaH, editor. Maryland (2014)
24. Ireson, C.R., Alavijeh, M.S., Palmer, A.M., Fowler, E.R., Jones, H.J.: The role of mouse tumour models in the discovery and development of anticancer drugs. *Br. J. Cancer*. **121**(2), 101–108 (2019). <https://doi.org/10.1038/s41416-019-0495-5>
25. Finkelstein, S.E., Heimann, D.M., Klebanoff, C.A., Antony, P.A., Gattinoni, L., Hinrichs, C.S., et al.: Bedside to bench and back again: how animal models are guiding the development of new immunotherapies for cancer. *J. Leukoc. Biol.* **76**(2), 333–337 (2004). <https://doi.org/10.1189/jlb.0304120>
26. Mozgunov, P., Jaki, T., Paoletti, X.: Randomized dose-escalation designs for drug combination cancer trials with immunotherapy. *J. Biopharm. Stat.* **29**(2), 359–377 (2019). <https://doi.org/10.1080/10543406.2018.1535503>

27. Lipsky, M.S., Sharp, L.K.: From idea to market: the drug approval process. *J. Am. Board Fam. Pract.* **14**(5), 362–367 (2001)
28. Weber, J.S., Hodi, F.S., Wolchok, J.D., Topalian, S.L., Schadendorf, D., Larkin, J., et al.: Safety profile of nivolumab monotherapy: a pooled analysis of patients with advanced melanoma. *J. Clin. Oncol.* **35**(7), 785–792 (2017). <https://doi.org/10.1200/jco.2015.66.1389>
29. Squibb B-M. Opdivo Package Insert https://packageinserts.bms.com/pi/pi_opdivo.pdf (2019)
30. Garrett-Mayer, E.: The continual reassessment method for dose-finding studies: a tutorial. *Clin. Trials.* **3**(1), 57–71 (2006). <https://doi.org/10.1191/1740774506cn1340a>
31. Yuan, Y., Lin, R., Li, D., Nie, L., Warren, K.E.: Time-to-event Bayesian optimal interval design to accelerate phase I trials. *Clin. Cancer Res.* **24**(20), 4921–4930 (2018). <https://doi.org/10.1158/1078-0432.Ccr-18-0246>
32. Mazarella, L., Duso, B.A., Trapani, D., Belli, C., D'Amico, P., Ferraro, E., et al.: The evolving landscape of 'next-generation' immune checkpoint inhibitors: a review. *Eur. J. Cancer.* **117**, 14–31 (2019). <https://doi.org/10.1016/j.ejca.2019.04.035>
33. Calandri, M., Solitto, F., Angelino, V., Moretti, F., Veltri, A.: The role of radiology in the evaluation of the immunotherapy efficacy. *J. Thorac. Dis.* **10**(Suppl 13), S1438–S1s46 (2018). <https://doi.org/10.21037/jtd.2018.05.130>
34. Vrankar, M., Unk, M.: Immune RECIST criteria and symptomatic pseudoprogression in non-small cell lung cancer patients treated with immunotherapy. *Radiol. Oncol.* **52**(4), 365–369 (2018). <https://doi.org/10.2478/raon-2018-0037>
35. Seymour, L., Bogaerts, J., Perrone, A., Ford, R., Schwartz, L.H., Mandrekar, S., et al.: iRECIST: guidelines for response criteria for use in trials testing immunotherapeutics. *Lancet Oncol.* **18**(3), e143–ee52 (2017). [https://doi.org/10.1016/S1470-2045\(17\)30074-8](https://doi.org/10.1016/S1470-2045(17)30074-8)
36. Jreige, M., Letovanec, I., Chaba, K., Renaud, S., Rusakiewicz, S., Cristina, V., et al.: (18)F-FDG PET metabolic-to-morphological volume ratio predicts PD-L1 tumour expression and response to PD-1 blockade in non-small-cell lung cancer. *Eur. J. Nucl. Med. Mol. Imaging.* **46**(9), 1859–1868 (2019). <https://doi.org/10.1007/s00259-019-04348-x>
37. Lee, T.S., Song, I.H., Shin, J.I., Park, Y.S., Kim, J.Y., Kim, K.I., et al.: PET imaging biomarkers of anti-EGFR immunotherapy in Esophageal squamous cell carcinoma models. *Cell.* **7**(11) (2018). <https://doi.org/10.3390/cells7110187>
38. Mohanty, S., Yerneni, K., Theruvath, J.L., Graef, C.M., Nejadnik, H., Lenkov, O., et al.: Nanoparticle enhanced MRI can monitor macrophage response to CD47 mAb immunotherapy in osteosarcoma. *Cell Death Dis.* **10**(2), 36 (2019). <https://doi.org/10.1038/s41419-018-1285-3>
39. Otoshi, T., Nagano, T., Tachihara, M., Nishimura, Y.: Possible biomarkers for cancer immunotherapy. *Cancers (Basel).* **11**, 7 (2019). <https://doi.org/10.3390/cancers11070935>
40. Lee, J.H., Long, G.V., Menzies, A.M., Lo, S., Guminski, A., Whitbourne, K., et al.: Association between circulating tumor DNA and pseudoprogression in patients with metastatic melanoma treated with anti-programmed cell death 1 antibodies. *JAMA Oncol.* **4**(5), 717–721 (2018). <https://doi.org/10.1001/jamaoncol.2017.5332>
41. Ngwa, W., Irabor, O.C., Schoenfeld, J.D., Hesser, J., Demaria, S., Formenti, S.C.: Using immunotherapy to boost the abscopal effect. *Nat. Rev. Cancer.* **18**(5), 313–322 (2018). <https://doi.org/10.1038/nrc.2018.6>
42. Mole, R.H.: Whole body irradiation; radiobiology or medicine? *Br. J. Radiol.* **26**(305), 234–241 (1953). <https://doi.org/10.1259/0007-1285-26-305-234>
43. Melosky, B., Juergens, R., Hirsh, V., McLeod, D., Leigh, N., Tsao, M.S., et al.: Amplifying outcomes: checkpoint inhibitor combinations in first-line non-small cell lung cancer. *Oncologist.* (2019). <https://doi.org/10.1634/theoncologist.2019-0027>
44. Savitsky, K., Yu, X.: Combined strategies for tumor immunotherapy with nanoparticles. *Clin. Transl. Oncol.* (2019). <https://doi.org/10.1007/s12094-019-02081-3>
45. Paller, C.J., Bradbury, P.A., Ivy, S.P., Seymour, L., LoRusso, P.M., Baker, L., et al.: Design of phase I combination trials: recommendations of the clinical trial design task force of the NCI investigational drug steering committee. *Clin. Cancer Res.* **20**(16), 4210–4217 (2014). <https://doi.org/10.1158/1078-0432.Ccr-14-0521>

46. Wages, N.A., Slingluff Jr., C.L., Petroni, G.R.: A phase I/II adaptive design to determine the optimal treatment regimen from a set of combination immunotherapies in high-risk melanoma. *Contemp. Clin. Trials*. **41**, 172–179 (2015). <https://doi.org/10.1016/j.cct.2015.01.016>
47. FDA. Expansion cohorts: use in first-in-human clinical trials to expedite development of oncology drugs and biologics guidance for industry. In: Services USDoHaH, editor. Maryland (2018)
48. Mansinho, A., Boni, V., Miguel, M., Calvo, E.: New designs in early clinical drug development. *Ann. Oncol.* (2019). <https://doi.org/10.1093/annonc/mdz191>
49. Prowell, T.M., Theoret, M.R., Pazdur, R.: Seamless oncology-drug development. *N. Engl. J. Med.* **374**(21), 2001–2003 (2016). <https://doi.org/10.1056/NEJMp1603747>
50. FDA. Adaptive Designs for Clinical Trials of Drugs and Biologics: Guidance for Industry. Maryland (2018)

Intravital Optical Imaging to Monitor Anti-Tumor Immunological Response in Preclinical Models



Gregory M. Palmer, Yuxiang Wang, and Antoine Mansourati

1 Introduction

Intravital microscopy has a long history of application to studying the tumor microenvironment, and in particular angiogenesis and vascular function. The technique has a long history dating back to the origins of the microscope [1], with modern techniques involving window chamber models following JC Sandison's use of a transparent window to visualize vascular growth implanted in a rabbit ear [2]. This was later adapted to tumor studies [3] and further refined by the development of the dorsal skin fold window chamber [4], which has been in widespread use in oncology studies. This field has seen a wide range of advancements in terms of imaging techniques, animal/tumor models, sources of contrast, and image analysis methods [5], which will be the focus of this chapter. In addition, in light of the unique capabilities of intravital microscopy to characterize functional parameters including immune function, as well as nanoparticle distribution and tissue interaction, and given the recent interest in these areas and the focus of this book, these applications will receive special emphasis in this treatment.

2 Immuno-Oncology

The immune system has long been speculated to play an important role in both suppressing the incidence of cancer, and in playing an important role in its treatment

G. M. Palmer (✉)

Department of Radiation Oncology, Duke University Medical Center, Durham, NC, USA

e-mail: greg.palmer@duke.edu

Y. Wang · A. Mansourati

Duke University School of Medicine, Durham, NC, USA

© Springer Nature Switzerland AG 2021

T. Vo-Dinh (ed.), *Nanoparticle-Mediated Immunotherapy*, Bioanalysis 12,

https://doi.org/10.1007/978-3-030-78338-9_4

outcomes. As early as 1908 Ehrlich postulated the role of the body's defense system in suppressing the development of cancer [6]. This is known today as immunosurveillance, which fits within the broader categorization of immunoediting [7]. This occurs in three phases, each of which is amenable to detection and characterization by intravital microscopy and so will be briefly described here. First, is the elimination phase, wherein the innate and adaptive immune systems together identify and destroy tumors before they become clinically detectable. The process of carcinogenesis involves mutation a wide range of stressors, which can thus activate the immune response. This has become widely accepted in particular as transgenic mouse models have allowed specific manipulations of immune function [8], and natural killer (NK) and cytotoxic T cells have been shown to play important roles in eliminating incipient tumors [7]. During the elimination phase, highly immunogenic mutations which would otherwise lead to cancer, are thought to be suppressed and eliminated prior to clinical observability, while some less immunogenic tumors are able proliferate and suppress the immune response in a variety of ways. This is known as immunoevasion, and can be achieved by a variety of mechanisms, including suppression of tumor antigens or MHC class I expression (which presents antigens to the immune system), release of immunosuppressive cytokines (e.g. IL-10, TGF- β), and expression of immune checkpoint ligands (e.g. PD-L1). Although it is relatively challenging to develop models suitable for imaging this phase of cancer initiation, carcinogen induced or genetically engineering mouse models enable predictable development of cancer, and metastatic colonization of tumor cells is also very amenable to intravital microscopy, e.g. [9–11]. Thus, these are active areas of research and sources of great interest for intravital imaging.

The second phase is equilibrium, at which phase tumors remain relatively static in size as a result of immune suppression of tumor progression [12]. There is also evidence for dormant metastatic tumor colonies or single cells that may be suppressed, in part, by immune function. Koebel et al. established this using immunocompetent mice treated with a low dose carcinogen 3-methylcholanthrene (MCA), which did not develop observable tumors. When the immune system was ablated, tumors rapidly appeared in half of the animals that had previously been suppressed in a dormant state [13]. It has proved relatively challenging however, to establish mouse models with stable disease controlled by immune function.

The final phase is escape, wherein tumors effectively escape control by the immune system. This can occur by a variety of mechanisms by which the tumor evades the immune system, including reduced tumor recognition (e.g. via loss of MHC class I), increased survival/resistance to cell death, or development of an immunosuppressive microenvironment. In this phase, the immune system loses the ability to control tumor growth. There is a complex interplay between anti-tumor immune function and pathologic activation of inflammatory and immunosuppressive pathways [14]. Intravital imaging has played a key role in expanding our understanding of how pathologic activation of inflammatory pathways as well as anti-tumor immune responses, can either act to support or inhibit tumor growth, angiogenesis, treatment resistance, invasion and metastasis [1, 9, 10, 14–16].

A renewed understanding of the role of the immune system and the great potential of enhancing anti-tumor immune function in cancer therapy has followed

from a series of successful clinical trials [17, 18]. These include notably the immune checkpoint inhibitors, as well as adoptive cell transfer (e.g. CAR T cell therapy), cancer vaccines (e.g. Sipuleucel-T), and cytokine or targeted therapies. Many of these strategies have been characterized using intravital microscopy or combined with nanoparticle-based approaches, as will be described in the following sections.

2.1 Use of Nanoparticles in Immune Therapy

The use of nanotechnology in tumor immune therapy strategies is driven by a number of uniquely favorable properties related to the ability of nanoparticles to effectively carry and deliver immune-modulating therapies across physical and biological barriers imposed by the tumor microenvironment [19–21]. These steps include delivery to the organ of interest (sufficiently avoiding clearance or uptake in other organs), entrance into the tissue site of interest (commonly via vascular extravasation), and finally delivery to the cellular or molecular target (via cellular uptake or binding). Tumors present unique challenges to this process due to their generally disorganized and inefficient vasculature and defense mechanisms such as multidrug resistance (MDR) which can effectively eliminate drugs from the tumor cells [22, 23], or anti-apoptotic mechanisms, which inhibit cell death and promote treatment resistance [24]. Nanoparticles are appealing in overcoming these physical and biological limitations. For example, through active or passive targeting, nanoparticles can deliver drug payloads more effectively to the specific target of interest, such as the lymph nodes or tumor cells [25–27]. Nanoparticles are also actively taken up by macrophages and dendritic cells via phagocytosis, which facilitates targeted activation of antigen presenting cells as well as the innate immune system [21, 28]. In addition, through combination therapy combining a payload drug with an inhibitor of MDR or anti-apoptotic pathways, it is possible to enhance therapeutic response through nanotechnology mediated treatments [19, 29].

3 Imaging Techniques

3.1 Advantages of Intravital Techniques

Intravital imaging has a number of key advantages that are particularly suitable for characterizing in vivo immune responses and tumor interactions. Notably, the ability of intravital microscopy to quantitatively assess a wide variety of specific physiologic, molecular, and cellular targets at high resolution. Longitudinal measurement of living systems enables dynamic characterization of the cascade of events relevant to tumor-immune interactions and the impact of therapy [14,

30, 31]. This section will briefly review some of the more common imaging modalities utilized in intravital microscopy along with their respective strengths and weaknesses. These are suitable for characterizing the most commonly utilized sources of contrast in intravital microscopy, namely fluorescence and absorption based contrast.

Fluorescence microscopy capitalizes on the use of fluorescent probes. These are molecules that absorb light in a wavelength dependent manner, which promotes an electron to an excited state. Some energy is lost as the electron undergoes nonradiative relaxation to the lowest vibrational energy level of the excited state. Then the fluorophore may emit a fluorescent photon at a longer wavelength (lower energy). This change in wavelength, referred to as the Stokes shift, facilitates separation of fluorescent light from the incident light by means of a wavelength dependent filter. This forms the basis for fluorescence microscopy. Because each fluorophore has a characteristic absorption and fluorescence emission spectrum, multiple fluorophores can be used in the same sample separated by wavelength. One important consideration in selecting a fluorophore for use *in vivo* is the optical properties of the tissue as well as the tissue autofluorescence (native fluorescence of biological molecules). Generally speaking, absorption and scattering decreases with increasing wavelength, allowing for deeper penetration of red and particularly near infrared light. There is a large drop off in hemoglobin absorption particularly above 600 nm, with a minimum in tissue attenuation occurring between approximately 700–900 nm, which is referred to as the near infrared window. In addition to this, and even more importantly for superficial imaging, is a reduction in background autofluorescence at longer wavelengths, which allows for much more sensitive detection of the fluorophore of interest. For this reason, red and far-red sources of fluorescence are ideal for all intravital imaging applications, and are essential for any deep tissue imaging.

3.2 Wide Field Microscopy and Imaging

The simplest and most widely available approach for intravital microscopy is the conventional wide field fluorescence microscope. This is useful for superficial imaging of exposed tissue, as with window chamber models, and is capable of imaging a wide range of functional, morphological, and molecular sources of contrast through use of fluorescence probes and intrinsic sources of tissue contrast [32]. However, it has limitations including that it has poor depth penetration, and so is limited to the very superficial layers of tissue on the order of <20–50 μm , beyond which, light scattering limits the ability to achieve sharp focus. Another limitation is the lack of depth sectioning, so any fluorescence signal generated outside of the focal plane is collected and contributes to the out of focus background signal. This makes imaging and resolution of fine details challenging in a sample with dense three dimensional fluorophore distribution (e.g. with fluorophore distributed throughout an optically thick tumor). Nevertheless, the advantage of simplicity and

widespread availability of such microscopes makes it a workhorse system for many imaging applications.

Brightfield microscopy is another approach that is useful in particular in resolving vasculature. This can be done in transmission or reflection mode, and is sensitive to attenuation of light by the sample, in particular absorption by blood in the visible wavelength range (described in more detail below). Each of these approaches can also be performed via either a conventional microscope or endoscopic imaging system.

3.3 Confocal Microscopy and Structured Illumination

Confocal imaging was originally invented by Marvin Minsky in 1955, with the goal of overcoming the resolution and depth limitations of available microscopes to facilitate studying brain function in intact tissues [33]. The principle behind confocal microscopes is that the illumination and fluorescence emission pass through pinholes in conjugate focal planes, such that out of focus light is rejected from the detector (such light is focused out of the plane of the pinhole). With the advent of high power, collimated, monochromatic light sources (lasers) such microscopes became more practical and have been a workhorse of intravital microscopy as well as endoscopy. This approach facilitated, for the first time, depth sectioned optical imaging in living systems, by which the imaging system selectively detected light originating from a single focal plane. This represents a tremendous advantage when imaging living tissue in order to be able to resolve cells and other structures in three dimensions in the native environment. Because of the use of the pinhole, and tightly focused light, only a single voxel of information is acquired at a time, and the sample must be scanned, typically achieved using movable mirrors to deflect the illumination spot over an x,y grid, and so raster scan the sample to build up a 2-dimensional data set. Including changes in the focal plan, a 3-dimensional data set can be obtained. This enables depth resolved imaging typically on the order of 100–250 μm maximum depth, dependent on the tissue optical properties and signal. With multiplexing of fluorophores at different wavelengths, this technique enables imaging tumor and immune cells, as well as other sources of contrast in their native environment in intact tissue. As such one is able to monitor tumor growth, angiogenesis, lymphocyte infiltration, tumor associated macrophages, and other relevant endpoints, to be discussed in more detail in the next sections [34–36].

Related to this, spinning disk confocal is an approach by which rather than a single pinhole, there is an array of pinholes on a disk, such that multiple spots can be imaged simultaneously. By spinning the disk, the sample can be radially scanned to build a 2-dimensional image. Another approach is structured illumination, in which a pattern is projected onto the sample (typically alternating bright and dark lines). These are swept across the sample and processed to reject any out of focus signal, such that only pixels showing sharp contrast of the pattern projected onto the focal plane is retained. An example of such an image is shown in Fig. 1, which

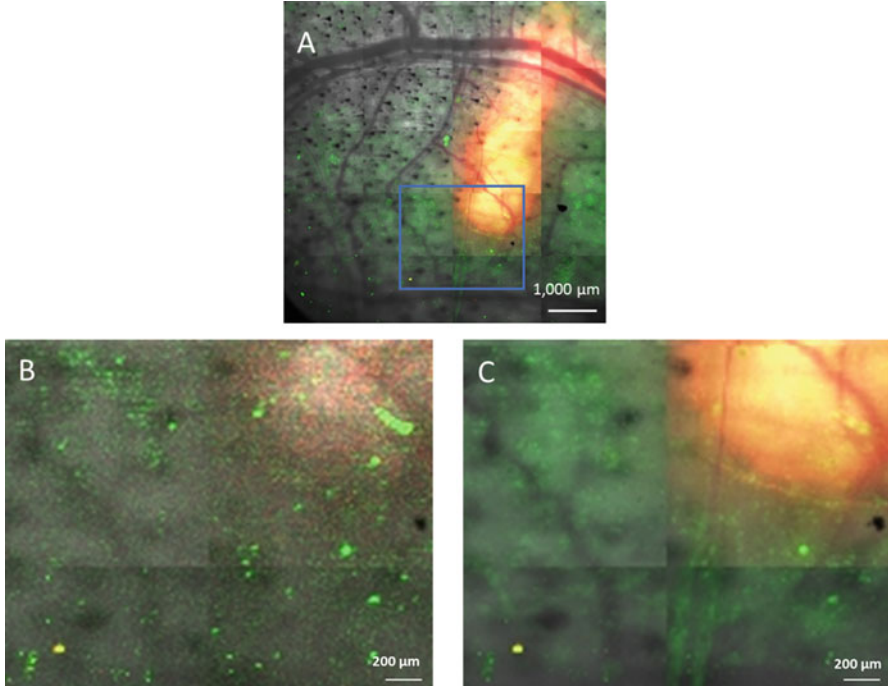


Fig. 1 Intravital imaging of a CX3CR1-GFP reporter mouse demonstrates presence of myeloid cell infiltration to the tumor 8 days following combination hyperthermia and immune checkpoint inhibition. Tumor cells are shown in red, with myeloid in green, overlaid on the bright field image in grayscale (**a**). Also shown is the difference between optically sectioned GFP imaging using the Zeiss Apotome.2 structured illumination system (**b**), as compared to the conventional fluorescence image (**c**). It can be seen that in the conventional fluorescence image, there is diffuse out of focus signal particularly prevalent in the tumor region (upper right), whereas in the optically sectioned image, individual cells and cell clusters in the focal plane can be resolved

also demonstrates the difference between optically sectioned and conventional fluorescence imaging.

3.4 Multiphoton Microscopy

Multiphoton microscopy is conceptually similar to a confocal, in that a tightly focused laser spot is scanned across the sample, however, in this case, depth sectioning is achieved not with an emission pinhole, but through a non-linear absorption process. This technique was first developed and applied to living systems by Denk, Strickler and Webb [37], and has since found widespread adoption for intravital imaging. At very high intensity, a molecule can absorb two or more photons simultaneously to excite the fluorophore to its excited state at lower energy

(longer wavelength) than would typically be absorbed. In this way, the fluorophore is efficiently excited only where the intensity is high enough, namely at the focal point. The key advantages of this approach include the use of longer wavelength light, which minimizes phototoxicity, and has increased penetration distance, as well as eliminating out of focus signal generation. For these reasons, the penetration depth is greater than confocal, typically in the range of 300–500 μm in tumors. The disadvantage is that it is generally more expensive and complex, requiring a high power, pulsed laser source. Multiphoton imaging is suitable for most of the same sources of contrast as the above, and has been applied for a wide range of immunology, cancer biology, and therapeutic endpoints [38–41].

3.5 Photoacoustic Microscopy

Photoacoustic microscopy is a more recent innovation that derives contrast based on the photoacoustic effect. This is the generation of ultrasonic waves due to the absorption of light by a chromophore. The details of this approach are reviewed elsewhere [42–46], but in brief, a pulsed or modulated laser is used to illuminate the tissue sample, which is absorbed by chromophores within the tissue. These produce ultrasound waves within the tissue that propagates through the tissue to be collected by an ultrasound transducer to produce an image. This can be related to the chromophore concentration and distribution through modeling techniques. It has the key advantage of having the high molecular specificity of optical imaging (due to wavelength specific optical absorption) combined with the penetration and resolution of ultrasound imaging. This can be applied to virtually any source of absorption contrast including many fluorophores fluorescence imaging. Notably intrinsic optical contrast due to hemoglobin absorption in the visible and NIR wavelength range enables quantification of vascular morphology and oxygen saturation, while exogenous absorbers in the NIR (where native tissue absorption is low) enable molecular imaging with high sensitivity and specificity (see below for more information on contrast mechanisms). This is a growing area of research with great potential to expand our knowledge of tumor immune interactions particularly as it facilitates *in vivo*, and whole animal imaging without the need for window chambers.

3.6 Other Microscopy Techniques

A wide variety of other advanced microscopy techniques are being developed or are commercially available that have relevance to some aspects of immune function that will not be described in detail here but are referenced for further interest. This includes optical coherence tomography (OCT) which is based on detection of reflected light using an interferometry based approach [47, 48]. Because scattering

is the primary source of contrast, it is more suited for imaging tissue morphology, however recent innovations enable characterization of dynamic signals such as vascular flow and absorption contrast such as hemoglobin oxygen saturation. Thus, functional indicators relevant to immune function can be characterized with this approach, which has distinct advantages of greater penetration depth and high resolution at depth (1–2 mm penetration). Other more recent innovations include nonlinear and pump-probe approaches to quantify absorption contrast, and super-resolution techniques for molecular imaging [34, 49–51].

4 Models and Methods of Quantifying Immune Function

In applying any approach to characterize tumor immunology, a key consideration is the biologic system to be studied as a means of understanding human disease. This is primarily achieved using mouse models, although some other models and even clinical approaches have been implemented. A wide range of model systems and sources of contrast are possible so this is not meant as a comprehensive resource but to discuss some of the more commonly employed and notable findings.

4.1 *Window Chamber Models*

As described above, window chamber models are essential for a variety of imaging approaches due to the inherent limitations on penetration depth of light. The dorsal skin fold window chamber is likely the most commonly utilized model for intravital microscopy and the first developed for use in oncology studies. It has a number of practical advantages, including relative simplicity of implementation and surgical technique required, and the relatively minimally invasive nature of the procedure, as it only involves the skin and is not very technically challenging. In addition, due to the thin and relatively transparent window chamber (single skin layer thickness), it is easily made compatible with standard microscopy techniques including transmission brightfield microscopy [32]. Limitations of this model include that the stromal cells present in the orthotopic tumor microenvironment are not present, and secondly, that the surgical procedure could itself induce an inflammatory response which could complicate immunology studies in particular, although this would be a feature common to other surgical window sites as well.

To better assess the immune microenvironment within the context of the original organ site, window chamber models have also been developed at other organ sites. These generally involve surgical dissection to expose the organ of interest and placement of a coverglass mounted on a frame, or alternatively a flexible film affixed to the surgical fenestration. One of the first such models was the mammary window for intravital imaging of breast cancer models originally developed by Shan et al. and later adapted to multimodality and immune cell imaging [52–55]. Another

model in widespread use is the cranial thinned skull or window chamber model, commonly employed for brain tumor research as well as brain function studies [56]. The thinned skull model removes the skin and some of the cortical bone such that the underlying brain can be imaged. This provides a minimally invasive approach amenable to long term or minimally disruptive imaging. The cranial window generally involves removal of a piece of the full thickness of the skull, exposing the cortex, and in some cases removing the dura mater for optimal image quality. A coverglass can then be affixed directly to the skull which creates a long term stable system for imaging. This type of approach has been previously applied to imaging nanoparticle uptake in the brain, as well as the initiation and development of brain metastases, and immune function in the tumor microenvironment [57–59]. Other models have been developed suitable for a wide range of tumor sites including the lungs [60–62], liver [63, 64], cremaster, lymph nodes, bone marrow, spleen, muscle, and skin [1, 65].

There are also a few sites suitable for intravital microscopy without a window chamber worth mentioning. One such site is the ear pinna. At this site, the skin is thin enough to facilitate intravital microscopy without the need for a surgical intervention, and this model has been used for a wide range of studies [66–68]. It is also possible to grow tumors there ectopically, the primary disadvantage being the extremely small space for tumor growth, which limits the size and duration for which tumors can be studied. Another option is the mucosa, for example the oral mucosa is accessible to intravital microscopy and facilitates imaging the vasculature and leukocyte interaction which has been studied for radiation effects on normal tissue [69]. Other sites are accessible by endoscopy or laparoscopy including the gastrointestinal tract and bladder and can be serially imaged, again without the need for permanent surgical placement of a window chamber which minimizes disruption of the tissue and immune function [70–73]. However, such approaches are more limited in the types of imaging that can be performed, tight size constraints, and ease of implementation, and there can be practical limitations in how readily the tumors can be identified and monitored.

4.2 Genetic Reporter Models of Immune Cells

One approach for intravital imaging of immune cells and function is the use of fluorescent or bioluminescent reporters. These enable specific labeling of immune cells or immune cell subsets, taking advantage of immune-specific promoters in genetically modified animals. There are many such models in the literature, but we will highlight a few of the more widely available and utilized models as well as a broad sample of imaging of different types of immune cells.

One such model is the widely utilized and commercially available CX3CR1-GFP model [74] (commercially available via Jackson Labs). This model was developed by replacing the CX3CR1 gene with a green fluorescent reporter in the C57BL/6 background strain. In this way GFP is expressed in cells that normally would express

CX3CR1, in particular monocytes, microglial cells, macrophages, and some NK and dendritic cells. This model has been used in a wide range of immunological studies, ranging from developmental biology to cancer immune therapy. In another model studying macrophage function, it was demonstrated that tumor associated macrophages contributed to increased vascular permeability as assessed by *in vivo* fluorescence imaging of leakage of a macromolecular fluorescent dextran [15]. The same study found that the recruitment of macrophages by CCR2 expression led to recruitment of CCR2+ monocytic cells to the tumor and contributed significantly to chemotherapeutic resistance [15]. These studies of macrophage function point to the unique ability of intravital imaging to elucidate complex interactions between tumor cells, the immune system, the tumor microenvironment, and therapy at a cellular and molecular level [75].

Other examples of models that have been reported in the literature include a neutrophil-specific reporter consisting of a Ly6G locus with a knockin expressing Cre recombinase and the red fluorescent reporter tdTomato [76]. There are also approaches for imaging natural killer (NK) cells, for example using a CXCR6-GFP reporter construct [77, 78]. Models have also been developed for imaging CD8+ T cells [79] and dendritic cells [80, 81]. This is not meant to be a comprehensive listing of existing models, but to point out that models exist for a wide range of immune cells subtypes, and given the rapid expansion of available tools for genetic manipulation, more and more models are being generated with different specific characteristics and applications. A number of existing reviews provide a more comprehensive overview on this topic [82–84].

A challenge however in applying such models is that depending on the reporter model chosen, multiple types or subsets of cells may express the reporter. One solution is to combine multiple reporters or to use functional approaches to distinguishing them, for example by use of nanoparticles that are preferentially phagocytosed by specific macrophage subtypes, which has been used to functionally characterize macrophage subpopulations [85]. In another recent example, a dual reporter with CX3CR1-GFP combined with CCR2-RFP (red fluorescent protein) was utilized to distinguish native microglial cells from migrating/infiltrating monocytes/macrophages in a model of glioblastoma [86].

A challenge to the aforementioned approaches is the need to develop a unique animal model for every immune cell population of interest, which can be challenging and time consuming. An alternative approach is to use a mouse model with constitutive reporter expression throughout the animal, and then use adoptive transfer to introduce specific immune cell subtype(s) into a recipient animal. In this way by use of flow cytometry, highly specific immune cell subtypes can be isolated, having persistent reporter expression such that lineage tracing and long term tracking of immune cell infiltrates is possible [87]. It should be noted that a challenge in using any such model described above is the potential alteration of immune function by means of the genetic manipulation. This can come at the expense of the native gene function as well as the introduction of potentially toxic or immunogenic genetic payloads [88], so in any such model, this potential effect should be considered.

4.3 Exogenous Sources of Contrast

Other approaches to imaging immune cells involve targeted imaging approaches to label cells *in vivo* with a source of fluorescence or other optical contrast. One such approach is to use a persistent dye or nanoparticle that binds to or is taken up by the cell and retained for long periods following *in vivo* administration. This approach mirrors the adoptive transfer studies described above but avoids the need for genetic manipulation, and is capable of tracking specific cell subsets, or using different color labels is capable of multiplexing multiple subsets in *ex vivo* live systems [89] or live animals *in vivo* through use of window chamber models [90]. A wide variety of approaches have been used, including uptake of fluorescent or optically active nanoparticles, which have been shown in a number of systems to be stably retained for long duration [91, 92]. The primary limitation of this approach is that the cell label will be diluted as the cells divide, so it can be less effective for proliferating cell types over longer durations.

Immunofluorescence labeling is the gold standard technique for tumor immune cell profiling due to the ability to characterize multiple cell surface and/or internal markers to distinguish different sub-populations in detail. *In vivo* approaches analogous to this have been implemented in the ear dermis through multi-color labeling of immune cell populations using fluorescent labeled antibodies [93]. Similar approaches have also been used to identify myeloid cell subpopulations and their different behaviors *in vivo* based on functional imaging and cell surface marker binding [94]. This type of approach facilitates flexible multicolor labeling without the need of a long development cycle to produce a reporter animal model, and can be particularly suitable for exploratory studies by avoiding the expense and time commitment of animal model development.

4.4 Other Sources of Contrast Including Functional Imaging of the Tumor and Tumor Microenvironment

In addition to direct imaging of immune cells within the tumor, there are a wide range of functional indicators that provide important information about the tumor microenvironment which can have direct effects on immune function [95]. This includes imaging apoptosis and cell death (as induced by immune function), as well as biosensors for a wide range of physiologic and molecular endpoints [96–98]. One notable example of this is tumor hypoxia. It is known that oxygen is required by immune cells for a variety of normal functions, and it has long been established that hypoxia is a key determinant of therapeutic response and tumor aggressiveness, and hypoxia sensing can be exploited as a key predictor of response [99, 100]. Through the development of advanced intravital imaging techniques it is now possible to study the direct effects on tumor cells vs. effects on the immune system or stromal cells. For example, phosphorescence lifetime as well

as ratiometric sensing of oxygen-quenched phosphors enables the study of tissue hypoxia *in vivo* [101–103]. Through the use of intravital imaging it has been demonstrated that there is a significant oxygen dependence on lymphocyte motility [104]. Specifically, it was found that T cell motility was sustained with local pO₂ above 5 mmHg, which a sharp drop in motility below this level, which could be rescued by breathing 100% oxygen. The use of oxygen-quenched phosphorescence in characterizing tissue hypoxia is thus an active area of research with important consequences on immune therapies, and improvement in tissue oxygenation could be a potential complementary strategy. A bioreducible probe for quantifying tissue oxygenation using photoacoustic imaging has also recently been reported, which is also suitable for *in vivo* sensing with the advantages of photoacoustics described above [105].

A related imaging technique is characterization of hemoglobin oxygen saturation, which has been accomplished by a variety of techniques, taking advantage of the differing absorption spectra of oxy- and deoxy-hemoglobin [32, 105, 106]. This is an absorption based measurement, and a variety of optical setups are possible, including bright field transmission imaging as with the dorsal skin fold window chamber, as well as reflectance mode imaging using cross polarization or oblique illumination [107–109]. Photoacoustic microscopy has also been applied to characterize hemoglobin oxygen saturation within microvessels in tumors in a variety of organ sites [43, 105, 110]. Similarly, there are published approaches for utilizing OCT based methods for quantifying hemoglobin oxygen saturation including a dual wavelength approach [47, 48], which offers practical advantages as discussed above.

Photoswitchable probes are a more recent innovation that has been applied to track specific immune cell populations and migration to and from specific locations. For example, the Kaede transgenic photoswitchable probe, irreversibly converts from green to red fluorescence upon exposure to UV light, and has been used to track migration of immune cell populations from the lymph nodes to other tissues [111]. A more recent innovation is the development of a photoswitchable probe for photoacoustic microscopy. In this case, photoactivation results in a reversible change in the absorption spectrum which allows for greater sensitivity and specificity of detection for multiplexed cellular imaging [112]. Figure 2 shows an example showing *in vivo* tumor imaging of a photoswitchable reporter demonstrating reporter expression within the tumor.

Another aspect of physiology and the tumor microenvironment that plays a key role in both immune function and nanoparticle mediated sensing and therapy is the vascular and lymphatic system. Owing to the hemoglobin absorption contrast mentioned above, a number of optical imaging approaches are able to image vascular morphology and blood flow, including bright field and other varieties of optical microscopy, OCT, and photoacoustic microscopy. For example, using video microscopy of transmitted light in a dorsal skin fold window chamber, it is possible to calculate flow speed and direction on a pixel wise basis to reconstruct the vascular network [61]. This is useful for characterizing angiogenesis, vasomotion, and vascular network morphology. It has also been widely utilized in

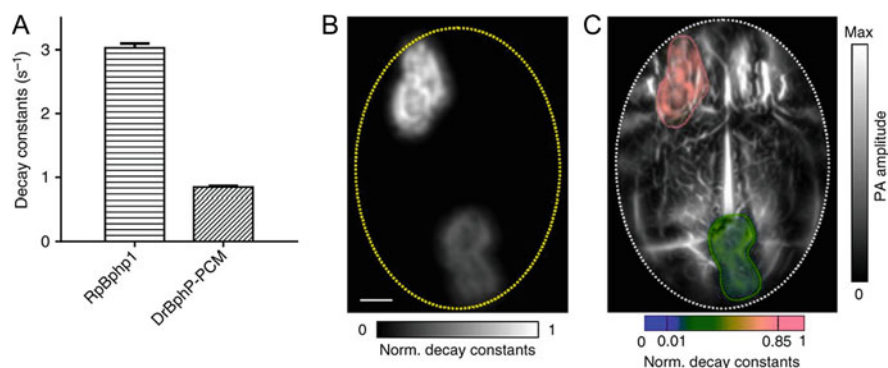


Fig. 2 Photoacoustic imaging of dual photoswitchable reporters having different decay constants at which they return to their ground state following photoactivation (a). This difference in decay constant facilitates multiplexed imaging of these separate reporters. This is demonstrated in two U87 glioblastoma models, transfected with different reporters, and grown in two separate tumors, which are distinguishable by decay constant imaging, scale 2 mm (b). Grayscale overlay shows the vasculature which is detected via hemoglobin absorption contrast (c). Adapted from Li et al. [112]

brain functional imaging, known as the intrinsic signal in which vessels dilate in response to neural activity [113, 114].

Video imaging of other sources of contrast enables study of vascular permeability, accumulation of nanoparticles, and leukocyte endothelial cell interactions. For example, using fluorescently labeled leukocytes, it is possible to examine sticking and rolling of such cells along the vessel wall [115]. Vascular contrast can also be achieved by fluorescence through use of macromolecular probes, such as fluorescently labeled dextrans or nanoparticles, which cannot readily leak out of most vessels as quickly as small molecules (although tumor vasculature is particularly leaky). Dextrans of varying sizes have been used to characterize vascular permeability and pore size through intravital microscopy [116]. In addition fluorescence contrast in both endothelial cells [117–119] and lymphatics [120, 121] is available through reporter model mouse strains and can be combined with intravital microscopy to better detect small vessels and migrating endothelial cells. Quantitative imaging of fluorescent nanoparticles intratumoral uptake has also been evaluated [122]. Optical imaging is particularly suited for characterizing drug delivery and release due to the ability to label the nanoparticle carriers and drug cargo with fluorescent dyes.

Finally, as these types of nanoparticle-mediated approaches for imaging and drug delivery have become more widely used, the interaction of these systems with the immune system and normal tissue function has become more apparent and needs to be considered. As one such example, the presence of a tumor in a mouse model has been shown to induce global immune changes which leads to enhanced nanoparticle clearance, possibly mediated by enhanced macrophage-mediated clearance and shift to a Th2 dominant immune phenotype [123]. An immune response may also be directed against the nanoparticles via the adaptive

immune system. Antibodies against PEG, commonly used as a surface coating on nanoparticles to enhance circulations times, have been shown to be generated in vivo and alter the distribution of PEGylated nanoparticles in vivo [124, 125]. A similar effect of enhanced clearance following repeat administration has been seen with viral particles [126]. Thus, the impact of tumor growth and potentially therapy needs to be accounted for when considering nanoparticle mediated therapy and imaging and this may be of particular relevance in studies of immune function.

5 Conclusion

This chapter has presented a broad overview of the technical and biological considerations when implementing intravital optical imaging for characterizing immune function in tumors. This is a growing and rapidly changing field, and intravital imaging presents a unique platform for studying dynamic functional interactions that can have a profound effect on tumor growth progression and treatment response.

References

1. Secklehner, J., Lo Celso, C., Carlin, L.M.: Intravital microscopy in historic and contemporary immunology. *Immunol. Cell Biol.* **95**, 506–513 (2017). <https://doi.org/10.1038/icb.2017.25>
2. Sandison, J.C.: The transparent chamber of the rabbit's ear, giving a complete description of improved technic of construction and introduction, and general account of growth and behavior of living cells and tissues as seen with the microscope. *Am. J. Anat.* **41**, 447–473 (1928). <https://doi.org/10.1002/aja.1000410303>
3. Ide, A., Baker, N., Warren, S.: Vascularization of the Brown Pearce rabbit epithelioma transplant as seen in the transparent ear chamber. *Am. J. Roentgenol.* **42**, 891–899 (1939)
4. Algire, G.H.: An adaptation of the transparent-chamber technique to the mouse. *J. Natl. Cancer Inst.* **4**, 1–11 (1943). <https://doi.org/10.1093/jnci/4.1.1>
5. Gabriel, E.M., Fisher, D.T., Evans, S., Takabe, K., Skitzki, J.J.: Intravital microscopy in the study of the tumor microenvironment: from bench to human application. *Oncotarget.* **9**, 20165–20178 (2018). <https://doi.org/10.18632/oncotarget.24957>
6. Ehrlich, P.: Über den jetzigen stand der Karzinomforschung. *Ned. Tijdschr. Geneesk.* **5**, 273–290 (1908)
7. Mittal, D., Gubin, M.M., Schreiber, R.D., Smyth, M.J.: New insights into cancer immunoeediting and its three component phases—elimination, equilibrium and escape. *Curr. Opin. Immunol.* **27**, 16–25 (2014). <https://doi.org/10.1016/j.coi.2014.01.004>
8. Shankaran, V., Ikeda, H., Bruce, A.T., White, J.M., Swanson, P.E., Old, L.J., Schreiber, R.D.: IFN γ and lymphocytes prevent primary tumour development and shape tumour immunogenicity. *Nature.* **410**, 1107–1111 (2001). <https://doi.org/10.1038/35074122>
9. Alexander, S., Weigel, B., Winkler, F., Friedl, P.: Preclinical intravital microscopy of the tumour-stroma interface: invasion, metastasis, and therapy response. *Curr. Opin. Cell Biol.* **25**, 659–671 (2013). <https://doi.org/10.1016/j.ceb.2013.07.001>
10. Headley, M.B., Bins, A., Nip, A., Roberts, E.W., Looney, M.R., Gerard, A., Krummel, M.F.: Visualization of immediate immune responses to pioneer metastatic cells in the lung. *Nature.* **531**, 513–517 (2016). <https://doi.org/10.1038/nature16985>

11. Hu, F., Martin, H., Martinez, A., Everitt, J., Erkanli, A., Lee, W.T., Dewhirst, M., Ramanujam, N.: Distinct angiogenic changes during carcinogenesis defined by novel label-free dark-field imaging in a hamster cheek pouch model. *Cancer Res.* **77**, 7109–7119 (2017). <https://doi.org/10.1158/0008-5472.CAN-17-1058>
12. Schreiber, R.D., Old, L.J., Smyth, M.J.: Cancer immunoediting: integrating immunity's roles in cancer suppression and promotion. *Science.* **331**, 1565–1570 (2011). <https://doi.org/10.1126/science.1203486>
13. Koebel, C.M., Vermi, W., Swann, J.B., Zerafa, N., Rodig, S.J., Old, L.J., Smyth, M.J., Schreiber, R.D.: Adaptive immunity maintains occult cancer in an equilibrium state. *Nature.* **450**, 903–907 (2007). <https://doi.org/10.1038/nature06309>
14. Torcellan, T., Stolp, J., Chtanova, T.: In vivo imaging sheds light on immune cell migration and function in cancer. *Front. Immunol.* **8**, 309 (2017). <https://doi.org/10.3389/fimmu.2017.00309>
15. Nakasone, E.S., Askautrud, H.A., Kees, T., Park, J.-H., Plaks, V., Ewald, A.J., Fein, M., Rasch, M.G., Tan, Y.-X., Qiu, J., Park, J., Sinha, P., Bissell, M.J., Frengen, E., Werb, Z., Egeblad, M.: Imaging tumor-stroma interactions during chemotherapy reveals contributions of the microenvironment to resistance. *Cancer Cell.* **21**, 488–503 (2012). <https://doi.org/10.1016/j.ccr.2012.02.017>
16. Zal, T., Chodaczek, G.: Intravital imaging of anti-tumor immune response and the tumor microenvironment. *Semin. Immunopathol.* **32**, 305–317 (2010). <https://doi.org/10.1007/s00281-010-0217-9>
17. Rosenberg, S.A.: Decade in review—cancer immunotherapy. *Nat. Rev. Clin. Oncol.* **11**, 630–632 (2014). <https://doi.org/10.1038/nrclinonc.2014.174>
18. Sharma, P., Wagner, K., Wolchok, J.D., Allison, J.P.: Novel cancer immunotherapy agents with survival benefit: recent successes and next steps. *Nat. Rev. Cancer.* **11**, 805–812 (2011). <https://doi.org/10.1038/nrc3153>
19. Blanco, E., Shen, H., Ferrari, M.: Principles of nanoparticle design for overcoming biological barriers to drug delivery. *Nat. Biotechnol.* **33**, 941–951 (2015). <https://doi.org/10.1038/nbt.3330>
20. Mitchell, M.J., Jain, R.K., Langer, R.: Engineering and physical sciences in oncology: challenges and opportunities. *Nat. Rev. Cancer.* **17**, 659–675 (2017). <https://doi.org/10.1038/nrc.2017.83>
21. Shen, H., Sun, T., Hoang, H.H., Burchfield, J.S., Hamilton, G.F., Mittendorf, E.A., Ferrari, M.: Enhancing cancer immunotherapy through nanotechnology-mediated tumor infiltration and activation of immune cells. *Semin. Immunol.* **34**, 114–122 (2017). <https://doi.org/10.1016/j.smim.2017.09.002>
22. Bar-Zeev, M., Livney, Y.D., Assaraf, Y.G.: Targeted nanomedicine for cancer therapeutics: towards precision medicine overcoming drug resistance. *Drug Resist. Updat.* **31**, 15–30 (2017). <https://doi.org/10.1016/j.drug.2017.05.002>
23. Dewhirst, M.W., Secomb, T.W.: Transport of drugs from blood vessels to tumour tissue. *Nat. Rev. Cancer.* **17**, 738–750 (2017). <https://doi.org/10.1038/nrc.2017.93>
24. Evans, M.K., Brown, M.C., Geradts, J., Bao, X., Robinson, T.J., Jolly, M.K., Vermeulen, P.B., Palmer, G.M., Gromeier, M., Levine, H., Morse, M.A., Van Laere, S.J., Devi, G.R.: XIAP regulation by MNK links MAPK and NFκB signaling to determine an aggressive breast cancer phenotype. *Cancer Res.* **78**, 1726–1738 (2018). <https://doi.org/10.1158/0008-5472.CAN-17-1667>
25. Jeanbart, L., Ballester, M., de Titta, A., Corthésy, P., Romero, P., Hubbell, J.A., Swartz, M.A.: Enhancing efficacy of anticancer vaccines by targeted delivery to tumor-draining lymph nodes. *Cancer Immunol. Res.* **2**, 436–447 (2014). <https://doi.org/10.1158/2326-6066.CIR-14-0019-T>
26. Liu, H., Moynihan, K.D., Zheng, Y., Szeto, G.L., Li, A.V., Huang, B., Van Egeren, D.S., Park, C., Irvine, D.J.: Structure-based programming of lymph-node targeting in molecular vaccines. *Nature.* **507**, 519–522 (2014). <https://doi.org/10.1038/nature12978>

27. Thomas, S.N., Vokali, E., Lund, A.W., Hubbell, J.A., Swartz, M.A.: Targeting the tumor-draining lymph node with adjuvanted nanoparticles reshapes the anti-tumor immune response. *Biomaterials*. **35**, 814–824 (2014). <https://doi.org/10.1016/j.biomaterials.2013.10.003>
28. Andón, F.T., Digifico, E., Maeda, A., Erreni, M., Mantovani, A., Alonso, M.J., Allavena, P.: Targeting tumor associated macrophages: the new challenge for nanomedicine. *Semin. Immunol.* **34**, 103–113 (2017). <https://doi.org/10.1016/j.smim.2017.09.004>
29. Batrakova, E.V., Kabanov, A.V.: Pluronic block copolymers. *J. Control. Release*. **130**, 98–106 (2008). <https://doi.org/10.1016/j.jconrel.2008.04.013>
30. Fukumura, D., Duda, D.G., Munn, L.L., Jain, R.K.: Tumor microvasculature and microenvironment: novel insights through Intravital imaging in pre-clinical models. *Microcirculation*. **17**, 206–225 (2010). <https://doi.org/10.1111/j.1549-8719.2010.00029.x>
31. Nobis, M., Warren, S.C., Lucas, M.C., Murphy, K.J., Herrmann, D., Timpson, P.: Molecular mobility and activity in an intravital imaging setting - implications for cancer progression and targeting. *J. Cell Sci.* **131** (2018). <https://doi.org/10.1242/jcs.206995>
32. Palmer, G.M., Fontanella, A.N., Shan, S., Hanna, G., Zhang, G., Fraser, C.L., Dewhirst, M.W.: In vivo optical molecular imaging and analysis in mice using dorsal window chamber models applied to hypoxia, vasculature and fluorescent reporters. *Nat. Protoc.* **6**, 1355–1366 (2011). <https://doi.org/10.1038/nprot.2011.349>
33. Minsky, M.: Memoir on inventing the confocal scanning microscope. *Scanning*. **10**, 128–138 (1988). <https://doi.org/10.1002/sca.4950100403>
34. Andresen, V., Pollok, K., Rinnenthal, J.-L., Oehme, L., Günther, R., Spiecker, H., Radbruch, H., Gerhard, J., Sporbart, A., Cseresnyes, Z., Hauser, A.E., Niesner, R.: High-resolution intravital microscopy. *PLoS One*. **7**, e50915 (2012). <https://doi.org/10.1371/journal.pone.0050915>
35. Leong, H.S., Steinmetz, N.F., Ablack, A., Destito, G., Zijlstra, A., Stuhlmann, H., Manchester, M., Lewis, J.D.: Intravital imaging of embryonic and tumor neovasculature using viral nanoparticles. *Nat. Protoc.* **5**, 1406–1417 (2010). <https://doi.org/10.1038/nprot.2010.103>
36. Naumenko, V., Van, S., Dastidar, H., Kim, D.-S., Kim, S.-J., Zeng, Z., Deniset, J., Lau, A., Zhang, C., Macia, N., Heyne, B., Jenne, C.N., Mahoney, D.J.: Visualizing oncolytic virus-host interactions in live mice using Intravital microscopy. *Mol. Ther. Oncolytics*. **10**, 14–27 (2018). <https://doi.org/10.1016/j.omto.2018.06.001>
37. Denk, W., Strickler, J.H., Webb, W.W.: Two-photon laser scanning fluorescence microscopy. *Science*. **248**, 73–76 (1990). <https://doi.org/10.1126/science.2321027>
38. Benson, R.A., Brewer, J.M., Garside, P.: Visualizing and tracking T cell motility in vivo. *Methods Mol. Biol.* **1591**, 27–41 (2017). https://doi.org/10.1007/978-1-4939-6931-9_3
39. Cahalan, M.D., Parker, I., Wei, S.H., Miller, M.J.: Two-photon tissue imaging: seeing the immune system in a fresh light. *Nat. Rev. Immunol.* **2**, 872–880 (2002). <https://doi.org/10.1038/nri935>
40. Germain, R.N., Castellino, F., Chieppa, M., Egen, J.G., Huang, A.Y.C., Koo, L.Y., Qi, H.: An extended vision for dynamic high-resolution intravital immune imaging. *Semin. Immunol.* **17**, 431–441 (2005). <https://doi.org/10.1016/j.smim.2005.09.003>
41. Perrin, L., Bayarmagnai, B., Gligorijevic, B.: Frontiers in intravital multiphoton microscopy of cancer. *Cancer Rep.*, e1192 (2019). <https://doi.org/10.1002/cnr2.1192>
42. Brunker, J., Yao, J., Laufer, J., Bohndiek, S.E.: Photoacoustic imaging using genetically encoded reporters: a review. *J. Biomed. Opt.*, 22 (2017). <https://doi.org/10.1117/1.JBO.22.7.070901>
43. Hu, S., Wang, L.V.: Photoacoustic imaging and characterization of the microvasculature. *J. Biomed. Opt.* **15**, 011101 (2010). <https://doi.org/10.1117/1.3281673>
44. Valluru, K.S., Willmann, J.K.: Clinical photoacoustic imaging of cancer. *Ultrasonography*. **35**, 267–280 (2016). <https://doi.org/10.14366/usg.16035>
45. Valluru, K.S., Wilson, K.E., Willmann, J.K.: Photoacoustic imaging in oncology: translational preclinical and early clinical experience. *Radiology*. **280**, 332–349 (2016). <https://doi.org/10.1148/radiol.16151414>

46. van den Berg, P.J., Daoudi, K., Steenbergen, W.: Review of photoacoustic flow imaging: its current state and its promises. *Photo-Dermatology*. **3**, 89–99 (2015). <https://doi.org/10.1016/j.pacs.2015.08.001>
47. Robles, F.E., Wilson, C., Grant, G., Wax, A.: Molecular imaging true-colour spectroscopic optical coherence tomography. *Nat. Photonics*. **5**, 744–747 (2011). <https://doi.org/10.1038/nphoton.2011.257>
48. Yin, B., Kuranov, R.V., McElroy, A.B., Kazmi, S., Dunn, A.K., Duong, T.Q., Milner, T.E.: Dual-wavelength photothermal optical coherence tomography for imaging microvasculature blood oxygen saturation. *J. Biomed. Opt.* **18**, 56005 (2013). <https://doi.org/10.1117/1.JBO.18.5.056005>
49. Puza, C.J., Warren, W.S., Mosca, P.J.: The changing landscape of dermatology practice: melanoma and pump-probe laser microscopy. *Lasers Med. Sci.* **32**, 1935–1939 (2017). <https://doi.org/10.1007/s10103-017-2319-2>
50. Shashkova, S., Leake, M.C.: Single-molecule fluorescence microscopy review: shedding new light on old problems. *Biosci. Rep.* **37** (2017). <https://doi.org/10.1042/BSR20170031>
51. Simpson, M.J., Wilson, J.W., Phipps, M.A., Robles, F.E., Selim, M.A., Warren, W.S.: Nonlinear microscopy of eumelanin and pheomelanin with subcellular resolution. *J. Invest. Dermatol.* **133**, 1822–1826 (2013). <https://doi.org/10.1038/jid.2013.37>
52. Kedrin, D., Gligorijevic, B., Wyckoff, J., Verkhusha, V.V., Condeelis, J., Segall, J.E., van Rheenen, J.: Intravital imaging of metastatic behavior through a mammary imaging window. *Nat. Methods*. **5**, 1019–1021 (2008). <https://doi.org/10.1038/nmeth.1269>
53. Schafer, R., Leung, H.M., Gmitro, A.F.: Multi-modality imaging of a murine mammary window chamber for breast cancer research. *BioTechniques*. **57**, 45–50 (2014). <https://doi.org/10.2144/000114191>
54. Shan, S., Sorg, B., Dewhirst, M.W.: A novel rodent mammary window of orthotopic breast cancer for intravital microscopy. *Microvasc. Res.* **65**, 109–117 (2003). [https://doi.org/10.1016/s0026-2862\(02\)00017-1](https://doi.org/10.1016/s0026-2862(02)00017-1)
55. Sobolik, T., Su, Y.-J., Ashby, W., Schaffer, D.K., Wells, S., Wikswo, J.P., Zijlstra, A., Richmond, A.: Development of novel murine mammary imaging windows to examine wound healing effects on leukocyte trafficking in mammary tumors with intravital imaging. *Intravital*. **5** (2016). <https://doi.org/10.1080/21659087.2015.1125562>
56. Dorand, R.D., Barkauskas, D.S., Evans, T.A., Petrosiute, A., Huang, A.Y.: Comparison of intravital thinned skull and cranial window approaches to study CNS immunobiology in the mouse cortex. *Intravital*, **3** (2014). <https://doi.org/10.4161/intv.29728>
57. Benbenishty, A., Gadrich, M., Cottarelli, A., Lubart, A., Kain, D., Amer, M., Shaashua, L., Glasner, A., Erez, N., Agalliu, D., Mayo, L., Ben-Eliyahu, S., Blinder, P.: Prophylactic TLR9 stimulation reduces brain metastasis through microglia activation. *PLoS Biol.* **17** (2019). <https://doi.org/10.1371/journal.pbio.2006859>
58. Qiao, S., Qian, Y., Xu, G., Luo, Q., Zhang, Z.: Long-term characterization of activated microglia/macrophages facilitating the development of experimental brain metastasis through intravital microscopic imaging. *J. Neuroinflammation*. **16**, 4 (2019). <https://doi.org/10.1186/s12974-018-1389-9>
59. Yuan, H., Wilson, C.M., Xia, J., Doyle, S.L., Li, S., Fales, A.M., Liu, Y., Ozaki, E., Mulfaul, K., Hanna, G., Palmer, G.M., Wang, L.V., Grant, G.A., Vo-Dinh, T.: Plasmonics-enhanced and optically modulated delivery of gold nanostars into brain tumor. *Nanoscale*. **6**, 4078–4082 (2014). <https://doi.org/10.1039/c3nr06770j>
60. Entenberg, D., Voiculescu, S., Guo, P., Borriello, L., Wang, Y., Karagiannis, G.S., Jones, J., Baccay, F., Oktay, M., Condeelis, J.: A permanent window for the murine lung enables high-resolution imaging of cancer metastasis. *Nat. Methods*. **15**, 73–80 (2018). <https://doi.org/10.1038/nmeth.4511>
61. Fontanella, A.N., Schroeder, T., Hochman, D.W., Chen, R.E., Hanna, G., Haglund, M.M., Secomb, T.W., Palmer, G.M., Dewhirst, M.W.: Quantitative mapping of hemodynamics in the lung, brain, and dorsal window chamber-grown tumors using a novel, automated algorithm. *Microcirculation*. **20**, 724–735 (2013). <https://doi.org/10.1111/micc.12072>

62. Looney, M.R., Bhattacharya, J.: Live imaging of the lung. *Annu. Rev. Physiol.* **76**, 431–445 (2014). <https://doi.org/10.1146/annurev-physiol-021113-170331>
63. Babes, L., Kubes, P.: Visualizing the tumor microenvironment of liver metastasis by spinning disk confocal microscopy. *Methods Mol. Biol.* **1458**, 203–215 (2016). https://doi.org/10.1007/978-1-4939-3801-8_15
64. Benechet, A.P., Ganzer, L., Iannacone, M.: Intravital microscopy analysis of hepatic T cell dynamics. *Methods Mol. Biol.* **1514**, 49–61 (2017). https://doi.org/10.1007/978-1-4939-6548-9_4
65. Sumen, C., Mempel, T.R., Mazo, I.B., von Andrian, U.H.: Intravital microscopy: visualizing immunity in context. *Immunity.* **21**, 315–329 (2004). <https://doi.org/10.1016/j.immuni.2004.08.006>
66. Bentolila, N.Y., Barnhill, R.L., Lugassy, C., Bentolila, L.A.: Intravital imaging of human melanoma cells in the mouse ear skin by two-photon excitation microscopy. *Methods Mol. Biol.* **1755**, 223–232 (2018). https://doi.org/10.1007/978-1-4939-7724-6_15
67. Chen, B.J., Jiao, Y., Zhang, P., Sun, A.Y., Pitt, G.S., Deoliveira, D., Drago, N., Ye, T., Liu, C., Chao, N.J.: Long-term in vivo imaging of multiple organs at the single cell level. *PLoS One.* **8**, e52087 (2013). <https://doi.org/10.1371/journal.pone.0052087>
68. Güç, E., Fankhauser, M., Lund, A.W., Swartz, M.A., Kilarski, W.W.: Long-term intravital immunofluorescence imaging of tissue matrix components with epifluorescence and two-photon microscopy. *J. Vis. Exp.* (2014). <https://doi.org/10.3791/51388>
69. Birer, S.R., Lee, C.-T., Choudhury, K.R., Young, K.H., Spasojevic, I., Batinic-Haberle, I., Crapo, J.D., Dewhirst, M.W., Ashcraft, K.A.: Inhibition of the continuum of radiation-induced normal tissue injury by a redox-active Mn porphyrin. *Radiat. Res.* **188**, 94–104 (2017). <https://doi.org/10.1667/RR14757.1.S1>
70. Dähn, S., Schwalbach, P., Maksan, S., Wöhleke, F., Benner, A., Kuntz, C.: Influence of different gases used for laparoscopy (helium, carbon dioxide, room air, and xenon) on tumor volume, histomorphology, and leukocyte-tumor-endothelium interaction in intravital microscopy. *Surg. Endosc.* **19**, 65–70 (2005). <https://doi.org/10.1007/s00464-003-9298-z>
71. Metildi, C.A., Tang, C.-M., Kaushal, S., Leonard, S.Y., Magistri, P., Tran Cao, H.S., Hoffman, R.M., Bouvet, M., Sicklick, J.K.: In vivo fluorescence imaging of gastrointestinal stromal tumors using fluorophore-conjugated anti-KIT antibody. *Ann. Surg. Oncol.* **20**(Suppl 3), S693–S700 (2013). <https://doi.org/10.1245/s10434-013-3172-6>
72. Oh, G., Yoo, S.W., Jung, Y., Ryu, Y.-M., Park, Y., Kim, K.H., Kim, S., Myung, S.-J., Chung, E.: Intravital imaging of mouse colonic adenoma using MMP-based molecular probes with multi-channel fluorescence endoscopy. *Biomed. Opt. Express.* **5**, 1677–1689 (2014). <https://doi.org/10.1364/BOE.5.001677>
73. Realdon, S., Dassie, E., Fassan, M., Dall’Olmo, L., Hatem, G., Buda, A., Arcidiacono, D., Diamantis, G., Zhang, H., Greene, M.I., Sturmiolo, G.C., Ruge, M., Alberti, A., Battaglia, G.: In vivo molecular imaging of HER2 expression in a rat model of Barrett’s esophagus adenocarcinoma. *Dis. Esophagus.* **28**, 394–403 (2015). <https://doi.org/10.1111/dote.12210>
74. Jung, S., Aliberti, J., Graemmel, P., Sunshine, M.J., Kreutzberg, G.W., Sher, A., Littman, D.R.: Analysis of fractalkine receptor CX(3)CR1 function by targeted deletion and green fluorescent protein reporter gene insertion. *Mol. Cell. Biol.* **20**, 4106–4114 (2000). <https://doi.org/10.1128/mcb.20.11.4106-4114.2000>
75. Rua, R., McGavern, D.B.: Elucidation of monocyte/macrophage dynamics and function by intravital imaging. *J. Leukoc. Biol.* **98**, 319–332 (2015). <https://doi.org/10.1189/jlb.4RI0115-006RR>
76. Hasenberg, A., Hasenberg, M., Männ, L., Neumann, F., Borkenstein, L., Stecher, M., Kraus, A., Engel, D.R., Klingberg, A., Seddigh, P., Abdullah, Z., Klebow, S., Engelmann, S., Reinhold, A., Brandau, S., Seeling, M., Waisman, A., Schraven, B., Göthert, J.R., Nimmerjahn, F., Gunzer, M.: Catchup: a mouse model for imaging-based tracking and modulation of neutrophil granulocytes. *Nat. Methods.* **12**, 445–452 (2015). <https://doi.org/10.1038/nmeth.3322>

77. Heymann, F., Niemietz, P.M., Peusquens, J., Ergen, C., Kohlhepp, M., Mossanen, J.C., Schneider, C., Vogt, M., Tolba, R.H., Trautwein, C., Martin, C., Tacke, F.: Long term intravital multiphoton microscopy imaging of immune cells in healthy and diseased liver using CXCR6.Gfp reporter mice. *J. Vis. Exp.* (2015). <https://doi.org/10.3791/52607>
78. Shapovalova, M., Pyper, S.R., Moriarity, B.S., LeBeau, A.M.: The molecular imaging of natural killer cells. *Mol. Imaging.* **17** (2018). <https://doi.org/10.1177/1536012118794816>
79. Oghumu, S., Dong, R., Varikuti, S., Shawler, T., Kampfrath, T., Terrazas, C.A., Lezama-Davila, C., Ahmer, B.M.M., Whitacre, C.C., Rajagopalan, S., Locksley, R., Sharpe, A.H., Satoskar, A.R.: Distinct populations of innate CD8+ T cells revealed in a CXCR3 reporter mouse. *J. Immunol.* **190**, 2229–2240 (2013). <https://doi.org/10.4049/jimmunol.1201170>
80. Lindquist, R.L., Shakhar, G., Dudziak, D., Wardemann, H., Eisenreich, T., Dustin, M.L., Nussenzweig, M.C.: Visualizing dendritic cell networks in vivo. *Nat. Immunol.* **5**, 1243–1250 (2004). <https://doi.org/10.1038/ni1139>
81. Tal, O., Lim, H.Y., Gurevich, I., Milo, I., Shipony, Z., Ng, L.G., Angeli, V., Shakhar, G.: DC mobilization from the skin requires docking to immobilized CCL21 on lymphatic endothelium and intralymphatic crawling. *J. Exp. Med.* **208**, 2141–2153 (2011). <https://doi.org/10.1084/jem.20102392>
82. Dubey, P.: Reporter gene imaging of immune responses to cancer: progress and challenges. *Theranostics.* **2**, 355–362 (2012). <https://doi.org/10.7150/thno.3903>
83. Li, M., Wang, Y., Liu, M., Lan, X.: Multimodality reporter gene imaging: construction strategies and application. *Theranostics.* **8**, 2954–2973 (2018b). <https://doi.org/10.7150/thno.24108>
84. Li, S., Chen, L.-X., Peng, X.-H., Wang, C., Qin, B.-Y., Tan, D., Han, C.-X., Yang, H., Ren, X.-N., Liu, F., Xu, C.-H., Zhou, X.-H.: Overview of the reporter genes and reporter mouse models. *Animal Model Exp. Med.* **1**, 29–35 (2018c). <https://doi.org/10.1002/ame2.12008>
85. Qie, Y., Yuan, H., von Roemeling, C.A., Chen, Y., Liu, X., Shih, K.D., Knight, J.A., Tun, H.W., Wharen, R.E., Jiang, W., Kim, B.Y.S.: Surface modification of nanoparticles enables selective evasion of phagocytic clearance by distinct macrophage phenotypes. *Sci. Rep.* **6** (2016). <https://doi.org/10.1038/srep26269>
86. Chen, Z., Feng, X., Herting, C.J., Garcia, V.A., Nie, K., Pong, W.W., Rasmussen, R., Dwivedi, B., Seby, S., Wolf, S.A., Gutmann, D.H., Hambarzumyan, D.: Cellular and molecular identity of tumor-associated macrophages in glioblastoma. *Cancer Res.* **77**, 2266–2278 (2017). <https://doi.org/10.1158/0008-5472.CAN-16-2310>
87. Rabinovich, B.A., Radu, C.G.: Imaging adoptive cell transfer based cancer immunotherapy. *Curr. Pharm. Biotechnol.* **11**, 672–684 (2010). <https://doi.org/10.2174/138920110792246528>
88. Ansari, A.M., Ahmed, A.K., Matsangos, A.E., Lay, F., Born, L.J., Marti, G., Harmon, J.W., Sun, Z.: Cellular GFP toxicity and immunogenicity: potential confounders in in vivo cell tracking experiments. *Stem Cell Rev.* **12**, 553–559 (2016). <https://doi.org/10.1007/s12015-016-9670-8>
89. Miller, M.J., Wei, S.H., Parker, I., Cahalan, M.D.: Two-photon imaging of lymphocyte motility and antigen response in intact lymph node. *Science.* **296**, 1869–1873 (2002). <https://doi.org/10.1126/science.1070051>
90. Coisne, C., Lyck, R., Engelhardt, B.: Live cell imaging techniques to study T cell trafficking across the blood-brain barrier in vitro and in vivo. *Fluids Barriers CNS.* **10**, 7 (2013). <https://doi.org/10.1186/2045-8118-10-7>
91. Lee, H.W., Gangadaran, P., Kalimuthu, S., Ahn, B.-C.: Advances in molecular imaging strategies for in vivo tracking of immune cells [WWW document]. *Biomed. Res. Int.* (2016). <https://doi.org/10.1155/2016/1946585>
92. Liu, Y., Huang, W., Xiong, C., Huang, Y., Chen, B.J., Racioppi, L., Chao, N., Vo-Dinh, T.: Biodistribution and sensitive tracking of immune cells with plasmonic gold nanostars. *Int. J. Nanomedicine.* **14**, 3403–3411 (2019). <https://doi.org/10.2147/IJN.S192189>
93. Kilarski, W.W., Güç, E., Teo, J.C.M., Oliver, S.R., Lund, A.W., Swartz, M.A.: Intravital immunofluorescence for visualizing the microcirculatory and immune microenvironments in the mouse ear dermis. *PLoS One.* **8**, e57135 (2013). <https://doi.org/10.1371/journal.pone.0057135>

94. Egeblad, M., Ewald, A.J., Askautrud, H.A., Truitt, M.L., Welm, B.E., Bainbridge, E., Peeters, G., Krummel, M.F., Werb, Z.: Visualizing stromal cell dynamics in different tumor microenvironments by spinning disk confocal microscopy. *Dis. Model. Mech.* **1**, 155–167 (2008). <https://doi.org/10.1242/dmm.000596>
95. Ramamonjisoa, N., Ackerstaff, E.: Characterization of the tumor microenvironment and tumor-stroma interaction by non-invasive preclinical imaging. *Front. Oncol.* **7**, 3 (2017). <https://doi.org/10.3389/fonc.2017.00003>
96. Conway, J.R.W., Warren, S.C., Timpson, P.: Context-dependent intravital imaging of therapeutic response using intramolecular FRET biosensors. *Methods.* **128**, 78–94 (2017). <https://doi.org/10.1016/j.ymeth.2017.04.014>
97. Smith, B.A., Smith, B.D.: Biomarkers and molecular probes for cell death imaging and targeted therapeutics. *Bioconjug. Chem.* **23**, 1989–2006 (2012). <https://doi.org/10.1021/bc3003309>
98. Zeng, W., Wang, X., Xu, P., Liu, G., Eden, H.S., Chen, X.: Molecular imaging of apoptosis: from micro to macro. *Theranostics.* **5**, 559–582 (2015). <https://doi.org/10.7150/thno.11548>
99. Chitneni, S.K., Palmer, G.M., Zalutsky, M.R., Dewhirst, M.W.: Molecular imaging of hypoxia. *J. Nucl. Med.* **52**, 165–168 (2011). <https://doi.org/10.2967/jnumed.110.075663>
100. Dewhirst, M.W., Cao, Y., Moeller, B.: Cycling hypoxia and free radicals regulate angiogenesis and radiotherapy response. *Nat. Rev. Cancer.* **8**, 425–437 (2008). <https://doi.org/10.1038/nrc2397>
101. Pogue, B.W., Feng, J., LaRochelle, E.P., Bruža, P., Lin, H., Zhang, R., Shell, J.R., Dehghani, H., Davis, S.C., Vinogradov, S.A., Gladstone, D.J., Jarvis, L.A.: Maps of in vivo oxygen pressure with submillimetre resolution and nanomolar sensitivity enabled by Cherenkov-excited luminescence scanned imaging. *Nat. Biomed. Eng.* **2**, 254–264 (2018). <https://doi.org/10.1038/s41551-018-0220-3>
102. Wolfbeis, O.S.: Luminescent sensing and imaging of oxygen: fierce competition to the Clark electrode. *BioEssays.* **37**, 921–928 (2015). <https://doi.org/10.1002/bies.201500002>
103. Zhang, G., Palmer, G.M., Dewhirst, M.W., Fraser, C.L.: A dual-emissive-materials design concept enables tumour hypoxia imaging. *Nat. Mater.* **8**, 747–751 (2009). <https://doi.org/10.1038/nmat2509>
104. Rytelwski, M., Haryutyunan, K., Nwajei, F., Shanmugasundaram, M., Wspanialy, P., Zal, M.A., Chen, C.-H., El Khatib, M., Plunkett, S., Vinogradov, S.A., Konopleva, M., Zal, T.: Merger of dynamic two-photon and phosphorescence lifetime microscopy reveals dependence of lymphocyte motility on oxygen in solid and hematological tumors. *J. Immunother. Cancer.* **7**, 78 (2019). <https://doi.org/10.1186/s40425-019-0543-y>
105. Chen, M., Chen, M., Knox, H.J., Knox, H.J., Tang, Y., Liu, W., Nie, L., Nie, L., Chan, J., Chan, J., Yao, J., Yao, J.: Simultaneous photoacoustic imaging of intravascular and tissue oxygenation. *Opt. Lett.* **OL 44**, 3773–3776 (2019). <https://doi.org/10.1364/OL.44.003773>
106. Rickard, A.G., Palmer, G.M., Dewhirst, M.W.: Clinical and pre-clinical methods for quantifying tumor hypoxia. *Adv. Exp. Med. Biol.* **1136**, 19–41 (2019). https://doi.org/10.1007/978-3-030-12734-3_2
107. Lee, J.A., Kozikowski, R.T., Sorg, B.S.: In vivo microscopy of microvessel oxygenation and network connections. *Microvasc. Res.* **98**, 29–39 (2015). <https://doi.org/10.1016/j.mvr.2014.11.007>
108. Shonat, R.D., Wachman, E.S., Niu, W., Koretsky, A.P., Farkas, D.L.: Near-simultaneous hemoglobin saturation and oxygen tension maps in mouse brain using an AOTF microscope. *Biophys. J.* **73**, 1223–1231 (1997). [https://doi.org/10.1016/S0006-3495\(97\)78155-4](https://doi.org/10.1016/S0006-3495(97)78155-4)
109. Wachman, E.S., Niu, W., Farkas, D.L.: AOTF microscope for imaging with increased speed and spectral versatility. *Biophys. J.* **73**, 1215–1222 (1997). [https://doi.org/10.1016/S0006-3495\(97\)78154-2](https://doi.org/10.1016/S0006-3495(97)78154-2)
110. Tzoumas, S., Ntziachristos, V.: Spectral unmixing techniques for optoacoustic imaging of tissue pathophysiology. *Philos. Trans. A Math. Phys. Eng. Sci.* **375** (2017). <https://doi.org/10.1098/rsta.2017.0262>

111. Tomura, M., Yoshida, N., Tanaka, J., Karasawa, S., Miwa, Y., Miyawaki, A., Kanagawa, O.: Monitoring cellular movement in vivo with photoconvertible fluorescence protein “Kaede” transgenic mice. *Proc. Natl. Acad. Sci. U. S. A.* **105**, 10871–10876 (2008). <https://doi.org/10.1073/pnas.0802278105>
112. Li, L., Shemetov, A.A., Baloban, M., Hu, P., Zhu, L., Shcherbakova, D.M., Zhang, R., Shi, J., Yao, J., Wang, L.V., Verkhusha, V.V.: Small near-infrared photochromic protein for photoacoustic multi-contrast imaging and detection of protein interactions in vivo. *Nat. Commun.* **9**, 2734 (2018a). <https://doi.org/10.1038/s41467-018-05231-3>
113. Chen-Bee, C.H., Agoncillo, T., Lay, C.C., Frostig, R.D.: Intrinsic signal optical imaging of brain function using short stimulus delivery intervals. *J. Neurosci. Methods.* **187**, 171–182 (2010). <https://doi.org/10.1016/j.jneumeth.2010.01.009>
114. Haglund, M.M., Ojemann, G.A., Hochman, D.W.: Optical imaging of epileptiform and functional activity in human cerebral cortex. *Nature.* **358**, 668–671 (1992). <https://doi.org/10.1038/358668a0>
115. Dirkx, A.E.M., Oude Egbrink, M.G.A., Kuijpers, M.J.E., van der Niet, S.T., Heijnen, V.V.T., Bouma-ter Steege, J.C.A., Wagstaff, J., Griffioen, A.W.: Tumor angiogenesis modulates leukocyte-vessel wall interactions in vivo by reducing endothelial adhesion molecule expression. *Cancer Res.* **63**, 2322–2329 (2003)
116. Dreher, M.R., Liu, W., Michelich, C.R., Dewhirst, M.W., Yuan, F., Chilkoti, A.: Tumor vascular permeability, accumulation, and penetration of macromolecular drug carriers. *J. Natl. Cancer Inst.* **98**, 335–344 (2006). <https://doi.org/10.1093/jnci/djj070>
117. Larina, I.V., Shen, W., Kelly, O.G., Hadjantonakis, A.-K., Baron, M.H., Dickinson, M.E.: A membrane associated mCherry fluorescent reporter line for studying vascular remodeling and cardiac function during murine embryonic development. *Anat. Rec. (Hoboken).* **292**, 333–341 (2009). <https://doi.org/10.1002/ar.20821>
118. Manzoor, A.A., Lindner, L.H., Landon, C.D., Park, J.-Y., Simnick, A.J., Dreher, M.R., Das, S., Hanna, G., Park, W., Chilkoti, A., Koning, G.A., ten Hagen, T.L.M., Needham, D., Dewhirst, M.W.: Overcoming limitations in nanoparticle drug delivery: triggered, intravascular release to improve drug penetration into tumors. *Cancer Res.* **72**, 5566–5575 (2012). <https://doi.org/10.1158/0008-5472.CAN-12-1683>
119. Zhu, J., Dugas-Ford, J., Chang, M., Purta, P., Han, K.-Y., Hong, Y.-K., Dickinson, M.E., Rosenblatt, M.I., Chang, J.-H., Azar, D.T.: Simultaneous in vivo imaging of blood and lymphatic vessel growth in Prox1-GFP/Flk1::myr-mCherry mice. *FEBS J.* **282**, 1458–1467 (2015). <https://doi.org/10.1111/febs.13234>
120. Hägerling, R., Pollmann, C., Kremer, L., Andresen, V., Kiefer, F.: Intravital two-photon microscopy of lymphatic vessel development and function using a transgenic Prox1 promoter-directed mOrange2 reporter mouse. *Biochem. Soc. Trans.* **39**, 1674–1681 (2011). <https://doi.org/10.1042/BST20110722>
121. Truman, L.A., Bentley, K.L., Smith, E.C., Massaro, S.A., Gonzalez, D.G., Haberman, A.M., Hill, M., Jones, D., Min, W., Krause, D.S., Ruddle, N.H.: ProxTom lymphatic vessel reporter mice reveal Prox1 expression in the adrenal medulla, megakaryocytes, and platelets. *Am. J. Pathol.* **180**, 1715–1725 (2012). <https://doi.org/10.1016/j.ajpath.2011.12.026>
122. Monsky, W.L., Fukumura, D., Gohongi, T., Ancukiewicz, M., Weich, H.A., Torchilin, V.P., Yuan, F., Jain, R.K.: Augmentation of transvascular transport of macromolecules and nanoparticles in tumors using vascular endothelial growth factor. *Cancer Res.* **59**, 4129–4135 (1999)
123. Kai, M.P., Brighton, H.E., Fromen, C.A., Shen, T.W., Luft, J.C., Luft, Y.E., Keeler, A.W., Robbins, G.R., Ting, J.P.Y., Zamboni, W.C., Bear, J.E., DeSimone, J.M.: Tumor presence induces global immune changes and enhances nanoparticle clearance. *ACS Nano.* **10**, 861–870 (2016). <https://doi.org/10.1021/acsnano.5b05999>

124. Park, K.: Impact of anti-PEG antibodies on PEGylated nanoparticles fate in vivo. *J. Control. Release.* **287**, 257 (2018). <https://doi.org/10.1016/j.jconrel.2018.09.014>
125. Zhang, P., Sun, F., Liu, S., Jiang, S.: Anti-PEG antibodies in the clinic: current issues and beyond PEGylation. *J. Control. Release.* **244**, 184–193 (2016). <https://doi.org/10.1016/j.jconrel.2016.06.040>
126. Shukla, S., Dorand, R.D., Myers, J.T., Woods, S.E., Gulati, N.M., Stewart, P.L., Commandeur, U., Huang, A.Y., Steinmetz, N.F.: Multiple administrations of viral nanoparticles alter in vivo behavior-insights from intravital microscopy. *ACS Biomater. Sci. Eng.* **2**, 829–837 (2016). <https://doi.org/10.1021/acsbiomaterials.6b00060>

Nanoparticle-Mediated Heating: A Theoretical Study for Photothermal Treatment and Photo Immunotherapy



Stephen J. Norton and Tuan Vo-Dinh 

1 Introduction

There is increasing interest in using nanoparticles for photothermal therapy for the treatment of many diseases such as cancer [1]. Photo immunotherapy hyperthermia (HT) is a treatment where heat is applied to a tumor or organ [2, 3]. The aim of HT is to increase tumor temperature above physiologic body temperature (37 °C) with the goal of directly inducing cellular damage to abrogate growth, as well as promote local and systemic antitumor immune effects. While high temperature HT (>55 °C) can actually induce immediate thermal death of targeted tumors, it is now clear that mild fever-range HT (<43 °C) can (i) enhance drug delivery to tumors, (ii) improve cancer cell sensitivity to other therapies, and (iii) trigger potent systemic anti-cancer immune responses [4–10]. Nanoparticle (NP)-mediated thermal therapy offers the potential to combine the advantages of precise cancer cell ablation with many benefits of mild HT in the tumor microenvironment, including radio-sensitization of hypoxic regions, enhancement of drug delivery, activation of thermosensitive agents and boosting the immune system. Nanoparticles, such as gold nanostars (GNS) can act as nano-sources of heat that can ablate tumor cells in their microenvironment. This feature improves tumor-targeting precision and permits the use of reduced laser energy required to destroy the targeted

S. J. Norton (✉)
Duke University, Durham, NC, USA
e-mail: sjnorton@duke.edu

T. Vo-Dinh
Fitzpatrick Institute for Photonics, Duke University, Durham, NC, USA
Department of Biomedical Engineering, Duke University, Durham, NC, USA
Department of Chemistry, Duke University, Durham, NC, USA
e-mail: tuan.vodinh@duke.edu

cancer cells. The ability to selectively heat tumor areas where GNS are located while keeping surrounding healthy tissues at lower temperatures offers significant advantages over other traditional thermal therapies, such as ultrasound, microwaves, radiofrequency. Nanoparticle-mediated photothermal therapy (PTT) can rapidly ablate tumor cells and induce mild hyperthermia to boost the immune system due to a natural propensity of GNS to extravasate from the tumor vascular network and accumulate in and around cancer cells [11, 12]. It is important to note that the resulting higher concentration of particles within the tumor tissue results in a higher temperature elevation there since, as we shall show, this elevation is directly proportional to the particle concentration in addition to the smaller elevation from tissue absorption. This enhanced permeability and retention (EPR) feature and the capacity to efficiently convert photon energy into heat make nanoparticles the ideal photothermal transducer for selective cancer therapy.

Nanoparticle absorption of near-infrared light has formed the basis of an effective thermal-therapy methodology as reported by numerous authors in the last two decades [13–34]. For the past few years our laboratory has been developing star-shaped gold nanoparticles, referred to as gold nanostars (GNS), for photothermal treatment immunotherapy [35–41]. As an ideal photothermal transducer for cancer therapy at the nanoscale level, GNS can be exploited for activation by near-infrared (NIR) light in deep tissue [39]. Our team has recently combined GNS-mediated photothermal therapy with immune checkpoint inhibitor-based immunotherapy to produce an effective two-pronged treatment modality referred to as Synergistic Immuno Photo Nanotherapy (SYMPHONY). We have demonstrated in murine models of peripheral tumors that precise GNS-mediated photothermal thermal ablation bolsters anti-PD-L1 therapy to permit eradication of both local and distant tumors, as well as the development of immunologic memory [40, 41].

Nobel metal nanoparticles embedded in tissue are exceptionally efficient at converting optical energy to heat. Maximum particle absorption occurs at the wavelength of the particle's plasmon resonance in which the particle's absorption cross section can be as high as an order of magnitude larger than the particle's geometric cross section [42]. Varying the size, geometry and composition of the particles permits the tuning of the resonance wavelength into the therapeutic window, roughly between 700 and 1100 nm. In this window, light penetration of three or four cm into tissue is possible. This is the wavelength range in which light scattering significantly dominates light absorption. Shifting the plasmon resonance into this range can be most easily achieved by varying the particle geometry, such as the shell thickness, the nanorod aspect ratio or the nanostar branch aspect ratio.

Each particle acts essentially as a point source of heat production, in which the optically-absorbed power is almost instantaneously transferred into the surrounding fluid due to the much higher thermal conductivity of a metallic particle relative to that of the surrounding fluid [43]. With a high concentration of particles, the temperature of the fluid can increase tens of degrees or more above the ambient temperature. As shown below, the resultant temperature elevation of the fluid is proportional to three factors: the particle absorption cross section, the particle concentration and the incident light intensity.

2 Theory

Noble metal nanoparticles exhibit strong absorption cross sections at wavelengths corresponding to their plasmon resonances. The absorption of optical energy is then converted to heat, which diffuses into the surrounding medium. Our objective here is to compute the temperature elevation from the light absorption of embedded particles using basic heat-flow theory for two relatively simple, but practical, geometries. In general there will be two contributions to the temperature elevation: (1) the absorption of light by the tissue and (2) the absorption by the plasmonic particles. We can treat these contributions separately and then add them. This addition is reasonable when the particle concentration is moderately sparse, which should hold under most practical conditions.

In the first case considered, the temperature elevation is calculated from heat flow arising from a point source of optical power inside a thermally-conducting medium. The assumption of a point source can be used as an approximate model of an optical fiber delivering power to the interior of a region of tissue, where we regard the tip of the fiber as the point source. In a homogeneous medium, the point source will give rise to a temperature profile with spherical symmetry with the temperature decreasing radially with distance from the source. The second geometry assumes a planewave incident on a distribution of particles in tissue. In both cases time-dependent solutions to the heat-flow equation can be found under the assumption of a uniform distribution of particles and that the optical properties of the tissue can also be approximated as uniform. The latter assumptions are idealizations, but render the heat-flow problem tractable. Although more complex problems can be performed using purely numerical algorithms, it should be noted that analytical solutions of this kind, based on relatively simple geometries, can be of value for a number of reasons. For example, analytical solutions can be used to validate or check numerical solutions. Also, analytically-derived formulas for the space and time dependence of temperature can be calculated much faster than most numerical methods, such as finite-element based methods. This can be an advantage when multiple calculations are needed in which parameters (optical and/or thermal) are varied. This is particularly important in carrying out, for example, a thermal inverse problem. In the latter, multiple forward problems are computed while varying one or more of the parameters of the system [44, 45]. We should also note that our problem represents a coupled system of light and heat transport. Analytical solutions that show explicitly how these phenomena interact may help in clarifying the role of some of the optical and thermal parameters that influence temperature. One example is the derivation of an explicit formula for the location of the peak temperature under planewave illumination and its dependence on these parameters. This peak value occurs because of competition between heat loss at the surface and heat loss in the interior due to absorption and perfusion. In another example, explicit formulas can be derived for the steady-state temperature, where the latter is approached asymptotically as time increases.

2.1 Heat Flow Equation

The heat flow equation for the temperature $T(\mathbf{r}, t)$ is given by [46]

$$\nabla^2 T(\mathbf{r}, t) - \frac{1}{\kappa} \frac{\partial T(\mathbf{r}, t)}{\partial t} - \frac{T(\mathbf{r}, t)}{\kappa \tau} = -\frac{A(\mathbf{r})}{k}, \quad (1)$$

where $A(\mathbf{r})$ [W/m^3] is a steady-state optical heat source, κ [m^2/s] and k [$\text{W}/^\circ\text{C m}$] are the thermal diffusivity and thermal conductivity of the medium, and τ [s] is the perfusion time constant. If the medium is tissue, the perfusion term in (1) accounts for loss of heat due to blood flow [46]. Typical values of τ may vary from tens of seconds to several minutes depending on the tissue type [47]. In (1) we will for convenience define $T(\mathbf{r}, t)$ as the elevation in temperature relative to the ambient temperature with the initial condition $T(\mathbf{r}, 0) = T_{amb}$, where the ambient temperature T_{amb} is assumed constant. For example, T_{amb} would be body temperature for an in-vivo study.

2.2 Optical Heat Sources

Optical absorption by the tissue and particles both contribute to the distributed heat source $A(\mathbf{r})$. To calculate the contribution to $A(\mathbf{r})$ from tissue absorption, we require the scattering and absorption coefficients of the tissue. For the contribution from particle absorption, we require the absorption cross section of an individual particle (which in general will be wavelength dependent) and the particle concentration. In our analysis, we shall employ the diffusion approximation for light transport within the tissue, which should hold when the wavelength resides within the therapeutic window (700 nm to 1000 nm). In this window multiple scattering dominates absorption. The diffusion equation for the light fluence rate $\phi(r)$ [W/m^2] under steady-state illumination is given by Wang and Wu [48], Vo-Dinh [49]:

$$\nabla^2 \phi(\mathbf{r}) - \mu_e^2 \phi(\mathbf{r}) = -\frac{\mu_e^2}{\mu_a} S(\mathbf{r}), \quad (2)$$

where μ_e [m^{-1}] and μ_a [m^{-1}] are, respectively, the effective attenuation coefficient and the absorption coefficient of the medium and $S(\mathbf{r})$ [W/m^3] is the source term. The fluence rate is defined as the integral of the specific intensity over the complete 4π solid angle [48]. The right-hand side of (2) is sometimes written as $S(\mathbf{r})/D$ using the relation $D = \mu_a/\mu_e^2$, where D is the diffusion coefficient.

The quantities, μ_e and μ_a , in (2) together with the source $S(\mathbf{r})$ will determine the light distribution in the tissue. In general, both the tissue and the nanoparticles contribute to the scattering and absorption coefficients. The total absorption coefficient may be written $\mu_a = \mu_{at} + \mu_{ap}$, where μ_{at} is the absorption coefficient of the tissue

and $\mu_{ap} = N\sigma_a$ is the absorption coefficient arising from the particles [48]. Here N [m^{-3}] is the particle number density and σ_a [m^2] the particle absorption cross section. The effective attenuation coefficient may be written $\mu_e = \sqrt{3}\mu_a(\mu_a + \mu'_s)$, where $\mu'_s = \mu_{st}(1 - g_t) + \mu_{sp}(1 - g_p)$ is the total reduced (or transport) scattering coefficient. In the latter expression, μ_{st} and μ_{sp} are the scattering coefficients of the tissue and particles, respectively, and g_t and g_p are their corresponding anisotropy factors. Typically, $g_t \approx 0.9$ and, for particles much smaller than a wavelength, $g_p = 0$ (that is, the particles scatter isotropically).

With the wavelength tuned to the plasmon resonance of the particles, the particle absorption coefficient, μ_{ap} , can be considerably larger than the tissue absorption coefficient, μ_{at} . This is desirable since in this case more optical energy is absorbed by the particles than the tissue. The above considerations show that the ratio of energy absorbed by the particles to that absorbed by the tissue is $N\sigma_a/\mu_{at}$. For typical values of these parameters, this ratio can exceed 10.

We shall consider two forms of the light source $S(\mathbf{r})$: a point source given by $S(r) = P_s\delta(r)/(4\pi r^2)$ and (2) a planewave source given by $S(z) = I_0\delta(z)$, where $\delta(\cdot)$ is the Dirac delta function. Here P_s [W] is the power emitted by the point source and I_0 [W/m^2] is the intensity of the incident planewave. One caveat is that the calculated heat production on the basis of diffusion theory will somewhat overestimate the temperature within one transport mean-free path length of the source. For typical tissue parameters, the transport mean-free length is on the order of 1 mm or less [50].

2.3 Heat Generation from a Point Source

Here we shall assume the heat source $A(\mathbf{r})$ is generated by a point source of light, which can serve as an approximate model of the illumination from the tip of an optical fiber embedded in tissue. For a point source at $r = 0$ emitting power P_s , the solution to (2) is [48]

$$\phi(r) = \frac{P_s\mu_e^2}{4\pi\mu_a} \frac{e^{-\mu_e r}}{r}. \quad (3)$$

The power per unit volume absorbed by the tissue at the radial distance r is $A(r) = \mu_a\phi(r)$ [W/m^3]. We can then write

$$A(r) = C \frac{e^{-\mu_e r}}{r}, \quad (4)$$

where

$$C \equiv \frac{P_s\mu_e^2}{4\pi}. \quad (5)$$

2.4 Heat Generation from a Planewave Source

For a planewave source propagating in the z direction the solution to (2) is [48]

$$\phi(z) = \begin{cases} \frac{I_0 \mu_e}{\mu_a} e^{-\mu_e z} & \text{for } z \geq 0 \\ 0 & \text{for } z < 0, \end{cases} \quad (6)$$

where I_0 is the incident light intensity. The planewave heat source is then $A(z) = \mu_a \phi(z)$, with the planewave fluence rate given by (6). We then can write

$$A(z) = K e^{-\mu_e z}, \quad (7)$$

for $z \geq 0$ with $K \equiv I_0 \mu_e$.

3 Temperature Elevation Using a Point Source of Optical Power

We begin by examining the general case assuming any spherically-symmetric source of heat production $A(r)$ [W/m^3]. Equation (1) becomes in spherical coordinates

$$\frac{1}{r^2} \frac{\partial}{\partial r} \left(r^2 \frac{\partial T}{\partial r} \right) - \frac{1}{\kappa} \frac{\partial T}{\partial t} - \frac{T}{\kappa \tau} = -\frac{A(r)}{k}. \quad (8)$$

In (8) we define $T(r, t)$ as the elevation in temperature relative to the ambient temperature with the initial condition $T(r, 0) = T_{amb}$.

3.1 Time-Dependent Temperature

It is convenient to solve (8) using a Green's function approach, where the Green's function, $g(r, t|r', t')$, is defined as a solution to

$$\frac{1}{r^2} \frac{\partial}{\partial r} \left(r^2 \frac{\partial g}{\partial r} \right) - \frac{1}{\kappa} \frac{\partial g}{\partial t} - \frac{g}{\kappa \tau} = -\frac{1}{r^2} \delta(r-r') \delta(t-t').$$

The solution to (8) can then be shown to be [51]

$$T(r, t) = \frac{1}{k} \int_0^\infty r'^2 dr' \int_0^t dt' A(r') g(r, t|r', t'). \quad (9)$$

The Green's function, g , is derived in Appendix 1 and is given by

$$g(r, t|r', t') = \frac{2\kappa}{\pi} u(t-t') \int_0^\infty j_0(r\rho) j_0(r'\rho) e^{-\kappa(\rho^2+1/\kappa\tau)(t-t')} \rho^2 d\rho, \quad (10)$$

where $u(\cdot)$ is the unit step function and $j_0(\cdot)$ is the spherical Bessel function of order zero. Substituting (10) into (9) and interchanging orders of integration, we obtain

$$T(r, t) = \frac{2\kappa}{\pi k} \int_0^\infty \rho^2 d\rho j_0(r\rho) \int_0^\infty r'^2 dr' A(r') j_0(r'\rho) \int_0^t dt' e^{-\kappa(\rho^2+1/\kappa\tau)(t-t')}. \quad (11)$$

We now define

$$\bar{A}(\rho) = \int_0^\infty A(r') j_0(r'\rho) r'^2 dr', \quad (12)$$

which is the spherical Hankel transform of $A(r)$. The inverse spherical Hankel transform is

$$A(r) = \frac{2}{\pi} \int_0^\infty \bar{A}(\rho) j_0(r\rho) \rho^2 d\rho. \quad (13)$$

Relation (13) can be confirmed using the relation

$$\int_0^\infty j_0(r\rho) j_0(r'\rho) r^2 dr = \frac{\pi}{2\rho^2} \delta(\rho - \rho'). \quad (14)$$

Performing the t' integral in (11) results in

$$T(r, t) = \frac{2}{\pi k} \int_0^\infty j_0(r\rho) \bar{A}(\rho) \left\{ \frac{1 - e^{-\kappa(\rho^2+1/\kappa\tau)t}}{\rho^2 + 1/\kappa\tau} \right\} \rho^2 d\rho. \quad (15)$$

This solution can be checked by substituting into the heat-flow equation (8) and using the identity (40) in Appendix 1 and (13).

We now assume the heat source $A(r)$ is generated by a point source of light, where $A(r)$ is given by (4). We first evaluate $\bar{A}(\rho)$ from (12) by substituting (4). Noting that $j_0(r'\rho) = \sin(r'\rho)/r'\rho$, we find

$$\bar{A}(\rho) = C \int_0^\infty \frac{e^{-\mu_e r'}}{r'} \frac{\sin(r'\rho)}{r'\rho} r'^2 dr' = \frac{C}{\mu_e^2 + \rho^2}.$$

Substituting this into (15), we obtain an expression for $T(r, t)$:

$$T(r, t) = \frac{2C}{\pi k} \int_0^\infty j_0(r\rho) \left\{ \frac{1 - e^{-\kappa(\rho^2+1/\kappa\tau)t}}{(\mu_e^2 + \rho^2)(\rho^2 + 1/\kappa\tau)} \right\} \rho^2 d\rho. \quad (16)$$

The integral (16) will require a numerical evaluation. However, the steady-state solution can be evaluated explicitly.

3.2 Steady-State Temperature

The steady-state solution follows by letting $t \rightarrow \infty$, in which case (16) simplifies to

$$T^{(ss)}(r) = \frac{2C}{\pi k} \int_0^\infty \frac{j_0(r\rho)\rho^2 d\rho}{(\mu_e^2 + \rho^2)(\rho^2 + 1/\kappa\tau)}. \quad (17)$$

Substituting $j_0(r\rho) = \sin(r\rho)/(r\rho)$, this integral can be evaluated to yield

$$T^{(ss)}(r) = \frac{C}{k} \left[\frac{e^{-r/\sqrt{\kappa\tau}} - e^{-r\mu_e}}{r(\mu_e^2 - 1/\kappa\tau)} \right].$$

The peak temperature will occur at the point $r = 0$, given by

$$T^{(ss)}(0) = \frac{C}{k(\mu_e + 1/\sqrt{\kappa\tau})}.$$

Comparing (16) and (17), one also can write

$$T(r, t) = T^{(ss)}(r) - \frac{2C}{\pi k} e^{-t/\tau} \int_0^\infty \frac{j_0(r\rho) e^{-\kappa t \rho^2} \rho^2 d\rho}{(\mu_e^2 + \rho^2)(\rho^2 + 1/\kappa\tau)},$$

where the integral on the right goes to zero as t increases. From this relation it is clear that when τ is small $T(r, t) \rightarrow T^{(ss)}(r)$ more rapidly, as expected from physical arguments. This equation can also be used to calculate the time required to achieve, for example, 50% of the steady-state temperature.

3.3 Cooling

When the source is turned off, the system will cool and approach the ambient temperature. If the source is turned off at $t = t_0$, the temperature obeys the following heat flow equation with the initial condition $T(r, t_0)$:

$$\frac{1}{r^2} \frac{\partial}{\partial r} \left(r^2 \frac{\partial T}{\partial r} \right) - \frac{1}{\kappa} \frac{\partial T}{\partial t} - \frac{T}{\kappa\tau} = 0 \quad (18)$$

for $t \geq t_0$. The temperature for $t \geq t_0$ is computed from [51]:

$$T(r, t) = \frac{1}{\kappa} \int_0^\infty g(r, t|r', t_0) T(r', t_0) r'^2 dr'. \quad (19)$$

This relation follows from the property that

$$\lim_{t \rightarrow t_0} g(r, t|r', t_0) = \frac{\kappa}{r^2} \delta(r - r').$$

To evaluate (19), we set $t' = t_0$ in (10) and $t = t_0$ in (16) and substitute the resulting expressions for $g(r, t|r', t_0)$ and $T(r, t_0)$ into (19). Interchanging orders of integration, performing the r' integral with the aid of (14), finally yields

$$T(r, t) = \frac{2C}{\pi k} \int_0^\infty j_0(r\rho) e^{-\kappa(\rho^2 + 1/\kappa\tau)(t-t_0)} \left\{ \frac{1 - e^{-\kappa(\rho^2 + 1/\kappa\tau)t_0}}{(\mu_e^2 + \rho^2)(\rho^2 + 1/\kappa\tau)} \right\} \rho^2 d\rho \quad (20)$$

for $t \geq t_0$. As a check, substituting (20) into (18) shows that the heat flow equation is satisfied with the initial condition $T(r, t_0)$.

We note finally that in the absence of perfusion ($\tau \rightarrow \infty$) we merely set terms of the form $1/\kappa\tau$ or $1/\sqrt{\kappa\tau}$ to zero in all of the above relations.

4 Temperature Elevation from a Planewave Source of Optical Power

Here we assume the heat source $A(z)$ is generated by an planewave normally-incident on a boundary separating two media, one optically absorbing and the other not absorbing (for example, an air-tissue interface). In this case, the light will generate the exponentially decaying heat source defined by (7). The resultant heat flow equation then becomes

$$\frac{\partial^2 T(z, t)}{dz^2} - \frac{1}{\kappa} \frac{\partial T(z, t)}{\partial t} - \frac{T(z, t)}{\kappa\tau} = -\frac{A(z)}{k}, \quad (21)$$

where $A(z) = K \exp(-\mu_e z)$ for $z \geq 0$ and $A(z) = 0$ for $z < 0$.

4.1 Thermal Boundary Conditions

There are three possible thermal boundary conditions at the interface $z = 0$ given by:

1. $T(0, t) = T_{amb}$
2. $\left. \frac{dT(z, t)}{dz} \right|_{z=0} = 0$
3. $\left. \frac{dT(z, t)}{dz} \right|_{z=0} + h[T(0, t) - T_{amb}] = 0$

In the third case, h is a heat transfer coefficient at the boundary. This case subsumes the first two as special cases; that is, cases 1 and 2 follow when $h \rightarrow \infty$ and $h = 0$, respectively. Boundary condition 1 arises when the boundary heat transfer is sufficiently large to maintain the boundary at the ambient temperature. Boundary condition 2 holds when the heat transfer is so low as to inhibit heat flux across the boundary (i.e., act as a thermal insulator). Boundary condition 3, sometimes called a convection boundary condition, is characterized by a heat transfer rate proportional to the temperature difference across the boundary. The heat transfer coefficient h can be measured by first heating the system and then recording the rate at which the system cools as a function of time.

4.2 Time-Dependent Temperature

The boundary conditions for $T(z, t)$ can be enforced by using a Green's function that satisfies these boundary conditions. In Appendix 1 the Green's functions that satisfy boundary conditions 1 and 2 are shown to be, respectively,

$$g_1(z, t|z', t') = \frac{2\kappa}{\pi} u(t-t') \int_0^\infty \sin(sz) \sin(sz') e^{-\kappa(s^2+1/\kappa\tau)(t-t')} ds \quad (22)$$

$$g_2(z, t|z', t') = \frac{2\kappa}{\pi} u(t-t') \int_0^\infty \cos(sz) \cos(sz') e^{-\kappa(s^2+1/\kappa\tau)(t-t')} ds. \quad (23)$$

As before, we will for convenience set $T_{amb} = 0$ so that $T(z, t)$ represents the temperature elevation above ambient. The derivation of the Green's function for boundary condition 3, denoted $g_3(z, t|z', t')$, is more involved and we state this function in Appendix 2. There we indicate the general procedure used to derive it.

Given the Green's function, the temperature is calculated from [51]

$$T_i(z, t) = \frac{1}{k} \int_0^\infty dz' \int_0^t dt' A(z') g_i(z, t|z', t'), \quad (24)$$

where $i = 1, 2, 3$. We illustrate this for case 1. Substituting (22) into (24) and interchanging orders of integration, we obtain

$$T_1(z, t) = \frac{2\kappa}{\pi k} \int_0^\infty ds \sin(sz) \int_0^\infty dz' A(z') \sin(sz'). \int_0^t dt' e^{-\kappa(s^2+1/\kappa\tau)(t-t')}. \quad (25)$$

We now define

$$\bar{A}(s) = \int_0^\infty A(z') \sin(sz') dz', \quad (26)$$

which is the sine transform of $A(z)$. The inverse sine transform is

$$A(z) = \frac{2}{\pi} \int_0^\infty \bar{A}(s) \sin(sz) ds.$$

Performing the t' integral in (25) results in

$$T_1(z, t) = \frac{2}{\pi k} \int_0^\infty \sin(sz) \bar{A}(s) \left\{ \frac{1 - e^{-\kappa(s^2+1/\kappa\tau)t}}{s^2 + 1/\kappa\tau} \right\} ds.$$

Substituting

$$A(z) = K e^{-\mu_e z}$$

into (26), we have

$$\bar{A}(s) = K \int_0^\infty e^{-\mu_e z'} \sin(sz') dz' = \frac{Ks}{\mu_e^2 + s^2},$$

so that

$$T_1(z, t) = \frac{2K}{\pi k} \int_0^\infty \frac{s \sin(sz)}{\mu_e^2 + s^2} \left\{ \frac{1 - e^{-\kappa(s^2+1/\kappa\tau)t}}{s^2 + 1/\kappa\tau} \right\} ds. \quad (27)$$

Similarly, for boundary condition 2, we have

$$T_2(z, t) = \frac{2K\mu_e}{\pi k} \int_0^\infty \frac{\cos(sz)}{\mu_e^2 + s^2} \left\{ \frac{1 - e^{-\kappa(s^2+1/\kappa\tau)t}}{s^2 + 1/\kappa\tau} \right\} ds. \quad (28)$$

In the absence of perfusion ($\tau \rightarrow \infty$) we replace the terms $1/\kappa\tau$ with zero in (27) and (28).

When the source is turned off, the system will cool and approach the ambient temperature. If the source is turned off at $t = t_0$, the temperature obeys the following

heat flow equation with the initial condition $T(z, t_0)$:

$$\frac{\partial^2 T(z, t)}{dz^2} - \frac{1}{\kappa} \frac{\partial T(z, t)}{\partial t} - \frac{T(z, t)}{\kappa \tau} = 0, \quad (29)$$

for $t \geq t_0$. The temperature for $t \geq t_0$ is computed from [51]:

$$T_i(z, t) = \frac{1}{\kappa} \int_0^\infty g_i(z, t|z', t_0) T_i(z', t_0) dz'. \quad (30)$$

We illustrate this assuming boundary condition 1. To evaluate this, we set $t' = t_0$ in (22) and $t = t_0$ in (27) and substitute the resulting expressions for $g_1(z, t|z', t_0)$ and $T_1(z, t_0)$ into (30). Interchanging orders of integration and performing the z' integral, finally yields

$$T_1(z, t) = \frac{2K}{\pi k} \int_0^\infty \frac{s \sin(sz)}{\mu_e^2 + s^2} e^{-\kappa(s^2 + 1/\kappa\tau)(t-t_0)} \left\{ \frac{1 - e^{-\kappa(s^2 + 1/\kappa\tau)t_0}}{s^2 + 1/\kappa\tau} \right\} ds \quad (31)$$

for $t \geq t_0$. As a check, substituting (31) into (29) shows that the heat flow equation is satisfied with the initial condition $T_1(z, t_0)$. Similarly, the cooling of $T_2(z, t)$ is given by

$$T_2(z, t) = \frac{2K\mu_e}{\pi k} \int_0^\infty \frac{\cos(sz)}{\mu_e^2 + s^2} e^{-\kappa(s^2 + 1/\kappa\tau)(t-t_0)} \left\{ \frac{1 - e^{-\kappa(s^2 + 1/\kappa\tau)t_0}}{s^2 + 1/\kappa\tau} \right\} ds. \quad (32)$$

Again, when there is no perfusion, we replace the terms $1/\kappa\tau$ with zero in (31) and (32).

4.3 Steady-State Temperature

The steady-state temperatures are obtained by letting $t \rightarrow \infty$ in (27) and (28), or

$$T_1^{(ss)}(z) = \frac{2K}{\pi k} \int_0^\infty \frac{s \sin(sz) ds}{(\mu_e^2 + s^2)(s^2 + 1/\kappa\tau)}$$

$$T_2^{(ss)}(z) = \frac{2K\mu_e}{\pi k} \int_0^\infty \frac{\cos(sz) ds}{(\mu_e^2 + s^2)(s^2 + 1/\kappa\tau)}.$$

These can be integrated to obtain

$$T_1^{(ss)}(z) = \frac{K}{k(1/\kappa\tau - \mu_e^2)} \left[e^{-\mu_e z} - e^{-z/\sqrt{\kappa\tau}} \right] \quad (33)$$

$$T_2^{(ss)}(z) = \frac{K}{k(1/\kappa\tau - \mu_e^2)} \left[e^{-\mu_e z} - \mu_e \sqrt{\kappa\tau} e^{-z/\sqrt{\kappa\tau}} \right]. \quad (34)$$

It is clear from (34) that in the absence of perfusion ($\tau \rightarrow \infty$) $T_2^{(ss)}(z)$ diverges. By differentiating the above expressions with respect to z and setting the derivatives to zero, we can find the value of z for which the steady-state temperature is maximum. For boundary condition 1 this value is found to be

$$z_{max} = \frac{\ln(\mu_e \sqrt{\kappa\tau})}{\mu_e - 1/\sqrt{\kappa\tau}}. \quad (35)$$

In general $z_{max} > 0$ when perfusion is present. In the absence of perfusion, z_{max} has no finite value. We also find that $z_{max} = 0$ for boundary condition 2 as expected. The steady-state temperature for boundary condition 3 is given in Appendix 2. In general we will have $z_{max} > 0$ for this boundary condition, but only when perfusion is present. By substituting z_{max} back into (33) and (34) explicit expressions can be found for the peak steady-state temperatures.

Finally, it may be useful to write the time-dependent solution (27) as

$$T_1(z, t) = T_1^{(ss)}(z) - \frac{2K}{\pi k} e^{-t/\tau} \int_0^\infty \frac{s \sin(sz) e^{-\kappa t s^2} ds}{(\mu_e^2 + s^2)(s^2 + 1/\kappa\tau)}, \quad (36)$$

where $T_1^{(ss)}(z)$ is given by (33) and the integral tends to zero as $t \rightarrow \infty$. Once again, this shows that $T_1(z, t) \rightarrow T_1^{(ss)}(z)$ more rapidly when τ is small. Similar expressions can be written for $T_2(z, t)$ and $T_3(z, t)$.

5 Simulations

Our objective here is to display the temperature elevations that can be achieved using representative values of the optical and thermal tissue parameters and typical values of nanoparticle cross sections and concentrations. We show temperature profiles computed from the preceding formulas using the following values: source parameters: $P_s = 0.1$ W, $I_0 = 1$ W cm⁻²; tissue thermal parameters: $k = 0.6$ W/C-m, $\kappa = 1.5 \times 10^{-7}$ m²s⁻¹; tissue optical parameters: $\mu_{at} = 0.10$ cm⁻¹, $\mu_{st} = 10$ cm⁻¹; nanoparticle parameters: $\sigma_a = 9.8 \times 10^{-11}$ cm², $\sigma_s = 9.8 \times 10^{-12}$ cm² and $N = 10^{11}$ cm⁻³. The values of the nanoparticle cross sections are, respectively, computed assuming an absorption efficiency of 5 and a scattering efficiency of 0.5 for a particle with a diameter of 50 nm. The efficiencies are defined as the ratio of the absorption and scattering cross sections to the particle's geometric cross section. These values are typical of plasmonic particles tuned to their plasmon resonance wavelength [42]. The efficiencies will vary depending on the particle size and shape.

We note that the temperature elevation will scale in direct proportion to the source magnitudes, P_s and I_0 .

5.1 Point Source Illumination

Figure 1 shows radial temperature profiles above the ambient temperature as a function of distance from a point source at three time intervals after the source is turned on and the steady-state temperature elevation. This calculation assumed no perfusion. Any finite value of the perfusion time constant will result in a reduced temperature. From the linearity of the heat flow equation, the temperature elevation arising from multiple point sources can be computed by adding the displaced temperature distribution from a single point source. Figure 2 shows a contour plot of the temperature elevation from a single point source assuming the temperature has achieved a steady-state; Fig. 3 is a contour plot of two point sources one cm apart, again assuming a steady-state. Figure 4 shows temperature elevation profiles with three values of the perfusion time constant τ in addition to no perfusion again assuming steady-state conditions. This plot clearly shows that perfusion can have a dramatic effect on temperature.

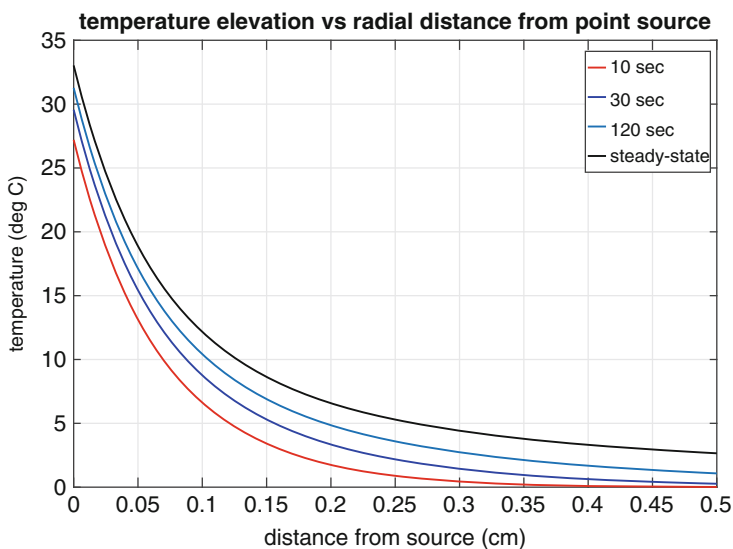


Fig. 1 Radial profiles of the temperature elevation at three time intervals and the steady-state elevation ($t \rightarrow \infty$). No perfusion is assumed

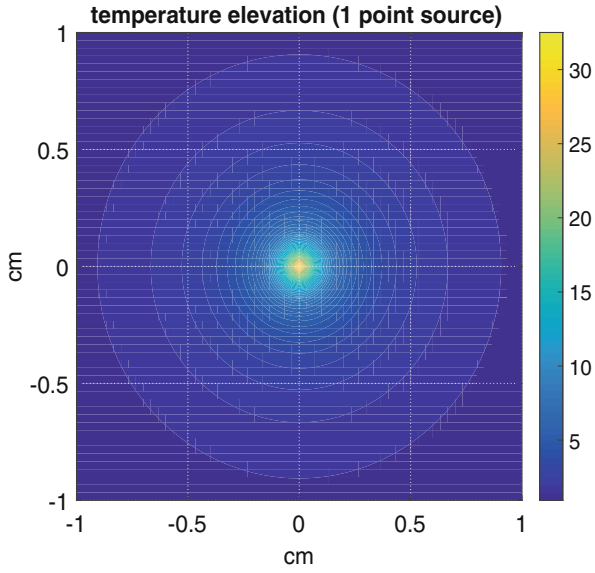


Fig. 2 Contour plot of the steady-state temperature elevation from a single point source. No perfusion is assumed

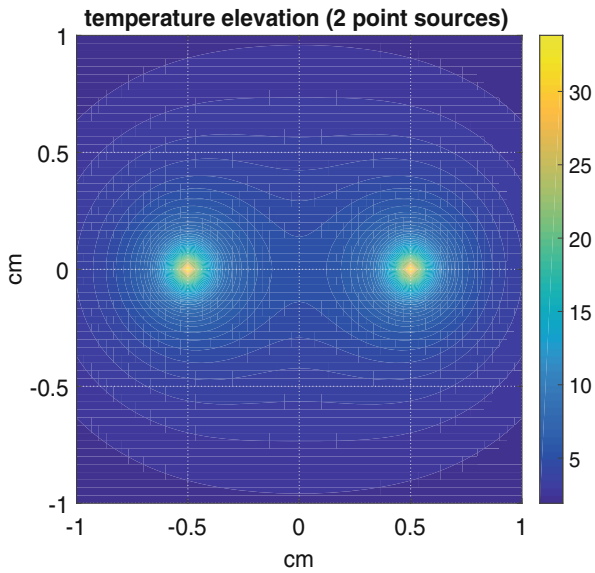


Fig. 3 Contour plot of the steady-state temperature elevation from two point sources one cm apart. No perfusion is assumed

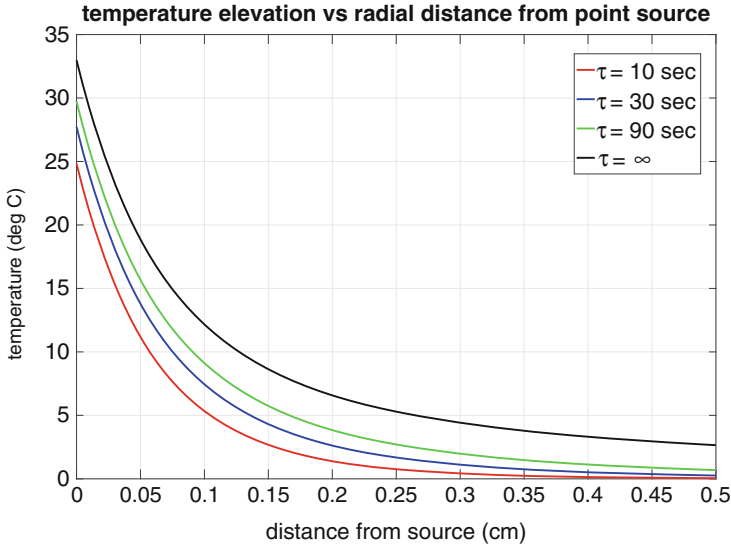


Fig. 4 Steady-state temperature elevation for three values of the perfusion time constant τ and no perfusion ($\tau = \infty$)

5.2 Planewave illumination

Figure 5 shows temperature-elevation profiles for three time intervals as well as the steady-state elevation under planewave illumination. This figure assumes boundary condition 1, in which the interface is held at the ambient temperature (assumed zero here) with a perfusion time constant of $\tau = 300$ s. Figure 6 shows a contour plot of the steady-state temperature elevation with $\tau = 300$ s. Figure 7 is similar to Fig. 5, but in the absence of perfusion ($\tau \rightarrow \infty$). Again, note that no perfusion, the steady-state elevation is large. Figure 8 shows the temperature elevation with boundary condition 1 with three values of the perfusion time constant as well as no perfusion ($\tau \rightarrow \infty$).

Figure 9 shows temperature elevation profiles at the same time intervals as before, but assuming boundary condition 2 (in which the boundary is insulating) with a perfusion time constant of $\tau = 300$ s. The steady-state elevation is also shown. Figure 10 is a contour plot of the steady-state temperature with $\tau = 300$ s. Figure 11 is the same as Fig. 9 with no perfusion ($\tau \rightarrow \infty$). In this case, in the absence of perfusion, there is no steady-state value; the temperature continues to increase without bound. These plots should be compared to those of Fig. 9. Finally, Fig. 12 shows plots of the temperature elevation with three values of the perfusion time constant.

Boundary condition 3, which assumes some heat flux across the boundary, will produce temperature profiles intermediate between the results for boundary conditions 1 and 2 depending on the value of the heat transfer coefficient, h .

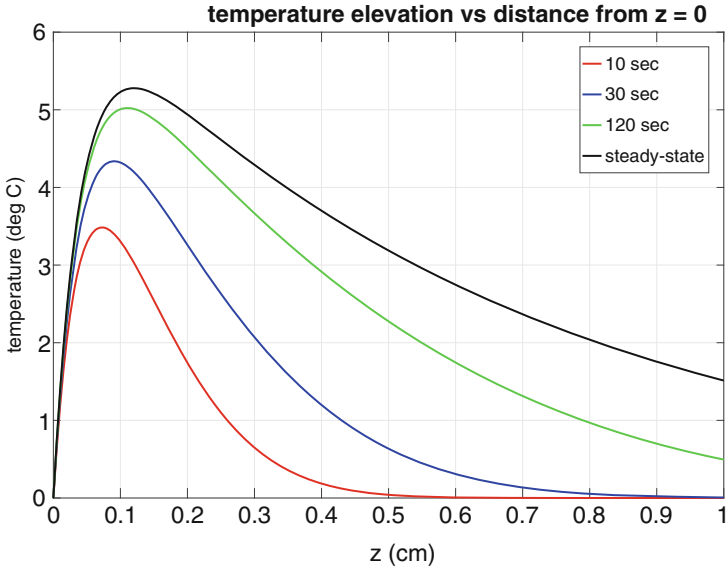


Fig. 5 The steady-state temperature elevation for three time intervals for the planewave source as a function of distance from the $z = 0$ plane. Boundary condition 1 is assumed with a perfusion time constant of $\tau = 300$ s

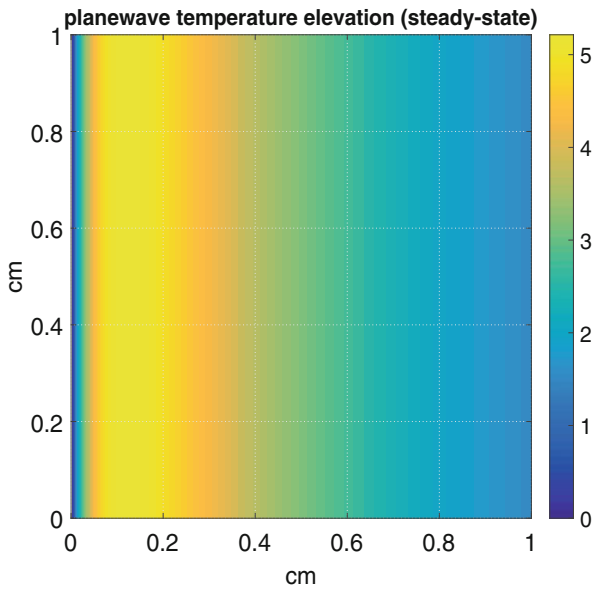


Fig. 6 Contour plot of the steady-state temperature elevation for a planewave source for boundary condition 1 and a perfusion time constant of $\tau = 300$ s

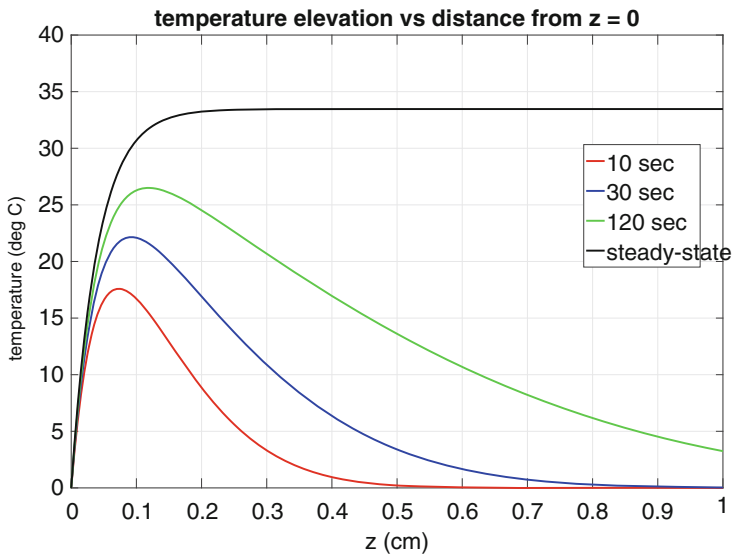


Fig. 7 Steady-state temperature elevation for three time intervals for the planewave source as a function of distance from the $z = 0$ plane. Boundary condition 1 is assumed with no perfusion ($\tau = \infty$)

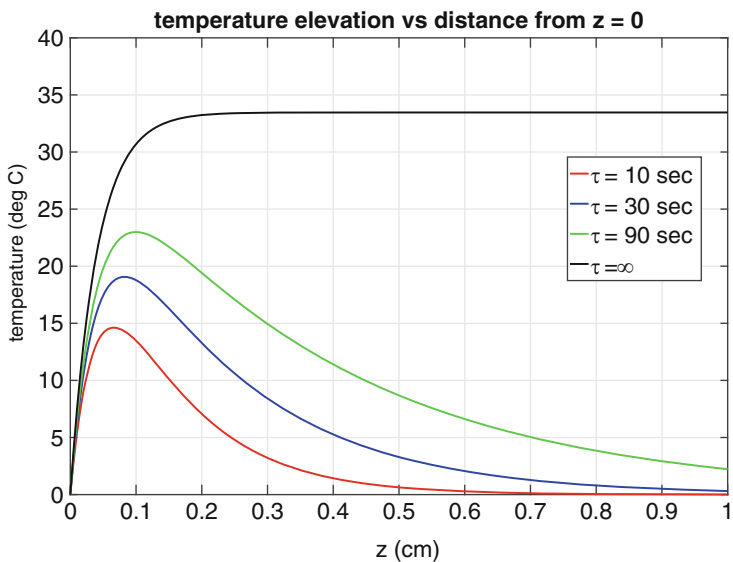


Fig. 8 Steady-state temperature elevation for three values of the perfusion time constant τ for the planewave source and boundary condition 1

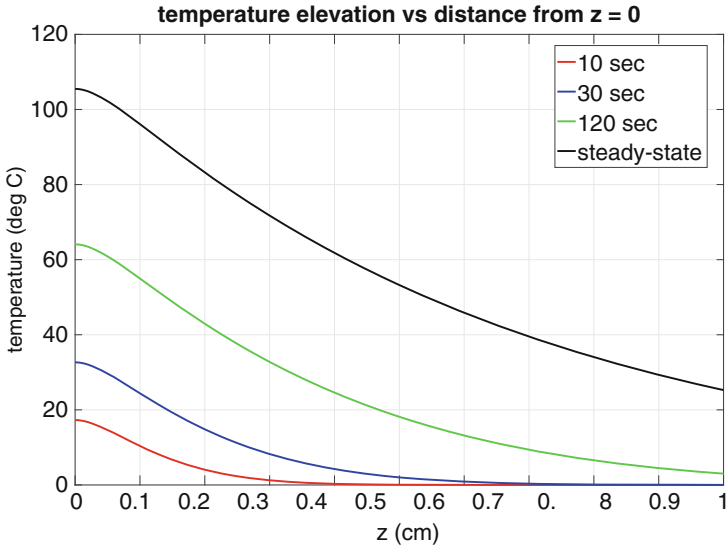


Fig. 9 Steady-state temperature elevation for three time intervals for the planewave source as a function of distance from the $z = 0$ plane. Boundary condition 2 is assumed with a perfusion time constant of $\tau = 300$ s

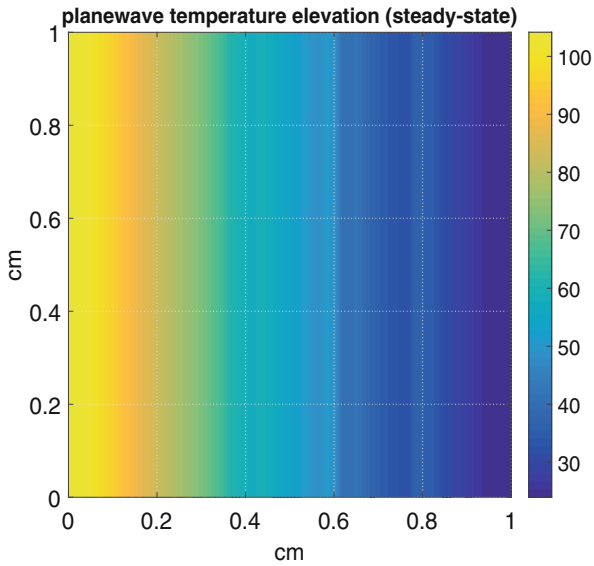


Fig. 10 Contour plot of the steady-state temperature elevation for a planewave source for boundary condition 2 with a perfusion time constant of $\tau = 300$ s

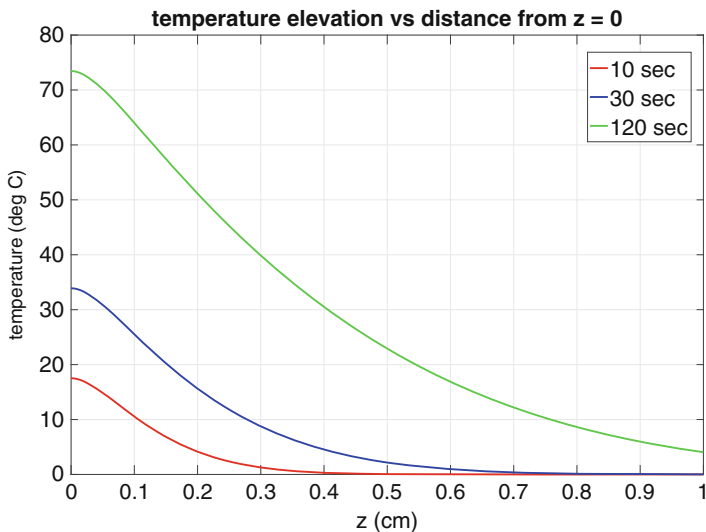


Fig. 11 Temperature elevation for three time intervals for a planewave source as a function of distance from the $z = 0$ plane. Boundary condition 2 is assumed with no perfusion ($\tau = \infty$). No steady-state elevation exists in this case

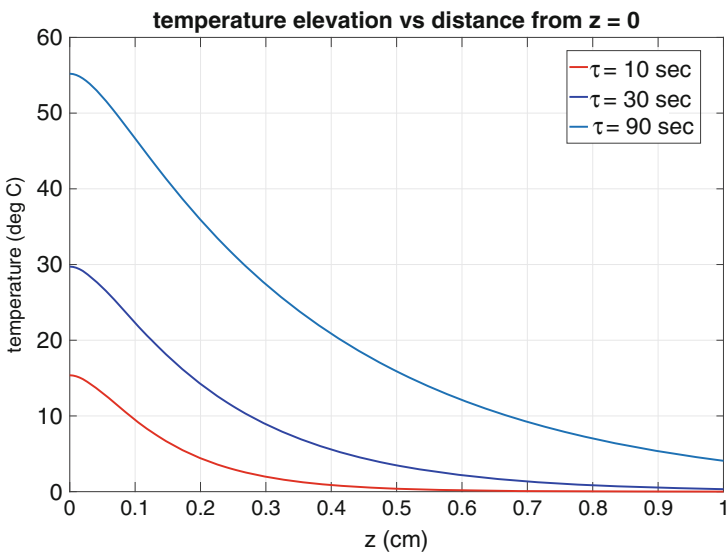


Fig. 12 Steady-state temperature elevation for three values of the perfusion time constant τ for a planewave source and boundary condition 2

6 Summary

The presence of plasmonic nanoparticles in tissue significantly enhances light absorption with a resultant elevation in temperature in regions of higher particle concentration. Part of this elevation will arise from tissue absorption, but this contribution will generally be less than that of particle absorption when the particles are tuned to their plasmon resonance. Given the particle concentration, their cross sections and tissue parameters, analytical solutions were derived for the space and time dependence of the temperature elevation under two types of optical illumination. The point-source solution is a reasonable model for a fiber emitting light embedded inside a region of tissue. For planewave illumination, three types of boundary conditions at the boundary interface were shown to give rise to different spatial temperature distributions. The point-source and planewave solutions require a single numerical integration and can be calculated rapidly. Moreover, explicit formulas for the steady-state temperature elevations have been derived. To obtain analytical solutions, we employed the diffusion approximation for light transport in tissue. This is a reasonable approximation within the therapeutic window in which scattering significantly dominates absorption. In the diffusion approximation, we require two tissue-dependent parameters to determine the light distribution: the effective scattering coefficient, μ_e , and the tissue absorption coefficient, μ_a . To estimate the heat source arising from nanoparticle absorption, we require the particle absorption and scattering cross sections, σ_a and σ_s , and the particle number density, N . The tissue thermal parameters are the tissue thermal conductivity, k , the tissue thermal diffusivity, κ and the thermal perfusion time constant, τ . For planewave illumination, the heat transfer coefficient at the boundary, h , may also be required depending on the boundary condition there. Most of these parameters can be measured in *in vitro* experiments, and some can be calculated, such as the nanoparticle absorption and scattering cross sections. For particles of complex shape (other than spheres, shells and spheroids), numerical calculations will be required for the cross sections. One result of the analysis, and the calculations presented here, is the significant sensitivity of the temperature elevation on the perfusion time constant. This time constant can not be measured *in vitro*, but will require an *in vivo* measurement or estimates based on published data for specific tissue types.

Acknowledgments This work was supported by the National Institutes of Health (1R01EB028078-01A1)

Appendix 1: Derivation of the Green's Functions

For a spherically-symmetric source, the Green's function, $g(r, t|r', t')$, for the diffusion equation is defined as the solution to

$$\frac{1}{r^2} \frac{\partial}{\partial r} \left(r^2 \frac{\partial g}{\partial r} \right) - \frac{1}{\kappa} \frac{\partial g}{\partial t} - \frac{g}{\kappa \tau} = -\frac{1}{r^2} \delta(r-r') \delta(t-t'). \quad (37)$$

To find $g(r, t|r', t')$, we employ the completeness relation for the spherical Bessel function $j_0(r\rho)$:

$$\int_0^\infty j_0(r\rho) j_0(r'\rho) \rho^2 d\rho = \frac{\pi}{2r^2} \delta(r-r'). \quad (38)$$

We now let [52]

$$g(r, t|r', t') = \int_0^\infty C_\rho(t, t') j_0(r\rho) j_0(r'\rho) \rho^2 d\rho, \quad (39)$$

and substitute into (37). Noting the relation,

$$\frac{1}{r^2} \frac{\partial}{\partial r} \left(r^2 \frac{\partial j_0(\rho r)}{\partial r} \right) + \rho^2 j_0(\rho r) = 0, \quad (40)$$

and using (38) for $\delta(r-r')/r^2$ on the right of (37), we obtain the following differential equation for $C_\rho(t, t')$:

$$\frac{1}{\kappa} \frac{dC_\rho}{dt} + (\rho^2 + 1/\kappa\tau) C_\rho = \frac{2}{\pi} \delta(t-t').$$

The solution to this equation is

$$C_\rho(t, t') = \frac{2\kappa}{\pi} u(t-t') e^{-\kappa(\rho^2 + 1/\kappa\tau)(t-t')},$$

where $u(t)$ is the unit step function. Substituting into (39), we obtain (10).

For a planewave source, the Green's function, $g(z, t|z', t')$, for the diffusion equation is defined as the solution to

$$\frac{\partial^2 g}{\partial z^2} - \frac{1}{\kappa} \frac{\partial g}{\partial t} - \frac{g}{\kappa \tau} = -\delta(z-z') \delta(t-t').$$

Using the same method as above, the free-space green's function is found to be

$$g(z, t|z', t') = \frac{\kappa}{\pi} u(t-t') \int_0^\infty \cos[s(z-z')] e^{-\kappa(s^2 + 1/\kappa\tau)(t-t')} ds.$$

To enforce boundary conditions 1 and 2 we employ linear combinations of the free-space Green's functions as follows. The Green's functions for boundary conditions 1 and 2 are, respectively, $g_1(z, t|z', t') = g(z, t|z', t') - g(z, t|-z', t')$ and $g_2(z, t|z', t') = g(z, t|z', t') + g(z, t|-z', t')$, which result in (22) and (23).

Appendix 2: Temperature Elevation for Boundary Condition 3

We can derive the temperature elevation for boundary condition 3 using the same approach as above once we have the Green's function $g_3(z, t|z', t')$ that enforces this boundary condition. One can show that

$$g_3(z, t|z', t') = g_2(z, t|z', t') + g_h(z, t|z', t'),$$

where $g_2(z, t|z', t')$ is given by (23) and

$$g_h(z, t|z', t') \equiv \frac{2h\kappa}{\pi} u(t-t') \int_0^\infty e^{-\kappa(t-t')(s^2+1/\kappa\tau)} \left\{ \frac{s \sin[(z+z')s] - h \cos[(z+z')s]}{h^2+s^2} \right\} ds.$$

The most straightforward method of deriving this result is to use Laplace transforms; the general procedure is outlined in [53]. The Green's function g_3 reduces to g_2 when $h = 0$. One can also show that $g_3 \rightarrow g_1$ in the limit $h \rightarrow \infty$.

The temperature elevation $T_3(z, t)$ is now obtained by substituting $g_3(z, t|z', t')$ into (24) and integrating with respect to z' and t' . This results in

$$T_3(z, t) = T_2(z, t) + T_h(z, t).$$

Here $T_2(z, t)$ is given by (28) and

$$T_h(z, t) \equiv \frac{2Kh}{\pi k} \int_0^\infty \frac{F_s(z)}{(s^2+h^2)(s^2+\mu_e^2)(s^2+1/\kappa\tau)} \left[1 - e^{-\kappa(s^2+1/\kappa\tau)t} \right] ds.$$

where

$$F_s(z) \equiv (\mu_e + h)s \sin(zs) + (s^2 - h\mu_e) \cos(zs).$$

When $h = 0$, we have $T_3(z, t) = T_2(z, t)$ and when $h \rightarrow \infty$, $T_3(z, t) \rightarrow T_1(z, t)$. The steady-state temperature ($t \rightarrow \infty$) may be written

$$T_3^{(ss)}(z) = T_2^{(ss)}(z) + T_h^{(ss)}(z),$$

where $T_2^{(ss)}(z)$ is given by (34) and

$$T_h^{(ss)}(z) \equiv \frac{2Kh}{\pi k} \int_0^\infty \frac{F_s(z) ds}{(s^2+h^2)(s^2+\mu_e^2)(s^2+1/\kappa\tau)}.$$

This can be readily integrated after expanding the integrand in partial fractions. After some algebra, we obtain

$$T_3^{(ss)}(z) = \frac{K}{k(1/\kappa\tau - \mu_e^2)} \left[e^{-\mu_e z} - \left(\frac{\mu_e + h}{1/\sqrt{\kappa\tau} + h} \right) e^{-z/\sqrt{\kappa\tau}} \right].$$

$T_3^{(ss)}(z)$ will have a peak temperature at some distance $z_{max} > 0$ that can be found by differentiating $T_3^{(ss)}(z)$ with respect to z and setting the derivative to zero. This results in

$$z_{max} = \frac{1}{(\mu_e - 1/\sqrt{\kappa\tau})} \ln \left[\frac{1 + h\sqrt{\kappa\tau}}{1 + h/\mu_e} \right].$$

This reduces to (35) when $h \rightarrow \infty$ and $z_{max} = 0$ when $h = 0$. Note that no finite z_{max} exists in the absence of perfusion.

References

1. Vines, J.B., Yoon, J.-H., Ryu, N.-E., et al.: Gold Nanoparticles for photothermal cancer therapy. *Front. Chem.* **7**, 167 (2019)
2. Falk, M.H., Issels, R.D.: Hyperthermia in oncology. *Int. J. Hyperthermia.* **17**(1), 1–18 (2001)
3. Owusu, R.A., Abern, M.R., Inman, B.A.: Hyperthermia as adjunct to intravesical chemotherapy for bladder cancer. *Biomed Res. Int.* **2013**, 262313 (2013)
4. Hildebrandt, B., Wust, P., Ahlers, O., et al.: The cellular and molecular basis of hyperthermia. *Crit. Rev. Oncol. Hematol.* **43**(1), 33–56 (2002)
5. Frey, B., Weiss, E.M., Rubner, Y., et al.: Old and new facts about hyperthermia-induced modulations of the immune system. *Int. J. Hyperthermia.* **28**(6), 528–542 (2012)
6. Schildkopf, P., Ott, O.J., Frey, B., et al.: Biological rationales and clinical applications of temperature controlled hyperthermia-implications for multimodal cancer treatments. *Curr. Med. Chem.* **17**(27), 3045–3057 (2010)
7. Wust, P., Hildebrandt, B., Sreenivasa, G., et al.: Hyperthermia in combined treatment of cancer. *Lancet. Oncol.* **3**(8), 487–497 (2002)
8. Pandita, T.K., Pandita S., Bhaumik S.R.: Molecular parameters of hyperthermia for radiosensitization. *Crit. Rev. Eukaryotic Gene Expr.* **19**(3), 235–251 (2009)
9. Takada, T., Yamashita, T., Sato, M., et al.: Growth inhibition of re-challenge B16 melanoma transplant by conjugates of melanogenesis substrate and magnetite nanoparticles as the basis for developing melanoma-targeted chemo-thermo-immunotherapy. *J Biomed. Biotechnol.* 457936 (2009)
10. Koning, G.A., Eggermont, A.M.M., Lindner, L.H., et al.: Hyperthermia and thermosensitive liposomes for improved delivery of chemotherapeutic drugs to solid tumors. *Pharm. Res.* **27**(8), 1750–1754 (2010)
11. Loo, C., Lin, A., Hirsch, L., et al.: Nanoshell-enabled photonics-based imaging and therapy of cancer. *Technol. Cancer Res. Treat.* **3**(1), 33–40 (2004)
12. Wang, C., Xu, L., Liang, C., et al.: Immunological responses triggered by photothermal therapy with carbon nanotubes in combination with anti-CTLA-4 therapy to inhibit cancer metastasis. *Adv. Mater.* **26**(48), 8154–8162 (2014)
13. Hirsch, L.R., Stafford, R.J., Bankson, J.A., et al.: Nanoshell-mediated near-infrared thermal therapy of tumors under magnetic resonance guidance. *PNAS* **100**, 13549–13554 (2003)
14. Pitsillides, C.M., Joe, E.K., Wei, X., et al.: Selective cell targeting with light-absorbing microparticles and nanoparticles. *Biophys. J.* **84**, 4023–4032 (2003)

15. Huang, X., El-Sayed, I.H., Qian, W., et al.: Cancer cell imaging and photothermal therapy in the near-infrared region by using gold nanorods. *J. Am. Chem. Soc.* **128**, 2115–2120 (2006)
16. Govorov, A.O., Zhang, W., Skeini, T., et al.: Gold nanoparticle ensembles as heaters and actuators: melting and collective plasmon resonances. *Nanoscale Res. Lett.* **1**, 84–90 (2006)
17. Elliott, A.M., Stafford, R.J., Schwartz, J., et al.: Laser-induced thermal response and characterization of nanoparticles for cancer treatment using magnetic resonance thermal imaging. *Am. Assoc. Phys. Med.* **34**(7), 3102–3108 (2007)
18. Reynoso, F.J., Lee, C.-D., Cheong, S.-K., et al.: Implementation of a multisource model for gold nanoparticle-mediated plasmonic heating with near-infrared laser by the finite element method. *Am. Assoc. Phys. Med.* **40**(7), 073301 (2007)
19. Roper, D.K., Ahn, W., Hoepfner, M.: Microscale heat transfer transduced by surface plasmon resonant gold nanoparticles. *J. Phys. Chem. C* **111**, 3636–3641 (2007)
20. Govorov, A.O., Richardson, H.H.: Generating heat with metal nanoparticles. *NanoToday* **2**, 30–38 (2007)
21. Jain, P.K., El-Sayed, I.H., Qian, W., et al.: Au nanoparticles target cancer. *NanoToday* **2**, 18–29 (2007)
22. Huang, X., Jain, P.K., El-Sayed, I.H., et al.: Plasmonic photothermal therapy (PPTT) using gold nanoparticles. *Lasers Med. Sci.* **23**, 217–228 (2008)
23. Sassaroli, E., Li, K.C.P., O'Neill, B.E.: Numerical investigation of heating of a gold nanoparticle and the surrounding microenvironment by nanosecond laser pulses for nanomedicine applications. *Phys. Med. Biol.* **54**, 5541–5560 (2009)
24. Cheong, S.-K., Krishnan, S., Cho, S.H.: Modeling of plasmonic heating from individual gold nanoshells for near-infrared laser-induced thermal therapy. *Med. Phys.* **36**(10), 4664–4671 (2009)
25. Richardson, H.H., Carlson, M.T., Tandler, P.J., et al.: Experimental and theoretical studies of light-to-heat conversion and collective heating in metal nanoparticle solutions. *Nano Lett.* **9**(3), 1139–1146 (2009)
26. Baffou, G., Quidant R., de Abajo, F.J.G.: Nanoscale control of optical heating in complex plasmonic systems. *ACS Nano* **4**, 709–716 (2010)
27. Huang, H.C., Rege, K., Heys, J.J.: Spatiotemporal temperature distribution and cancer cell death in response to extracellular hyperthermia induced by gold nanorods. *ACS Nano* **4**, 2892–2900 (2010)
28. Sanchot, A., Baffou, G., Marty, R., et al.: Plasmonic nanoparticle networks for light and heat concentration. *ACS Nano* **6**, 3434–3440 (2012)
29. Qina, Z., Bischof, J.C.: Thermophysical and biological responses of gold nanoparticle laser heating. *Chem. Soc. Rev.* **41**, 1191–1217 (2012)
30. Essone Mezeme, M., Brosseau, C.: Engineering nanostructures with enhanced thermoplasmonic properties for biosensing and selective targeting applications. *Phys. Rev. E* **87**, 012722 (2013)
31. Baffou, G., Quidant, R.: Thermo-plasmonics: using metallic nanostructures as nano-sources of heat. *Laser Photonics Rev.* **7**, 171–187 (2013)
32. Liu, Y., Ashton, J.R., Moding, E.-J., et al.: A plasmonic gold nanostar theranostic probe for in vivo tumor imaging and photothermal therapy. *Theranostics* **5**, 946–960 (2015)
33. Norton, S.J., Vo-Dinh, T.: Photothermal effects of plasmonic metal nanoparticles in a fluid. *J. Appl. Phys.* **116**, 083105 (2016)
34. Yuan, H., Fales, A.M., Vo-Dinh, T.: TAT peptide-functionalized gold nanostars: enhanced intracellular delivery and efficient NIR photothermal therapy using ultralow irradiance. *J. Am. Chem. Soc.* **134**(28), 11358–11361 (2012)
35. Liu, Y., Ashton, J.R., Moding, E.J., et al.: A plasmonic gold nanostar theranostic probe for in vivo tumor imaging and photothermal therapy. *Theranostics* **5**(9), 946–960 (2015)
36. Khoury, C.G., Vo-Dinh, T.: Gold nanostars for surface-enhanced Raman scattering: synthesis, characterization and optimization. *J. Phys. Chem. C Nanometer. Interfaces.* **112**(48), 18849–18859 (2008)
37. Yuan, H., Khoury, C.G., Hwang, H., et al.: Gold nanostars: surfactant-free synthesis, 3D modelling, and two-photon photoluminescence imaging. *Nanotechnology* **23**(7), 075102 (2012)

38. Yuan, H., Khoury, C.G., Wilson, C.M., et al.: In vivo particle tracking and photothermal ablation using plasmon-resonant gold nanostars. *Nanomedicine* **8**(8), 1355–1363 (2012)
39. Yuan, H., Wilson, C.M., Xia J., et al.: Plasmonics-enhanced and optically modulated delivery of gold nanostars into brain tumor. *Nanoscale* **6**(8), 4078–4082 (2014)
40. Liu, Y., Maccarini, P., Palmer, G.M., et al.: Synergistic immuno photothermal nanotherapy (SYMPHONY) for the treatment of unresectable and metastatic cancers. *Sci. Rep.* **7**, 1–6 (2017)
41. Liu, Y., Chongsathidkiet, P., Crawford, B.M., et al.: Plasmonic gold nanostar-mediated photothermal immunotherapy for brain tumor ablation and immunologic memory. *Immunotherapy* **11**, 1293–1302 (2019)
42. Jain, P.K., Lee, K.S., El-Sayed, I.H., et al.: Calculated absorption and scattering properties of gold nanoparticles of different size, shape and composition: applications in biological imaging and biomedicine. *J. Phys. Chem. B* **110**, 7238–7248 (2006)
43. Koblinski, P., Cahill, D.G., Bodapati, A., et al.: Limits of localized heating by electromagnetically excited nanoparticles. *J. Appl. Phys.* **100**, 054305 (2006)
44. Norton, S.J.: A general nonlinear inverse transport algorithm using forward and adjoint flux computations. *IEEE Trans. Nuclear Sci.* **44**(2), 153–162 (1997)
45. Norton, S.J.: Iterative inverse scattering algorithms: methods of computing Fréchet derivatives. *J. Acoust. Soc. Am.* **106**(5), 2653–2660 (1999)
46. Hyborg, W.L.: Solutions of the bio-heat transfer equation. *Phys. Med. Biol.* **33**, 785–792 (1988)
47. Holmes, K.R.: A tabulation of blood perfusion rates from the literature for specific tissues and organs was compiled by Professor Kenneth R. Holmes. This list is available online at <http://users.ece.utexas.edu/~valvano/research/right.html> under the heading “Thermal Properties by Kenneth Holmes”
48. Wang, L.V., Wu, H.-I.: *Biomedical Optics*, Chapter 5. Wiley, Hoboken (2007)
49. Vo-Dinh, T. (ed.): *Biomedical Photonics Handbook*, Chapter 2. CRC Press, New York (2003)
50. Wang, L.V., Wu, H.-I.: *Biomedical Optics*, Appendix A. Wiley, Hoboken (2007)
51. Morse, P.M., Feshbach, H.: *Methods of Theoretical Physics*, p. 860. McGraw-Hill, New York (1953)
52. Morse, P.M., Feshbach, H.: *Methods of Theoretical Physics*, p. 864. McGraw-Hill, New York (1953). This general approach is known as the eigenfunction expansion method for computing the Green’s function. Here the eigenfunctions are the spherical Bessel functions
53. Carslaw, H.S., Jaeger, J.C.: *Conduction of Heat in Solids*, 2nd edn., p. 358. Oxford University Press (1959)

Part II
Nanosystems for Biomedical Applications

Nanoparticle Systems Applied for Immunotherapy in Various Treatment Modalities



Vanessa Cupil-Garcia, Bridget M. Crawford, and Tuan Vo-Dinh 

1 Introduction

There is a critical need for novel technologies to effectively treat and ultimately reduce cancer recurrences, treatment costs, number of radical cystectomies, and mortality. The development of better and targeted treatments continues in the long and drawn out war against cancer. The high cancer relapse rates following treatments of chemotherapy and radiation therapy has encouraged many researchers to focus on employing the human body's own defense system as a tool to combat cancer. Cancer immunotherapy has shown promise as an alternative to the current forms of cancer treatment and is the subject of ongoing and extensive research. The goal of immunotherapy treatment is to recruit tumor killing immune cells already present in the tumor microenvironment, initiating an antitumor immune response. Although certain tumors are moderately responsive to immunotherapy, including microsatellite instable cancers, response rates for the majority remain low, as tumors exhibit primary, adaptive, and acquired resistance to cancer immunotherapy [1, 2].

V. Cupil-Garcia (✉)

Fitzpatrick Institute for Photonics, Duke University, Durham, NC, USA

Department of Chemistry, Duke University, Durham, NC, USA

e-mail: vanessa.cupil.garcia@duke.edu

B. M. Crawford

Fitzpatrick Institute for Photonics, Duke University, Durham, NC, USA

Department of Biomedical Engineering, Duke University, Durham, NC, USA

T. Vo-Dinh

Fitzpatrick Institute for Photonics, Duke University, Durham, NC, USA

Department of Biomedical Engineering, Duke University, Durham, NC, USA

Department of Chemistry, Duke University, Durham, NC, USA

e-mail: tuan.vodinh@duke.edu

Recent developments in the fields of nanotechnology and bioengineering afford new approaches that can dramatically improve not only the safety but also the efficacy of cancer immunotherapy [3–5]. Since the immune system is spatiotemporally controlled, therapies that influence the immune system should be spatiotemporally controlled as well, in order to maximize the therapeutic index. Nanoparticles and biomaterials allow for defined localization, pharmacokinetics and co-delivery of immunomodulatory compounds, eliciting responses that cannot be achieved upon administration of such compounds when free in solution. The safety and efficacy of immunotherapy can be improved by incorporating different therapeutic agents into engineered biomaterials for targeting specific immune reactions. Nanoparticle carriers can be loaded with biological molecules and even cells, therefore making them useful for the targeted delivery of antigens, vaccines, proteins, or other immunotherapeutic agents to the desired site. The convergence of cancer immunotherapy, nanotechnology, bioengineering, and drug delivery is most opportune, as each of these fields has matured independently to the point that they can now be combined synergistically and used to complement the others. A diagram rendering a representative example of nanoparticle activation of the innate and adaptive immune system is shown in Fig. 1. This chapter provides an overview of the development and applications of various nanoparticle platforms for enhanced immunotherapy as well as in combination with other treatments, including photothermal therapy (PTT), photodynamic therapy (PDT), and chemotherapy [6].

2 Widening the Therapeutic Window

The therapeutic window refers to the range of doses that optimize between efficacy and toxicity, achieving the greatest therapeutic benefit without resulting in unacceptable side-effects or toxicity. Drug delivery technologies can focus the action of immunostimulatory payloads on particular cells or tissues, thereby minimizing systemic dissemination and undesirable side effects. Safer systemic administration is highly desirable as intravenous injection is much more readily translated to the point of care as compared to intratumoral or peritumoral injection. The physicochemical properties of nanoparticles, including size, shape, surface charge, and surface functionalization, are crucial factors in the development of a drug delivery system. The delivery mechanism of nanoparticles depends greatly on the enhanced permeability and retention (EPR) effect, a process by which accumulation of particles in tumors occurs following systemic administration. Studies have demonstrated that nanoparticles with elongated shapes, such as nanorods, have greater internalization potential compared to their spherical counterparts. Additionally, surface functionalization can allow for increased circulation time or active targeting to a desired site, thereby increasing specificity of treatment. Although nanoparticles containing cancer cell-intrinsic drugs must deliver their payload to the vast majority of cancer cells within the tumor to confer meaningful benefit, even a modest accrual of immunotherapy-loaded particles can elicit robust

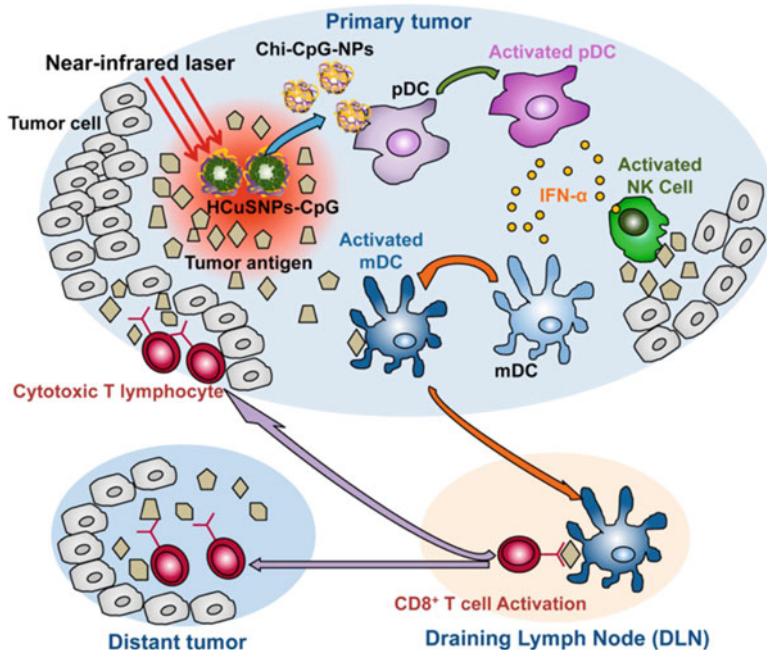


Fig. 1 Representative example of immunomodulation using multifunctional nanoparticles. Diagram of Chitosan-Coated Hollow Copper Sulfide Nanoparticles conjugated to cytosine guanine motifs (HCuSNPs-CpG) for photothermal immunotherapy of breast cancer. After PTT treatment using NIR light, the nanoparticles transform to chitosan- CpG nanocomplexes (Chi-CpG-NPs). This results in uptake into Toll-like receptor 9-rich endosomes of plasmacytoid dendritic cells (pDCs). The pDCs secrete interferon- α (IFN- α) after stimulation from CpG. pDCs promote innate immunity via NK cell activation. In tandem HCuSNPs PTT ruptures and kills the tumor cells causing the release of tumor-associated antigens to myeloid dendritic cells (mDCs). Activated pDCs secrete IFN- α and cause mDCs to transform into antigen-presenting cells. The APCs travel to tumor-draining lymph nodes (DLNs) and prime antigen specific T cells. The adaptive immune response is due to antigen-specific CD8⁺ T cells entering circulation into primary and untreated metastatic tumors in different locations known as the “effector phase.” Adapted from [6]

anti-tumor responses. Since immune cells can proliferate as well as propagate the response by activating complementary immune cells, then modest accumulation of immunotherapy-loaded nanoparticles can generate a desirable and beneficial immune response.

Releasing small quantities of therapy over an extended period of time can lead to sustained local treatment rather than immediate saturation and subsequent dispersion of a compound. While intratumoral or peritumoral injections of naked cytokines, antibodies, or agonists allow for local treatment, they result in systemic exposure as well as toxicity since the drugs diffuse away rapidly [7]. For example, recombinant cytokines injected intratumorally into patients’ lesions can be detected systemically within 30 minutes, leading to toxicities that equal those following systemic injection [8–10]. Kwong et al. demonstrated that by anchoring the agonist

anti-CD137 (a co-stimulatory molecule also known as 4-1BB) and an IL-2-Fc domain fusion protein to liposomes of appropriate size restricted the distribution of the biologics to the tumor parenchyma and tumor-draining lymph nodes, where T cells are primed by antigen-presenting cells (APCs) [11]. By preventing leakage into circulation following local administration into mice, a majority of the primary tumors were cured without lethal inflammatory toxicity that was associated with the same intratumoral injection without liposomes (i.e., in solution).

3 Enhancing Adoptive-Cell Therapy

Adoptive-cell therapy is becoming an increasingly important strategy in immunotherapy. Examples include transgenic T cell receptor (TCR) products [12], tumor-infiltrating lymphocytes (TILs) [13, 14] and chimeric antigen receptor (CAR) T cells – which have been approved by the US FDA for the treatment of B cell acute lymphoblastic leukemia [15] and B cell non-Hodgkin lymphoma [16, 17]. Nanotechnology can be applied *ex vivo* to activate and expand T cells prior to their adoptive transfer. Because antigen-specific T cells are often present at low amounts, the ability to increase the quantity of these important cells is beneficial. The standard protocol for preparing autologous T cells for adoptive transfer involves using spherical superparamagnetic polymer particles coated with anti-CD3 and anti-CD28 antibodies, known as Dynabeads™, which are first-generation artificial APCs (aAPCs) [18, 19]. Additionally, aAPCs have been made by functionalizing iron-dextran nanoparticles with a major histocompatibility complex (MHC)-immunoglobulin (Ig) dimer and a co-stimulatory CD28 antibody [20]. Using magnetic columns, antigen-specific CD8⁺ T cells bound to the aAPCs are enriched and separated from bulk leukocyte populations [21]. The aPAC size, concentration, and ligand choice and density impact the recovery, activation, and expansion of the T cell populations. Mimicking the natural antigen presentation of physiological APCs can greatly improve the antitumor properties of the T cells.

4 Improving Payload Delivery

Owing to their dimensions, nanoparticles naturally mimic bacteria or viruses and are therefore readily recognized by various types of immune cells, including APCs. For instance, a synthetic engineered bacterial vector acted as a potent adjuvant for anticancer immunotherapy [22]. Also, the biomaterial carrier of the nanoparticle itself can serve as an adjuvant, allowing for simpler production without the need for a separate agonist of innate immunity. Recently, GNPs have been applied in immunotherapies including cancer antigen and immune adjuvant delivery. GNPs alone have been shown to stimulate the immune system and thus prove to be attractive candidates for adjuvant delivery. Thermal ablation and light triggered

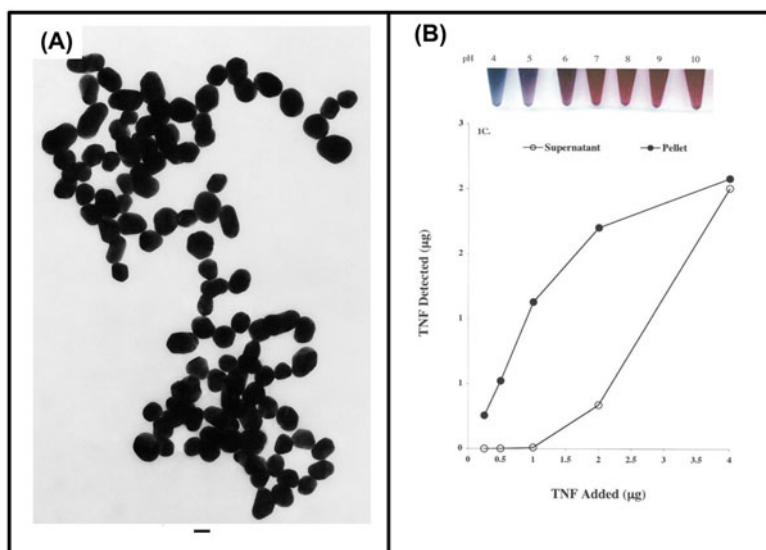


Fig. 2 CYT-6091 Colloidal Gold Clinical Trial for Treatment of Cancer. (a) Representative transmission electron microscopy images of the colloidal gold nanoparticles used in the study. (b) pH binding studies to determine the optimal binding of TNF to the colloidal gold nanoparticles for enhance therapy. Adapted from [25]

release could be combined with delivery of nucleic acid immune adjuvants, such as toll like receptor (TLR) agonists, as promising immune therapies. For instance, the CpG oligonucleotide adjuvant has been conjugated to gold chitosan nanoparticles and demonstrated an enhanced effect of CpG *in vitro* and *in vivo* as compared to free CpG [6, 23]. CpG molecules are short DNA sequences that mimic bacterial DNA and thus stimulate immune cells via interaction with TLR9, found in the endolysosomal compartments of cells, where GNPs are rapidly uptaken within phagocytic immune cells. It was found that GNP functionalized with triethylene glycol (TEG) modified CpG resulted in enhanced TNF- α secretion as well as inhibition of tumor growth compared to free CpG [24].

In another study, TNF- α was linked to the surface of 33-nm GNP via thiolated polyethylene glycol (PEG-SH) to promote delivery of the cytokine to MC-38 colon carcinoma tumors following intravenous injection in tumor-bearing mice [25]. Paciotti et al. demonstrated that TNF functionalized GNP resulted in maximal antitumor response with lower doses of TNF and decreased off-site toxicity compared to TNF alone. Results demonstrating binding curves for TNF to colloidal gold nanoparticles from this study are shown in Fig. 2. This work, under the name CYT-6091, was further expanded by Goel et al. in 2005 during phase 1 clinical trials for 29 patients with solid tumors that were not responsive to traditional therapies [26]. It was found that three times the maximum tolerated dose of TNF previously reported was systemically administered without adverse effects. Bischof et al. have

also used CYT-6091 as a vascular disrupting agent in conjugation with cryosurgery or hyperthermia [27]. A synergistic antitumor response was demonstrated that was greater than the sum of the treatments alone.

Several groups have studied GNPs for their ability to deliver large vaccine payloads, including Lin and co-workers who used 30-nm GNPs functionalized with self-assembling modified PEG and tumor-associated antigen peptides as a cancer vaccine platform, termed gold nanovaccine (AuNV) [28]. It was found that the AuNV was able to stimulate T cells with a four-fold enhanced efficacy as compared to free antigen peptide. Nanotechnology formulations can be used to load multiple modalities into the same formulation, whether these be small molecules, nucleic acids, polypeptides, or cells. This ability to co-entrap has particular utility in the context of vaccines, as co-encapsulating both antigen and adjuvant ensures that both vaccine components are delivered concurrently to the same APCs. If delivered separately, those APCs that take up the antigen in the absence of the adjuvant become tolerogenic. The co-delivery of adjuvants with antigens has proven to be highly effective, leading to a study by Jon and colleagues using 7-nm GNPs functionalized with red fluorescent protein (RFP) as a model antigen and CpH 1668 as the adjuvant [29]. In agreement with results of a study by Penades et al., they demonstrated that GNP systems that mimic viral properties are attractive vaccine candidates due to their improved lymph node accumulation and interaction with APCs [30].

Targeting of lymph nodes substantially enhances the efficacy and safety of systemic vaccination. Antigens and adjuvants can be efficiently delivered to lymph nodes by conjugating them to lipophilic albumin-binding tails using a polar linker that promotes solubility, thereby significantly improving antitumor efficacy and reducing systemic toxicity [31]. High-density lipoprotein-mimicking nanodiscs coupled with antigen peptides and adjuvants have the ability to enhance the co-delivery of antigen and adjuvant to lymphoid organs and sustain antigen presentation by APCs. When combined with anti-PD-1 and anti-CTLA-4 therapy, the nanodisc vaccines eliminated established mouse colorectal and melanoma tumors [32].

Since nucleic acid-based vaccines are susceptible to nuclease-mediated hydrolysis, the use of nanocarriers greatly enhance their stability. mRNA contains both specificity (encoded antigen) and function (adjuvant), thus every cell that takes up the mRNA has potential to induce productive immunity rather than tolerance. Lipids have been used extensively to increase the efficiency of nucleic acid cargo delivery [4]. For example, Kranz et al. demonstrated that dendritic cells can be targeted *in vivo* by systemically administered RNA-lipoplexes (RNA-LPX) by adjusting the net charge. The LPX protected the RNA from extracellular ribonucleases and mediates its efficient uptake and expression of encoded antigens by local APCs, generating robust effector and memory T cell responses and inducing the rejection of established tumors in multiple mouse models of cancer [33].

While small molecules, cytokines, and antibodies can benefit from targeted delivery to relevant tissues or cell types, nucleic acids often require drug delivery solutions in order to transit across hydrophobic, tightly packed cell membranes. Nanoparticles can also facilitate payload release from membrane-bound compartments into the cytosol following endocytosis or phagocytosis. Lipid nanoparticles,

polymeric particles and aptamer-conjugates have been used to achieve small-interfering RNA (siRNA)-mediated silencing of transcripts in mice, although the efficiency of delivery is quite low [34]. Among the most exciting application of nucleic acid delivery is the use of targeted polymeric nanoparticles to transfect primary human T cells or hematopoietic stem cells following *in vitro* incubation.

5 Combinational Cancer Immunotherapy with Nanoparticles

Nanoparticle-based phototherapies have been widely studied and used for their strong efficacy, minimal invasiveness, and negligible side effects in tumor elimination. In addition to directly killing tumor cells through heat or ROS, PTT, PDT, and chemotherapy, nanoparticles can also induce antitumor immunity by incorporating other immunotherapeutic molecules. With the aid of photosensitive nanoparticle platforms, immune-modulating agents delivered to a specific site are expected to be more powerful in tumor destruction and effective immune activation.

5.1 Nanoparticle-Based Photothermal Immunotherapy

Hyperthermia (HT) is a treatment where heat is applied to a tumor or organ [35, 36]. While high temperature HT (>55 °C) can induce immediate thermal death (ablation) to targeted tumors, mild fever-range HT (40–43 °C) can be used to (1) improve drug delivery to tumors, (2) improve cancer cell sensitivity to anti-cancer therapy, and (3) trigger potent systemic anti-cancer immune responses [37–40]. Nanoparticle (NP)-mediated thermal therapy offers the potential to combine the advantages of precise cancer cell ablation [41] with many benefits of mild HT in the tumor microenvironment, including radio-sensitization of hypoxic regions [42], enhancement of drug delivery [43], activation of thermosensitive agents [44], and boosting the immune system [45].

Metallic nanostructures have gained particular interest in nanomedicine research due to their ability to interact with electromagnetic (EM) radiation, which stems from their confinement of electrons to produce quantum effects. Noble metal plasmonic nanostructures, like gold and silver nanoparticles, are most commonly used due to their relative inertness and visible and near-infrared absorption bands. Gold nanoparticles have been found useful for *in vivo* applications due to their biocompatibility, while silver nanoparticles have larger molar extinction coefficients, leading to more sensitive *in vitro* assays. Plasmonic gold nanoparticles (GNP) have been brought to the forefront of cancer research in recent years because of their facile synthesis and surface modification, tunable size, shape and optical properties, and biocompatibility. High quality, high yield and size controllable colloidal gold can be quickly prepared by the well-known citrate reduction method [46–48]. Among nanoparticles used for light-induced (photo) thermal therapy

(PTT), gold nanostars (GNS) are of particular interest as they offer a wide-range of optical tunability by engineering subtle changes in their geometry. The multiple sharp branches on GNS create a “lightning rod” effect that enhances local EM field dramatically and concentrates heating [49, 50]. Our team pioneered GNS development using a novel surfactant-free synthesis method for safe and effective star-shaped nanoparticle generation [49–52]. We have shown that this unique tip-enhanced plasmonic property of GNS can be tuned to the near infrared (NIR) ‘diagnostic-therapeutics’ optical window, where photons travel further in healthy tissue to be ‘captured’ and converted into heat by GNS that specifically accumulate within a tumor [53].

Key features to consider when selecting a particle for photothermal therapy are the maximum absorption wavelength (λ_{\max}) and absorption cross-section, as well as the size of the particle. Synthesis advancement in the last decade has allowed for development of gold nanoparticles of different shapes and structures, including gold nanospheres, gold-silica nanoshells, hollow gold nanoshells, gold nanocages, gold nanorods, and gold nanostars, which all show largely red-shifted properties boosting their values in photothermal cancer therapy. This review will briefly discuss various gold nanoparticles for PTT of cancer, while more extensive reviews of GNPs for PTT can be found elsewhere [54].

Gold nanoparticles have recently been applied in immunotherapies, including cancer antigen and immune adjuvant delivery, as well as combination therapies with photothermal therapy. GNPs inevitably accumulate at high concentrations in the liver and spleen and as such, it is important to understand how GNPs alone may interact with the immune system. Villiers et al. examined the effect of GNPs on the immune system through their ability to perturb the functions of dendritic cells (DC), a major component of both innate and acquired immune response, and showed that GNPs are not cytotoxic even at high concentrations [55]. Furthermore, the phenotype of the DC is unchanged, indicating that there is no activation of the DC; however, the secretion of cytokines is significantly modified after internalization of GNP into endocytic compartments indicating a potential perturbation of the immune response. When investigating the effect of GNPs on macrophages *in vitro*, Hsu et al. determined that GNPs can induce proinflammatory cytokine expression [56]; however, other groups have found that GNPs can inhibit toll like receptor 9 (TLR9)- and IL-1 β -mediated inflammatory responses [57, 58]. Both of these studies demonstrated response induction or inhibition by GNPs in a size-dependent manner, with smaller particle sizes (<5 nm) having the highest impact on the immune response.

Although gold nanoparticle-mediated PTT has shown potential to be effective on its own, this treatment type is limited to accessible sites and is therefore not currently applicable to metastatic disease. As such, recent research has investigated whether the immune response following PTT can be enhanced to treat distant sites not accessible by PTT. Shan and colleagues found that tumor cell necrosis following gold nanoshell thermal treatment *in vitro* caused the release of damage associated molecular patterns (DAMPs), but this release did not induce stimulation of macrophages [59]. Visaria and colleagues found that pre-treatment with tumor necrosis factor alpha (TNF- α) by conjugating it to gold nanoparticles allowed for

enhanced damage caused by hyperthermia; however, they did not assess the effects of combined PTT and TNF- α pretreatment [60]. These researchers hypothesized that TNF treatment induced inflammatory pathways that caused vascular damage at the tumor site. Although this method promoted tumor death at the local site, its efficacy in treating distant tumors was not demonstrated.

The systemic effects of PTT to promote a tumor specific immune response against a distant tumor was assessed by Bear et al. in a melanoma model of subcutaneous B16-ovalbumin tumor [61]. It was determined that infiltration of CD4+ helper T cells and CD8+ cytotoxic T cells mediated this response; however, there was also a significant increase in myeloid derived suppressor cells (MDSCs) at the spleen and distant site compared to mice that did not receive treatment, consequently failing to slow the growth of B16-F10 tumors and enhancing the growth of distant lung metastases. They also discovered that PTT was followed by a systemic increase in inflammatory cytokines, such as IL-6 and IL-1 β , suggesting that PTT can produce immune stimulatory and immune inhibitory effects that could be exploited in the treatment of metastatic disease. To test this, they adoptively transferred gp100-specific pmel T cells following PTT. The combination of local control by PTT and systemic antitumor immune reactivity provided by adoptively transferred T cells not only prevented primary tumor recurrence post-ablation, but also inhibited tumor growth at distant sites and stopped the outgrowth of lung metastases.

A different type of combination therapy utilizes PTT agents as delivery vehicles for immune modulatory agents such as drugs, oligonucleotides or proteins. The use of plasmonic nanoparticles as immunotherapy carriers provides a number of advantages including potentially targeted delivery, enhanced therapeutic effect, and reduced adverse outcomes. An example of such was demonstrated by Xia et al. as they developed gold nanocages containing doxorubicin and coated with thermally-responsive polymer for release of chemotherapy upon heating [62]. Similarly, Li et al. demonstrated that using doxorubicin-loaded hollow gold nanoshells for combined PTT and chemotherapy was more effective than either treatment alone *in vivo* and also reduced the systemic toxicity of doxorubicin [63]. Because doxorubicin has been shown to cause immunogenic cell death in cancer cells, the inflammatory response, antigen release and immunogenic apoptosis caused by combination PTT and chemotherapy could cause a potent immune response against metastatic cancer sites [64].

Additionally, an attractive approach that has been recently studied is the use of immune cells as a targeted delivery system by loading macrophages, T cells or DCs with GNPs. Macrophages containing gold nanoshells with a core radius of 60 nm and shell thickness of 27 nm have been shown to successfully deliver nanoshells to the hypoxic center of tumor spheroids and allowed for enhanced photoinduced cell death and tumor reduction [65]. Foster et al. demonstrated that human T cells can be loaded with 45 nm GNP *ex vivo* and migrate to tumor sites in a human tumor xenograft mouse model [66]. It was found that loaded T cells did not lose function or viability and that the *in vivo* tumor targeting was improved four-fold with the T cell delivery system as compared intravenous injection of free PEGylated GNPs. Such a system has potential for enhanced delivery of GNP for tumor PTT.

Recently, our group has developed a novel synergistic immune-phototherapy (SYMPHONY), which has demonstrated successful treatment of both primary and distant tumors for bladder cancer within mice [67]. The SYMPHONY therapy combines GNS-mediated photothermal therapy and immune checkpoint inhibitor, anti-PD-L1 antibody. The GNS-mediated photothermal therapy can be used to activate the immune system and generate a synergistic effect by combining with anti-PD-L1 immunotherapy. For the SYMPHONY group, 80 mg/kg GNS was administrated through tail vein. One day after GNS injection, laser treatment was performed on the primary tumor but not for the distant tumor. Anti-PD-L1 antibody was IP administrated after laser irradiation and every 3 days. On day 49, only SYMPHONY group had survival (2 mice) and all mice in other groups did not survive. Both primary tumor and distant tumor were completely cured for one mouse and no tumor recurred in the following 3 months. Tumors rechallenged was performed by injecting cancer cells, after which no tumor development was identified, indicating the existence of memorized immunoresponse, “cancer vaccine effect”. Both the primary tumor, which was laser treated, as well as the distant tumor, which did not receive laser treatment show therapeutic response from SYMPHONY treatment. Immune cell phenotyping was performed to investigate immunoresponse from SYMPHONY and suggested that the synergistic effect observed from SYMPHONY group may be due to the following reasons: First, the dying tumor cells after GNS-mediated photothermal therapy could release tumor-specific antigens, damage-associated molecular pattern molecules (DAMPs), and heat shock proteins (HSPs) into surrounding microenvironment, which can be considered as a local anti-cancer vaccination process. Second, the included PD-1/PD-L1 immune checkpoint inhibition reverse immunosuppression factor to make tumor exposed to generated cancer specific cytotoxic immune cells. The mechanism for inducing a cancer immune memory response is depicted in Fig. 3. Also shown in Fig. 3 are transmission electron microscopy images of the gold nanostar and high degree of tunability afforded by changing the amount of silver nitrate in the synthesis. Such tunability also shifts the plasmon resonance and absorption of the gold nanostar into the NIR making them effective PTT nanoparticles. SYMPHONY is a powerful and promising modality in the development of an anti-cancer vaccine candidate.

5.2 Nanoparticle-Based Photodynamic Immunotherapy

Photodynamic therapy has been clinically proven to treat various diseases in a manner that is highly selective with low toxicity and negative side effects. Additionally, this minimally invasive technique is quite reproducible. PDT holds promise for treating cancer by selectively retaining photosensitizers in tumor sites. Activating the photosensitizers using a specific wavelength of excitation light generates singlet oxygen and other reactive oxygen species (ROS), leading to apoptosis and necrosis of tumor cells.

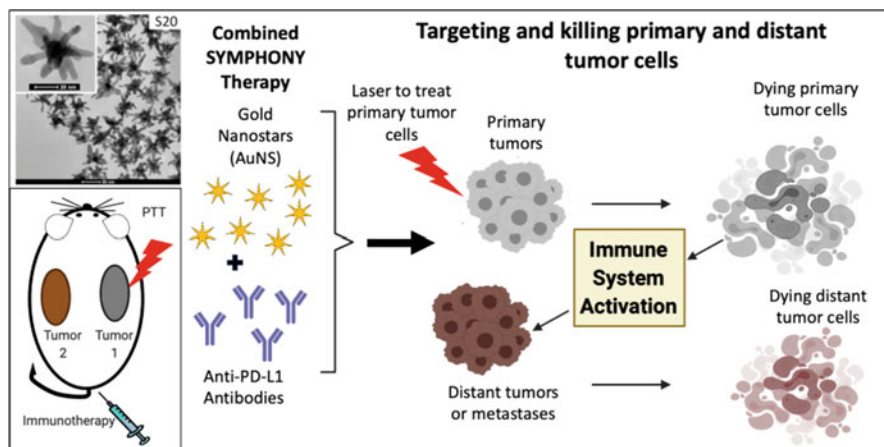


Fig. 3 Photothermal therapy combined with immunotherapy to generate immunological memory against cancer. Transmission electron microscopy (TEM) images of gold nanostars (AuNS) formed using silver nitrate. S20 refers to final concentration of 20 μM silver nitrate. Scale bars = 50 nm (top right inset). Adapted from [50]. Schematic illustration demonstrating SYMPHONY modality to treat metastatic bladder cancer. Adapted from ref. [67] and created with BioRender.com. Notably, only SYMPHONY mice were tumor free (40%) after treatment and survived rechallenge (20%) due to generated cancer vaccine effect. Adapted from ref. [67]

Traditional photosensitizers are poorly soluble, easily affected by the body's internal environment and enzymatic molecules, and untargeted. Several nanomaterials that have been widely studied for their effectiveness in treating cancer by PTT are also valuable as PDT agents. Yu et al. developed graphene oxide coated (HPPH)-PEG-HK nanoparticles loaded with a photosensitizer PS HPPH. Potent antitumor effects induced by activated DCs and CD8+ T cells were observed on both primary tumors and lung metastasis [68].

Fales et al. reported the synthesis of SERS label-tagged gold nanostars, coated with a silica shell containing methylene blue photosensitizing drug as a nanoplatform possessing a combined capability for SERS detection and singlet oxygen generation for photodynamic therapy [69]. The gold nanostars were tuned for maximal absorption in the NIR and tagged with a NIR dye for surface-enhanced resonance Raman scattering (SERRS). Silica coating was used to encapsulate the photosensitizer methylene blue in a shell around the particles. Upon 785-nm excitation, SERS from the Raman dye was observed, while excitation at 633 nm showed fluorescence from methylene blue. Measurement of singlet oxygen generation from the methylene blue encapsulated particles showed a significant increase as compared to the particles synthesized without methylene blue, demonstrating the potential for this nanoplatform for theranostics, i.e. both SERS detection and PDT [69]. Another theranostics nanoplatform was developed by loading the photosensitizer, protoporphyrin IX, onto a Raman-labeled gold nanosatr [70]. A cell-penetrating peptide, TAT, enhanced intracellular accumulation of the nanoparticles in order

to improve their delivery and efficacy. The plasmonic gold nanostar platform was designed to increase the Raman signal via the surface-enhanced resonance Raman scattering (SERRS) effect. Theranostic SERS imaging and photodynamic therapy using this nanoconstruct were demonstrated on BT-549 breast cancer cells [70]. A folate receptor (FR)-targeted theranostic nanocomposite was also developed for SERS imaging and PDT. FR-specific SERS detection and PDT were demonstrated *in vitro* using two FR-positive cancer cell lines and one FR-negative cancer cell lines [71].

As an alternative to other polymeric and/or inorganic nanocarriers and nanoconjugates, which may also deliver photosensitizers to the inside of the target cells, protein nanocages provide a unique vehicle of biological origin for the intracellular delivery of photosensitizing molecules for PDT by protecting the photosensitizers from reactive biomolecules in the cell membranes, and yet providing a coherent, critical mass of destructive power (by way of singlet oxygen generation) upon specific light irradiation for photodynamic therapy of tumor cells. Yan et al. have demonstrated the successful encapsulation of methylene blue (MB) in apoferritin via a dissociation-reassembly process controlled by pH [72, 73]. The resulting MB-containing apoferritin nanocages show a positive effect on singlet oxygen production, and cytotoxic effects on MCF-7 human breast adenocarcinoma cells when irradiated at 633-nm wavelength.

Although PDT seems to be more immunostimulatory than PTT, PDT alone exhibits lower stimulation and activation effects on both innate and adaptive immunity than mainstream cancer immunotherapy combined with immune-modulating agents. Introducing immune-modulating agents into PDT treatment has recently been used to enhance PDT immunotherapy, leading to tumor inhibition and improved survival. Immune checkpoint blockade (ICB) agents, which could reverse the negative regulatory signals between the immune system and tumor cells, have been used to enhance antitumor immune responses induced by PDT. Such strategies will be explored in this section from a wide array of nanoparticles combined with PDT.

Upconversion particles have emerged as robust nanomaterials to generate novel combination cancer therapies [74]. Upconversion luminescence is the non-linear optical process that leads conversion of two or more higher-energy output photons of a shorter wavelength [75]. Upconversion nanomaterials containing rare earth metals have multiple benefits as they have a reduced autofluorescence background, higher tissue penetration depth, and increased photostability [75]. Upconversion nanoparticles coated in polymers delivered chlorin photosensitizer to tumors in mice and caused increased singlet oxygen production under NIR light which marks their promise as an *in vivo* cancer treatment [75]. Recently a multifunctional upconversion particle combined with CTLA4 has been developed for treatment of colorectal cancer [76]. The upconversion particle contained chlorin and adjuvant imiquimod (R837), which is a Toll-like-receptor-7 agonist. The multitasking upconversion nanoparticle immunotherapy treatment with NIR light decreased localized tumor growth, as well as distant metastases. Remarkably the treatment also prevented tumor growth after rechallenging with tumor cells in the surviving

mice. In their work, they also noted the maturation of dendritic cells triggered by the treatment and secretion of cytokines. Central memory CD8+ T cells (CD3+, CD8+, CD44+, CD62L−) percentages were higher in the combined treatment compared to the various control groups. Regulatory T cells were also inhibited while a long-term immune memory effect was produced [76]. All in all, it is evident that that PDT combined with ICBs improved antitumor immunity [76]. Combined PDT/ICBs significantly improved DC activation and maturation after PDT treatment with the aid of CTLA-4 checkpoint blockade, and exhibited robust antitumor immunity that suppressed the growth of both local and distant tumors. Such a cancer immunotherapy strategy could introduce immune memory cells during treatment, preventing tumor recurrence via a vaccine effect.

Aptamers and DNA construct nanomaterials have high specificity and selectivity for proteins, such as cell receptors found in cancerous tissue; thus, they pose as promising methods for targeting proteins and delivering treatments. Using this strategy and a method to enhance the optical abilities of aptamers Jin and coworkers incorporated upconversion nanophosphors nanoparticles with the photosensitizer pyropheophorbide and an aptamer probe conjugated to doxorubicin [77]. In the presence of cancer cells, the unique nanoformulation could produce cytotoxic $^{1}O_2$, and additionally release doxorubicin when irradiated with NIR light. The aptamer was designed to target the PTK 7 protein expressed on the surface cancer cells shown in Fig. 4a. *In vivo* and histological studies confirmed only tumor damage without harming other organ systems [77]. In another notable example, DNA G-quadruplex nanostructures with entrapped photosensitizers and hemin were successfully applied for improved PDT therapy and overcame hypoxia resistance [78]. The DNA G-quadruplex inhibited antiapoptotic protein B-cell lymphoma 2 (Bcl-2) expression rendering an increase of apoptosis in tumors [78].

Organic nanomaterials such as those made of lipids are of great interest due their ability to clear the reticuloendothelial system (RES). Liposomes can be synthesized from commercially available cholesterol and natural or synthetic phospholipids. Under saturated conditions in an aqueous media, amphiphilic phospholipid molecules spontaneously form lipid bilayers making their synthesis rapid and facile [79]. In 1995 the first FDA approved doxorubicin-liposomal drug coated in polyethylene glycol (PEG) chains were approved [80]. Liposomes have also been used to encapsulate DNA and antigens in the development of vaccines [81]. Liposomes have been used to encapsulate other materials such as dyes for biomedical imaging, PTT, chemotherapy and nanosensing rendering them versatile and promising nanoformulations for cancer therapy [82–84]. Likewise, functionalization of nanomaterials with molecules to enhance their circulation times and tumor uptake to enhance immune effects has been explored for their ability to clear the RES. Cheng et al. found that TCPP porphyrin nanoparticles coated with PEG with larger molecular weights had increased tumor uptake. On the contrary, PEG with lower molecular weights were better suited for renal clearance, which is an important aspect to explore when designing safe and efficient cancer therapeutics [85]. Towards the understanding of designing PDT liposome therapeutics, Chlorin and metformin were both incorporated inside liposomes due to the hydrophilic nature of

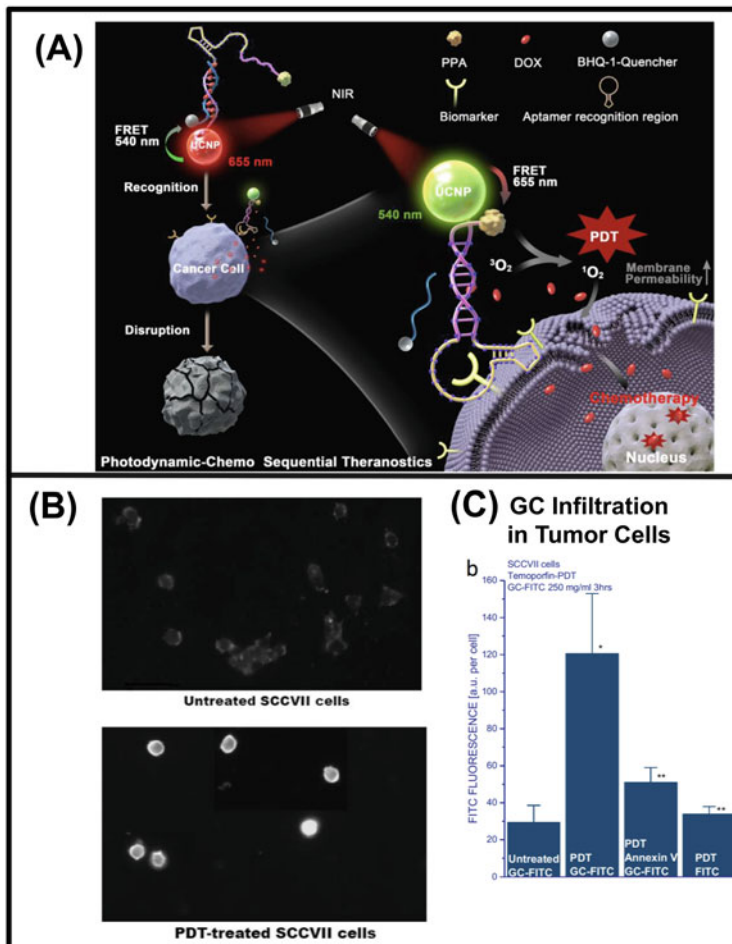


Fig. 4 Combined nanoformulations for PDT to modulate immune response. **(a)** Schematic depiction of upconversion nanophosphor (UCNP)-aptamer/ssDNA-pyropheophorbide- a (PPA)-doxorubicin (DOX) nanoformulation applied for cancer photodynamic–chemo sequential theranostics for treatment of HeLa tumors. Adapted from [77]. **(b)** Fluorescence images of PDT-treated and non PDT-treated squamous cell carcinoma (SCCVII) incubated with N-dihydrogalactochitosan(GC)-FITC demonstrating successful infiltration of GC inside the cells. Adapted from ref. [88]. **(c)** Amounts of GC bound to cells based on GC-associated FITC fluorescence. Adapted from ref. [88]

the inner cavity and hydrophobicity of the outer cavity for PDT treatment of three different mouse models [86]. Metformin incorporation was shown to increase tumor oxidation and therapeutic effects due to its ability to inhibit activity of complex I in the mitochondrial electron transport chain [86].

Feng and co-workers used a different approach to enhance PDT and induce synergistic effects by using a sequentially activated tumor therapy. In their design,

the drug AQ4N is activated in hypoxic environments to kill tumor cells. Thus, coloaded of chlorin and AQ4N inside liposomes induced hypoxia but also severe tumor blood vascular damage. These liposomes were also loaded with copper isotopes allowing for PET, fluorescence, and photoacoustic imaging [87]. In addition, N-dihydrogalactochitosan (GC) as an adjunct for immunomodulation during PDT has been researched by Korbelik et al. In treatment of squamous cell carcinoma using this organic nanoformulation they found a decrease in the numbers of myeloid suppressor cells [88]. The results showed an enhanced binding of GC to PDT treated cells allowing for better uptake and presentation of tumor antigens demonstrated in Fig. 4b [88].

5.3 Nanoparticle-Based Chemo-Immunotherapy

Chemotherapy treatment kills malignant cancer cells by using molecules that are toxic to rapidly dividing cells. After drug screening models improved and the onset of medical oncology, combination chemotherapy was demonstrated to cure childhood leukemia and Hodgkin's disease in research that occurred between 1960–1970 [89]. Today chemotherapy remains a widely used therapy by oncologists. Currently adjuvant chemotherapy is universally employed and evolving as new drugs are continuously screened and combined with targeted treatments [89]. For instance, chemotherapy drugs, such as methotrexate and cisplatin were been shown to be the single best agents in the treatment of head and neck cancer [90]. Also, targeted therapies, such as those that target tyrosine kinase receptors, select and kill subpopulations of cells in a more specific manner than broad chemotherapeutic agents [91]. Immunogenic cell death is of great interest in activating the immune system to increase the efficacy of cancer fighting treatments. Tumor antigens and endogenous danger signals (ATP, heat shock proteins, calreticulin, and high-mobility group box1 protein) released during the death of tumor cells promote activation of dendritic cells and antigen-specific T-cells [92]. Certain combination chemotherapy treatments have been shown to generate cancer-specific adaptive immunity via immunogenic cell death in the tumor tissue [64]. Delivery of both chemotherapy drugs such as Doxil in conjunction with antibodies, check point inhibitors, or cell stress inducers to elicit ICD have the potential to establish enhanced adaptive immune response to tumor antigens and stronger cancer killing potency [93, 94].

However, chemotherapy causes detrimental effects on normal tissues and thus broad negative side effects in the patient. Also, cancerous tissues can develop drug resistance and lead to relapse. For instance in triple negative breast cancer, patient resistance to chemotherapy is prevalent and relapse rate is high [95]. Multiple genetic mutations in cancer also pose challenges for targeted therapies. Survival times for patients also remains low for certain cancers treated with chemotherapy as in bladder cancer treatment, where cisplatin-based combination chemotherapy treatments yield an overall survival of 14–15 months [96]. In effect, new com-

combination treatments need to be explored to increase immune activation, survival, rate and prognosis of patients. Nanoparticle-based therapeutics in recent years have emerged as promising candidates for treatment due to their passive targeting capabilities and high therapeutic efficacy to modulate and probe the immune system in combination with chemotherapy [97, 98]. Furthermore, nanoparticle encapsulation of immunogenic cell death inducing molecules and chemotherapeutic agents has shown an increase in anti-tumor effects than free immunogenic cell death inducers [99].

Plasmonic nanomaterials have been shown to be effective drug carriers for chemotherapeutic drugs under laser excitation. Particularly, Zhong and co-workers utilized gold nanorods coated with PEG-*b*-PCL-lipoic acid ester block copolymer for targeted chemotherapy of glioma xenografts [100]. The nanoparticles were directed for targeted chemotherapy using cRGD functionalization, as cRGD has a strong affinity with $\alpha v \beta 3$ integrin receptors that are over-expressed on tumor cells such as malignant glioma cells, breast cancer cells, bladder cancer cells, and prostate cancer cells. NIR laser remotely triggers drug release of Doxorubicin in the tumor environment and induces an antitumor effect. The treatment generated 100% mice survival and a complete impediment of tumor growth [100]. Their previous work also demonstrated inhibition of drug-sensitive and drug resistant cancer cells while maintaining high spatial and temporal rate control of drug release [101]. An akin approach was undertaken by Zheng et al. who designed a gold nanostar encapsulated in a liposome and silica shell which contained doxorubicin (hydrophilic) and docetaxel (hydrophobic) [102]. Upon NIR irradiation release of the drugs ensued inhibition of tumor growth of MDA-MB-231 and MCF-7 cells, thus demonstrating a multimodal therapy and delivery of hydrophilic-hydrophobic chemotherapy agents [102]. Other research groups used gold nanostars functionalized with a targeting peptide and doxorubicin. The multifunctional nanostars were used for successful photothermal, photodynamic, and chemical therapy which had a higher therapeutic efficiency and synergistic properties compared to the individual stand-alone treatments [103]. Also, combined chemotherapy with gold nanoparticle mediated photothermal therapy has demonstrated a strong antitumor immune response against distant untreated tumors in 85% of the mice cohort in the study [104].

Magnetite nanoparticles with superparamagnetic properties can generate heat following exposure to an alternating magnetic field [105]. In a recent work, primary and metastatic tumors were treated with magnetite nanoparticle-based intracellular hyperthermia and subsequently produced heat shock proteins [105]. Further studies used antimelanoma chemotherapy agents, 4-S-cysteaminy phenol propionyl derivatives, functionalized on magnetite nanoparticles for the treatment of melanoma [106]. Chemo-thermo-immuno treatment with these particles led to heat shock protein 72 production and a melanoma-specific CD8+ T-cell response indicating a systemic antimelanoma immune response. The researchers noted that the heat shock protein-antigen peptide complex release from dying tumor cells was caused by dendritic cells and increased the cross-presentation of the antigenic peptide as part of the MHC class I molecules [106]. These researchers also constructed a 3D melanoma spheroid culture array using magnetic cell patterning to assess NPrCAP

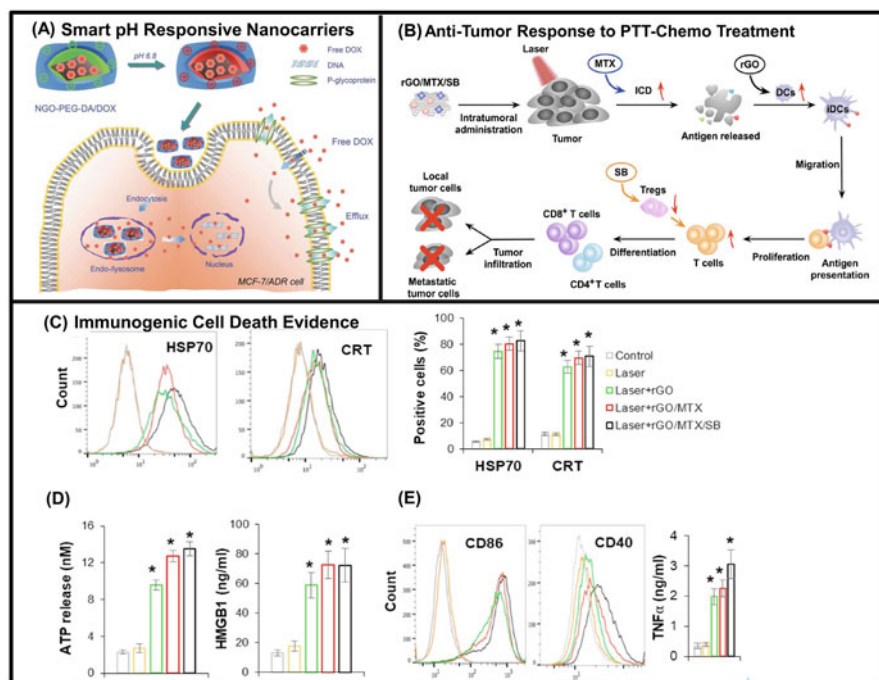


Fig. 5 Chemotherapy approaches for synergistic tumor treatments and immunogenic cell death stimulated by combined synergistic therapy. **(a)** Depiction of the acidic extracellular environment in tumors that allows for charge reverse NGO-PEG-DA/DOX complex. After cellular uptake, DOX release is triggered. Adapted from [108]. **(b)** Schematic illustrating antitumor immune response mechanism following nanographene oxide (rGO) with mitoxantrone (chemotherapeutic agent, MTX) and SB-431542 (transforming growth factor beta inhibitor, SB) based PTT. Adapted from ref. [109]. **(c)** 3 h after GO/MTX/SB PTT therapy, expression of heat shock protein (HSP70) and calreticulin (CRT) on the surface of tumor cells was established using flow cytometry. Adapted from [109]. **(d)** ATP and high-mobility group box 1 (HMGB1) extracellularly released from tumor cells 12 hrs following rGO/MTX/SB PTT therapy. Adapted from [109]. **(e)** Graph showing the expression of CD86 and CD40 and secretion of $\text{TNF}\alpha$ from bone marrow-derived dendritic cells, following rGO/MTX/SB PTT treatment of tumor cells. Adapted from ref. [109]

and heat treatment. Their model proved to be more effective in determining the anti-proliferative effect, half-maximal inhibitory concentration, and spheroid size compared to the 2D model [107].

Smart nanomaterials capable of releasing their cargo, such as drugs, upon external stimulation are novel avenues in the path to find cancer combating agents. Such a smart carrier was developed by Feng and researchers which consists of a pH-responsive nanomaterial to enhance uptake in the acidic tumor microenvironment [108]. The 2,3-dimethylmaleic anhydride coating on PEG and polymer decorated graphene oxide nanoparticles allows for pH reversibility. Furthermore, this smart nanoparticle encapsulates doxorubicin for a slow efflux of drug in lysosomes inside tumor cells shown in Fig. 5a. Synergistic therapeutic effects were observed in

comparison with free doxorubicin due to increased cell-killing in wild-type and drug-resistant cancer cells [108]. In a separate study mitoxantrone and a transforming growth factor beta inhibitor were loaded onto reduced graphene oxide for a triple therapy consisting of photothermal, chemotherapy, and immunotherapy. Following treatment with the graphene oxide system, 70% of the mice entered remission and resisted rechallenge with tumor cells. Immunophenotyping of the treatment groups found an increase in tumor-specific cytotoxic CD8+ T lymphocytes and less regulatory T cells in distant tumors. Their study demonstrated an inhibition of the tumor immunosuppressive environment and an astonishing *in situ* vaccination following treatment depicted in Fig. 5b–e [109].

Chitosan nanoparticles have been widely explored in conjunction with dyes as NIR responsive organic nanoformulations for cancer therapy. A novel multimodal particle composed of chitosan encasing a chemotherapeutic drug (gemcitabine) and a catalyst of H₂ production([FeFe]TPP) for hydrogen chemotherapy was recently probed for its efficacy [110]. Sun and coworkers showed that the H₂ nanogenerator was capable of diminishing mitochondrial function, inhibit ATP synthesis, and indirectly reduce P-gp protein transport in bladder cancer cells [110]. Organic nanomaterials, such as those made from polymers have also yielded promising results in the development of cancer therapeutics. Artificially inducing immunogenic cell death with 2′3′-cyclic guanosine monophosphate-adenosine monophosphate 2′cGAMP stimulator interferon genes using hollow polymeric nanoshells combined with other therapies is a novel endeavor that led to restraint in tumor progression and prolonging of overall survival [111]. Delivery of cGAMP inside the nanoshells *in vitro* and *in vivo* primed the cells for synthetic immunogenic cell death followed by cytotoxic treatment with chemotherapeutic drugs and antibody immunotherapy (anti-CTLA4 mAb) in B16F10 mice models. The treatment elicited high levels of IFN-β, immunogenic cell debris, and antigen specific T-cells [111]. Nanoparticles activated by pH combined with chemotherapy have also been explored by Liu et al. They illustrate that nanoscale coordination polymers with an acidic sensitive linker and high Z number element hafnium ions are capable of inducing mitochondrial damage and stop the cell cycle of tumor cells in the G1 phase. The biodegradable nanoparticle is also a radiosensitizer inducing tumor destruction due to the incorporation of Hafnium ions. All in all, their nanoradiosensitizer combined with chemotherapy demonstrate synergistic outcomes *in vitro* and *in vivo* [112].

Liposomes are vesicles that can be effectively cleared via the RES and have shown great promise in oncology [84, 113, 114]. The expression of indoleamine 2,3-dioxygenase 1 (IDO) is contributor to immunosuppression in numerous cancers such as colorectal cancer, and Shen and collaborators synthesized a liposome loaded with oxaliplatin and alkylated NLG919 (an IDO inhibitor) [115]. Their study was efficient in treating subcutaneous and orthotopic murine colorectal tumor models and determined that treatment of tumors with the bifunctional liposome prevented degradation of tryptophan to immunosuppressive kynurenine. Antitumor efficiency was effective due to the higher amounts of TNF-α and IFN-γ in groups treated with the bifunctional liposome. In addition, they observed an increase in the intratumoral

CD8+ T cells while the amount of Tregs cells was significantly lower. Dendritic cell maturation in the lymph nodes was also a full order of magnitude higher in the combined treatment group versus the mice in the control groups [115]. Other chemotherapy active liposomes targeting the IDO pathway combined with PD-1 blocking antibodies effectively eradicated breast cancer tumors and distant lung metastases [116]. The work effectively showed uptake of dying tumor cell by dendritic cells, tumor antigen presentation and the recruitment of naïve T-cells thereby proving the efficacy of the combined approach. Also seen in the work was activation of perforin- and IFN- γ releasing cytotoxic T-cells. Synergistic effects were also observed due to the recruitment of CD8+ cytotoxic T lymphocytes (CTLs), absence of Tregs, and an incrementation in CD8+/FOXP3+ T-cell ratios [116]. In another example, Doxorubicin loaded inside high-density lipoprotein-mimicking nano discs were used to prime tumors in conjunction with anti-PD-1 and generated a strong CD8+ T cell response [117]. Remarkably, the treatment also increased epitope recognition to antigens, neoantigens, and whole tumor cells. Complete tumor eradication was observed in CT26 and MC38 colon carcinoma tumors (80 to 88%). Moreover, the treatment prevented complete tumor recurrence in surviving mice [117].

Seth and colleagues administered paclitaxel and immuno-stimulating agent toll-like receptor-7 (TLR-7) agonist-imiquimod dispersed inside an organic poly (g-glutamic acid) polymer nanoparticle to a mouse melanoma tumor model [113]. *In vitro*, they found an anti-tumor response consisting of enhanced secretion of pro-inflammatory and Th1 cytokines. The *in vivo* experiments confirmed the uptake of release antigen by dendritic cells as there was a dramatic inhibition of tumor sizes across the study and lack of secondary tumor development [118]. A one of a kind biodegradable coordination polymer utilizing Zn-ions added with polyethylene glycol, doxorubicin, and 4-phenylimidazole (PI) has been characterized by Tian et al. [119]. PI is an inhibitor of indoleamine 2,3-dioxygenase, which promotes immunosuppression by recruiting immunosuppressive regulatory T cells. After the combined therapy immune cells were examined via flow cytometry and demonstrated a higher CD3+ and CD8+ T cell infiltration, while intratumoral regulatory T cells were down regulated. IDO inhibition was also exhibited as Kyn/Trp ratios were much lower. Also, CD3+, CD8+, CD62L-, CD44+ effector memory T cells were much higher in the combined treatment group ZnPI-PEG/DOX than the control [119]. Another method to treat cancer through inhibition of the IDO pathway exploited the use of mesoporous silica nanoparticles with a porous interior encapsulating indoximod, an IDO inhibitor [120]. The interior of the mesoporous silica nanoparticle also contained oxaliplatin, the chemotherapeutic drug. Tumor reduction and eradication was observed when pancreatic tumors in mice were treated via direct tumor injection or intravenous biodistribution of the multifunctional particle. The innate immune system was also affected since there was an increase in expression of high motility group box 1 and calreticulin. The researchers also observed recruitment of cytotoxic T lymphocytes concurrent with the downregulation of Foxp3+ T cells [120].

6 Conclusion

Cancer continues to be a devastating global problem and cancer metastasis is involved in more than 90% of cancer related deaths [121]. Conventional treatments to treat cancer have been ineffective in improving survival. Nanoparticles are emerging as a pivotal technology with over one thousand nano-enabled consumer products on the market worldwide in a variety of industries ranging from electronics, therapeutics, medical treatments, and textiles [122–125]. In biomedicine, nanoparticles are ideal candidates for the treatment of diseases and in the development of a cancer vaccine [126]. Due to the enhanced permeability and retention effect (EPR), nanoparticles are preferentially absorbed in tumor sites. In effect, they accumulate in the plasma and in tumors.

Plasmonic-active metallic nanoparticles have gained much interest in biomedical research because of their ability to be used for photothermal therapy and photodynamic therapy in order to eradicate tumors. Absorption of plasmonic and organic nanoparticles with the use of dyes can be tuned to the near infrared (NIR) window, which is favorable for *in vivo* applications because tissue penetration is maximized and attenuation of light by blood and tissue is minimized in this spectral range [127].

Abnormalities of tumor vasculature such as hypervascularization, abnormal vascular architecture, overproduction of permeability factors that trigger extravasation, and lack of lymphatic drainage allows for the accumulation of nanoparticles [97]. Nanoparticles ranging from 20 to 200 nm in size show fast drainage into the lymph nodes and are taken up by dendritic cells, which is favorable for presentation of antigens. Ultimately, research studies have demonstrated that nanoparticles are pivotal in the fight against cancer because of their ability to innately modulate the immune system. Combining them with antigens, adjuvants, chemotherapeutic drugs, and other therapies further their capacity in eradicating local and distant tumors and eliciting a powerful immune memory response to protect patients from cancer recurrence. Now more than ever advancing research towards finding the most efficacious orthogonal nanomedicine approach to ultimately produce a cancer vaccine is paramount in the fight against cancer.

Acknowledgements This work was supported by National Institutes of Health (1R01EB028078-01A1).

References

1. Yarchoan, M., Hopkins, A., Jaffee, E.M.: Tumor mutational burden and response rate to PD-1 inhibition. *N. Engl. J. Med.* **377**(25), 2500 (2017)
2. Sharma, P., et al.: Primary, adaptive, and acquired resistance to cancer immunotherapy. *Cell.* **168**(4), 707–723 (2017)
3. Riley, R.S., et al.: Delivery technologies for cancer immunotherapy. *Nat. Rev. Drug Discov.*, 1 (2019)

4. Jeanbart, L., Swartz, M.A.: Engineering opportunities in cancer immunotherapy. *Proc. Natl. Acad. Sci.* **112**(47), 14467–14472 (2015)
5. Manolova, V., et al.: Nanoparticles target distinct dendritic cell populations according to their size. *Eur. J. Immunol.* **38**(5), 1404–1413 (2008)
6. Guo, L.R., et al.: Combinatorial photothermal and Immuno cancer therapy using chitosan-coated hollow copper sulfide nanoparticles. *ACS Nano.* **8**(6), 5670–5681 (2014)
7. Milling, L., Zhang, Y., Irvine, D.J.: Delivering safer immunotherapies for cancer. *Adv. Drug Deliv. Rev.* **114**, 79–101 (2017)
8. Pfreundschuh, M.G., et al.: Phase I study of intratumoral application of recombinant human tumor necrosis factor. *Eur. J. Cancer Clin. Oncol.* **25**(2), 379–388 (1989)
9. van Herpen, C.M., et al.: Intratumoral rIL-12 administration in head and neck squamous cell carcinoma patients induces B cell activation. *Int. J. Cancer.* **123**(10), 2354–2361 (2008)
10. Bartsch, H.H., et al.: Intralesional application of recombinant human tumor necrosis factor alpha induces local tumor regression in patients with advanced malignancies. *Eur. J. Cancer Clin. Oncol.* **25**(2), 287–291 (1989)
11. Kwong, B., et al.: Localized immunotherapy via liposome-anchored anti-CD137+IL-2 prevents lethal toxicity and elicits local and systemic antitumor immunity. *Cancer Res.* **73**(5), 1547–1558 (2013)
12. Robbins, P.F., et al.: A pilot trial using lymphocytes genetically engineered with an NY-ESO-1-reactive T-cell receptor: long-term follow-up and correlates with response. *Clin. Cancer Res.* **21**(5), 1019–1027 (2015)
13. Bobisse, S., et al.: Sensitive and frequent identification of high avidity neo-epitope specific CD8+ T cells in immunotherapy-naïve ovarian cancer. *Nat. Commun.* **9**(1), 1092 (2018)
14. Tran, E., et al.: Cancer immunotherapy based on mutation-specific CD4+ T cells in a patient with epithelial cancer. *Science.* **344**(6184), 641–645 (2014)
15. Maude, S.L., et al.: Tisagenlecleucel in children and young adults with B-cell lymphoblastic leukemia. *N. Engl. J. Med.* **378**(5), 439–448 (2018)
16. Neelapu, S.S., et al.: Axicabtagene ciloleucel CAR T-cell therapy in refractory large B-cell lymphoma. *N. Engl. J. Med.* **377**(26), 2531–2544 (2017)
17. Schuster, S.J., et al.: Chimeric antigen receptor T cells in refractory B-cell lymphomas. *N. Engl. J. Med.* **377**(26), 2545–2554 (2017)
18. Hollyman, D., et al.: Manufacturing validation of biologically functional T cells targeted to CD19 antigen for autologous adoptive cell therapy. *J. Immunother.* **32**(2), 169 (2009)
19. Huang, X., et al.: Sleeping beauty transposon-mediated engineering of human primary T cells for therapy of CD19+ lymphoid malignancies. *Mol. Ther.* **16**(3), 580–589 (2008)
20. Perica, K., et al.: Magnetic field-induced T cell receptor clustering by nanoparticles enhances T cell activation and stimulates antitumor activity. *ACS Nano.* **8**(3), 2252–2260 (2014)
21. Perica, K., et al.: Enrichment and expansion with nanoscale artificial antigen presenting cells for adoptive immunotherapy. *ACS Nano.* **9**(7), 6861–6871 (2015)
22. Zheng, B.B., et al.: Bacterium-Mimicking Vector with Enhanced Adjuvanticity for Cancer Immunotherapy and Minimized Toxicity. *Adv. Funct. Mater.* **29**, 33 (2019)
23. Badie, B., Berlin, J.M.: The future of CpG immunotherapy in cancer. *Immunotherapy.* **5**(1), 1–3 (2013)
24. Lin, A.Y., et al.: Gold Nanoparticle Delivery of Modified CpG Stimulates Macrophages and Inhibits Tumor Growth for Enhanced Immunotherapy. *PLoS One.* **8**, 5 (2013)
25. Paciotti, G.F., et al.: Colloidal gold: a novel nanoparticle vector for tumor directed drug delivery. *Drug Deliv.* **11**(3), 169–183 (2004)
26. Goel, R., et al.: Biodistribution of TNF-alpha-coated gold nanoparticles in an in vivo model system. *Nanomedicine.* **4**(4), 401–410 (2009)
27. Shenoi, M.M., et al.: Nanoparticle preconditioning for enhanced thermal therapies in cancer. *Nanomedicine.* **6**(3), 545–563 (2011)
28. Lin, A.Y., et al.: High-density sub-100-nm peptide-gold nanoparticle complexes improve vaccine presentation by dendritic cells in vitro. *Nanoscale Res. Lett.* **8** (2013)

29. Lee, I.H., et al.: Imageable antigen-presenting gold nanoparticle vaccines for effective cancer immunotherapy in vivo. *Angew. Chem. Int. Ed. Engl.* **51**(35), 8800–8805 (2012)
30. Arnáiz, B., et al.: Cellular uptake of gold nanoparticles bearing HIV gp120 oligomannosides. *Bioconjug. Chem.* **23**(4), 814–825 (2012)
31. Liu, H., et al.: Structure-based programming of lymph-node targeting in molecular vaccines. *Nature.* **507**(7493), 519 (2014)
32. Kuai, R., et al.: *Designer vaccine nanodiscs for personalized cancer immunotherapy.* *Nature Materials.* **16**(4), 489 (2017)
33. Kranz, L.M., et al.: Systemic RNA delivery to dendritic cells exploits antiviral defence for cancer immunotherapy. *Nature.* **534**(7607), 396 (2016)
34. Ramishetti, S., Peer, D.: Engineering lymphocytes with RNAi. *Adv. Drug Deliv. Rev.* **141**, 55–66 (2019)
35. Falk, M.H., Issels, R.D.: Hyperthermia in oncology. *Int. J. Hyperth.* **17**(1), 1–18 (2001)
36. Owusu, R.A., Abern, M.R., Inman, B.A.: *Hyperthermia as adjunct to intravesical chemotherapy for bladder cancer.* *Biomed. Res. Int.*, 7 (2013)
37. Hildebrandt, B., et al.: The cellular and molecular basis of hyperthermia. *Crit. Rev. Oncol. Hematol.* **43**(1), 33–56 (2002)
38. Frey, B., et al.: Old and new facts about hyperthermia-induced modulations of the immune system. *Int. J. Hyperth.* **28**(6), 528–542 (2012)
39. Schildkopf, P., et al.: Biological rationales and clinical applications of temperature controlled hyperthermia—implications for multimodal cancer treatments. *Curr. Med. Chem.* **17**(27), 3045–3057 (2010)
40. Wust, P., et al.: Hyperthermia in combined treatment of cancer. *Lancet Oncol.* **3**(8), 487–497 (2002)
41. Loo, C., et al.: Nanoshell-enabled photonics-based imaging and therapy of cancer. *Technol. Cancer Res. Treat.* **3**(1), 33–40 (2004)
42. Pandita, T.K., Pandita, S., Bhaumik, S.R.: Molecular parameters of hyperthermia for radiosensitization. *Crit. Rev. Eukaryot. Gene Expr.* **19**(3), 235–251 (2009)
43. Takada, T., et al.: Growth inhibition of Re-Challenge B16 melanoma transplant by conjugates of melanogenesis substrate and magnetite nanoparticles as the basis for developing melanoma-targeted chemo-thermo-immunotherapy. *J. Biomed. Biotechnol.*, 13 (2009)
44. Koning, G.A., et al.: Hyperthermia and thermosensitive liposomes for improved delivery of chemotherapeutic drugs to solid tumors. *Pharm. Res.* **27**(8), 1750–1754 (2010)
45. Wang, C., et al.: Immunological responses triggered by photothermal therapy with carbon nanotubes in combination with anti-CTLA-4 therapy to inhibit cancer metastasis. *Adv. Mater.* **26**(48), 8154–8162 (2014)
46. Turkevich, J., Stevenson, P.C., Hillier, J.: A study of the nucleation and growth processes in the synthesis of colloidal gold. *Discuss. Faraday Soc.* **11**, 55–75 (1951)
47. Turkevich, J., Garton, G., Stevenson, P.: The color of colloidal gold. *J. Colloid Sci.* **9**, 26–35 (1954)
48. Frens, G.: Controlled nucleation for the regulation of the particle size in monodisperse gold suspensions. *Nat. Phys. Sci.* **241**(105), 20 (1973)
49. Khoury, C.G., Vo-Dinh, T.: Gold nanostars for surface-enhanced Raman scattering: synthesis, characterization and optimization. *J. Phys. Chem. C.* **112**(48), 18849–18859 (2008)
50. Yuan, H., et al.: Gold nanostars: surfactant-free synthesis, 3D modelling, and two-photon photoluminescence imaging. *Nanotechnology.* **23**, 1361–6528 (2012) (Electronic)
51. Liu, Y., et al.: A plasmonic gold nanostar theranostic probe for in vivo tumor imaging and photothermal therapy. *Theranostics.* **5**(9), 946–960 (2015)
52. Yuan, H., et al.: In vivo particle tracking and photothermal ablation using plasmon-resonant gold nanostars. *Nanomedicine.* **8**(8), 1355–1363 (2012)
53. Yuan, H., Fales, A.M., Vo-Dinh, T.: TAT peptide-functionalized gold Nanostars: enhanced intracellular delivery and efficient NIR photothermal therapy using ultralow irradiance. *J. Am. Chem. Soc.* **134**(28), 11358–11361 (2012)

54. Abadeer, N.S., Murphy, C.J.: Recent Progress in cancer thermal therapy using gold nanoparticles. *J. Phys. Chem. C*. **120**(9), 4691–4716 (2016)
55. Villiers, C.L., et al.: Analysis of the toxicity of gold nano particles on the immune system: effect on dendritic cell functions. *J. Nanopart. Res.* **12**(1), 55–60 (2010)
56. Yen, H.J., Hsu, S.H., Tsai, C.L.: *Cytotoxicity and immunological response of gold and silver nanoparticles of different sizes*. *Small*. **5**(13), 1553–1561 (2009)
57. Tsai, C.-Y., et al.: Size-dependent attenuation of TLR9 signaling by gold nanoparticles in macrophages. *J. Immunol.* **188**(1), 68–76 (2012)
58. Sumbayev, V.V., et al.: Gold nanoparticles downregulate interleukin-1 β -induced pro-inflammatory responses. *Small*. **9**(3), 472–477 (2013)
59. Nguyen, H.T., et al.: Activation of inflammasomes by tumor cell death mediated by gold nanoshells. *Biomaterials*. **33**(7), 2197–2205 (2012)
60. Visaria, R.K., et al.: Enhancement of tumor thermal therapy using gold nanoparticle–assisted tumor necrosis factor- α delivery. *Mol. Cancer Ther.* **5**(4), 1014–1020 (2006)
61. Bear, A.S., et al.: Elimination of metastatic melanoma using gold nanoshell-enabled photothermal therapy and adoptive T cell transfer. *PLoS One*. **8**(7), e69073 (2013)
62. Yavuz, M.S., et al.: Gold nanocages covered by smart polymers for controlled release with near-infrared light. *Nat. Mater.* **8**(12), 935 (2009)
63. You, J., et al.: Photothermal-chemotherapy with doxorubicin-loaded hollow gold nanospheres: a platform for near-infrared light-triggered drug release. *J. Control. Release*. **158**(2), 319–328 (2012)
64. Casares, N., et al.: Caspase-dependent immunogenicity of doxorubicin-induced tumor cell death. *J. Exp. Med.* **202**(12), 1691–1701 (2005)
65. Choi, M.-R., et al.: A cellular Trojan horse for delivery of therapeutic nanoparticles into tumors. *Nano Lett.* **7**(12), 3759–3765 (2007)
66. Kennedy, L.C., et al.: T cells enhance gold nanoparticle delivery to tumors in vivo. *Nanoscale Res. Lett.* **6** (2011)
67. Liu, Y., et al.: Synergistic Immuno Photothermal Nanotherapy (SYMPHONY) for the treatment of unresectable and metastatic cancers. *Sci. Rep.* **7**(1), 8606 (2017)
68. Yu, X., et al.: Inhibiting metastasis and preventing tumor relapse by triggering host immunity with tumor-targeted photodynamic therapy using photosensitizer-loaded functional Nanographenes. *ACS Nano*. **11**(10), 10147–10158 (2017)
69. Fales, A.M., Yuan, H., Vo-Dinh, T.: Silica-coated gold nanostars for combined surface-enhanced Raman scattering (SERS) detection and singlet-oxygen generation: a potential nanoplatform for theranostics. *Langmuir*. **27**(19), 12186–12190 (2011)
70. Fales, A.M., Yuan, H., Vo-Dinh, T.: Cell-penetrating peptide enhanced intracellular Raman imaging and photodynamic therapy. *Mol. Pharm.* **10**(6), 2291–2298 (2013)
71. Fales, A.M., Crawford, B.M., Vo-Dinh, T.: Folate receptor-targeted theranostic nanoconstruct for surface-enhanced Raman scattering imaging and photodynamic therapy. *ACS Omega*. **1**(4), 730–735 (2016)
72. Yan, F., et al.: *Apoferitin protein cages: a novel drug nanocarrier for photodynamic therapy*. *Chem. Commun. (Camb.)*. **38**, 4579–4581 (2008)
73. Yan, F., et al.: Cellular uptake and photodynamic activity of protein nanocages containing methylene blue photosensitizing drug. *Photochem. Photobiol.* **86**(3), 662–666 (2010)
74. Wang, C., Cheng, L., Liu, Z.: Upconversion nanoparticles for photodynamic therapy and other cancer therapeutics. *Theranostics*. **3**(5), 317–330 (2013)
75. Wang, C., et al.: Near-infrared light induced in vivo photodynamic therapy of cancer based on upconversion nanoparticles. *Biomaterials*. **32**(26), 6145–6154 (2011)
76. Xu, J., et al.: Near-infrared-triggered photodynamic therapy with multitasking upconversion nanoparticles in combination with checkpoint blockade for immunotherapy of colorectal cancer. *ACS Nano*. **11**(5), 4463–4474 (2017)
77. Jin, X., et al.: Aptamer-functionalized upconverting nanoformulations for light-switching cancer-specific recognition and in situ photodynamic–chemo sequential theranostics. *ACS Appl. Mater. Interfaces*. (2020)

78. Yang, Y., et al.: G-Quadruplex-based nanoscale coordination polymers to modulate tumor hypoxia and achieve nuclear-targeted drug delivery for enhanced photodynamic therapy. *Nano Lett.* **18**(11), 6867–6875 (2018)
79. Lasic, D.D.: The mechanism of vesicle formation. *Biochem. J.* **256**(1), 1–11 (1988)
80. Barenholz, Y.: Doxil (R)—the first FDA-approved nano-drug: lessons learned. *J. Control. Release.* **160**(2), 117–134 (2012)
81. Gregoriadis, G., Saffie, R., deSouza, J.B.: *Liposome-mediated DNA vaccination*. *FEBS Lett.* **402**(2–3), 107–110 (1997)
82. McNamara, K.P., Rosenzweig, Z.: Dye-encapsulating liposomes as fluorescence-based oxygen nanosensors. *Anal. Chem.* **70**(22), 4853–4859 (1998)
83. Miranda, D., et al.: Highly-soluble cyanine J-aggregates entrapped by liposomes for in vivo optical imaging around 930 nm. *Theranostics.* **9**(2), 381–390 (2019)
84. Yoon, H.J., et al.: Liposomal indocyanine green for enhanced photothermal therapy. *ACS Appl. Mater. Interfaces.* **9**(7), 5683–5691 (2017)
85. Cheng, L., et al.: *Renal-Clearable PEGylated Porphyrin Nanoparticles for Image-guided Photodynamic Cancer Therapy*. *Adv. Funct. Mater.* **27**, 34 (2017)
86. Song, X.J., et al.: Liposomes co-loaded with metformin and chlorin e6 modulate tumor hypoxia during enhanced photodynamic therapy. *Nano Res.* **10**(4), 1200–1212 (2017)
87. Feng, L.Z., et al.: Theranostic liposomes with HypoxiaActivated prodrug to effectively destruct hypoxic tumors post-photodynamic therapy. *ACS Nano.* **11**(1), 927–937 (2017)
88. Korbely, M., et al.: N-dihydrogalactochitosan as immune and direct antitumor agent amplifying the effects of photodynamic therapy and photodynamic therapy-generated vaccines. *Int. Immunopharmacol.* **75** (2019)
89. DeVita, V.T., Chu, E.: A history of cancer chemotherapy. *Cancer Res.* **68**(21), 8643–8653 (2008)
90. Mead, G.M., Jacobs, C.: Changing-role of chemotherapy in treatment of head and neck-cancer. *Am. J. Med.* **73**(4), 582–595 (1982)
91. Petrelli, A., Giordano, S.: From single- to multi-target drugs in cancer therapy: when aspecificity becomes an advantage. *Curr. Med. Chem.* **15**(5), 422–432 (2008)
92. Krysko, D.V., et al.: Immunogenic cell death and DAMPs in cancer therapy. *Nat. Rev. Cancer.* **12**(12), 860–875 (2012)
93. Kroemer, G., et al.: Immunogenic cell death in cancer therapy. *Annu. Rev. Immunol.* **31**(1), 51–72 (2013)
94. Rios-Doria, J., et al.: Doxil synergizes with cancer immunotherapies to enhance antitumor responses in syngeneic mouse models. *Neoplasia.* **17**(8), 661–670 (2015)
95. Ahmadzade, T., Reid, G., McKenzie, D.R.: Fundamentals of siRNA and miRNA therapeutics and a review of targeted nanoparticle delivery systems in breast cancer. *Biophys. Rev.* **10**(1), 69–86 (2018)
96. Kim, H.S., Seo, H.K.: Immune checkpoint inhibitors for urothelial carcinoma. *Investig Clin Urol.* **59**(5), 285–296 (2018)
97. Greish, K.: Enhanced permeability and retention (EPR) effect for anticancer nanomedicine drug targeting. *Cancer Nanotechnol Methods Protocols.* **624**, 25–37 (2010)
98. Kobayashi, K., et al.: Surface engineering of nanoparticles for therapeutic applications. *Polym. J.* **46**(8), 460–468 (2014)
99. Zhao, X., et al.: Inducing enhanced immunogenic cell death with nanocarrier-based drug delivery systems for pancreatic cancer therapy. *Biomaterials.* **102**, 187–197 (2016)
100. Zhong, Y.N., et al.: cRGD-directed, NIR-responsive and robust AuNR/PEG-PCL hybrid nanoparticles for targeted chemotherapy of glioblastoma in vivo. *J. Control. Release.* **195**, 63–71 (2014)
101. Zhong, Y., et al.: Gold nanorod-cored biodegradable micelles as a robust and remotely controllable doxorubicin release system for potent inhibition of drug-sensitive and -resistant cancer cells. *Biomacromolecules.* **14**(7), 2411–2419 (2013)

102. Cai, Z., et al.: NIR-triggered chemo-photothermal therapy by thermosensitive gold Nanostar@mesoporous silica@liposome-composited drug delivery systems. *ACS Appl. Bio Mater.* **3**(8), 5322–5330 (2020)
103. Su, G., et al.: Mesoporous silica-coated gold nanostars with drug payload for combined chemo-photothermal cancer therapy. *J. Drug Target.* **27**(2), 201–210 (2019)
104. Bisker, G., et al.: Controlled release of rituximab from gold nanoparticles for phototherapy of malignant cells. *J. Control. Release.* **162**(2), 303–309 (2012)
105. Jimbow, K., et al.: Melanoma-targeted chemothermotherapy and in situ peptide immunotherapy through HSP production by using melanogenesis substrate, NPrCAP, and magnetite nanoparticles. *J. Skin Cancer.* **2013**, 742925–742925 (2013)
106. Sato, A., et al.: Melanoma-targeted chemo-thermo-immuno (CTI)-therapy using N-propionyl-4-S-cysteaminyphenol-magnetite nanoparticles elicits CTL response via heat shock protein-peptide complex release. *Cancer Sci.* **101**(9), 1939–1946 (2010)
107. Yamamoto, S., et al.: Three-dimensional magnetic cell array for evaluation of anti-proliferative effects of chemo-thermo treatment on cancer spheroids. *Biotechnol. Bioprocess Eng.* **20**(3), 488–497 (2015)
108. Feng, L.Z., et al.: Smart pH-responsive nanocarriers based on Nano-graphene oxide for combined chemo- and photothermal therapy overcoming drug resistance. *Adv. Healthc. Mater.* **3**(8), 1261–1271 (2014)
109. Zhou, F., et al.: Photo-activated chemo-immunotherapy for metastatic cancer using a synergistic graphene nanosystem. *Biomaterials.* **265**, 120421 (2021)
110. Sun, R., et al.: Photoactivated H2 nanogenerator for enhanced chemotherapy of bladder cancer. *ACS Nano.* **14**(7), 8135–8148 (2020)
111. Chattopadhyay, S., et al.: Synthetic immunogenic cell death mediated by intracellular delivery of STING agonist Nanoshells enhances anticancer chemo-immunotherapy. *Nano Lett.* **20**(4), 2246–2256 (2020)
112. Liu, J.J., et al.: pH-Sensitive dissociable nanoscale coordination polymers with drug loading for synergistically enhanced chemoradiotherapy (vol 27, 1703832, 2017). *Adv. Funct. Mater.* **29**, 51 (2019)
113. Sessa, G., Weissmann, G.: *Phospholipid spherules (liposomes) as a model for biological membranes.* *J. Lipid Res.* **9**(3), 310 (1968)
114. Yoon, H.-J., et al.: Photothermally amplified therapeutic liposomes for effective combination treatment of cancer. *ACS Appl. Mater. Interfaces.* **10**(7), 6118–6123 (2018)
115. Shen, F.Y., et al.: Oxaliplatin-/NLG919 prodrugs-constructed liposomes for effective chemoimmunotherapy of colorectal cancer. *Biomaterials.* **255** (2020)
116. Lu, J.Q., et al.: Breast cancer chemo-immunotherapy through liposomal delivery of an immunogenic cell death stimulus plus interference in the IDO-1 pathway. *ACS Nano.* **12**(11), 11041–11061 (2018)
117. Kuai, R., et al.: *Elimination of established tumors with nanodisc-based combination chemoimmunotherapy.* *Sci. Adv.* **4**(4), eaao1736 (2018)
118. Seth, A., Heo, M.B., Lim, Y.T.: Poly (γ -glutamic acid) based combination of water-insoluble paclitaxel and TLR7 agonist for chemo-immunotherapy. *Biomaterials.* **35**(27), 7992–8001 (2014)
119. Tian, L., et al.: *Coordination Polymers Integrating Metalloimmunology with Immune Modulation to Elicit Robust Cancer Chemoimmunotherapy.* *CCS Chemistry.*
120. Lu, J., et al.: Nano-enabled pancreas cancer immunotherapy using immunogenic cell death and reversing immunosuppression. *Nat. Commun.* **8**(1), 1811 (2017)
121. Jemal, A., et al. *Global cancer statistics.* (1542–4863 (Electronic))
122. Zhang, L., et al.: Nanoparticles in medicine: therapeutic applications and developments. *Clin. Pharmacol. Therapeut.* **83**(5), 761–769 (2008)
123. Kamysny, A., Magdassi, S.: Conductive nanomaterials for printed electronics. *Small.* **10**(17), 3515–3535 (2014)

124. Dastjerdi, R., Montazer, M.: A review on the application of inorganic nano-structured materials in the modification of textiles: focus on anti-microbial properties. *Colloids Surfaces B-Biointerfaces*. **79**(1), 5–18 (2010)
125. Vance, M.E., Kuiken, T., Vejerano, E. P., McGinnis, S.P., Hochella, M.F., Jr., Rejeski, D. and Hull, M.S., *Nanotechnology in the Real World: Redeveloping the Nanomaterial Consumer Products Inventory*. (2019)
126. Kreyling, W.G., Semmler-Behnke, M., Chaudhry, Q.: A complementary definition of nano-material. *Nano Today*. **5**(3), 165–168 (2010)
127. Smith, A.M., Mancini, M.C., Nie, S.M.: BIOIMAGING second window for in vivo imaging. *Nat. Nanotechnol.* **4**(11), 710–711 (2009)

Design of Nanostructure Materials to Modulate Immunosuppressive Tumour Microenvironments and Enhance Cancer Immunotherapy



Seung Mo Jin, Sang Nam Lee, Hong Sik Shin, and Yong Taik Lim

1 Introduction

1.1 History and Conventional Methods of Cancer Therapy

Fossils attest to the time since when long cancer has prevailed in human history. The presence of cancer has already been shown in fossilized bone tumours, ancient Egyptian mummies, and other ancient sources. Clues suggesting osteosarcoma, a bone cancer, have been found in Egyptian mummies. Cancer has long been associated with human history [1].

However, the scientific study of cancer began just a few centuries ago. In the nineteenth century, the development of microscopy enabled pathological study of tissues and resulted in its correlation with cancer. Many doctors and scientist studied “How to kill these mutated tissues,” and many clinical treatments were established to kill tumour tissue. Chemotherapy, radiotherapy, and surgery are the most common and conventional cancer treatments, which aim to kill tumour tissue using chemical drugs, radiation, and physical methods, respectively. These methods have been developed over the years, and they effectively kill cancer cells. Advancements in these technologies have decreased the number of people suffering from cancer and increased the cure rate [2, 3]. However, several obstacles exist that prohibit people

Seung Mo Jin, Sang Nam Lee and Hong Sik Shin contributed equally.

S. M. Jin · S. N. Lee · H. S. Shin · Y. T. Lim (✉)

Department of Nano Engineering, SKKU Advanced Institute of Nanotechnology (SAINT),
Suwon, Gyeonggi-do, Republic of Korea

School of Chemical Engineering, Sungkyunkwan University, Suwon, Gyeonggi-do, Republic of
Korea

e-mail: yongtaik@skku.edu

from conquering cancer. First, the human body cannot endure high toxicity from chemo drugs because the drugs can kill normal cells (high toxicity and low efficacy). Owing to a cancer cell's abnormal proliferation rate and metastasis, the part to be irradiated or operated on (low specificity) cannot be specified. Moreover, even if the doctor diagnoses the patient and completely treats the cancer, it often recurs in the patient (short-term effect). Finally, the tumour does not exist in isolation; it exists in correlation with various immune cells and immuno-responsible factors such as cytokines, chemokines, enzymes, and reactive oxygen species (ROS) (tumour microenvironment). Furthermore, these correlations usually result in therapeutic resistance against chemo drugs and radiation during treatment [4].

1.2 Emergence of Cancer Immunotherapy

To overcome the aforementioned problems, we need another cancer treatment strategy with properties such as “low toxicity,” “high efficacy,” “high specificity,” and “long term effect.” Moreover, we must consider and adjust immune-responsive factors. The concept of “cancer immunotherapy” has emerged in this context. Immunotherapy in medicine involves treating various diseases such as cancer, allergies, autoimmune diseases and infectious diseases using immune system components such as antibodies, cytokines and dendritic cells. Immunotherapy provides specificity, more effective, less toxic, secondary effects and better tolerance to clinical practice [5].

“Cancer immunotherapy” uses the host's inherent immune system to treat cancer and imparts a memory effect to the immune system that can inhibit cancer relapse. Normal anti-cancer immunity involves identifying and removing early malignant cells expressing tumour-related antigens (TAAs) [6]. And complicate immune system such as dendritic cells (DC), macrophages, plasma cells, cytokines, antibodies, and helper T cells all work together to prevent tumour development [7]. To initiate the anticancer response, TAAs that are presented by antigen-presenting cells (APCs) such as DCs form complexes with MHC class I molecules to activate cytotoxic T lymphocytes (CTLs). Activated CTLs specifically kill cancer cells based on the information from TAAs. After killing whole cancer cells in the host, the activated T cell converts to a “memory T cell” and establishes the memory effect for the specific cancer.

1.3 Hurdle of Early Cancer Immunotherapy

These described mechanisms are similar to the concept of vaccination for infectious disease. Following up on the idea of vaccines, the first cancer immunotherapy focused on TAA generation, antigen presentation by APCs, and activation of CTLs, which are called a “cancer vaccine.”

Unfortunately, after a number of cancer vaccine have been conducted and tested in clinical practice, but only one cancer vaccine has been approved; sipuleucel-T in prostate cancer [8]. The most serious problem is that many cancer vaccines could induce a tumour-specific T cell response without objective anti-tumour activity [9]. This finding suggests that priming the tumour-specific T cell response is not the key for conquering cancer. There are some factors that inhibit the CTL response.

The early cancer vaccine trials gave us an insight: there are factors that hinder the anti-tumour response. In this book chapter, we describe the “Factors that suppress anti-tumour response in cancer immunotherapy” and introduce “Designed nanostructure materials as a strategy to overcome the immunosuppressive tumour microenvironment.”

1.4 Expansion of Cancer Immunotherapy

As previously mentioned, traditional cancer immunotherapy also just considers “killing tumour cells” regardless of considering the complexity of immune response of the tumour microenvironment (TME) and their potential response to treatment. As the technology has advanced, it has revealed that tumour cells have their own mechanism to interact with TME, and they usually escape cancer therapy using it. Therefore, the discovery of TME suggests a new direction to overcome the immune suppressive environment to cancer immunotherapy.

Conventionally, the tumour, T cell, APCs, and NK cells was the environment interacting with tumour and immunologic effector cells in cancer therapy. In recent years, the concept of the environment surrounding the tumour enlarged and was called the “tumour microenvironment (TME).” The TME contains T cells, APCs, NK cells, **(1) immune suppressive cells** (myeloid-derived suppression cells (MDSCs), tumour-associated macrophages (TAMs), and regulatory T cells (Treg)), **(2) cytokines and chemokines** (inflammatory(anti-tumoural) TNF- α , IL-12, IL-6, IFN- γ cytokines, anti-inflammatory (pro-tumoural) IL-10, TGF- β cytokines, angiogenic cytokine VEGF, cell-promoting cytokines/chemokines like CCL 22 and GM-CSF), and **(3) enzymes controlling TME-related cell metabolism** (IDO, arginase, and NOS2) [10].

1.5 Immune Suppressive Cells in TME

Regulatory T (Treg) cells are a Foxp3-expressing T cell subpopulation that plays a role in immunological self-tolerance and homeostasis. Treg-mediated immune suppression is important for negative regulation of immune-mediated inflammation, autoimmune disease, and allergies. However, Treg is a strong immune suppressor in context of cancer. The high expression of the IL-2 receptor on Treg can deprive IL-2 from T cells and disturb proliferation [11]. Also, CD39 and CD73, ectoenzymes

highly expressed on Tregs, facilitate adenosine elaboration and initiate the adenosine signalling pathway to inhibit effector T cell proliferation and DC function [12]. TIGIT is a surface molecule on Tregs that induces immunosuppressive cytokines IL-10 and TGF- β when Tregs interact with DCs [13].

Macrophages are involved in various immune responses in our body and most inflammatory responses. However, these macrophages change to become pro-tumoural tumour-associated macrophages (TAMs) when the tumour progresses. While the tumour growing, the inflammatory Th1 response dominant tumour microenvironment changes to an anti-inflammatory dominant condition. In response to the change, the macrophages polarize to TAMs via IL-4 (CD4+ T cells/tumour cell secreted), colony stimulating factor-1 (CSF-1), GM-CSF, TGF- β , arginase-1, and other factors. TAMs induce T cell apoptosis, Treg recruitment to the tumour site and inhibit T cells/NK cells and angiogenesis via vascular endothelial growth factor (VEGF) secretion.

The myeloid-derived suppressor cells (MDSCs) generated in bone marrow migrate to lymphoid organs or the tumour site and become the one of most important parts of the tumour microenvironment. Both lymphoid organ and tumour microenvironment migrated MDSCs play an immune-suppressive role. The MDSCs in the tumour microenvironment especially inhibit CD3/CD28-mediated T cell proliferation. Furthermore, MDSCs generate pro-tumoural metabolic control enzymes like arginase and NOS2 in some tumour types.

1.6 Cytokines and Chemokines in TME

As mentioned in previous paragraphs, cytokines and chemokines are important components in the tumour microenvironment. The immune response in our body can completely differ depending on the dominant cytokines or chemokines.

For example, when a tumour established, immune cells in our body try to exclude tumour cells and consequently generate inflammatory cytokines. Inflammatory cytokines like “tumour necrosis factor- α (TNF- α),” “IFN- γ ,” and “IL-6” initiate the anti-tumoural immune response by signalling various immune cells.

However, the inflammatory conditions reverse to an anti-inflammatory condition and the anti-inflammatory cytokines become dominant due to the tumour’s immune suppressive mechanism. Anti-inflammatory cytokines like TGF- β and IL-10 stimulate the suppressive immune cells (Treg, TAMs, and MDSCs) and form a pro-tumoural TME.

In addition to those cytokines, several cytokines and chemokines are associated with the tumour microenvironment. For example, vascular endothelial growth factor (VEGF) facilitates angiogenesis around the tumour to supply enough nutrients for tumour growth. Also, angiogenesis induces tumour cell migration and metastasis. Expression of CCL2, the chemokine known as a monocyte chemo attractant, positively correlates with tumour-associated macrophage (TAM) infiltration, tumour vascularization, and angiogenesis [14].

1.7 Organized Interaction Between TME

There are many tumour microenvironment immune suppressive factors elaborated in this chapter. Since the human immune system is not a fixed system, the immune suppressive factors interact with each other and sometimes yield a negative synergy effect.

For example, the facilitation of MDSCs effects itself and increases Treg and TAM infiltration to the tumour site, stimulating them via anti-inflammatory cytokines. Furthermore, the enzymes secreted by MDSCs induce Treg and TAM differentiation. Likewise, it is difficult to overcome the immune suppressive tumour microenvironment because other factors interact with each other. Therefore, the key to cancer immunotherapy is the effective delivery of the appropriate drug to the immune system based on knowledge of interactions between immunological factors.

1.8 Immune Checkpoint and ICBT Combination

2018 was very meaningful year for cancer immunotherapy because the Nobel Prize for Physiology or Medicine was awarded to James P. Allison and Tasuku Honjo for inspiring research into “immune checkpoint blockade therapy (ICBT).” ICBT suggests new directions for cancer immunotherapy.

Immune checkpoint is a signalling pathway that inactivates immune cells. The immune checkpoint can be regarded as one tumour escaping mechanism, and it explains how the immune suppressive cells (containing tumour cells) can regulate the other immune cells.

Representative immune checkpoint molecules PD-1, PDL-1, and CTLA-4 are expressed on the immune cells or tumour cells and inhibit the immune response of cytotoxic T lymphocytes (CTLs), antigen-presenting cells (APCs), or B cells. Therefore, it is important to learn how to “block the immune checkpoint” to effectively administer immunotherapy in a patient. Also, the antibodies that combine with these ligands and block their role are the “blockbusters” of the pharmaceutical market: α PD-1, α PDL-1, and CTLA-4. Recent reports have shown that many patients suffering from various malignancies benefit from ICBT and mainstream of immunotherapy against it.

1.9 Hurdle of Recent Cancer Immunotherapy

Even though immune checkpoint blockade therapy seems like a dream drug in cancer immunotherapy, recent studies have shown its limitations. Most tumour have immune suppressive conditions and usually do not respond to the immune system.

These non-immunogenic tumours are called “cold tumours”. The expression of the immune checkpoint is low because of the tumour microenvironment of the cold tumour, so ICBT is not effective on these tumours. Another problem is related to toxicity. In addition to tumours and target cells, other normal cells express the immune checkpoint. When immune checkpoint inhibitor is injected, it can induce immune-related adverse events (irAEs) and systemic immune disorders like autoimmune disease.

1.10 Design of Nanostructures to Overcome the Hurdle of Recent Cancer Immunotherapy

Although there are remaining limitations, cancer immunotherapy is a promising therapeutic method for conquering cancer. In recent years, there have been many studies and technical developments to overcome limitations. In this chapter, we want to highlight some of these advances. A number of nano-materials are used in the cancer immunotherapy field for increased therapeutic effect, including liposomes, emulsion, core-shell particles, nano-rods, nano-structured hydrogel/scaffold, and lipid nanoparticles. We introduce the “designed nanostructure” as one strategy to overcome the immunosuppressive TME and modulate cold tumours into hot tumours (Fig. 1).

2 Nanomaterials for the Modulation of Immunosuppressive Cells in TME

2.1 Regulatory T Cells (Treg Cells)

Regulatory T cells are a type of CD4⁺ T cells which express high CD25 and FOXP3 [15]. Treg cells are characterized as CD4⁺CD25⁺FOXP3⁺ Treg cells, and they were originally noted to have important roles in maintaining the normal physiological state by moderating immune destruction and preventing autoimmune disease occurrence [16]. In case of cancer, Treg cells typically accumulate in the tumour microenvironment (TME) and promote immunosuppression by modulating several mechanisms such as immunosuppressive cytokine secretion and down-regulation of immune cell activation after direct cellular contact [16]. For example, intratumoural accumulation of Treg cells increases transforming growth factor beta (TGF- β) levels in the tumour microenvironment and inhibits infiltration of immune cells such as effector T cells, dendritic cells (DCs), natural killer cells (NK), natural killer T cells (NKT), and B cells [17].

One of the simplest ways to cope with immune suppression by Treg cells is to deplete them. Molecules such as cyclophosphamide and Raf kinase inhibitors

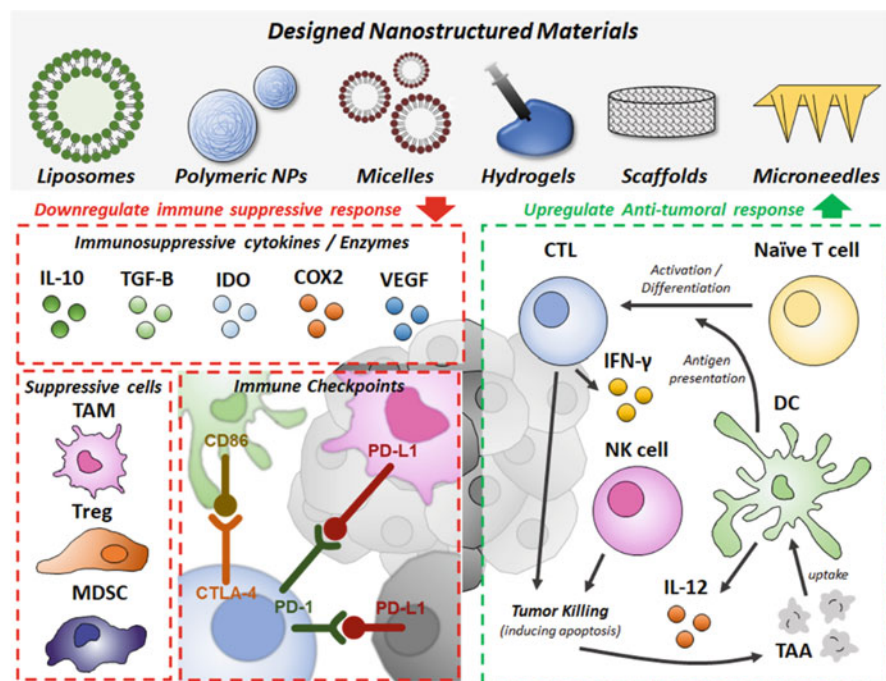


Fig. 1 Schematic illustration of designed nanomaterials which can modulate immune suppressive factors and anti-tumor response in tumor microenvironment

can selectively deplete Treg cells. In addition, monoclonal antibodies targeting Treg cell-associated surface molecules such as CD25 or CTLA-4 can mediate Treg cell depletion. Nanomaterials can be used to prepare these molecules for Treg cell modulation strategies [18]. However, several clinical attempts to increase the anti-tumour immune response via systemic depletion of Treg cells showed limited effects. This could be explained by recent studies showing that the effect of systemic depletion of Treg cells is not permanent because Teff cells are quickly converted to Treg cells [19]. To overcome this barrier, Kazuhide Sato et al. designed a near-infrared (NIR)-photoactivated radical-generating photodynamic dye (IRDye 700DX) conjugated to the anti-Fab fragment of an anti-CD25 antibody for CD25-targeting near-infrared photoimmunotherapy (NIR-PIT) for local depletion of Treg cells [20]. When the NIR light is applied to the lesion part, selective depletion of intratumoural local Treg cells occurs without eliminating the local effector immune cells or Treg cells in other organs. The increased ratio of CD8⁺ T cells and NK cells over Treg cells in the tumour microenvironment induces subsequent immune cell-mediated tumour elimination.

Another alternative approach is to manipulate Treg cell function. Cristiano Sacchetti et al. tried to selectively modulate resident Treg cells in the tumour microenvironment. They focused on the glucocorticoid-induced TNFR-related

receptor (GITR) because it showed higher overexpression on intratumoural Treg cells than splenic Treg cells, compared to other reported Treg-specific markers (folate receptor 4, CD103, and CD39) [21]. They synthesized PEG-modified single-walled carbon nanotubes (PEG-SWCNTs) coated with a GITR ligand via a biotin-neutravidin interaction with PEG chain, and they showed that ligands against Treg-specific receptors drive selective internalization of PEG-SWCNTs into intratumoural Treg cells. This investigation opens the possibility of Treg-selective functional manipulation. Another example of targeted modulation of Treg cell function was suggested by Ou W et al. They developed Treg cell-targeting nanoparticles by conjugating the tLyp1 peptide, which has a high affinity for the Nrp1 receptor expressed in intratumoural Treg cells [15]. Nanoparticles have good stability, and show effective Treg cell targeting, and high tumour accumulation. By incorporating imatinib (IMT), a tyrosine kinase inhibitor that blocks STAT3 and STAT5 signalling, in the nanoparticles, they enhanced downregulation of immunosuppressive Treg cells.

2.2 Myeloid-Derived Suppressor Cells (MDSC)

Myeloid-derived suppressor cells (MDSC) are a diverse population of immature myeloid cells that are generated in the bone marrow. In case of tumour patients, they migrate from bone marrow to peripheral lymphoid organs and tumours to mediate formation of an immune-suppressive condition in the tumour microenvironment [22]. MDSC-mediated tumour immune escape is achieved via multiple mechanisms, including expression of arginase (ARG1), inducible NOS (iNOS), immune suppressive cytokines (TGF- β , IL-10), and COX-2 to neutralize the anti-tumour function of effector immune cells [23, 24].

Z.Xu et al. developed a mannose-modified lipid calcium phosphate (LCP) nanoparticle (NP)-based vaccine containing both tumour-specific antigen (tyrosinase related protein 2 (Trp2) peptide) and adjuvant (CpG). Although the *in vivo* cytotoxic T lymphocyte (CTL) response generated by the LCP-Trp2 vaccination is strong, it is only effective in the early stages of tumour progression (4 days after tumour inoculation) and not in the late stage of tumour growth (13 days after tumour inoculation) [25] because the vaccination effect is compromised by tumour-associated immune suppression. To abrogate immune suppression, Meirong Huo et al. developed tumour-targeting PLGA-PEG-MBA micelles encapsulating a tyrosine kinase inhibitor and sunitinib base to work in a synergistic manner with the developed vaccine [26]. The synergistic effect decreased the percentage of immune suppressive cells (MDSCs and Tregs) in the tumour microenvironment, increased cytotoxic T cell infiltration, and produced a shift from a Th2 to Th1 pattern, resulting in tumour regression. Similarly, Yan Zhao et al. focused on the anti-inflammatory triterpenoid methyl-2-cyano-3,12-dioxooleana-1,9(11)-dien-28-oate (CDDO-Me), a broad spectrum inhibitor of several signalling pathways that blocks the immunosuppressive function of myeloid-derived suppressor cells

(MDSC) [27]. Encapsulating CDDO-Me in a PLGA nanoparticle increases the accessibility of the immune-modulating agent to CD11b⁺ cells (macrophages and MDSCs) after a single injection and alters the cytokine expression profiles of those immune suppressive cells, finally producing a favourable environment for CTL immune responses.

Cancer vaccine treatment after surgical removal of tumour produces a lower response compared to that in intact tumours despite the small tumour size due to immune suppression in the tumour microenvironment [28]. For postsurgical treatment, the synthetic immune niche (immuneCare-DISC, iCD) is peritumourally implanted in an advanced-stage primary 4T1 breast tumour model [29]. Gemcitabine released by iCD inhibits immunosuppressive MDSCs in the tumour and spleen and up-regulates the cancer vaccine effect. iCD prevents tumour recurrence and generates systemic antitumour immunity, as evidenced by the antitumour effect in the lung.

Moreover to the implantable scaffold, in another study, they tried to overcome the post-surgical formed tumour microenvironment with syringeable nanogel [30]. Syringeable immunomodulatory multidomain nanogel (iGel), which is composed by the electrostatic interaction of multi-vesicular liposome and nanoliposome, enabled the local and extended release of immunomodulatory drugs (Fig. 2). By inducing immunogenic cell death and MDSCs depletion simultaneously, the iGel successfully reshape the immunosuppressive tumour microenvironment and synergize with checkpoint therapies.

Polymeric micelles with a chemically conjugated 6-thioguanine (TG) via a disulphide bond to block the copolymer were synthesized by Laura Jeanbart et al. [31] 6-thioguanine is a cytotoxic drug that kills Mo-MDSCs in tumour-bearing mice. The intradermally-injected sub-30 nm micelle loaded with 6-thioguanine (MC-TG) drains through lymphatics to target skin-draining LNs, and is taken up by resident antigen-presenting cells. Biodistribution studies show that micelles are readily taken up by Mo-MDSCs in the LNs, spleen, and tumours compared to in free TG. Therefore, MC-TG, along with micelles, efficiently depletes Mo-MDSCs in the spleen, tumours, and G-MDSC in the draining LNs, boosting T cell-mediated anti-tumour responses.

Two typical cationic polymers—cationic dextran (C-dextran) and polyethyleneimine (PEI)—are known to stimulate macrophages to produce Th1-inducing cytokine IL-12 via the Toll-like receptor 4 (TLR4) signalling pathway and re-polarize M2 type macrophages to M1 type macrophages [32]. Further study showed that a similar effect occurs in MDSCs. MDSCs stimulated by the two cationic polymers re-polarized from M2- to M1-type, and the authors, by a knock-out mouse study, showed that TLR4 signalling triggered the stimulation [33]. Detailed examination of isolated MDSCs from the tumour indicated that C-dextran and PEI-treated groups secreted higher levels of the pro-inflammatory cytokines IL-12 and TNF- α , but lower levels of the anti-inflammatory cytokines IL-10 and TGF- β compared to the control group. Moreover, the cationic polymers increased NOS2 expression, and they decreased transcription of Arg1 in MDSCs. As a result, re-polarized MDSCs restored both immune surveillance in the tumour microenvironment and infiltration

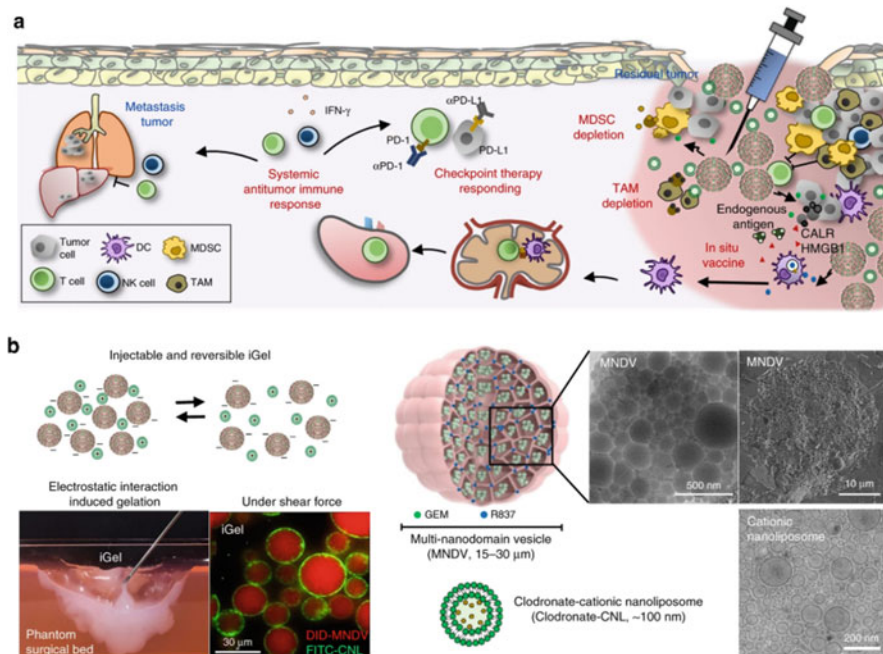


Fig. 2 Syringeable immunotherapeutic nanogel composed with MNDV and cationic nanoliposome reshapes the tumor microenvironment. **(a)** Schematic illustration shows after surgery, immunotherapeutic drugs (GEM, R837, Clodronate) in nanogel can convert immunosuppression in tumor microenvironment. **(b)** Principle and characteristic of nanogel formation. (Reproduced from Chanyoung Song et al. 2019)

of $CD4^+$ and $CD8^+$ T cells, which led to tumour eradication in 4T1 tumour-bearing mice.

Meng Yu et al. developed an intravenously-injected BSA-based nanoregulator incorporating MnO_2 and PI3K γ inhibitor IPI549 [34]. The nanoregulator is highly sensitive to the acidic and H_2O_2 -enriched tumour environment due to the oxygen-generating reduction of MnO_2 , resulting in collapse and fast release of IPI549 in the tumour microenvironment. Alleviation of hypoxia by MnO_2 downregulated PD-L1 expression and released IPI549 in the tumour microenvironment, binding to PI3K γ on MDSC, and resulting in MDSC suppression. As a result, the nanoregulator enhanced infiltration of $CD4^+$ helper T cells and cytotoxic $CD8^+$ T cells and decreased regulatory T cell infiltration, enhancing the T cell-mediated anti-tumour response.

2.3 *Tumour-Associated Macrophages (TAM)*

Tumour-associated macrophages (TAM) identify an alternatively-activated macrophage (“M2” polarized) rather than a classically-activated macrophage (“M1” polarized), secrete a range of anti-inflammatory cytokines such as interleukin-10 (IL-10), TGF- β (Transforming growth factor-beta) to suppress pro-inflammatory cytokine interleukin-12 (IL-12) secretion in intratumoural dendritic cells, and cytotoxic CD8⁺ T cell activation [35, 36]. It can subsequently stimulate tumour angiogenesis and drive tumour metastasis.

Several ligands binding to macrophage membrane receptors such as mannose or folate are well known for macrophage targeting. Based on these ligands, several delivery systems have been developed for macrophage-specific modulation. For example, Yu Wang et al. developed intravenously administered bio-responsive polymeric complex (P³AB) to target and eliminate tumour-associated macrophages (TAM) in the tumour microenvironment [36]. The polymeric complex consists of a core-shell structure. In the core part, bisphosphonate (macrophage-killing drug) is conjugated to glucomannan, which has affinity for the macrophage mannose receptor. The shell comprises poly(ethylene glycol) (PEG), poly(lactic-co-glycolic acid) (PLGA), and matrix metalloprotease (MMP) cleavable peptides in the tumour microenvironment. MMP cleavable peptide enables P³AB to respond to the tumour microenvironment (TME), and enables the core part to be efficiently delivered to tumour-associated macrophages (TAMs), rendering TAM-targeting cancer immunotherapy successful.

However, receptors for the ligands are also expressed in normal epithelial and dendritic cells. For higher specificity, Joao Conde et al. designed an M2 macrophage-specific peptide sequence (M2pep) to lower binding to non-targeted leukocytes and preferentially bind to tumour-associated macrophages (TAMs) [37]. They synthesized M2pep functionalized gold nanoparticles (AuNPs) incorporating vascular endothelial growth factor (VEGF) siRNA. Successful delivery of VEGF siRNA to tumour-associated macrophages (TAM) via M2pep-functionalized AuNPs blocked the high expression of angiogenic factors.

Several mechanisms in tumour cells facilitate the formation of an immune-suppressive microenvironment. For example, tumour-associated macrophages (TAM) are polarized toward a pro-tumorigenic M2 phenotype and phagocytosis by macrophages is blocked [38]. First, tumour cells secrete macrophage colony stimulating factor (MCSF), which binds to tyrosine kinase CSF-1R expressed on monocytes and macrophage. This recruits tumour-associated macrophages and differentiates toward M2-type macrophages. Second, tumour cells disturb the phagocytosis activity of macrophages by expressing an “eat me not” signal, CD47, which binds to SIRP α on macrophages. As the case stands, Ashish Kulkarni et al. designed a supramolecule consisting of an inhibitor of colony stimulating factor 1 receptor (CSF-1R) and SIRP α -blocking antibodies. The supramolecule binds with macrophages via SIRP α , blocking the CD47-SIRP α signalling axis. Meanwhile, CSF-1R inhibitor consistently acts on macrophages, enhancing repolarization of

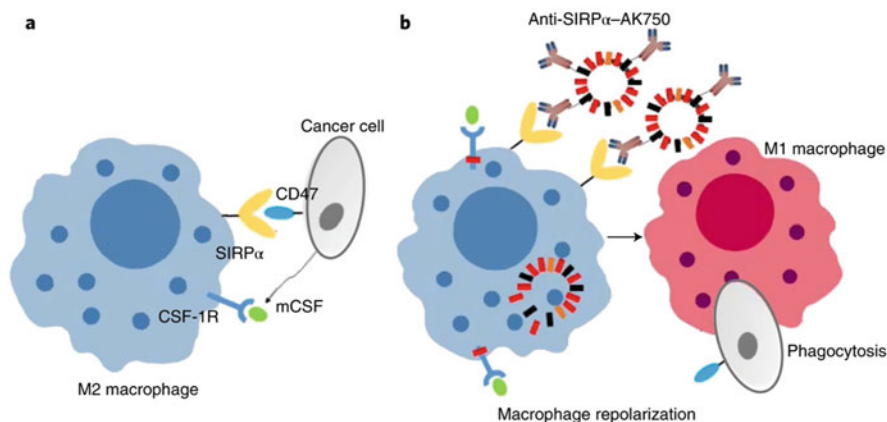


Fig. 3 A designer self-assembled supramolecule targets and repolarizes the tumor-associated macrophage. **(a)** Cancer cells inhibit phagocytosis of macrophage and polarize macrophages to the immunosuppressive ‘M2’ phenotype by blocking SIRP α and exploiting CSF-1R signaling, respectively. **(b)** Supramolecule induces repolarization of an M2 macrophage to anti-tumoral M1 macrophage by dual blocking SIRP α and CSF-1R signaling. (Reproduced from Ashish Kulkarni et al. 2018)

M2-to-M1 macrophages. Blocking the CD47-SIRP α and MCSF-CSF-1R signalling axes at the same time improves anti-tumour and anti-metastatic efficiencies in both melanoma and breast cancer models (Fig. 3).

Polarization of macrophages can be classified by cell shape-based high-content image analysis conducting by computational automated segmentation [39]. Christopher B. Rodell et al. extracted features of single cells such as cellular radius, axis lengths, compactness, and eccentricity, which are correlated with the polarized phenotype of macrophage. Based on the high content image analysis, 38 drugs (including tyrosine kinase inhibitors, colony-stimulating factor 1 receptor inhibitors, and Toll-like receptor agonists) were used for treatment of M2 polarized murine monocytes to observe the degree of M1 polarization. The R848 (TLR7/8 agonist) indicated the largest polarization. The poorly soluble drug R848 was solubilized by hydrophilic modified β -cyclodextrin (CD), and the amide bond between succinyl- β -cyclodextrin and L-lysine under aqueous conditions enabled the formation of a supramolecular drug reservoir. Systemically injected CDNP-R848 in multiple tumour types alters the phenotype of intratumoural macrophage toward to the M1 phenotype, suppresses the tumour growth and inhibits the tumour re-challenge.

3 Nanomaterials for the Modulation of Immunosuppressive Factors in TME

3.1 Indoleamine 2,3-Dioxygenase (IDO)

Indoleamine 2,3-dioxygenases (IDO) are immune-regulatory factors related to tryptophan metabolism. Specifically, they are tryptophan catabolic enzymes that catalyse the conversion of tryptophan into kynurenine. Tryptophan depletion and increased kynurenine perform immune-suppressive functions [40]. Tryptophan depletion stimulates effector T cell and natural killer cell autophagy, and increase in kynurenine up-regulates regulatory T cell and MDSC activation [41]. Importantly, IDO is associated with immune checkpoint inhibitor resistance, and combined IDO inhibitors with immune checkpoint inhibitors are an alternative cancer immunotherapy strategy.

Abhinav P. Acharya et al. developed a peri-tumoural injectable hydrogel called the immunomodulatory molecule delivery system (iMods) that enables targeted intracellular delivery of the IDO inhibitor 1-methyl tryptophan (1-MT). Along with 1-MT, iMods provides simultaneous intracellular delivery of tumour antigen (OVA) and adjuvant (poly(I:C)) and extracellular delivery of a checkpoint inhibitor (anti-PD-L1) [42]. Targeting multiple immunomodulators to their respective targets is possible by designing iMods as specific stimuli-responsive materials. For example, IDO inhibitors and vaccine components, which should be delivered to the cytosol, are encapsulated in pH-triggered degradable alginoketal particles. Meanwhile, alginoketal particles are mixed with a thermo-responsive polymer poly(ethylene glycol)-poly(serinol hexamethylene urethane) or poly(ethylene glycol)-poly-(serinol hexamethylene urethane) (ESHU) to form stable gels at 37 °C with anti-PD-L1 loaded for cell membrane delivery. *In vivo* injection of iMods enhances the ratio of CD8⁺ T cells/Treg cells in both tumour and tumour draining lymph nodes. Moreover, iMods generates systemic anti-tumour immunity.

It was revealed that even effective treatment by photo thermal therapy (PTT) or mild heat treatment upregulates heat shock protein (HSP) and indoleamine 2,3-dioxygenase (IDO) to accelerate tumour margin growth [43]. Therefore, combination with an IDO inhibitor is expected to further enhance the efficacy of photo thermal therapy. IR780 and NLG919 were selected as the photosensitizer and IDO inhibitor, respectively, and they were co-encapsulated in micelles synthesized with amphipathic polymer MPEG-PCL to effectively accumulate in the tumour and migrate to the lymph node through the lymphatic system. NLG919/IR780 micelle-mediated photo thermal therapy and IDO inhibition stimulate T cell activation and inhibit primary tumour and distant tumour growth, thus showing a systemic effect.

The immunogenic cell death (ICD)-inducible capacity of a few chemo-drugs (Oxaliplatin, Doxorubicin, Paclitaxel, and others) can be applied for chemotherapy in various cancer models. However, the immunogenic effects of these chemo-drugs could be concealed by the inducible immunosuppressive effects of locally overexpressed indoleamine 2,3-dioxygenase 1 (IDO1) in the tumour microenviron-

are widely being made. Yanqi Ye et al. engineered a microneedle (MN)-based transcutaneous delivery platform for the synergistic therapeutic effect of anti-PD-1 and 1-methyl tryptophan, which represent an immune checkpoint inhibitor and IDO inhibitor, respectively [46]. The sustained delivery system enhances the local retention of the agents, increasing the ratio of cytotoxic T lymphocytes to regulatory T cells and reducing toxicity from agents leaking into systemic circulation. Another strategy for local treatment with an immune checkpoint inhibitor and an IDO inhibitor was developed by Shuangjiang Yu et al. [47] An injectable polypeptide-based gel depot was developed for sustained release of anti-PD-L1 and D-1-methyl tryptophan, IDO inhibition, and ROS level control in the tumour microenvironment to treat a melanoma tumour model. The gel was formed with a triblock copolymer comprising a central poly(ethylene glycol) (PEG) block sided by polypeptide blocks containing ROS-responsive L-methionine (Me) and D-1-methyl tryptophan. At the optimized concentration of the triblock copolymer, the sol-to-gel transition temperature is modified to body temperature to enable *in-situ* hydrogel gelation. The thermogelling ROS-responsive hydrogel-based localized drug delivery platform successfully sustains local co-delivery of anti-PD-L1 and D-1-methyl tryptophan and enhances the antitumour efficacy compared to that of free drugs.

3.2 Cyclooxygenase 2 (COX-2)

Cyclooxygenase 2 (COX-2) is an inducible enzyme associated with inflammatory diseases and carcinogenesis via induction of pro-inflammatory cytokines and growth factors [48]. In cancer diseases, COX-2 and its products, especially prostaglandin E2 (PGE2), stimulate the AKT, NF- κ B, and ERK1/2 signalling pathways to promote tumour proliferation, angiogenesis, metastasis, and immunosuppression [49]. In detail, the COX-2/PGE2 pathway leads M1 to M2 phenotype polarization of macrophage, and down-regulates the maturation of dendritic cells and their expression of MHC class II molecules which present antigen to T cells [48]. COX-2 helps maintain MDSCs and promotes T cell differentiation into regulatory T cells. Therefore, COX-2 and its product PGE2 are widely recognized as therapeutic targets for immune resistance modulation in cancer treatment.

Nonsteroidal anti-inflammatory drugs (NSAIDs) have been widely used as COX inhibitors. However, since most them are poorly water soluble, it is difficult to apply them in the clinic. Therefore, co-solvents or delivery systems are required for further applications. Raghavendra Gowda et al. encapsulated celecoxib (COX-2 inhibitor) in a nanoliposomal-based agent that converts the drug to be soluble when administered intravenously [50]. They co-encapsulated Plumbagin (STAT3 inhibitor) in the nanoliposome so that these drugs can be simultaneously released at an optimal ratio for maximal synergistic effects with a minimal dose. The simultaneous inhibition of COX-2 and STAT3 in the melanoma tumour model decreased levels of several key cyclins important in melanoma development and significantly reduced tumour growth. In another study, celecoxib was locally delivered using

alginate hydrogel developed by Yongkui Li et al., which helped sustain the release of a high concentration of celecoxib in the peripheral circulation and in tumour regions [51]. Locally delivering celecoxib with hydrogel showed similar inhibition of tumour growth compared to daily intragastrical administration (i.g.). However, it significantly extended the survival time, indicating that the hydrogel maximizes celecoxib's effects. They also loaded anti-PD-1 in the hydrogel and synergistically enhanced the anti-tumour effects. The co-loaded hydrogel successfully increases the CD4⁺IFN- γ ⁺ and CD8⁺IFN- γ ⁺ T cells and reduces regulatory T cells and MDSCs in the tumour. Moreover, the representative anti-angiogenic chemokines CXCL9 and CXCL10 and immune-suppressive factors like IL-1, COX-2 were all down-regulated.

3.3 TGF- β

Transforming growth factor-beta (TGF- β) is involved in regulating immune cell activity which is crucial for maintaining normal tissue homeostasis. However, TGF- β is a major immune suppressive cytokine that promotes tumour growth by inducing an immune suppressive microenvironment in the context of the tumour microenvironment, which includes T regs (regulatory T cell), M2 macrophages, and results in angiogenesis and metastasis [52–54]. Moreover, TGF- β suppresses the anti-tumoral activity of pro-inflammatory immune cells. TGF- β prohibits dendritic cell (DC) migration to draining lymph nodes, which is essential for transporting tumour antigens. DCs affected by TGF- β differentiate to tolerogenic DCs and promote Treg differentiation. TGF- β is also strongly involved in M2 macrophage differentiation, which is a representative tumour-promoting antigen-presenting cell (APCs). In particular, TGF- β greatly affects T-cell systems. TGF- β induces Treg differentiation and inhibits naïve T cell differentiation to Th1 (type 1 T helper cell) and Th1 cell proliferation. Finally, TGF- β -induced Tregs regulate effector T cell function [52]. With its varied immunosuppressive mechanisms, TGF- β affects the tumour-promoting environment around the tumour. TGF- β regulation can be a powerful strategy in cancer immunotherapy. Zhou et al. developed a hydroxy ethyl starch-poly lactide (HES-PLA) nanoparticle that is co-encapsulated with TGF- β inhibitor (LY2157299) and an anti-cancer drug (doxorubicin) [55]. Insufficient chemotherapy can activate the TGF- β pathway and promote tumour metastasis. DOX (doxorubicin) in the HES-PLA nanoparticle can induce antitumor effect, but the heterogenous DOX distribution induces the up-regulation of TGF- β to promote tumour distribution. The co-delivered LY2157299 inhibits the TGF- β signalling pathway and successfully prohibits metastasis of 4 T1 breast cancer cells. Moreover, the antitumor effect and overall survival rates in the DOX/LY co-delivered group significantly increased in the 4 T1 murine breast cancer model. Park et al. focused on inhibition of the TGF- β immunosuppressive property [56]. They developed polymeric nano-liposome (nanolipogels; nLGs) containing the pro-inflammatory cytokine IL-2 and a TGF- β inhibitor drug, SB-505124-complexed cyclodextrins

to overcome the immunoinhibitory nature of TMEs. IL-2 and TGF- β inhibitor encapsulated in nLGs were consistently released and significantly increased the antitumor effect and survival rate of tumour-bearing mice. Moreover, NK cell activity and the population of tumour-infiltrating CD8⁺ T cells were also increased. Elevated TGF- β level greatly affects a cancer vaccine's therapeutic effect [40]. Xu et al. developed a lipid-calcium-phosphate (LCP) nanoparticle (NP) and liposome-protamine-hyaluronic acid (LPH) NP to enhance the CTL response and modulate the suppressive microenvironment [57]. LCP NP is loaded with tumour antigen (Trp 2 peptide) and adjuvant (CpG oligonucleotide) to evoke dendritic cell-mediated systemic immune response. In addition, LPH NP is designed to deliver anti-TGF- β siRNA, which down-regulates TGF- β levels in the tumour microenvironment. Co-delivery of LCP vaccine and LPH NP showed significant tumour regression compared to that in the LCP vaccine-only-treated group in late tumour stages. Moreover, the population of tumour-infiltrating CD8⁺ T cell increased in the LCP vaccine and LPH NP combination groups in late tumour stages.

3.4 Interleukin-10

Interleukin-10 (IL-10) is a representative anti-inflammatory cytokine controlling the immune suppressive TMEs. IL-10 is produced in the inflammatory environment by various immune cells: macrophages, myeloid DC, CD4⁺Foxp3⁺ Treg, and CD4⁺Foxp3⁻ regulatory T cells. IL-10 production in the inflammatory environment regulates the stimulated immune system after a proper immune response to minimize the damage due to self-reactive immune response. Such immune regulation is very important to maintain the immune system. However, IL-10 production is a very critical hurdle for immunotherapy in TMEs. It was reported that TLR7 agonist cream application increased IL-10 production by CD4⁺ Foxp3⁻ T cells to significantly reduce its therapeutic effect in a mammary tumour model [58]. Importantly, IL-10-producing immune cells are the same cell with IFN- γ secreting cells [59]. Type 1 T helper cells, the main anti-tumoural immune cells, are the main source of the IFN- γ cytokine, which is crucial for the antitumour effect. IL-10 production is also highly induced by Th1 cells, by a process called self-regulation. Since IL-10 acts as a defender against immune system over-response, IL-10-related therapy should be done in the intermediate level.

Shen et al. developed a lipid-protamine-DNA (LPD)-based nanoparticle loaded with IL-10 trap genes [60]. In addition to IL-10 trapping genes, the C-X-C motif chemokine ligand 12 (CXCL12), the key factor for inhibiting T-cell infiltration, was also loaded in the LPD nanoparticle to inhibit CXCL-12 functions and enhance the number of tumour-infiltrating T-cells. Even the IL-10 trap alone group showed reduced immune suppressive cells and inhibition of tumour growth in the murine 4T1 model. In the combination CXCL-12 and IL-10 trap group, a synergetic anti-tumour effect was observed based on both inhibition of immune suppressive cells

and enhancement of tumour-infiltration by CD8⁺ T cells, NK cells, and activated DCs in the 4T1 breast cancer model.

3.5 Vascular Endothelial Growth Factor (VEGF)

Vascular endothelial growth factor (VEGF) is a key angiogenesis mediator involved in the excessive formation of abnormal blood vessels in cancer [61]. VEGF directly affects endothelial cells to induce angiogenesis. Angiogenesis results in abnormal and inefficient blood vessels, and the formed blood vessels then supply oxygen and nutrients essential for tumour progression. Moreover, the formed blood vessels can be a path for tumour cell metastasis [61]. VEGF also acts as a chemoattractant for Tregs, increasing the population of tumour-infiltrating Tregs. In addition, VEGF reduces the action of antitumoral immune cells (DC, M1 macrophage, and cytotoxic T cell) and promotes immunosuppressive cell expansion (MDSC, M2 macrophage, and Treg) [62, 63]. VEGF pathway inhibition can normalize abnormal blood vessels and modulate the immune suppressive environment of TMEs. Normalization implies the conversion of an abnormal blood vessel to a regular normal blood vessel with high perfusion. However, anti-angiogenesis therapy results in a few issues, depending on inhibition degree. Excessive pruning of abnormal blood vessels leads to highly decreased perfusion, which induces an immunosuppressive environment [9]. Moreover, excessive reduction of blood vessels can result in the very low drug delivery efficiency [64]. In addition, Yang et al. reported that discontinuance of VEGF inhibition therapy can enhance metastasis via revascularization of liver blood vessels [65]. Retained release with proper dose of drug is essential for anti-VEGF therapy. To block angiogenesis and enhance intra-tumoral drug penetration, Chen et al. fabricated liposome-polycation nanoparticles loaded with VEGF siRNA and doxorubicin (DOX) [66]. Moreover, DSAA(N,N-distearyl-N-methyl-N-2-(N'-arginyl) aminoethyl ammonium chloride), a down-regulator of drug transporter proteins (P-glycoprotein), was incorporated in liposomes to overcome multiple drug resistance (MDR) and specifically target tumour cells, and the nanoparticles were modified with anisamide (AA). Intravenous delivery of VEGF siRNA with Dox (1.2 mg/kg)-loaded targeted nanoparticles showed a significant anti-tumoral effect. Chung et al. developed a polymeric gene carrier system to efficiently deliver VEGF-suppressing siRNA (siVEGF) to the tumour [67]. To enhance tumour targeting, the cationic cysteine-ending 9-mer arginine oligopeptide (CR9C)-based carrier was PEGylated. Eight intravenous injections of PEG-CR9C/siVEGF (1 mg/kg) oligopeptoplexes significantly reduced the intratumoral VEGF protein level in the subcutaneous SCC-7 xenograft tumour model and improved antitumor efficacy without any significant toxicity.

3.6 Immune Check Point Blockade

Currently, immune checkpoint blockade therapy (ICBT) is the most promising approach for cancer immunotherapy. In the tumour microenvironment, the tumour overexpresses many kinds of immune suppressive ligands such as PD-L1 to escape from the tumour-hostile immune system. Another checkpoint molecule, CTLA-4, is expressed on T cells; it downregulates T cell functions and upregulates Treg. Such immune checkpoints play a key role in producing immunosuppressive conditions [68].

Even if ICBT shows potential for becoming a new trend in cancer immunotherapy, the current results for systemic injection of these immune checkpoint blocking agents show low selectivity and the potential for causing immune-related adverse events (irAEs) [69].

3.6.1 α PD-L1

PD-L1 is usually expressed on the tumour cell surface and APCs. When PD-L1 on APCs binds to PD-1 on T cells, it induces Treg differentiation of CD4⁺ T cells. In addition, the PD-L1 on tumour cells binds to CD8⁺ T cells to regulate the T cell antitumour response [70]. Therefore, blocking PD-L1 or PD-1 is an effective approach in cancer immune therapy, and a number of nanostructure-based delivery systems for immune checkpoint inhibitors were developed and have been reported.

Recently, Wang et al. developed the anti-PD-L1 mAb delivering system by using the unique properties of platelets for reducing the risk of tumour recurrence and metastasis after surgery [71] (Fig. 5a). Liposomal nanohybrid cerasomes aimed to PD-L1 improve anti-tumour treatments. The cerasomes showed better performance than nontargeted delivery of PD-L1 antibody and paclitaxel in terms of anti-tumour effect and inhibiting metastasis. The dual-labelled cerasomes enable MRI/NIRF dual-mode detection and treatment of solid tumours [72].

Schneck et al. synthesized an “immunoswitch” that switches the cancer immunity cycle and increases immune cell antitumour activity (Fig. 5b). Nanoparticles coated with two different antibodies that simultaneously block aPD-L1 and 4-1BB T cell stimulation pathway enhance effector-target cell conjugation and offering bypass for delivering the information of tumour antigens [73].

aPD-1 and aPD-L1 mAb treatment sometimes shows unprecedented clinical response, hence the approach sometimes containing the engineering cellular nanovesicles (NV) for presenting PD-1 receptor. The NV can bind with PD-L1 and block its role of immune-regulation [74].

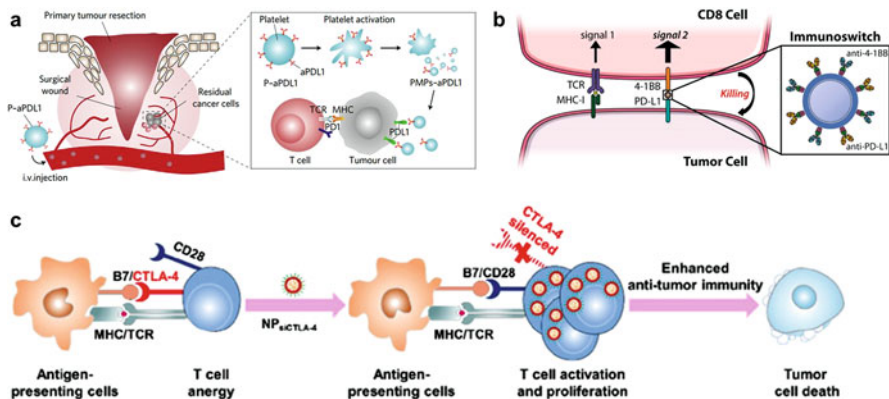


Fig. 5 Development of ICBT and nanomaterial based immunotherapy combination strategies. (a) The anti-PD-L1 expressing platelet blocking PD-L1 on tumor and reduce post-surgical tumour recurrence and metastasis (Reproduced from Chao Wang et al. 2017). (b) “immunoswitch” particle which conjugated with anti-4-1BB and anti-PD-L1 delay tumor growth and extend survival in multiple in vivo models of murine melanoma and colon cancer (Reproduced from Alyssa K. Kosmides et al. 2017). (c) siCTLA-4 containing NP silences CTLA-4 expressing and enhancing T cell mediated anti-tumour immunity (Reproduced from Shi-Yong Li et al. 2015)

3.6.2 α PD-1

As described before, when the PD-1 expressed on T cells binds to PD-L1, it regulates the antitumour response of T cells in various ways. Blocking the PD-1 ligand with an antibody is another important strategy in cancer therapy.

Zhen Gu et al. synthesized aPD-1 encapsulated CpG oligonucleotide chain-based “nano-cocoon” for programmed delivery of aPD-1 and CpG. To control the release of immune stimulants, they used a triglycerol monostearate (TGMS)-coated enzyme capable of digesting the CpG chain and generating CpG fragments. When the particle reaches tumour sites, the TGMS coating is uncovered by proteolytic enzymes abundant in tumours. As result, the “nano-cocoon” is divided to CpG and induces CpG and aPD-1 release to tumours [75].

3.6.3 α CTLA-4

CTLA-4, also known as CD152, is expressed on Tregs or activated T cells and down-regulates immune responses. In addition, it plays the role of an “off” switch, binding with CD80 or CD86 on APCs related to antigen presentation. Therefore, blocking CTLA-4 can up-regulate the cytotoxic effect of T cells and antigen presentation of APCs.

Melief et al. developed anti-CTLA-4 into montanide ISA-51 (water-in-oil emulsion) which can control burst release of the cargo for subcutaneous administration

[76]. This delivery system offering eightfold lower dose than conventionally needed and reducing systemic serum antibody level.

Chenghong Lei et al. reported similar strategy that synthesized nanoporous structure containing antibodies for adapting lower dose and sustained release [77].

Wang et al. synthesized nanoparticle by poly(ethylene glycol)-block-poly (d,l-lactide) and siCTLA-4 with N-bis(2-hydroxyethyl)-N-methyl-N-(2-cholesteryloxycarbonyl aminoethyl) ammonium bromide which can effectively load antibodies in double emulsion technique. The siCTLA-4 in nanoparticle can delivered into T cells and silencing CTLA-4 expression mRNA. Then the protein level of CTLA-4 are decreased and it induces regulate of T regs. Furthermore, the systemic injection of this nanoparticle increases T cell infiltration to tumour and inhibits B16 tumour growth [78] (Fig. 5c).

4 Conclusion

Over a decade, cancer immunotherapy has been focused on cancer vaccines to enhance the antitumoural response of effector immune cells. However, the cancer vaccines suffered from low therapeutic effect. As it was revealed that the immunosuppressive tumour microenvironment is a major hurdle for cancer immunotherapy, several studies related to TME reprogramming have been reported. Moreover, combination immunotherapy with nanotechnology has emerged as a new strategy for cancer immunotherapy to overcome low delivery and reduce systemic toxicity. An enormous number of studies showed enhanced therapeutic effects of nanotechnology-mediated immunotherapy. (Table 1) Moreover, combination therapy with ICBT and a TME reprogramming agent can significantly increase the ICBT response rate. However, there are several hurdles to translate this to clinical application despite the therapeutic effects being enhanced by TME reprogramming. First, immunotherapeutic agent toxicity is the most important criterion for clinical application. Although some therapeutic strategies have maximized effects, they are not useful if they are toxic. Even in nanotechnology combined immunotherapy, adverse reactions and toxicity effects were observed in clinical trials [79]. Second, priming tumour-specific immune cells is crucial to both enhance the therapeutic effect and reduce systemic side effects. The specific killing ability of effector T cells increases the efficacy of the administered therapeutic agent and prevents healthy tissue death. To increase tumour specificity of T cells, many other strategies were tried. Among the strategies, use of neo-antigens (antigen peptides that have tumour-specific sequences) have emerged as a promising strategy. Many studies have shown that a neo-antigen-compromised immunotherapy platform produces highly enhanced therapeutic effect [80–82]. Besides these strategies, the most important factor is drug kinetics. Dose, biodistribution, release time from nanocarriers, and targeting ability are the key factors that determine therapeutic efficacy. In conclusion, a well-designed nano-platform combined with an immune activator (cancer vaccine, ICBT, neo-antigen), and a TME reprogramming agent will yield promising antitumoural effects and reduce systemic toxicity.

Table 1 The therapeutic strategies for the immune suppressive factors

Target	Material	Therapeutic agent	Strategy	Ref
T reg cells	NIR-photoactivated radical-generating photodynamic dye & Anti-Fab fragment of an anti-CD25	Near-infrared photoimmunotherapy (NIR-PIT)	Targeting Treg with Anti-Fab and local depletion of Treg by near-infrared photoimmunotherapy (NIR-PIT)	[20]
	Glucocorticoid-induced TNFR-related receptor (GITR)	–	Driving selective internalization of PEG-SWCNTs into the Treg	[21]
	Nrp1 receptor	Imatinib	Targeting Nrp1 receptor on reg surface membrane to enhance imatinib, tyrosine kinase inhibitor of STAT3 and STAT5	[15]
MDSC	Sigma 1 receptor in	Sunitinib	Targeting Sigma 1 receptor on melanoma cells by anisamide ligand for targeted sunitinib	[26]
	Sigma 1 receptor in	Triterpenoid methyl-2-cyano-3,12-dioxoolenane-1,9(11)-dien-28-oate (CDDO-Me)	Anisamide analog-mediated delivery of CDDO-Me PLGA NPs to inhibit proliferation and promote apoptosis of cell, MDSC and T reg cells.	[27]
	–	Gemcitabine	Depleting MDSC directly MDSCdepleting agent (Gemcitabine)	[29]
	Monocytic MDSC	6-thioguanine PEG-PPS copolymer nanoscale polymeric micelle	Using ultra-small polymer nanoparticle to enhance antigen-presenting cell target efficiency.	[31]
	TLR4 in MDSC	Cationic dextran liposome & PEI cationic liposome	Polarizing MDSCs to M1 phenotype	[33]

	PI3K γ pathway in MDSC	BSA-MnO ₂ nanoparticle	IPI549 (PI3K γ inhibitor)	Inhibiting PI3K γ on MDSC to enhance the infiltration of CD4+ helper T cells and CD8+ T cells	[34]
TAM	Macrophage mannose receptor (MMR)	Peptideconjugated PEG-PLGA bio-responsive core/shell complex	Macrophage-killing alendronate (ALN) & macrophage-affinitive, natural gluco- mannan polymer (BSP)	Targeting MMR of TAM to induce MMP responsive cleavage of core/shell complex for releasing of macrophage-killing agents.	[36]
	TAM	RNAi-M2pep-AuNPs	Anti-VEGF siRNA	Specifically targeting TAM by M2 peptide and silencing VEGF expression siRNA	[37]
IDO	IDO in Treg	Alginate particles in ESHU hydrogel (iMods)	1-methyl-DL-tryptophan, Poly(L: C) & anti-PD-L1	Simultaneous administration of multiple immune modulators; 1-MT (Treg suppression), poly(L: C) (T eff induction) and anti-PD-L1 (Teff maintenance)	[42]
	IDO in tumor	mPEG-PCL micelles loaded with NLG919/IR780	NLG919 & PTT with IR780 & Anti-PD-L1	Suppression of IDO activity which is upregulated by hotothermal therapy (PTT)	[43]
	IDO in T reg	Mesoporous silica nanoparticles with indoximod conjugated phospholipid bilayer (IND-MSNP)	Indoximod & oxaliplatin (OX)	Direct or intravenous injection of OX/IND-MSNP to induce synergistic immunotherapy of immunogenic cell death and IDO inhibition	[44]

(continued)

Table 1 (continued)

Target	Material	Therapeutic agent	Strategy	Ref
–	Binary cooperative prodrug nanoparticle (BCPN) with two NLG91 conjugat bond	NLG919 & oxaliplatin (OXA)	Deliver-acidity responsive NLG919 prodrug with OXA to induce enhanced immune response	[45]
–	Microneedle consist of m-HA (Hyaluronic acid) based nanoparticle loaded with 1-MT and anti-PD1	1-methyl-DL-tryptophan (1-MT) & anti-PD1	Direct delivery of 1-MT and anti-PD1 to tumor by hyaluronidase mediated disruption of nanoparticles	[46]
–	1-MT conjugated thermo-gelling ROS-responsive polypeptide gel	1-MT & anti-PD-L1	Local injection of thermo-gelling gel to inhibit T reg function and reduce the local ROS level	[47]
COX-2	PEGylated L- α -Phosphatidylcholine (ePC) nanoliposome	Celecoxib & plumbagin	Inhibition of COX-2 and STAT3 pathway simultaneously	[50]
–	Alginate hydrogel	Celecoxib & anti-PD-1	Sustain release of celecoxib to tumor regions	[51]
TGF- β	HES-PLA nanoparticle	Doxorubicin & LY2157299 (TGF- β inhibitor)	Co-delivery of Doxorubicin and TGF- β inhibitor to eliminate the insufficient chemotherapy promoted metastasis	[55]
TGF- β receptor 1	PEGylated nanolipogel (nLG) containing β -cyclodextrin complex	iL-2 & SB505124 (TGF- β inhibitor)	Systemic and intratumoral injection of nLG to enhance intratumoral activated CD8+ T-cell infiltration	[56]

	–	Lipid-calcium-phosphate (LCP) nanoparticle & liposome-protamine-hyaluronic acid (LPH) nanoparticle	CpG oligonucleotide & anti-TGF- β siRNA	Delivery of two different system to enhance CTL response and remove suppressive microenvironment simultaneously	[57]
IL-10	–	Lipid-protamine-DNA nanoparticle	IL-10 & C-X-C motif chemokine ligand 12 (CXCL12) trap	Co-delivery of two trap genes with one particle to inhibit the immune suppressive factors (iL-10 and CXCL12)	[60]
VEGF	Sigma receptor 1 in tumor	Cationic liposome-polycation-DNA (LPD) and anionic liposome-polycation-DNA (LPD- II) with anisamide modification	Doxorubicin & anti-VEGF siRNA	Targeting tumor with anisamide ligand and co-delivering of anticancer drug (doxorubicin) and anti-VEGF siRNA	[66]
		PEGylated cationic cysteine-ended 9-mer arginine oligopeptide (CR9C)	Anti-VEGF siRNA	Systemic delivery of polymeric gene carrier	[67]

References

1. Asghar, U., Witkiewicz, A.K., Turner, N.C., Knudsen, E.S.: The history and future of targeting cyclin-dependent kinases in cancer therapy. *Nat. Rev. Drug Discov.* **14**, 130–146 (2015). <https://doi.org/10.1038/nrd4504>
2. Morrison, W.B.: Cancer chemotherapy: an annotated history. *J. Vet. Intern. Med.* **24**, 1249–1262 (2010). <https://doi.org/10.1111/j.1939-1676.2010.0590.x>
3. Delaney, G., Jacob, S., Featherstone, C., Barton, M.: The role of radiotherapy in cancer treatment. *Cancer.* **104**, 1129–1137 (2005). <https://doi.org/10.1002/cncr.21324>
4. Binnewies, M., Roberts, E.W., Kersten, K., et al.: Understanding the tumor immune microenvironment (TIME) for effective therapy. *Nat. Med.* **24**, 541–550 (2018). <https://doi.org/10.1038/s41591-018-0014-x>
5. Arruebo, M., Vilaboa, N., Sáez-Gutierrez, B., et al.: Assessment of the evolution of cancer treatment therapies. *Cancers (Basel).* **3**, 3279–3330 (2011). <https://doi.org/10.3390/cancers3033279>
6. Pardoll, D.: Cancer and the immune system: basic concepts and targets for intervention. *Semin. Oncol.* **42**, 523–538 (2015). <https://doi.org/10.1053/j.seminoncol.2015.05.003>
7. Klener, P., Otahal, P., Lateckova, L., Klener, P.: Immunotherapy approaches in cancer treatment. *Curr. Pharm. Biotechnol.* **16**, 771–781 (2015). <https://doi.org/10.2174/1389201016666150619114554>
8. Kantoff, P.W., Higano, C.S., Shore, N.D., et al.: Sipuleucel-T immunotherapy for castration-resistant prostate cancer. *N. Engl. J. Med.* **363**, 411–422 (2010). <https://doi.org/10.1056/NEJMoa1001294>
9. Melero, I., Gaudernack, G., Gerritsen, W., et al.: Therapeutic vaccines for cancer: an overview of clinical trials. *Nat. Rev. Clin. Oncol.* **11**, 509–524 (2014). <https://doi.org/10.1038/nrclinonc.2014.111>
10. Kapadia, C.H., Perry, J.L., Tian, S., et al.: Nanoparticulate immunotherapy for cancer. *J. Control. Release.* **219**, 167–180 (2015). <https://doi.org/10.1016/j.jconrel.2015.09.062>
11. Pandiyan, P., Zheng, L., Ishihara, S., et al.: CD4+CD25+Foxp3+ regulatory T cells induce cytokine deprivation-mediated apoptosis of effector CD4+ T cells. *Nat. Immunol.* **8**, 1353–1362 (2007). <https://doi.org/10.1038/ni1536>
12. Deaglio, S., Dwyer, K.M., Gao, W., et al.: Adenosine generation catalyzed by CD39 and CD73 expressed on regulatory T cells mediates immune suppression. *J. Exp. Med.* **204**, 1257–1265 (2007). <https://doi.org/10.1084/jem.20062512>
13. Yu X, Harden K, C Gonzalez L, et al (2009) The surface protein TIGIT suppresses T cell activation by promoting the generation of mature immunoregulatory dendritic cells. *Nat. Immunol.* 10:48–57. doi:<https://doi.org/10.1038/ni.1674>
14. O’Hayre, M., Salanga, C.L., Handel, T.M., Allen, S.J.: Chemokines and cancer: migration, intracellular signalling and intercellular communication in the microenvironment. *Biochem. J.* **409**, 635–649 (2008). <https://doi.org/10.1042/BJ20071493>
15. Ou, W., Thapa, R.K., Jiang, L., et al.: Regulatory T cell-targeted hybrid nanoparticles combined with immuno-checkpoint blockage for cancer immunotherapy. *J. Control. Release.* **281**, 84–96 (2018). <https://doi.org/10.1016/j.jconrel.2018.05.018>
16. Tormoen, G.W., Crittenden, M.R., Gough, M.J.: Role of the immunosuppressive microenvironment in immunotherapy. *Adv. Radiat. Oncol.* **3**, 520–526 (2018). <https://doi.org/10.1016/j.adro.2018.08.018>
17. Beyer, M., Schultze, J.L.: Review article regulatory T cells in cancer. *Blood.* **108**, 804–811 (2006). <https://doi.org/10.1182/blood-2006-02-002774>. Supported
18. Jonuleit, H., Bopp, T., Becker, C.: Treg cells as potential cellular targets for functionalized nanoparticles in cancer therapy. *Nanomedicine.* **11**, 2699–2709 (2016). <https://doi.org/10.2217/nmm-2016-0197>

19. Valzasina, B., Piconese, S., Guiducci, C., Colombo, M.P.: Tumor-induced expansion of regulatory T cells by conversion of CD4+CD25- lymphocytes is thymus and proliferation independent. *Cancer Res.* **66**, 4488–4495 (2006). <https://doi.org/10.1158/0008-5472.CAN-05-4217>
20. Hasegawa, Y., Nakamura, Y., Choyke, P.L., et al.: Spatially selective depletion of tumor-associated regulatory T cells with near-infrared photoimmunotherapy. *Sci. Transl. Med.* **8**, 352ra110–352ra110 (2016). <https://doi.org/10.1126/scitranslmed.aaf6843>
21. Sacchetti, C., Rapini, N., Magrini, A., et al.: In vivo targeting of intratumor regulatory t cells using peg-modified single-walled carbon nanotubes. *Bioconjug. Chem.* **24**, 852–858 (2013). <https://doi.org/10.1021/bc400070q>
22. Kumar, V., Patel, S., Tcyganov, E., Gabrilovich, D.I.: The nature of myeloid-derived suppressor cells in the tumor microenvironment. *Trends Immunol.* **37**, 208–220 (2016). <https://doi.org/10.1016/j.it.2016.01.004>
23. Marvel, D., Gabrilovich, D.I.: Myeloid-derived suppressor cells in the tumor microenvironment: expect the unexpected. *J. Clin. Invest.* **125**, 3356–3364 (2015). <https://doi.org/10.1172/JCI80005>
24. Wu, C., Muroski, M.E., Miska, J., et al.: Repolarization of myeloid derived suppressor cells via magnetic nanoparticles to promote radiotherapy for glioma treatment. *Nanomed. Nanotechnol. Biol. Med.* **16**, 126–137 (2019). <https://doi.org/10.1016/j.nano.2018.11.015>
25. Xu, Z., Ramishetti, S., Tseng, Y.C., et al.: Multifunctional nanoparticles co-delivering Trp2 peptide and CpG adjuvant induce potent cytotoxic T-lymphocyte response against melanoma and its lung metastasis. *J. Control. Release.* **172**, 259–265 (2013). <https://doi.org/10.1016/j.jconrel.2013.08.021>
26. Huo, M., Zhao, Y., Satterlee, A.B., et al.: Tumor-targeted delivery of sunitinib base enhances vaccine therapy for advanced melanoma by remodeling the tumor microenvironment. *J. Control. Release.* **245**, 81–94 (2017). <https://doi.org/10.1016/j.jconrel.2016.11.013>
27. Zhao, Y., Huo, M., Xu, Z., et al.: Nanoparticle delivery of CDDO-Me remodels the tumor microenvironment and enhances vaccine therapy for melanoma. *Biomaterials.* **68**, 54–66 (2015). <https://doi.org/10.1016/j.biomaterials.2015.07.053>
28. Predina, J., Eruslanov, E., Judy, B., et al.: Changes in the local tumor microenvironment in recurrent cancers may explain the failure of vaccines after surgery. *Proc. Natl. Acad. Sci.* **110**, E415–E424 (2013). <https://doi.org/10.1073/pnas.1211850110>
29. Phuengkham, H., Song, C., Um, S.H., Lim, Y.T.: Implantable synthetic immune niche for spatiotemporal modulation of tumor-derived immunosuppression and systemic antitumor immunity: postoperative immunotherapy. *Adv. Mater.* **30**, 1–9 (2018). <https://doi.org/10.1002/adma.201706719>
30. Song, C., Phuengkham, H., Kim, Y.S., et al.: Syringeable immunotherapeutic nanogel reshapes tumor microenvironment and prevents tumor metastasis and recurrence. *Nat. Commun.* **10**, 3745 (2019). <https://doi.org/10.1038/s41467-019-11730-8>
31. Jeanbart, L., Kourtis, I.C., van der Vlies, A.J., et al.: 6-Thioguanine-loaded polymeric micelles deplete myeloid-derived suppressor cells and enhance the efficacy of T cell immunotherapy in tumor-bearing mice. *Cancer Immunol. Immunother.* (2015). <https://doi.org/10.1007/s00262-015-1702-8>
32. Chen, H., Li, P., Yin, Y., et al.: The promotion of type 1 T helper cell responses to cationic polymers in vivo via toll-like receptor-4 mediated IL-12 secretion. *Biomaterials.* **31**, 8172–8180 (2010). <https://doi.org/10.1016/j.biomaterials.2010.07.056>
33. He, W., Liang, P., Guo, G., et al.: Re-polarizing myeloid-derived suppressor cells (MDSCs) with cationic polymers for cancer immunotherapy. *Sci. Rep.* **6**, 1–13 (2016). <https://doi.org/10.1038/srep24506>
34. Yu, M., Duan, X., Cai, Y., et al.: Multifunctional nanoregulator reshapes immune microenvironment and enhances immune memory for tumor immunotherapy. *Adv. Sci.* **1900037** (2019). <https://doi.org/10.1002/adv.201900037>
35. Liu, Y., Cao, X.: Immunosuppressive cells in tumor immune escape and metastasis. *J. Mol. Med.* **94**, 509–522 (2016). <https://doi.org/10.1007/s00109-015-1376-x>

36. Wang, Y., Guo, G., Feng, Y., et al.: A tumour microenvironment-responsive polymeric complex for targeted depletion of tumour-associated macrophages (TAMs). *J. Mater. Chem. B*, **5**, 7307–7318 (2017). <https://doi.org/10.1039/c7tb01495c>
37. Conde, J., Bao, C., Tan, Y., et al.: Dual targeted immunotherapy via in vivo delivery of biohybrid RNAi-peptide nanoparticles to tumor-associated macrophages and cancer cells. *Adv. Funct. Mater.* **25**, 4183–4194 (2015). <https://doi.org/10.1002/adfm.201501283>
38. Kulkarni, A., Chandrasekar, V., Natarajan, S.K., et al.: A designer self-assembled supramolecule amplifies macrophage immune responses against aggressive cancer. *Nat. Biomed. Eng.* **2**, 589–599 (2018). <https://doi.org/10.1038/s41551-018-0254-6>
39. Rodell, C.B., Arlauckas, S.P., Cuccarese, M.F., et al.: TLR7/8-agonist-loaded nanoparticles promote the polarization of tumour-associated macrophages to enhance cancer immunotherapy. *Nat. Biomed. Eng.* **2**, 578–588 (2018). <https://doi.org/10.1038/s41551-018-0236-8>
40. Munn, D.H., Mellor, A.L.: IDO in the tumor microenvironment: inflammation, counter-regulation, and tolerance. *Trends Immunol.* **37**, 193–207 (2016). <https://doi.org/10.1016/j.it.2016.01.002>
41. Liu, M., Wang, X., Wang, L., et al.: Targeting the IDO1 pathway in cancer: from bench to bedside. *J. Hematol. Oncol.* **11**, 1–12 (2018). <https://doi.org/10.1186/s13045-018-0644-y>
42. Acharya, A.P., Sinha, M., Ratay, M.L., et al.: Localized multi-component delivery platform generates local and systemic anti-tumor immunity. *Adv. Funct. Mater.*, **27** (2017). <https://doi.org/10.1002/adfm.201604366>
43. Peng, J., Xiao, Y., Li, W., et al.: Photosensitizer micelles together with IDO inhibitor enhance cancer photothermal therapy and immunotherapy. *Adv. Sci.* **5** (2018). <https://doi.org/10.1002/advs.201700891>
44. Lu, J., Liu, X., Liao, Y.P., et al.: Nano-enabled pancreas cancer immunotherapy using immunogenic cell death and reversing immunosuppression. *Nat. Commun.*, **8** (2017). <https://doi.org/10.1038/s41467-017-01651-9>
45. Feng, B., Zhou, F., Hou, B., et al.: Binary cooperative prodrug nanoparticles improve immunotherapy by synergistically modulating immune tumor microenvironment. *Adv. Mater.* **30**, 1–10 (2018). <https://doi.org/10.1002/adma.201803001>
46. Ye, Y., Wang, J., Hu, Q., et al.: Synergistic transcutaneous immunotherapy enhances antitumor immune responses through delivery of checkpoint inhibitors. *ACS Nano*, **10**, 8956–8963 (2016). <https://doi.org/10.1021/acsnano.6b04989>
47. Yu, S., Wang, C., Yu, J., et al.: Injectable bioresponsive gel depot for enhanced immune checkpoint blockade. *Adv. Mater.* **30**, 1–8 (2018). <https://doi.org/10.1002/adma.201801527>
48. Liu, B., Qu, L., Yan, S.: Cyclooxygenase-2 promotes tumor growth and suppresses tumor immunity. *Cancer Cell Int.* **15**, 2–7 (2015). <https://doi.org/10.1186/s12935-015-0260-7>
49. Park, W., Oh, Y.T., Han, J.H., Pyo, H.: Antitumor enhancement of celecoxib, a selective Cyclooxygenase-2 inhibitor, in a Lewis lung carcinoma expressing Cyclooxygenase-2. *J. Exp. Clin. Cancer Res.* **27**, 1–9 (2008). <https://doi.org/10.1186/1756-9966-27-66>
50. Gowda, R., Kardos, G., Sharma, A., et al.: Nanoparticle-based celecoxib and plumbagin for the synergistic treatment of melanoma. *Mol. Cancer Ther.* **16**, 440–452 (2017). <https://doi.org/10.1158/1535-7163.mct-16-0285>
51. Li, Y., Fang, M., Zhang, J., et al.: Hydrogel dual delivered celecoxib and anti-PD-1 synergistically improve antitumor immunity. *Onco. Targets. Ther.* **5**, 1–12 (2016). <https://doi.org/10.1080/2162402X.2015.1074374>
52. Gorelik, L., Flavell, R.A.: Transforming growth factor-beta in T-cell biology. *Nat. Rev. Immunol.* **2**, 46–53 (2002). <https://doi.org/10.1038/nri704>
53. Akhurst, R.J., Hata, A.: Targeting the TGF β signalling pathway in disease. *Nat. Rev. Drug Discov.* **11**, 790 (2012)
54. Chen, W., Ten Dijke, P.: Immunoregulation by members of the TGF β superfamily. *Nat. Rev. Immunol.* **16**, 723 (2016)
55. Qi, S.S., Sun, J.H., Yu, H.H., Yu, S.Q.: Co-delivery nanoparticles of anti-cancer drugs for improving chemotherapy efficacy. *Drug Deliv.* **24**, 1909 (2017)

56. Park, J., Wrzesinski, S.H., Stern, E., et al.: Combination delivery of TGF- β inhibitor and IL-2 by nanoscale liposomal polymeric gels enhances tumour immunotherapy. *Nat. Mater.* **11**, 895–905 (2012). <https://doi.org/10.1038/nmat3355>
57. Xu, Z., Wang, Y., Zhang, L., Huang, L.: Nanoparticle-delivered transforming growth factor- β siRNA enhances vaccination against advanced melanoma by modifying tumor microenvironment. *ACS Nano.* **8**, 3636 (2014). <https://doi.org/10.1021/nm500216y>
58. Lu, H., Wagner, W.M., Gad, E., et al.: Treatment failure of a TLR-7 agonist occurs due to self-regulation of acute inflammation and can be overcome by IL-10 blockade. *J. Immunol.* **184**, 5360–5367 (2010). <https://doi.org/10.4049/jimmunol.0902997>
59. O'Garra, A., Vieira, P.: TH1 cells control themselves by producing interleukin-10. *Nat. Rev. Immunol.* **7**, 425 (2007)
60. Shen, L., Li, J., Liu, Q., et al.: Local blockade of interleukin 10 and C-X-C motif chemokine ligand 12 with nano-delivery promotes antitumor response in murine cancers. *ACS Nano.* **12**, 9830 (2018). <https://doi.org/10.1021/acs.nano.8b00967>
61. Carmeliet, P.: VEGF as a key mediator of angiogenesis in cancer. *Oncology.* **69**(Suppl 3), 4–10 (2005). <https://doi.org/10.1159/000088478>
62. Ellis, L.M., Hicklin, D.J.: VEGF-targeted therapy: mechanisms of anti-tumor activity. *Nat. Rev. Cancer.* **8**, 579 (2008)
63. Terme, M., Pernot, S., Marcheteau, E., et al.: VEGFA-VEGFR pathway blockade inhibits tumor-induced regulatory T-cell proliferation in colorectal cancer. *Cancer Res.* **73**, 539–549 (2013). <https://doi.org/10.1158/0008-5472.CAN-12-2325>
64. Fukumura, D., Kloepper, J., Amoozgar, Z., et al.: Enhancing cancer immunotherapy using antiangiogenics: opportunities and challenges. *Nat. Rev. Clin. Oncol.* **15**, 325–340 (2018). <https://doi.org/10.1038/nrclinonc.2018.29>
65. Yang, Y., Zhang, Y., Iwamoto, H., et al.: Discontinuation of anti-VEGF cancer therapy promotes metastasis through a liver revascularization mechanism. *Nat. Commun.* **7**, 12680 (2016). <https://doi.org/10.1038/ncomms12680>
66. Chen, Y., Bathula, S.R., Li, J., Huang, L.: Multifunctional nanoparticles delivering small interfering RNA and doxorubicin overcome drug resistance in cancer. *J. Biol. Chem.* **285**, 22639 (2010). <https://doi.org/10.1074/jbc.M110.125906>
67. Chung, J.Y., Ul Ain, Q., Lee, H.L., et al.: Enhanced systemic anti-angiogenic siVEGF delivery using PEGylated oligo- d -arginine. *Mol. Pharm.* (2017). <https://doi.org/10.1021/acs.molpharmaceut.7b00282>
68. Phuengkham, H., Ren, L., Shin, I.W., Lim, Y.T.: Nanoengineered immune niches for reprogramming the immunosuppressive tumor microenvironment and enhancing cancer immunotherapy. *Adv. Mater.*, 1803322 (2019). <https://doi.org/10.1002/adma.201803322>
69. Cousin, S., Italiano, A.: Molecular pathways: immune checkpoint antibodies and their toxicities. *Clin. Cancer Res.* **22**, 4550–4555 (2016). <https://doi.org/10.1158/1078-0432.CCR-15-2569>
70. Francisco, L.M., Salinas, V.H., Brown, K.E., et al.: PD-L1 regulates the development, maintenance, and function of induced regulatory T cells. *J. Exp. Med.* **206**, 3015–3029 (2009). <https://doi.org/10.1084/jem.20090847>
71. Wang, C., Sun, W., Ye, Y., et al.: In situ activation of platelets with checkpoint inhibitors for post-surgical cancer immunotherapy. *Nat. Biomed. Eng.* **1**, 0011 (2017). <https://doi.org/10.1038/s41551-016-0011>
72. Du, Y., Liang, X., Li, Y., et al.: Liposomal nanohybrid cerasomes targeted to PD-L1 enable dual-modality imaging and improve antitumor treatments. *Cancer Lett.* **414**, 230–238 (2018). <https://doi.org/10.1016/j.canlet.2017.11.019>
73. Kosmides, A.K., Sidhom, J.-W., Fraser, A., et al.: Dual targeting nanoparticle stimulates the immune system to inhibit tumor growth. *ACS Nano.* **11**, 5417–5429 (2017). <https://doi.org/10.1021/acs.nano.6b08152>
74. Zhang, X., Wang, C., Wang, J., et al.: PD-1 blockade cellular vesicles for cancer immunotherapy. *Adv. Mater.* **30**, 1707112 (2018). <https://doi.org/10.1002/adma.201707112>

75. Wang, C., Sun, W., Wright, G., et al.: Inflammation-triggered cancer immunotherapy by programmed delivery of CpG and anti-PD1 antibody. *Adv. Mater.* **28**, 8912–8920 (2016). <https://doi.org/10.1002/adma.201506312>
76. Fransen, M.F., van der Sluis, T.C., Ossendorp, F., et al.: Controlled local delivery of CTLA-4 blocking antibody induces CD8+ T-cell-dependent tumor eradication and decreases risk of toxic side effects. *Clin. Cancer Res.* **19**, 5381–5389 (2013). <https://doi.org/10.1158/1078-0432.CCR-12-0781>
77. Lei, C., Liu, P., Chen, B., et al.: Local release of highly loaded antibodies from functionalized nanoporous support for cancer immunotherapy. *J. Am. Chem. Soc.* **132**, 6906–6907 (2010). <https://doi.org/10.1021/ja102414t>
78. Li, S.-Y., Liu, Y., Xu, C.-F., et al.: Restoring anti-tumor functions of T cells via nanoparticle-mediated immune checkpoint modulation. *J. Control. Release.* **231**, 17–28 (2016). <https://doi.org/10.1016/j.jconrel.2016.01.044>
79. Zuckerman, J.E., Gritli, I., Tolcher, A., et al.: Correlating animal and human phase Ia/Ib clinical data with CALAA-01, a targeted, polymer-based nanoparticle containing siRNA. *Proc. Natl. Acad. Sci. U. S. A.* **111**, 11449–11454 (2014). <https://doi.org/10.1073/pnas.1411393111>
80. Guo, Y., Lei, K., Tang, L.: Neoantigen vaccine delivery for personalized anticancer immunotherapy. *Front. Immunol.* **9**, 1499 (2018). <https://doi.org/10.3389/fimmu.2018.01499>
81. Keskin, D.B., Anandappa, A.J., Sun, J., et al.: Neoantigen vaccine generates intratumoral T cell responses in phase Ib glioblastoma trial. *Nature.* **565**, 234–239 (2019)
82. Ott, P.A., Hu, Z., Keskin, D.B., et al.: An immunogenic personal neoantigen vaccine for patients with melanoma. *Nature.* **547**, 217–221 (2017). <https://doi.org/10.1038/nature22991>

Plasmonic Gold Nanostars for Immuno Photothermal Nanotherapy to Treat Cancers and Induce Long-Term Immunity



Tuan Vo-Dinh , Brant A. Inman, Paolo Maccarini, Gregory M. Palmer, Yang Liu, and Wiguins Etienne

1 Introduction

According to the World Health Organization, cancer is the second leading cause of death globally with about 1 in 6 deaths is due to cancer [1]. Most metastatic cancers, which have spread beyond their organ of origin, still remain incurable. Nanomedicine has produced many advances in cancer treatment over the past few decades. Nanoparticles have received increasing interest in medical applications due to their unique efficacy and specificity in diagnostics, bioimaging and therapy [2]. Of particular interest is the use of nanoparticle-mediated thermal therapy for precise tumor cell ablation [3] radio-sensitization of hypoxic regions [4], enhancement of drug delivery [5], activation of thermosensitive agents [6], and enhancement of the immune system [7]. A special type of metallic nanoparticles, made of gold

T. Vo-Dinh (✉) · Y. Liu

Fitzpatrick Institute for Photonics, Duke University, Durham, NC, USA

Department of Biomedical Engineering, Duke University, Durham, NC, USA

Department of Chemistry, Duke University, Durham, NC, USA

e-mail: tuan.vodinh@duke.edu

B. A. Inman

Division of Urology, Duke Cancer Institute, Durham, NC, USA

Duke University Medical Center, Durham, NC, USA

P. Maccarini

Department of Electrical and Computer Engineering, Duke University, Durham, NC, USA

G. M. Palmer

Department of Radiation Oncology, Duke University Medical Center, Durham, NC, USA

W. Etienne

Department of Surgery, Duke University Medical Center, Durham, NC, USA

and silver and referred to as “plasmonic” nanoparticles, has used for biomedical applications because they exhibit enhanced optical and electromagnetic properties. For over three decades, our laboratory has actively involved in the development of plasmonic nanosystems for a wide variety of applications ranging from medical diagnostics [8–12] to cancer treatment using nanoparticle-mediated photothermal treatment [10, 13–15]. In particular, gold nanostars (GNS) also provide an excellent platform for chemical sensing and diagnostics using surface-enhanced Raman scattering (SERS), a spectrochemical technique of great interest in our laboratory for over three decades [11, 16–20]. Due to their selective absorption into tumors via enhanced permeability and retention feature and the photothermal efficiency to convert photon energy into heat, GNS are also the ideal photothermal transducers for selective cancer therapy. Furthermore, the combined use of GNS-mediated photothermal treatment with immunotherapy can broaden and enhance the efficacy of immunotherapy. This chapter provides an overview of the development and application of plasmonic GNS in combination with immunotherapy—a treatment referred to as Synergistic Immuno Photothermal Nanotherapy (SYMPHONY)—which can dramatically enhance the efficacy of immunotherapy. SYMPHONY was found to be capable to eradicate primary “treated” tumors and also produce the immune-mediated destruction of distant “untreated” metastatic tumors and ultimately create an anticancer ‘vaccine’ effect [21–23].

2 Gold Nanostars: A Versatile and Effective Platform for Photothermal Therapy

Plasmonic nanoparticles are a special kind of metallic nanoparticles that exhibit enhanced optical and electromagnetic properties. The term “plasmonic” is derived from the word plasmon, which refers to oscillations of conduction electrons in metallic nanostructures under the excitation light (e.g., laser) that irradiates the surface. These oscillations of electrons on the surface, called a “surface plasmon”, produce intense electromagnetic (EM) fields, leading to enormous increase in Raman scattering by 10^6 – 10^8 orders of magnitude. Raman spectroscopy is a sensing modality that allows for the optical detection of molecular and vibrational spectral information. The plasmonic effect, which produces intense Raman signals, has led to the great interest for the development SERS detection technique in many research laboratories worldwide [24].

Nanoparticle-Mediated Hyperthermia. Hyperthermia (HT) is a treatment where heat is applied to a tumor or organ [25, 26]. Thermal death (ablation) to targeted tumors can be induced by high-temperature HT (>55 °C). On the other hand, mild fever-range HT (40–43 °C) can be used to (1) improve drug delivery to tumors, (2) improve cancer cell sensitivity to anti-cancer therapy, and (3) trigger potent systemic anti-cancer immune responses [27–30]. Conventional HT techniques, such as ultrasound, microwaves, radiofrequency, have been widely used for tumor treatment. These methods are only macroscopically confined to the tumor area

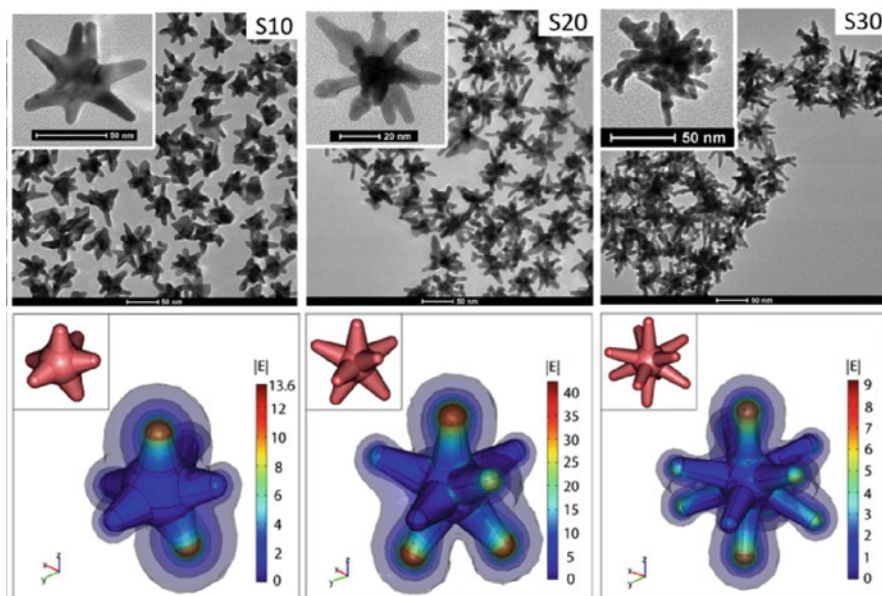


Fig. 1 Plasmonics-active gold nanostars. (Top) Transmission electron microscopy images of gold nanostars (GNS) formed under different Ag^+ concentrations (S10: $10 \mu\text{M}$, S20: $20 \mu\text{M}$, S30: $30 \mu\text{M}$), leading to different branch numbers. Scale bar 50 nm; (Bottom) 3D modeling and simulation of $|E|$ in the vicinity of the nanostars in response to a z-polarized plane wave incident E-field of unit amplitude, propagating in the y-direction, and with a wavelength of 800 nm. The GNSs' structure has multiple sharp branches that produce the numerous curvatures responsible for the 'lightning rod' effect that strongly enhances the local electromagnetic field when subject to light stimulation. The calculations indicate that the electromagnetic (EM) field at the GNS tips is dramatically enhanced, which reflects an intense tip-enhanced plasmonic effect. The insets depict the 3D geometry of the stars. Diagrams are not to scale. (Adapted from Reference 37)

but cannot target or ablate cancer cells at the microprecision scale. The use of nanoparticle (NP)-mediated thermal therapy has the advantage of precise cancer cell ablation [3] with many benefits of mild HT in the tumor microenvironment, including radio-sensitization of hypoxic regions [4], enhancement of drug delivery [5], activation of thermosensitive agents [6] and boosting the immune system.

The plasmonic properties of different types of nanoparticles, configurations, and their photothermal effects have been investigated theoretically [31–35]. Among nanoparticles used for light-induced (photo) thermal therapy (PTT), gold nanostars (GNS) offer several advantages, such as a wide-range of optical tunability by engineering subtle changes in their geometry. The GNS structure has multiple sharp branches that create a “lightning rod” effect, which can enhance local electromagnetic (EM) field dramatically (Fig. 1); under laser excitation, this unique feature of GNS can effectively absorb photons and concentrate heating into cancer cells [13, 36–38]. Photothermal treatment using GNS can rapidly ablate tumor cells and induce mild hyperthermia in their microenvironment to boost the immune

system due to a natural propensity of GNS to extravasate from the tumor vascular network and accumulate in and around cancer cells, offers an important advantage of nanoparticle-mediated therapy [14].

Surfactant-Free Synthesis of Biocompatible Gold Nanostars. With the goal of developing biocompatible nanoparticles for *in vivo* applications, our group introduced a surfactant-free synthesis chemistry that does not require toxic reagents for producing GNS [37]. This surfactant-free synthesis of nanostars can achieve high monodispersity and plasmon tunability. Unlike other NPs that require elaborate chemical synthesis processes, our high-yield GNS synthesis method is simple and rapid to perform in less than 30 seconds at room temperature. The synthesis method for GNS requires no addition of a toxic polymer surfactant, e.g., cetyl-trimethylammonium bromide (CTAB), rendering the GNS biocompatible and having a surface easy to functionalize. The presence of Ag^+ is necessary for nanostar formation. Without Ag^+ , it forms polydisperse rods and spheres. The major role of Ag^+ is believed not to form Ag branches but to assist the anisotropic growth of Au branches on certain crystallographic facets on multi-twinned citrate seeds, but not single crystalline CTAB seeds. The consistency and reproducibility of physical, chemical, optical and therapeutic properties of nanoparticles, which is mainly governed by their morphological features, are important for the effectiveness and reliability of branched gold nanoparticles in biomedical applications. In a systematic bottom-up synthesis approach, we have investigated in detail the optimization of the bottom-up synthesis that improves reproducibility and homogeneity of plasmonic branched-nanoparticles, and the modulation of the morphology, particularly the branch density, dimensions and sharpness of branches to obtain desired optical properties and/or loading capacities of therapeutic agents on nanoparticles [39].

Optical Tunability of GNS. Gold nanostars can be synthesized in a controlled fashion and exploited as potential candidates for near infrared NIR excitation and absorption in the tissue “optical window”, where photons travel further in healthy tissue to be ‘captured’ and converted into heat by GNS within a cancer [37]. HT methods using photons present several important challenges that need to be addressed. Within the optical tissue window, most tissues are sufficiently weak absorbers to permit significant penetration of light. This optical window ranges from 600 to 1300 nm, i.e., from the orange/red region of the visible spectrum into the NIR. At the short-wavelength end, the window is bound by the absorption of hemoglobin, in both its oxygenated and deoxygenated forms. At shorter wavelengths the absorption of many more biomolecules in tissue becomes important, including DNA and the amino acids tryptophan and tyrosine. At the longer wavelengths (infrared end) of the window, light penetration is limited by the absorption properties of water. Within the “therapeutic window”, scattering is dominant over absorption, and so the propagating light becomes diffuse, although not necessarily entering into the diffusion limit. Figure 2 shows a schematic diagram of the optical window of tissue [40].

The optical absorption properties of GNS can be tuned from the visible to the NIR spectral regions (700–1200 nm) by engineering subtle changes in their geometry. Increasing the concentrations of Ag^+ progressively red-shifted the plasmon

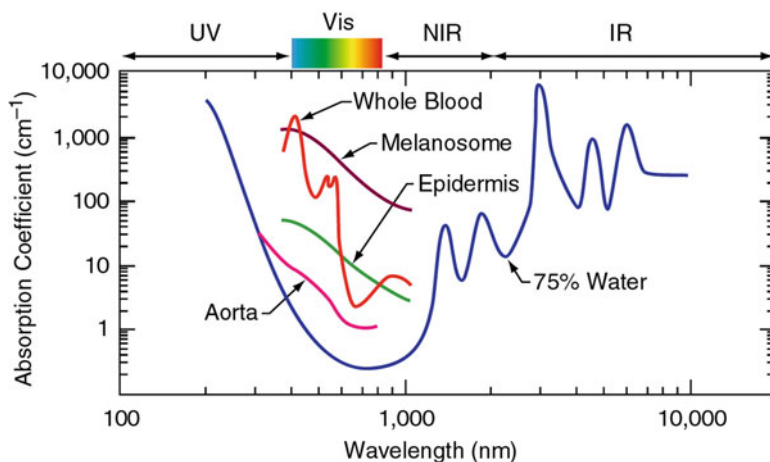


Fig. 2 The “Optical Window” of tissue and absorption spectra of biological components (Adapted From Ref 40)

band by forming longer, sharper, and more numerous branches (Fig. 3a, b) [37]. For instance, the GNS labelled S10 has a few protrusions, while S30 exhibit multiple long, sharp branches that appear to branch even further. The nanostars’ plasmon peaks are tunable from 600 to 1000 nm by a and by adjusting the Ag^+ concentration using a constant seed amount in our experimental studies and theoretical simulation using the finite-element model (FEM) electromagnetic software COMSOL Multiphysics program (Fig. 3c). A visible change in the solution colour from dark blue to dark grey was observed as the plasmon red-shifts and broadens. Both the plasmon peak position and spectral width followed a linear trend with increasing Ag^+ concentration. We have developed GNS that can produce efficient photothermal effects at 1064-nm laser wavelength, which is used in an FDA-approved laser wavelength used in a laser interstitial thermal therapy system (Monteris Medical) to treat patients with intracranial tumors. The GNS were synthesized using the modified approach based on the surfactant-free method developed by our laboratory [37]. Briefly, 12-nm gold sphere nanoparticles synthesized by reducing HAuCl_4 with trisodium citrate were used as seeds, and subsequently were rapidly mixed with AgNO_3 , ascorbic acid and HAuCl_4 . The ratio between seeds and HAuCl_4 or AgNO_3 was tuned to achieve high absorption at 1064 nm. The synthesized GNS were coated with SH-mPEG (M.W. 5000) to improve *in vivo* stability and circulation time. PEG-functionalized GNS nanoparticles were condensed and the gold mass concentration was measured with inductively coupled plasma mass spectrometry (ICP-MS). Figure 3d, e show the transmission emission microscopy (TEM) image and the absorption spectrum of GNS engineered to have absorption near 1000 nm.

The “Lightning Rod” Effect of Gold Nanostars. The optical properties of the nanostar geometry and plasmon bands have been investigated theoretically using numerical simulations [41]. When light is incident on a metallic nanoparticle,

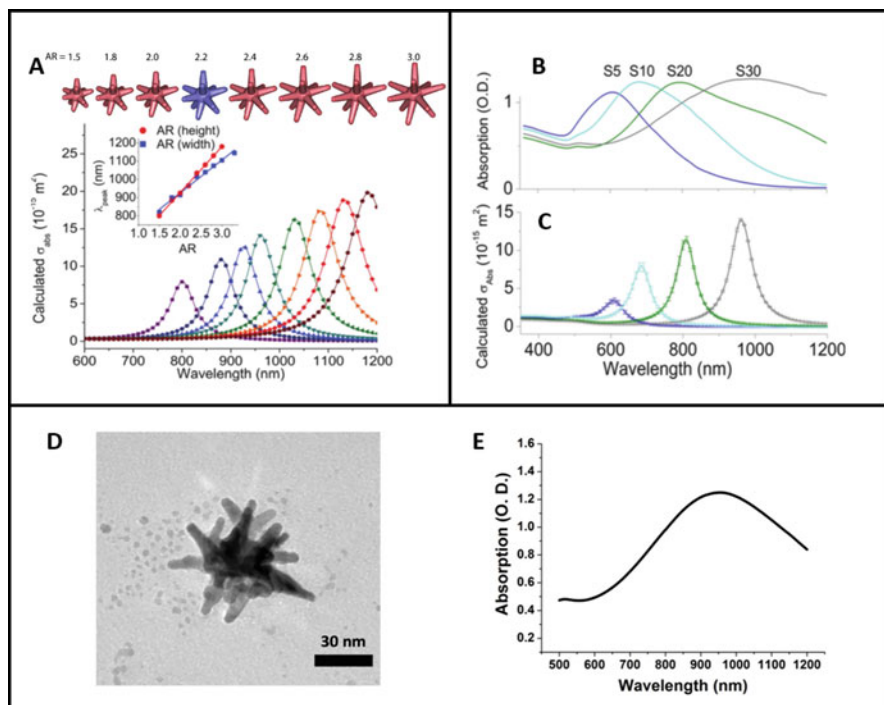


Fig. 3 Tunability of gold nanostars. (a) The scatter plots of polarization-averaged absorption against aspect ratio (AR) tuned by varying branch height while keeping the base width, core and tip diameters and branch number, constant. Their corresponding 3-D geometry is on top, where the blue one is the original model for S30 nanostars in Fig. 1. (inset) The linear relationship between plasmon peak position and AR, in turn, varying branch height (red, $R^2 = 0.997$) and base width (blue, $R^2 = 0.987$), keeping all other parameters constant. (b) Absorbance spectra of the star solutions (~ 0.1 nM) in citrate buffer. (c) The corresponding FEM-generated absorption spectra of nanostars embedded in water. The solved data points (± 1 SD) were interpolated with a spline fit. (Adapted from Ref. 37). (d) Transmission emission microscopy (TEM) image of a gold nanostar engineered to have absorption near 1000 nm. (e) Absorption spectrum of the plasmon band of gold nanostars around 1000 nm

plasmon resonances can significantly enhance the optical electric field (E-field) inside and near the surface of the particle. The wavelength of the peak E-field enhancement is affected by certain particle characteristics, including its size, shape and the wavelength dependence of its dielectric constant. The finite-element model (FEM) electromagnetic software COMSOL Multiphysics was used to calculate the E-field enhancement of a nanostar. Figure 4 depicts a contour plot of the magnitude of the electric field showing that the largest E-field enhancement occurs at the tips of the branches of the star. The combination of the resonance enhancement and the “lighting-rod effect” associated with the large curvature at the tips results in the large field enhancement at the tips of the star. This curvature creates a larger surface charge density and consequently a higher electric field. As a result, the

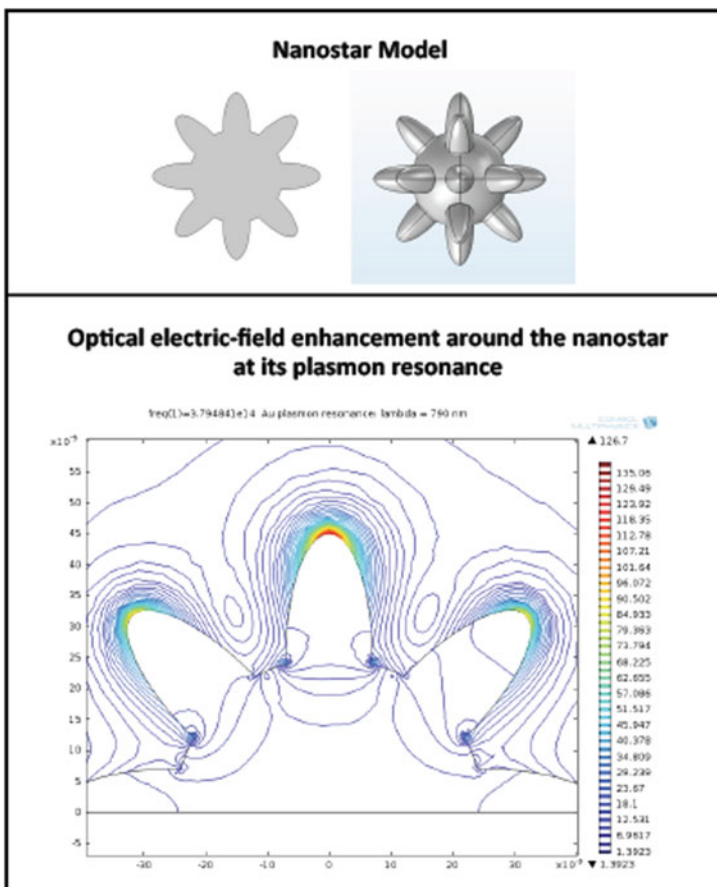


Fig. 4 The lightning rod effect in Gold Nanostar. Top: Cross-section and 3D view of our model of a nanostar; Bottom: Contour plot of electromagnetic field enhancement using COMSOL multiphysics calculations, showing the largest E-field enhancement occurring at the tips of the branches of the star (Adapted from Reference 41)

nanostar can generate E-field “hot spots” that can greatly exceed the enhancement of smoother particles such as nanospheres. Theoretical calculations have shown that GNS have the highest absorption-to-scattering ratio of the commonly used plasmonic gold nanoparticles, which is consistent with high conversion efficiency. The results of our calculations underline the advantages that makes the selection of nanostars an optimal choice for *in vivo* studies where tissue absorption are expected to substantially decrease the laser excitation. This is important as *in vivo* application has to be performed with power densities below the ANSI standard for maximum permissible exposure on the skin.

Enhanced Permeability and Retention. As with other nanoparticles, GNS sizes can be controlled so that they passively accumulate in tumors due to the enhanced

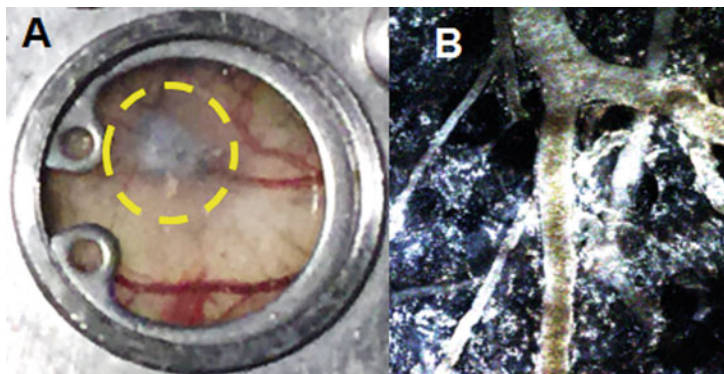


Fig. 5 The EPR effect showing GNS accumulation in tumor using via window chamber (a) and TPL imaging (b)

permeability and retention (EPR) effect of tumor vasculature. The EPR effect is a result of the inherent leakiness of the tumor vasculature, which is underdeveloped and allows nanoparticles to escape the circulation and accumulate passively in tumors. In addition, retention of nanoparticles in the tumor is enhanced by the lack of an efficient lymphatic system which would normally carry extravasated fluid back to the circulation. To take advantage of the EPR effect nanoparticles must be designed to have a narrow size range between approximately 10 and 100 nm. GNS take advantage of the EPR effect because they can be synthesized to have hydrodynamic sizes that fit well in the 10–100 nm size ranges. GNS can even be used to target sites that are traditionally very difficult to access with drugs like the brain. We have demonstrated selective accumulation of GNS in tumor following IV injection of GNS in the tail veins in a mouse study with a window chamber set-up on the tumor area. Figure 5a, shows GNS accumulation into the tumor area (black color) after intravenous tail vein injection, demonstrating the EPR effect. Figure 5b shows a two-photon photoluminescence (TPL) image through the window chamber, revealing that GNS have leaked through the blood vessels and penetrated into tumor interstitial space. The EPR effect was further illustrated in another study where GNS labeled with a Raman reporter, p-mercaptobenzoic acid (pMBA), were injected intravenously via the tail vein of mice with xenograft sarcomas [14]. Gold nanostars exhibit very intense SERS signal due to strong local field enhancement at the tips of the nanostar spikes. The SERS signals from the GNS that accumulated within each tumor and contralateral leg muscle were measured. Figure 6a shows the SERS spectrum for 30-nm GNS and 60-nm GNS in the sarcoma and normal muscle. The characteristic SERS peaks of pMBA on GNS at 1067 and 1588 cm^{-1} were detected in the tumor, but not in the contralateral leg muscle, which shows that SERS has the capability to differentiate tumor from normal muscle [14]. Figure 6b shows a picture of a mouse with primary sarcomas 3 days after 30-nm GNS injection. Significant GNS accumulation can be seen in the tumor, but not in the normal leg muscle of the contralateral leg, underlining the effectiveness of the EPR

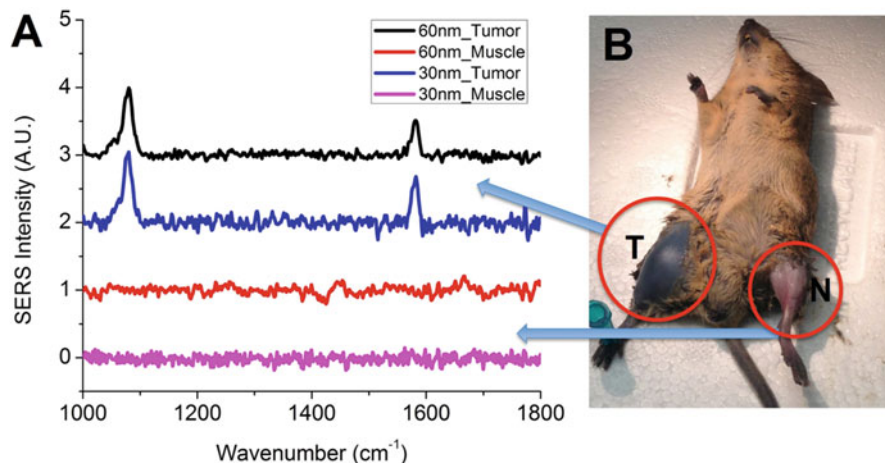
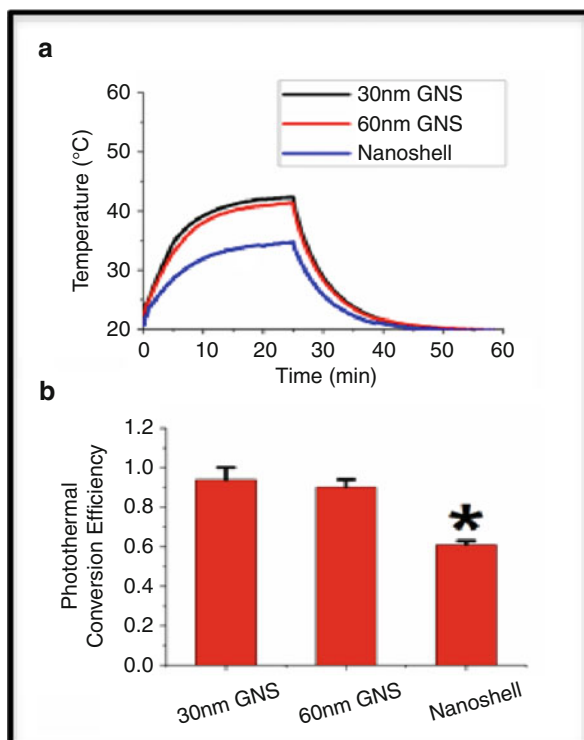


Fig. 6 The enhanced permeation and retention effect. (a) In vivo SERS spectra of 30-nm and 60-nm GNS nanoprobe with pMBA reporter. Unique SERS peaks can be detected at 1067 and 1588 cm^{-1} in the tumor, but not in the normal muscle. Baselines are artificially offset to visualize each spectrum individually. (b) Mouse with primary sarcomas 3 days after 30-nm GNS injection. Significant GNS accumulation can be seen in the tumor (T), but not in the normal leg muscle of the contralateral leg (N). (Adapted from Reference 14)

effect. The results demonstrate the possibility to externally detect tumors using non-invasive SERS monitoring, due to preferential accumulation of GNS into tumors.

Efficient GNS-Mediated Photothermal Effect. GNS convert light to heat with higher efficiency than for other GNP such as nanoshells, as confirmed by the temperature profiles in Fig. 7 [14, 37]. We used PTT (0.57 W/cm^2) and measured temperature changes in 0.2 nM GNS solution and water. The ability to safely target single tumor cells with a high level of efficacy and specificity can be obtained with GNS. Their multiple sharp branches acting like “lightning rods” can convert safely and efficiently light into heat. The rapidly increasing temperature indicates that GNS can be used very successfully for photothermal ablation. We chose nanoshells as a benchmark for our GNS comparison, because nanoshells are under clinical trial for photothermal therapy. The high photon-to-heat conversion efficiency and precise uptake in tumor via the EPR effect make GNS the ideal photothermal transducer for selective cancer therapy at the nanoscale level. Due to the combination of EPR effect and the high photon-to-heat conversion, there is significant reduction of the laser energy needed to precisely destroy the targeted cancer cells in which GNS preferentially. GNS, which accumulate in and around cancer cells, can be triggered with light to rapidly achieve high ablative intratumoral temperatures ($>55 \text{ }^\circ\text{C}$) and can also induce milder fever-range ($41\text{--}43 \text{ }^\circ\text{C}$) hyperthermia in the tumor microenvironment..

Fig. 7 Comparative photothermal studies of gold nanostars and gold nanoshells. **(a)** Higher temperature profiles for GNS **(b)** Higher PTT conversion efficiency for GNS vs less efficient gold nanoshells **(b)** (Adapted from Reference 14)



3 Combination Photo Immuno Therapy: SYMPHONY

Immunotherapy of Cancer. A variety of strategies have been used to treat cancer (e.g., chemotherapy, radiotherapy), but currently immunotherapy has emerged as one of the most promising modalities to treat cancer. In recent years, immunotherapy with specific immune checkpoint inhibitors provides a promising way to break the tumor immunosuppressive environment. It has been observed that the immune system does recognize and often eliminate small tumors but tumors that become clinical problems block antitumor immune responses with immunosuppression orchestrated by the tumor cells. There has been great interest in developing strategies to reverse this tumor-mediated immunosuppression in order improve cancer immunotherapy outcomes. The immune checkpoints are normally safeguards used by the body to prevent inappropriate or overactivation of the immune response. However, many tumors have acquired the ability to manipulate these checkpoints to switch the immune system into a nonresponsive state. Because immune checkpoints consist of ligand–receptor interactions, they can be readily blocked by antibodies or modulated by ligands or receptors. The cytotoxic T-lymphocyte-associated antigen 4 (CTLA4), the first immune checkpoint receptor to be clinically targeted, is

expressed exclusively on T cells where it primarily regulates the amplitude of the early stages of T cell activation.

Another immune-checkpoint receptor, PD-1, is emerging as a promising target. A new T cell co-stimulation (immune checkpoint) molecule called programmed death ligand 1 (PD-L1) was associated with bacillus Calmette-Guérin (BCG) immunotherapy failure and stage progression in bladder cancer [42]. Further studies subsequently confirmed this findings and showed associations with worse survival [43–45]. The PD-L1 immune checkpoint is commonly expressed by many cancers as a method of immune evasion [46, 47]. PD-L1 binds to the PD-1 receptor found on activated T cells and inhibits cytotoxic T-cell function, thus escaping the immune response from T-cell. Using animal models of cancer [46, 48], PD-L1 blockade was demonstrated to offer a potential possibility. A soluble form of PD-L1 was found to exist in cancer patients and retains its immunosuppressive activity [49, 50]. The therapeutic anti-PD-L1 antibody is designed to block the PD-L1/PD-1 interaction and reverse tumor-mediated immunosuppression. Blocking the PD-L1/PD-1 axis has been shown to be highly beneficial in many human tumors and used as a cancer treatment modality [51, 52]. However, current antibodies work only for a limited number of patients and can become ineffective with time.

Synergistic Combination Nano-Immunotherapy. We have introduced a combination treatment modality referred to as Synergistic Immuno Photo Nanotherapy (SYMPHONY), which combines GNS-mediated photothermal therapy with immune checkpoint inhibitor immunotherapy, designed to treat both primary tumors and secondary tumor cells (used as a metastatic model) as well as induce a long-term immunity against cancer [21–23]. Several synergistic processes could contribute to the efficacy of SYMPHONY (Fig. 8). First, localized GNS-mediated PTT using NIR laser irradiation is used to kill primary tumor cells. Following PTT treatment, dying tumor cells could release tumor-associated antigens (TAAs), damage-associated molecular pattern molecules (DAMPs), heat shock proteins (HSPs), etc. In general, DAMPs are intracellular molecules that are normally hidden in live cells. However, when cells are damaged or dying, DAMPS are released and acquire immunostimulatory properties. DAMPS have been shown to exert various effects on antigen-presenting cells (APCs), such as maturation, activation and antigen processing/presentation. APCs, which are present in the tissue or in local draining lymph nodes, process the tumor antigens and present tumor-derived peptides to T cells. Combining anti-PD-L1 treatment with tumor antigen presentation will activate tumor-specific T cells that will attack both in the primary and distant/metastatic cancer cells. This is particularly important in the primary tumor bed, hypoxic-oxygenated boundary, where it is believed metastatic/differentiating/proliferating potential is maximum.

In vivo studies using murine models have revealed that the two-pronged SYMPHONY approach, combining immune-checkpoint inhibition and GNS-mediated photothermal therapy, was capable of destroying primary tumors treated by laser irradiation; furthermore. Destruction of untreated distant tumors in mice implanted with the MB49 bladder cancer cell line was also observed [21]. The SYMPHONY treatment also triggered an anti-tumor immune memory that prevented tumor

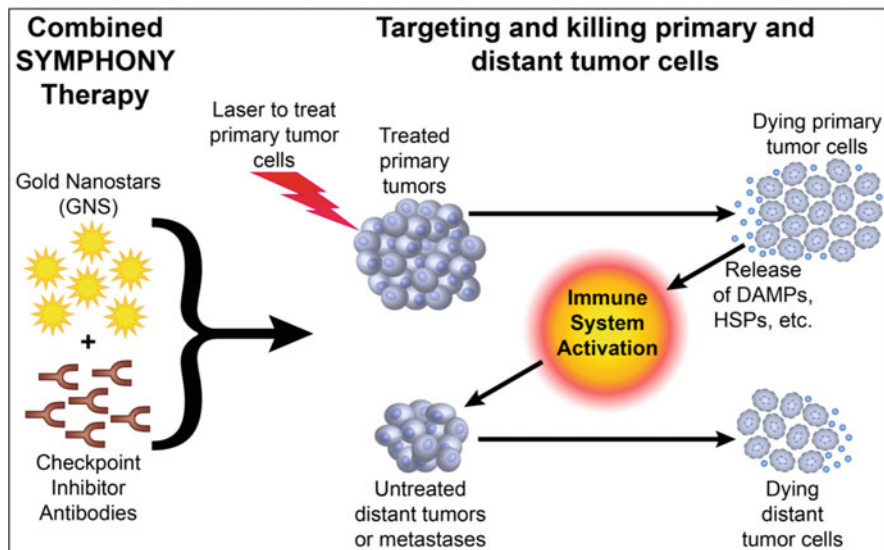


Fig. 8 The synergistic therapeutic concept SYMPHONY. First, localized GNS and NIR irradiation kill primary cancer cells. Dying cells release tumor-specific antigens and damage-associated molecular pattern molecules (DAMPs), as heat shock proteins (HSPs). DAMPs mediate maturation, activation, processing/presentation of antigen-presenting cells (APCs). Synergizing tumor antigen presentation with checkpoint inhibitor antibodies (e.g. anti-PD1 or anti-PD-L1) activates tumor-specific T cells to attack primary and metastatic tumors]

growth in cured mice when they were re-challenged with a second injection cancer cells, showing a ‘vaccine’ effect not observed in PTT or immunotherapy alone. In our study MB49 bladder cancer cells were implanted into C57BL/6 mice (250,000/100,000 cells in right/left flank, respectively) [21]. One day after nanostar injection, the photothermal therapy treatment was performed with an 808-nm laser for 10 minutes at a power density of 0.6 W/cm^2 . One half hour after laser irradiation, anti-PD-L1 antibody (200 μg per mouse) was intraperitoneally injected. The antibody was repeatedly injected every 3 days until the end of the experiment.

Figure 9a shows the results of the two-pronged SYMPHONY treatment modality. When laser light was used to activate GNS that had accumulated in the tumor, specific interactions between the light and nanoparticles resulted in local generation of heat (i.e., local PTT), which selectively killed the tumor cells. The second arm of therapy involved use of a highly specific molecule, anti-PD-L1 antibody, which inhibits a key pathway by which cancer cells suppress the antitumor immune response. Strong cancer growth and rapid death occurred in control distant tumors (no SYMPHONY treatment) (Fig. 9b). On the other hand, not only was there significant shrinkage of the primary tumor treated with GNS (Fig. 9c), but there was also dramatic growth inhibition/reversal of the untreated distant tumor (which was not treated with laser light) as seen in Fig. 9d. This can be explained by activation of a potent abscopal immune response, which treated not only primary but distant

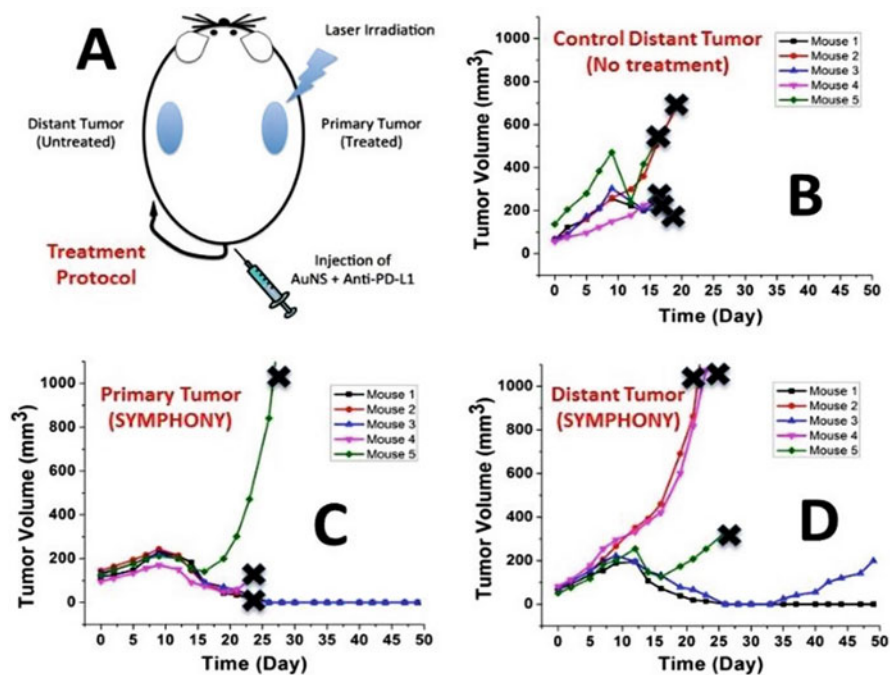


Fig. 9 (a) Diagram of SYMPHONY procedure. (b) Distant tumor sizes rapid change for blank control (similar for primary control). Primary (c) and distant (d) tumor sizes change for SYMPHONY group (Mice 1-black dots- was ultimately cured). x indicates sacrificed mice. (Adapted from Reference 21)

tumor as well, and resulted in an 80% tumor response rate and an unprecedented durable complete response (cure) in 20% of mice [21].

Figure 10 shows the Kaplan-Meier (K-M) overall survival curve, which underlines the significant improvement of SYMPHONY over anti-PD-L1 immune therapy alone. At the end of 49 days, the survival rate for the SYMPHONY group was 40%, while it was 0% for all other control groups including the anti-PD-L1-antibody therapy alone group. Anti-PD-L1 therapy by itself did show therapeutic effects compared to the untreated control group, but was not as efficient as SYMPHONY. Mice treated with SYMPHONY survived up to 12 months with no tumor recurrence.

To study the effects of photothermal therapy and PD-L1 treatment on anti-tumor immune response by immune cell phenotyping, spleens and tumors were collected from a separate cohort of MB49-tumor-bearing mice 7 days post treatment. In spleens, we found that combination treatment of GNS-PTT and anti-PD-L1 significantly increased the percentage of total T cells, CD4, CD8 T cells and B cells. The absolute numbers of total T cells, CD4 T cells and B cells were also increased in the mice receiving combination treatment. On the other hand, both the percentage and cell number of MDSC (myeloid-derived suppressor cells) were significantly reduced in the combination treatment group. We investigated the roles

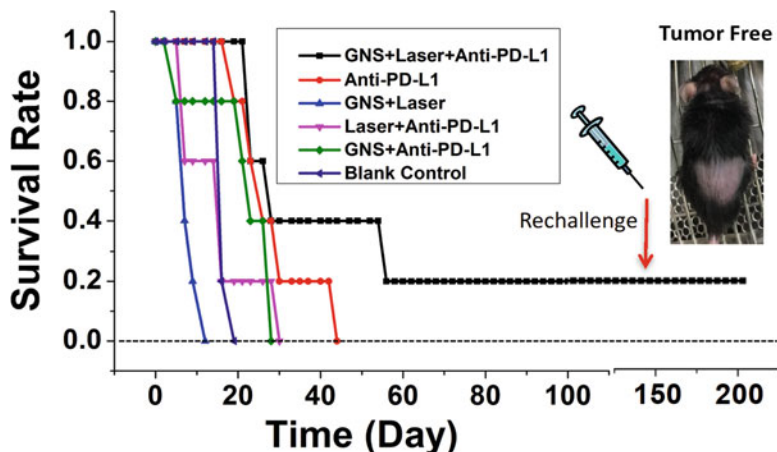


Fig. 10 Kaplan-Meier (K-M) overall survival curve for aggressive bladder cancer murine models. Mice were sacrificed when: (1) single tumor volume larger than 1000 mm^3 . (2) total tumor volume larger than 1500 mm^3 . (3) ulceration. GNS (2 mg per mouse) was intravenously (IV) injected through tail vein on Day 0 and laser treatment (808 nm, 0.6 W/cm^2) was performed on Day 1. Anti-PD-L1 antibody was intraperitoneally (IP) injected every 3 days (200 μg per injection) only PTT+Anti-PDL1 group has two survival mice (40%) after 49 days. As of today (>200 days) one mouse (20%) is deemed cured even after a tumor rechallenge experiment at day 145 [Inset]. All control groups have no survival mouse at day 43). (Adapted from Reference 21)

of photothermal therapy and PD-L1 treatment for PD-1 expression on T cells. Our results indicated that the combination treatment not only upregulated PD-1 expression on CD4 and CD8 T cells but also increased the percentage and cell number of PD-1⁺CD4 and PD-1⁺CD8 T cells).

Abscopal Effects and Long-Term Immunity against Cancer. An abscopal effect occurs when distant untreated tumors regress during treatment of a primary tumor. Abscopal effects are thought to be due to immune activation and generally indicate the induction of effective immunity. We have preliminarily evidence of a profound abscopal effect with SYMPHONY (Fig. 9d). Additionally, we performed rechallenge experiments in long-term (>90 day) survivors of SYMPHONY-treated MB49 tumors. Repeated MB49 injections did not lead to tumors recurrence. This exciting result indicates that SYMPHONY had induced effective long-lasting immunity against MB49 (Fig. 10, **Top right insert**) and if optimally exploited could pave the way to eradication of many hard-to-treat metastatic cancers.

4 Conclusion

Plasmonic nanoparticles such as gold nanostars have unique properties that allow them to amplify the optical properties of the excitation light and thus increase the

effectiveness of light-based photothermal tumor ablation. The unique properties of GNS, which contribute to plasmonics-amplified immune nanotherapy for cancer, include: (1) plasmonic nano-enhancers of light, (2) nano-targeting of tumor cells, (3) nano-sources for heating tumor cells from the inside (4) nano-activators of the immune system, and (5) synergistic amplification of immunomodulation. The combination of checkpoint blockade immunotherapy with GNS-mediated photothermal therapy offers the promise to address one of the most challenging problems in the treatment of metastatic cancer. Broadening and stabilizing the effect of PD-L1/PD1 inhibitors can be achieved with nanoparticle-mediated synergistic thermal therapies. Our results have indicated that by using a combination of immune-checkpoint inhibition and GNS-mediated photothermal therapy it is possible to achieve complete eradication of primary treated tumors as well as distant untreated tumors in mice. Immunotherapies could thus synergistically benefit from targeted thermal nanotherapies, especially when hyperthermia around immune-checkpoint inhibitors in the tumor bed is combined with precise thermal ablation of cancer cells. The effectiveness of the combination of plasmonic GNS-enabled photothermal ablation and PD-L1 immunomodulation was demonstrated to be synergistic (not just additive) and delayed rechallenge with repeated tumor injections did not lead to new tumor formation, indicating that the combined treatment induced effective long-lasting immunity against cancer.

Acknowledgements This work was supported by National Institutes of Health (1R01EB028078-01A1) and the Department of Defense (W81XWH-17-1-0567).

References

1. World Health Organization. Fact Sheets on Cancer (2021): <https://www.who.int/news-room/fact-sheets/detail/cancer>
2. He, Q., Guo, S., Qian, S., Chen, X.: Development of individualized anti-metastasis strategies by engineering nanomedicines. *Chem. Soc. Rev.* **44**, 6258–6286 (2015)
3. Loo, C., et al.: Nanoshell-enabled photonics-based imaging and therapy of cancer. *Technol. Cancer Res. Treat.* **3**(1), 33–40 (2004)
4. Pandita, T.K., Pandita, S., Bhaumik, S.R.: Molecular parameters of hyperthermia for Radiosensitization. *Crit. Rev. Eukaryot. Gene Expr.* **19**(3), 235–251 (2009)
5. Takada, T., Yamashita, T., Sato, M., Sato, A., Ono, I., Tamura, Y., et al.: Growth inhibition of re-challenge B16 melanoma transplant by conjugates of melanogenesis substrate and magnetite nanoparticles as the basis for developing melanoma-targeted chemo-thermo-immunotherapy. *J. Biomed. Biotechnol.* **2009**, 457936 (2009)
6. Koning, G.A., Eggermont, A.M.M., Lindner, L.H., ten Hagen, T.L.M.: Hyperthermia and thermosensitive liposomes for improved delivery of chemotherapeutic drugs to solid tumors. *Pharm. Res.* **27**(8), 1750–1754 (2010)
7. Wang, C., Xu, L., Liang, C., Xiang, J., Peng, R., Liu, Z.: Immunological responses triggered by photothermal therapy with carbon nanotubes in combination with anti-CTLA-4 therapy to inhibit cancer metastasis. *Adv. Mater.* **26**(48), 8154–8162 (2014)
8. Wang, H.N., Vo-Dinh, T.: Multiplex detection of breast cancer biomarkers using plasmonic molecular sentinel nanoprobe. *Nanotechnology.* **20**, 065101 (2009)

9. Vo-Dinh, T., Wang, H.N., Scaffidi, J.: Plasmonic nanoprobe for SERS biosensing and bioimaging. *J. Biophotonics*. **3**, 89–102 (2010)
10. Vo-Dinh, T., Fales, A.M., Griffin, G.D., Khoury, C.G., Liu, Y., Ngo, H., Norton, S.J., Register, J.K., Wang, H.N., Yuan, H.: Plasmonic nanoprobe: from chemical sensing to medical diagnostics and therapy. *Nanoscale*. **5**, 10127–10140 (2013)
11. Vo-Dinh, T., Liu, Y., Fales, A.M., Ngo, H., Wang, H.N., Register, J.K., Yuan, H., Norton, S.J., Griffin, G.D., SERS: Nanosensors and nanoreporters: Golden opportunities in biomedical applications. *WIREs Nanomed. Nanobiotechnol.* **7**, 17–33 (2015)
12. Wang, H.N., Crawford, B.M., Fales, A.M., Bowie, M.L., Seewaldt, V.L., Vo-Dinh, T.: Multiplexed detection of MicroRNA biomarkers using SERS-based inverse molecular sentinel (iMS) Nanoprobes. *J. Phys. Chem. C*. **120**, 21047 (2016)
13. Yuan, H., Fales, A.M., Vo-Dinh, T.: TAT peptide-functionalized gold nanostars: enhanced intracellular delivery and efficient NIR photothermal therapy using ultralow irradiance. *J. Am. Chem. Soc.* **134**(28), 11358–11361 (2012)
14. Liu, Y., Ashton, J.R., Moding, E.J., Yuan, H., Register, J.K., Fales, A.M., Choi, J., Whitley, M.J., Zhao, X., Qi, Y., Ma, Y., Vaidyanathan, G., Zalutsky, M.R., Kirsch, D.G., Badea, C.T., Vo-Dinh, T.: A plasmonic gold nanostar theranostic probe for in vivo tumor imaging and photothermal therapy. *Theranostics*. **5**(9), 946–960 (2015)
15. Yuan, H., Khoury, C.G., Wilson, C.M., Grant, G.A., Bennett, A.J., Vo-Dinh, T.: In vivo particle tracking and photothermal ablation using plasmon-resonant gold nanostars. *Nanomed. Nanotechnol. Biol. Med.* **8**(8), 1355–1363 (2012)
16. Vo Dinh, T., Hiramoto, M.Y.K., Begun, G.M., Moody, R.L.: Surface enhanced Raman spectroscopy for trace organic analysis. *Anal. Chem.* **56**, 1667 (1984)
17. Vo-Dinh, T.: Surface-enhanced Raman spectroscopy using metallic nanostructures. *TrAC-Trends Anal. Chem.* **17**, 557–582 (1998)
18. Vo-Dinh, T., Dhawan, A., Norton, S.J., Khoury, C.G., Wang, H.N., Misra, V., Gerhold, M.D.: Plasmonic nanoparticles and nanowires: design, fabrication and application in sensing. *J. Phys. Chem. C*. **114**, 7480–7488 (2010)
19. Crawford, B.M., Wang, H.N., Stolarchuk, C., Von Furstenberg, R., Strobbia, P., Zhang, D., Qin, X., Owzar, K., Garman, K.S., Vo-Dinh, T.: Plasmonic nanobiosensors for detection of MicroRNA cancer biomarkers in clinical samples. *Analyst*. **145**, 4587–4594 (2020)
20. Cupil-Garcia, V., Strobbia, P., Crawford, B.M., Wang, H.N., Ngo, H., Liu, Y., Vo-Dinh, T.: Plasmonic nanoplatforms: from surface-enhanced Raman scattering sensing to biomedical application. *J. Raman Spectrosc.*, Published on line: 12 December 2020. <https://doi.org/10.1002/jrs.6056>
21. Liu, Y., Maccarini, P., Palmer, G.M., Etienne, W., Zhao, Y., Lee, C.T., Ma, X., Inman, B.A., Vo-Dinh, T.: Synergistic immuno photothermal nanotherapy (SYMPHONY) for the treatment of unresectable and metastatic cancers. *Sci. Rep.* **7**, 8606 (2017)
22. Vo-Dinh, T., Inman, B.A.: What potential does plasmonics-amplified synergistic immuno photothermal nanotherapy have for treatment of cancer. *Nanomedicine*. **13**(2), 139–144 (2018)
23. Liu, Y., Chongsathidkiet, P., Crawford, B.M., Odion, R., Dechant, C.A., Kemeny, H.R., Cui, X., Maccarini, P.F., Lascola, C.D., Fecci, P.E., Vo-Dinh, T.: Plasmonic gold nanostar-mediated photothermal immunotherapy for brain tumor ablation and immunologic memory. *Immunotherapy*. **11**, 1293–1302 (2019)
24. Langer, J., Jimenez de Aberasturi, D., Aizpurua, J., Alvarez-Puebla, R.A., Augu e, B., Baumberg, J., Bazan, G.C., et al.: Present and future of surface enhanced Raman scattering. *ACS Nano*. **14**(1), 28–117 (2020)
25. Falk, M.H., Issels, R.D.: Hyperthermia in oncology. *Int. J. Hyperth.* **17**(1), 1–18 (2001)
26. Owusu, R.A., Abern, M.R., Inman, B.A.: Hyperthermia as adjunct to intravesical chemotherapy for bladder cancer. *Biomed. Res. Int.* **2013**, 262313 (2013)
27. Hildebrandt, B., Wust, P., Ahlers, O., et al.: The cellular and molecular basis of hyperthermia. *Crit. Rev. Oncol. Hematol.* **43**(1), 33–56 (2002)
28. Frey, B., Weiss, E.M., Rubner, Y., et al.: Old and new facts about hyperthermia-induced modulations of the immune system. *Int. J. Hyperth.* **28**(6), 528–542 (2012)

29. Schildkopf, P., Ott, O.J., Frey, B., et al.: Biological rationales and clinical applications of temperature controlled hyperthermia—implications for multimodal cancer treatments. *Curr. Med. Chem.* **17**(27), 3045–3057 (2010)
30. Wust, P., Hildebrandt, B., Sreenivasa, G., et al.: Hyperthermia in combined treatment of cancer. *Lancet Oncol.* **3**(8), 487–497 (2002)
31. Norton, S.J., Vo-Dinh, T.: Optical response of linear chains of metal nanospheres and nanospheroids. *J. Opt. Soc. Am.* **25**, 2767 (2008)
32. Norton, S.J., Vo-Dinh, T.: Spectral bounds on plasmon resonances for Ag and Au prolate and oblate nanospheroids. *J. Nano.* **2**, 029501 (2008)
33. Khoury, C.G., Norton, S.J., Vo-Dinh, T.: Plasmonics of 3-D Nanoshell dimers using multipole expansion and finite element method. *ACS Nano.* **3**, 2776–2788 (2009)
34. Khoury, C.G., Norton, S.J., Vo-Dinh, T.: Investigating the plasmonics of a dipole-excited silver nanoshell: Mie theory versus finite element method. *Nanotechnology.* **21**, 315203 (2010)
35. Norton, S.J., Vo-Dinh, T.: Photothermal effects of plasmonic metal nanoparticles in a fluid. *J. Appl. Phys.* **119**(8), 083105 (2016)
36. Khoury, C.G., Vo-Dinh, T.: Gold Nanostars for surface-enhanced Raman scattering: synthesis, characterization and optimization. *J. Phys. Chem. C. Nanomater. Interfaces.* **112**, 18849–18859 (2008)
37. Yuan, H., Khoury, C.G., Hwang, H., Wilson, C.M., Grant, G.A., Vo-Dinh, T.: Gold nanostars: surfactant-free synthesis, 3D modelling, and two-photon photoluminescence imaging. *Nanotechnology.* **23**(7), 075102 (2012)
38. Yuan, H., Khoury, C.G., Wilson, C.M., Grant, G.A., Bennett, A.J., Vo-Dinh, T.: In vivo particle tracking and photothermal ablation using plasmon-resonant gold nanostars. *Nanomedicine.* **8**(8), 1355–1363 (2012)
39. Indrasekara, A.S.D.S., Johnson, S.D., Odion, R.A., Vo-Dinh, T.: A systematic bottom-up synthesis: manipulation of the geometry and modulation of the optical response of surfactant-free gold Nanostars. *ACS Omega.* **3**(2), 2202 (2018)
40. Mobley, J., Vo-Dinh, T.: Optical properties of tissues, chapter 2. In: Vo-Dinh, T. (ed.) *Biomedical Photonics Handbook*, 2nd edn. CRC Press, Taylor and Francis, Boca Raton, London, New York (2015)
41. Register, J.K., Fales, A.M., Wang, H., Cho, E.H., Boico, A., Pradhan, S., Kim, J., Schroeder, T., Wisniewski, N.A., Klitzman, B., Vo-Dinh, T.: In vivo detection of SERS-encoded plasmonic nanostars in small and large animal models. *Anal. Bioanal. Chem.* **407**(27), 8215–8224 (2015)
42. Fabris, V.T., Lodillinsky, C., Pampena, M.B., Belgorosky, D., Lanari, C., Eijan, A.M.: Cytogenetic characterization of the murine bladder cancer model MB49 and the derived invasive line MB49-I. *Cancer Genet.* **205**(4), 168–176 (2012)
43. Chen, F., Zhang, G., Cao, Y., Hessner, M.J., See, W.A.: MB49 murine urothelial carcinoma: molecular and phenotypic comparison to human cell lines as a model of the direct tumor response to bacillus Calmette-Guerin. *J. Urol.* **182**(6), 2932–2937 (2009)
44. Gunther, J.H., Jurczok, A., Wulf, T., et al.: Optimizing syngeneic orthotopic murine bladder cancer (MB49). *Cancer Res.* **59**(12), 2834–2837 (1999)
45. Loskog, A., Ninalga, C., Hedlund, T., Alimohammadi, M., Malmstrom, P.U., Totterman, T.H.: Optimization of the MB49 mouse bladder cancer model for adenoviral gene therapy. *Lab. Anim.* **39**(4), 384–393 (2005)
46. Kirsch, I., Vignali, M., Robins, H.: T-cell receptor profiling in cancer. *Mol. Oncol.* **9**(10), 2063–2070 (2015)
47. Oghumu, S., Terrazas, C.A., Varikuti, S., et al.: CXCR3 expression defines a novel subset of innate CD8+ T cells that enhance immunity against bacterial infection and cancer upon stimulation with IL-15. *FASEB J.* **29**(3), 1019–1028 (2015)
48. Jung, S., Aliberti, J., Graemmel, P., et al.: Analysis of fractalkine receptor CX(3)CR1 function by targeted deletion and green fluorescent protein reporter gene insertion. *Mol. Cell. Biol.* **20**(11), 4106–4114 (2000)
49. Roth, T.J., Sheinin, Y., Lohse, C.M., et al.: B7-H3 ligand expression by prostate cancer: a novel marker of prognosis and potential target for therapy. *Cancer Res.* **67**(16), 7893–7900 (2007)

50. Inman, B.A., Frigola, X., Harris, K.J., et al.: Questionable relevance of gamma delta T lymphocytes in renal cell carcinoma. *J. Immunol.* **80**(5), 3578–3584 (2008)
51. Inman, B.A., Sebo, T.J., Frigola, X., et al.: PD-L1 (B7-H1) expression by urothelial carcinoma of the bladder and BCG-induced granulomata: associations with localized stage progression. *Cancer.* **109**(8), 1499–1505 (2007)
52. Bellmunt, J., Mullane, S.A., Werner, L., et al.: Association of PD-L1 expression on tumor-infiltrating mononuclear cells and overall survival in patients with urothelial carcinoma. *Ann. Oncol.* **26**(4), 812–817 (2015)

Nanotechnologies for Photothermal and Immuno Cancer Therapy: Advanced Strategies Using Copper Sulfide Nanoparticles and Bacterium-Mimicking Liposomes for Enhanced Efficacy



Binbin Zheng and Wei Lu

For decades, cancer has remained one of the major diseases threatening human health due to its refractoriness and metastasis. The rapid development of nanotechnology has provided new opportunities for complete elimination of cancer. Therapies such as photothermal and immuno cancer therapy are gaining more recognition as new treatment modalities in clinic. Photothermal therapy (PTT) is a non-invasive and local treatment modality that harnesses the absorption of near-infrared (NIR) laser by an optical absorbing agent to generate heat for ablating cancer cells. Cancer immunotherapy stimulates the host immune system to prevent, target, control and eliminate cancer cells, which are known to develop various mechanisms of immune escape.

PTT can induce precise cancer cell ablation effectively with minimal side effects to the healthy tissues nearby. However, due to the limited penetration depth of the laser, PTT is restricted to treat the subcutaneous or surgically exposed tumors. It is much less effective for metastatic tumors. On the contrary, although immunotherapy can help establish the systemic antitumor immunity with long-lasting memory responses, which shows great promises to prevent tumor metastasis and recurrence, it is relatively ineffective to eradicate solid primary tumors. Investigators are becoming aware of the potential value to combine PTT and immunotherapy to endow unique synergistic mechanisms to eradicate cancer cells [1, 2].

Copper sulfide nanoparticles (CuSNPs) are gradually emerging as promising NIR-responsive photothermal coupling agents for PTT [3–5]. On the other hand, several pattern recognition receptors (PRRs) have been identified in the innate immune systems of mammals, among which Toll like receptors (TLRs) and nucleotide binding oligomerization domain (NOD) like receptors (NLRs) are well

B. Zheng · W. Lu (✉)

Key Laboratory of Smart Drug Delivery, Ministry of Education, & State Key Laboratory of Molecular Engineering of Polymers, School of Pharmacy, Fudan University, Shanghai, China
e-mail: wlu@fudan.edu.cn

© Springer Nature Switzerland AG 2021

T. Vo-Dinh (ed.), *Nanoparticle-Mediated Immunotherapy*, Bioanalysis 12,
https://doi.org/10.1007/978-3-030-78338-9_9

191

studied and characterized. TLRs are the transmembrane receptors, whereas NLRs are the cytoplasmic receptors. Both of them are predominantly expressed in several immune cells and critical to elicit humoral and cellular immune responses. Encouraging progresses in immunotherapy based on optimized adjuvant formulations of ligands for TLRs and NLRs have been made in numerous preclinical and clinical tests [6–8]. In this chapter, we provide a brief introduction on CuSNPs as biodegradable alternatives to gold nanopatforms for PTT, followed by the description on the engineering of bacterium-mimicking liposomes for adjuvant immunotherapy. Finally, several recent studies examining the anti-tumor therapeutic effects using CuSNPs or/and adjuvant formulations based on bacterium-mimicking strategy for combinatorial photothermal and immuno cancer therapy are discussed.

1 Copper Sulfide Nanoparticles

PTT employs the photothermal coupling agents and NIR light energy sources to eradicate cancer cells locally at the primary tumor site, through which the light is converted to heat to kill the cancer cells. Currently, many nanopatforms such as gold nanoparticles (AuNPs), CuS nanoparticles and carbon nanotubes, have been proved to improve the efficacy of cancer PTT based on the efficient photothermal conversion effect.

PTT is required to destroy tumor cells by heating them to above 40 °C while keeps minimal injury to the surrounding healthy tissues [9]. Therefore, non-specific absorption of heat by surrounding tissues from the laser source has imposed a major limitation on the shallow therapeutic window of PTT, which has motivated the search of photoabsorbers with increased photothermal efficiency. AuNPs are the most widely studied photothermal agents, which can strongly absorb light as the result of the phenomenon called localized surface plasmon resonance (LSPR) and efficiently convert the absorbed light into heat by the fast electron–phonon and phonon–phonon processes [10]. In spite of the advantages such as bioinert properties and high photothermal conversion efficiency, AuNPs are considered barely biodegradable, raising concerns regarding their long-term metabolism [11].

CuSNPs, as one of the suitable candidates, have several properties different from AuNPs. Firstly, the raw material and production cost of CuSNPs is much lower than that of AuNPs rendering CuSNPs much easier to large-scale applications. Secondly, the inherent absorption wavelength of CuSNPs peaks at about 900 nm right in the NIR range, ideal for *in vivo* application with its low background absorption and deep penetration in tissues. Thirdly, unlike AuNPs that rely on LSPR to absorb NIR laser, the photothermal effects of CuSNPs stem from the intra-band *d-d* transition of Cu^{2+} . Since the LSPR absorption of AuNPs is determined by the dielectric constant of the surrounding medium, their absorption peak may change when delivered from the tubes to the tumor tissues. In contrast, the absorption wavelength of CuSNPs is rather constant because the intra-band transitions are not affected by the solvent environment. In addition, CuSNPs can be easily synthesized to as small as about

3 nm in size with complete photothermal effects [12]. The ultra-small size can be quickly cleared by kidney. Last but not least, AuNPs are almost nonmetabolizable while CuSNPs are considered biodegradable nanoparticles *in vivo*. The long-termed accumulation of AuNPs can induce an irreversible toxicity in the liver which can be avoided to the great extent in CuSNPs treatment [11].

1.1 Synthesis of CuSNPs

CuSNPs can be classified as solid CuSNPs and hollow CuSNPs (HCuSNPs) (Fig. 1). The synthesis of monodisperse and stable nanoparticles is of great importance for biomedical applications. Various methods have been developed to prepare CuSNPs.

1.1.1 Hydrothermal/Solvothermal Methods

The major drawback of reaction by simply mixing Cu and S powder together is the large-sized product and the requirement for high reaction temperature. In order to overcome these shortcomings, hydrothermal or solvothermal methods are commonly adapted for CuSNPs preparation which have the advantages of simple preparation, relatively low temperature and high purity of the products. For example, precursor of Cu (i.e., CuO or CuCl₂) and S (i.e., Na₂S or thiourea) are autoclaved at 130–170 °C for several hours to synthesize CuSNPs in diameter of about 13 nm [15]. Li and his coworkers synthesized CuSNPs with small diameter (~11 nm) by simply mixing aqueous solution of CuCl₂, sodium citrate, and Na₂S at room

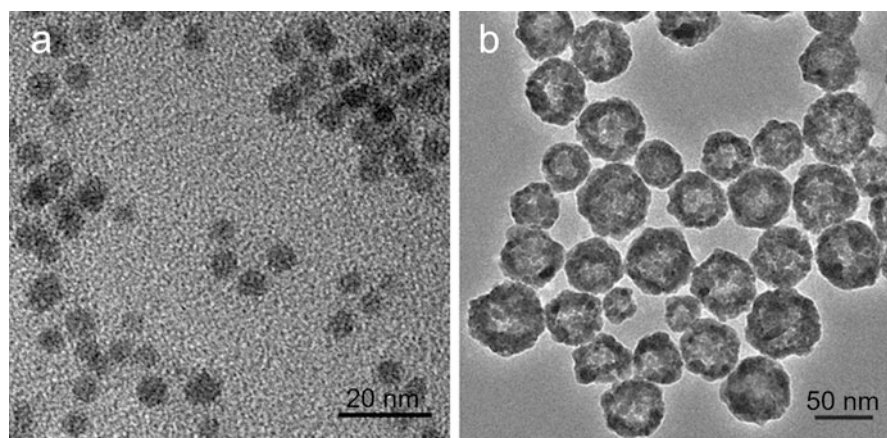


Fig. 1 Transmission electron microscopy images of solid CuSNPs (a) and HCuSNPs (b). (Adapted with permissions [13, 14]. Copyright 2014, American Chemical Society and 2012, Wiley-VCH)

temperature with subsequent reaction for 15 min at 90 °C [16]. The morphology and size of CuSNPs can be well controlled by adjusting the amount of copper sources, reaction temperature and time.

1.1.2 Microwave Irradiation

Compared to hydrothermal methods, microwave irradiation is a simpler, faster, and more energy efficient preparation procedure. CuSNPs can be successfully synthesized with the same Cu and S sources in ethylene glycol medium assisted by the cyclic irradiation of different microwave powers (~180 W) and exposure time (~20 min) [17].

1.1.3 Direct Dry-Grinding Synthesis

Lipophilic CuSNPs are of interest for drug delivery to hydrophobic tissues. However, lipophilic CuSNPs prepared by traditional methods such as cation exchange, hot injection or solventless approach are not able to absorb NIR light and require additional complex oxidization for PTT applications [18]. A new method has been developed by directly grinding copper (II) acetylacetonate with sulfur in oleylamine in the ambient environment for a few minutes followed by mild heat [19]. The obtained lipophilic CuSNPs are of uniform size with about 10 nm in diameter and demonstrate the photothermal effects.

Other reported methods for the synthesis of CuSNPs include sonochemical synthesis, surfactant-based synthesis and enzymatic treatment of dextran stabilized CuS nanosuspensions to produce nanoparticles [20–22].

1.1.4 Hollow CuSNPs Synthesis

One of the challenging issues for PTT application of solid CuSNPs is their weak absorbance of NIR light. The development of core-shell nanostructure of CuSNPs has proved to improve the nanoparticles absorbance and emissions [23]. HCuSNPs (Fig. 1b) have gained much attention due to their high photothermal conversion efficiency and drug loading capacity [24]. HCuSNPs are usually obtained by template-assisted methods with different types of core supports including surfactant micelle microemulsions, poly-(styrene-acrylic) latex particles and Cu₂O nanoparticles [24].

Wu and his coworkers have developed a fast and mild fabrication method based on the chemical transformation from Cu₂O spheres as sacrificial templates to CuS hollow spheres [23]. The Cu₂O spheres are loose aggregates of Cu₂O NPs. S²⁻ in the solution reacts with the Cu₂O on the surface of Cu₂O spheres to produce CuSNPs surrounding the Cu₂O spheres. With more CuSNPs produced on the surface, a shell structure composed of CuSNPs is formed. Under the driving force

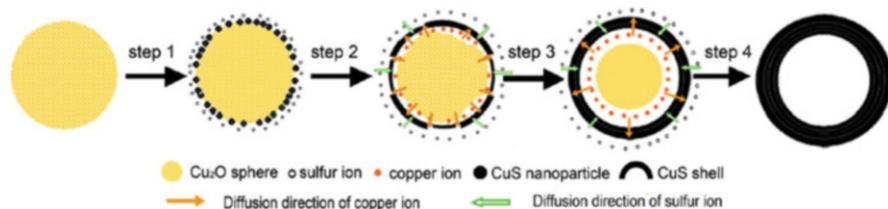


Fig. 2 Schematic illustration of growth of HCuSNPs using Cu_2O nanoparticles as core supports (Adapted with permission [23]. Copyright 2009, American Chemical Society)

of concentration gradient, the reaction continues until Cu ions are exhausted and the inner cavity is formed (Fig. 2).

1.2 Biomedical Applications of CuSNPs

1.2.1 Photothermal Therapy

CuSNPs are becoming widely recognized agents for PTT due to their unique optical properties and biocompatibility. In this technique, NIR wavelength ranging from 650 to 1350 nm is well known for its transparency to biological tissues. Once the nanoparticles reach the tumor site, NIR laser is applied and transformed into heat quickly in several minutes by CuSNPs. With precisely adjusting the position and diameter of the laser beam, PTT can kill tumor cells by heating them to over 40°C without affecting the surrounding tissues (See Fig. 3) [25]. In addition, the hypoxic and acidic microenvironment make tumor cells more sensitive to heat than normal cells [26]. Such strategy has been successfully applied to treating several cancer models in mice [25, 27, 28].

1.2.2 Drug Delivery

HCuSNPs are excellent drug delivery systems because of their large surface with numerous pores which are feasible for chemical functionalization and drug loading. HCuSNPs have been coated with polyetherimide (PEI) to introduce amine groups on the surface and then functionalized with the bovine serum albumin–folic acid (BSA–FA) complexes through the formation of amide bonds. With the surface modification of BSA, the HCuS–BSA–FA NPs have acquired stealthiness in the circulation system and could target tumor sites by enhanced permeability and retention (EPR) effects. The grafted FA segments on the surface could enhance the internalization of nanoparticles by receptor-mediated endocytosis. The HCuS–BSA–FA NPs can be further loaded with indocyanine green (ICG), a NIR absorbing fluorescent dye to achieve enhanced photothermal therapeutic effects [29].

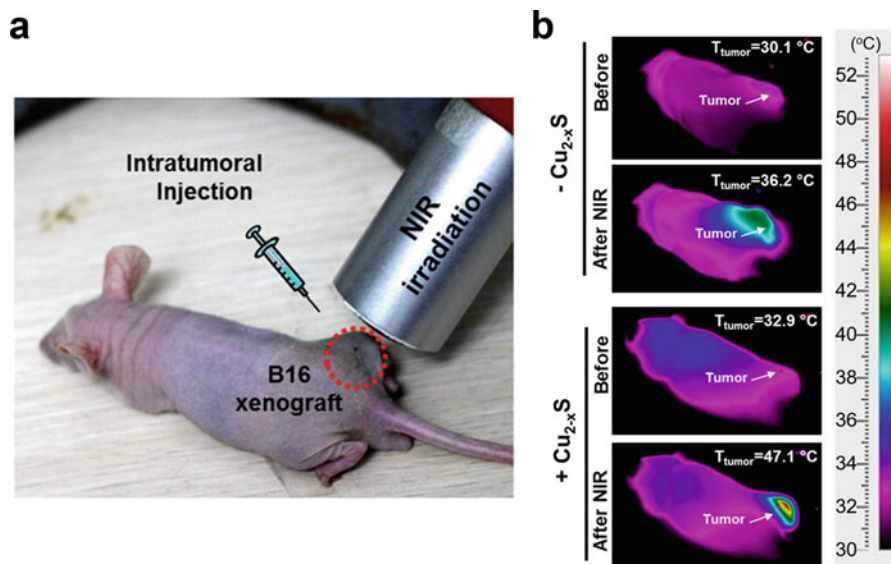


Fig. 3 PTT treatment on mice bearing B16 xenograft with CuSNPs. (a) The image of a B16 tumor-bearing nude mouse receiving PTT treatment. CuSNPs were injected intratumorally (15 mg/kg), immediately followed by NIR irradiation (0.6 W/cm², 100 s). Circle, B16 tumor, (b) Infrared thermal images of the tumor site post injection in non-treated (*upper*) and CuSNPs-treated (*lower*) mice (Adapted with permission [25]. Copyright 2015, American Chemical Society)

We have reported a photothermal ablation-enhanced transdermal drug delivery methodology based on HCuSNPs (Fig. 4). By using short (femto- to nanosecond) pulsed NIR irradiation (1.3–2.6 W/cm²), HCuSNPs could be heated to a high temperature within a few seconds. The heat was then quickly transmitted to the tissues locally. Such pulsed-heating strategy ensures that HCuSNPs efficiently decompose the stratum corneum locally without irritating the surrounding tissues. The resulted skin disruption has been proved to increase the permeability of human growth hormone [14]. Considering the distribution of antigen-presenting cells like Langerhans cells in epidermis, such photothermal ablation based delivery strategy is particularly beneficial for vaccine delivery with macromolecules such as protein antigens and oligonucleotides to these target cells.

2 Bacterium-Mimicking Liposomes

Immunotherapy presents a new paradigm for cancer therapy. By inducing the immune cells to recognize and kill tumor cells, immunotherapy relies on the activated host anti-tumor immune systems rather than the exogenous weapons such as irradiation or chemical drugs to eradicate cancers, which are particularly effective

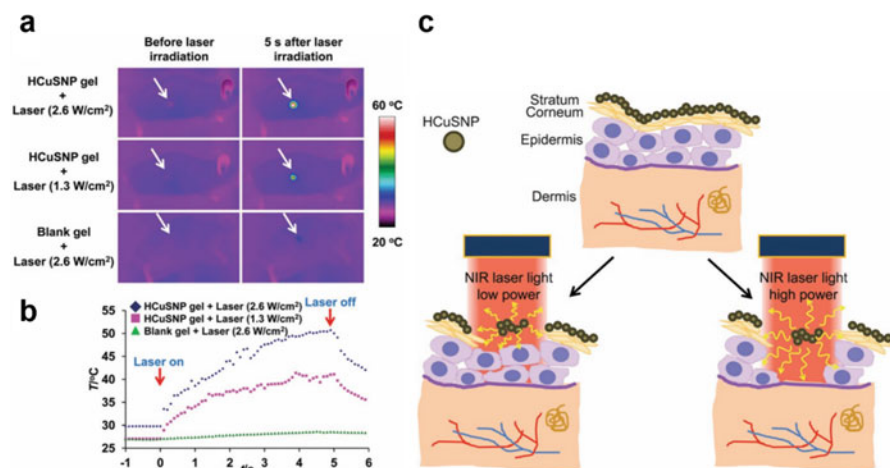


Fig. 4 Photothermal ablation of skin mediated by HCuSNPs. (a) Infrared thermal images of nude mice receiving laser irradiation. Mice were topically applied with gel with or without HCuSNPs followed by the laser treatment. Arrows, treated skin area, (b) Plots of average temperature in the treated skin area versus irradiation time, (c) Schematic illustration of photothermal ablation of skin by HCuSNPs with NIR laser irradiation (Adapted with permission [14]. Copyright 2012, Wiley-VCH)

in controlling cancer metastasis and relapse. Numerous kinds of immunotherapy including immune checkpoint inhibitors, adoptive T cells transfer and cancer vaccines have showed great promise for anti-tumor efficacy in preclinical and clinical tests. Cancer vaccines harness the tumor antigens to induce the therapeutic immune responses. Successful cancer vaccines rely on the optimized adjuvants to aid the poorly immunogenic antigens to establish powerful and durable anti-tumor immunity. Recent development of innate immunity reveals that PRRs are central to the innate immune response and are considered as key targets for developing effective adjuvants [30].

TLRs and NLRs belong to the family of PRRs in the host innate immunity. They are able to sense and recognize the conserved microbial components, usually termed as pathogen associated molecular patterns (PAMPs), as well as endogenous danger signals generally referred to damage-associated molecular patterns (DAMPs). The recognition of PAMPs or DAMPs by TLRs or NLRs occurs in different cellular compartments including the plasma membrane, cytoplasm and endolysosomes. The subcellular localization of PRRs copes with their respective ligands. For example, TLR1/2/4/6 recognize components derived from bacterial cell wall and are found mainly on the plasma membrane. TLR3/7/8/9 are expressed exclusively in intracellular vesicles such as the endoplasmic reticulum and endolysosomes, where they recognize microbial nucleic acids. NOD1 and NOD2 are general sensors of peptidoglycan distributed in the cytoplasm [31, 32].

PRRs signal through multiple pathways with different kinds of adaptor molecules such as myeloid differentiation primary-response protein 88 (MyD88), Toll/interleukin-1 receptor domain-containing adaptor protein inducing interferon- β (TRIF) and caspase activating recruitment domain 9 (CARD9) to stimulate innate immune responses. Two key circuits termed as nuclear factor kappa B (NF- κ B) and interferon regulatory factor (IRF) pathways involving three transcription factors NF- κ B, IRF3, and IRF7 are activated by these PRRs to induce the expression of proinflammatory cytokines and type I interferons that are essential in comprehensive activation of immune systems [33].

2.1 Adjuvant of Ligands for Toll-Like Receptors and NOD-Like Receptors

In nature, there exists various kinds of PRR-activating PAMPs including bacterial and viral nucleic acids (dsRNA for TLR3, ssRNA for TLR7/8, CpG motif containing DNA for TLR9), flagellin (which signal through TLR5), lipopolysaccharide (LPS for TLR4), lipoteichoic acid and lipopeptide (for TLR2) as well as peptidoglycan (for NOD1 and NOD2). These natural ligands are potent stimulators for innate immunity but many of them are too toxic for clinical applications. To reduce the risk of adverse effects to minimum, efforts are focused on the development of less toxic derivatives with chemical modifications. Among them, monophosphoryl lipid A (MPLA) and mifamurtide are the two best examples [8, 34].

Pioneering work conducted by Ribí and his colleagues to separate the immunostimulatory potency of LPS from its endotoxic side effects with chemical modifications has resulted in the synthesis of MPLA. It is derived from LPS by removal of the acyl chains, polysaccharide side groups and phosphates (Fig. 5). The toxicity of MPLA is reduced to 0.08% as that of LPS while retains most of the parent molecule's immuno stimulation potency [34]. MPLA represents the new total synthetic TLR-based vaccine adjuvant which is approved for clinical application [6].

Mifamurtide is a stimulator of NOD2 and a synthetic molecule derived from muramyl dipeptide (MDP). Although MDP is recognized as the minimal component of the mycobacterial peptidoglycan responsible for the potent adjuvanticity, it is too pyrogenic to be clinically used in humans. In the early 1980s, mifamurtide, also called liposomal muramyl tripeptide phosphatidyl ethanolamine (L-MTP-PE), has been developed. It is a liposomal formulation of the MTP-PE, derived from the covalent addition of Alanin and dipalmitoyl phosphatidyl ethanolamine to MDP (Fig. 6). Compared with MDP, mifamurtide is less toxic, longer held in the body and more effective to activate immune cells. In several Phase I and II clinical trials, mifamurtide has been proved to be efficient for anti-tumor therapy by activating monocyte in circulation [35].

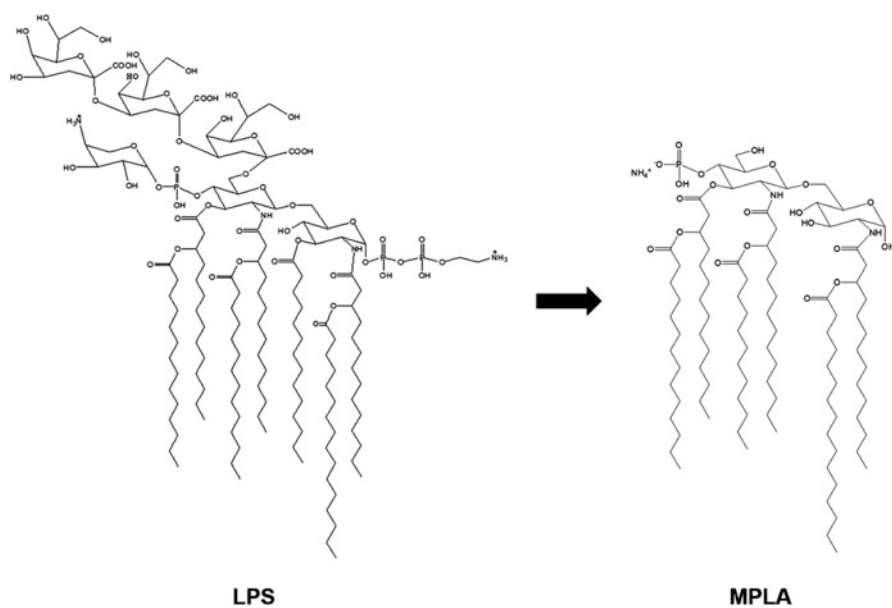


Fig. 5 The molecular structure of LPS from cell wall of *Salmonella minnesota* and its detoxified component MPLA

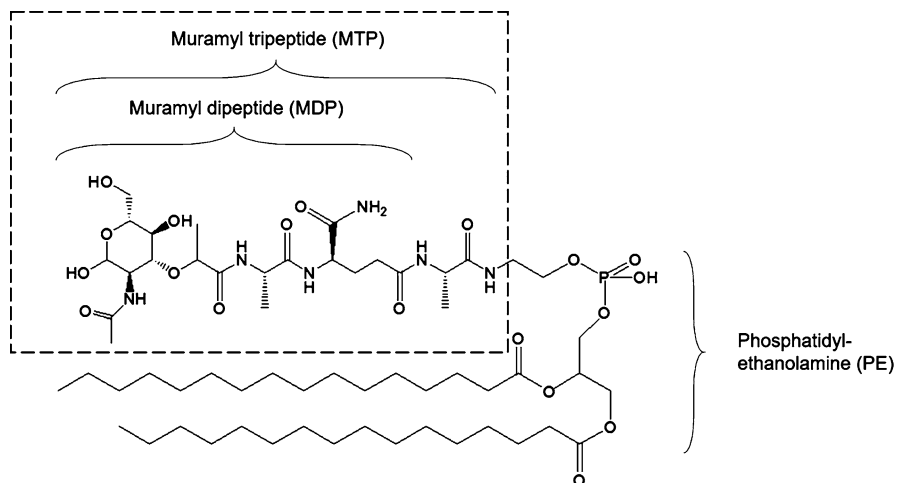


Fig. 6 The molecular structure of L-MTP-PE

2.2 *Engineering of Bacterium-Mimicking Liposomes as Adjuvants for Cancer Vaccines*

Many synthetic adjuvants developed based on TLR or NLR are proved to be safe and well-tolerated in humans. However, most of the clinical treatments based on these agonists as monotherapies or simple combination are proved to be unsatisfactory for anti-cancer therapeutics [36, 37]. It is of great interest to select these molecules to achieve an optimal combination with enhanced adjuvanticity. In fact, immune cells such as macrophages and dendritic cells utilize various kinds of TLRs and NLRs to detect and recognize bacteria. It is likely that these PAMPs cooperatively activate multiple PRRs and signal transduction pathways. Therefore, engineering a synthetic adjuvant delivery system composed of multiple TLR and NLR agonists which mimics the morphology and structure of bacteria may boost the immune system much more effectively than the monotherapy of adjuvant. The bacterium-mimicking vectors (BMVs) have been constructed based on this hypothesis [38]. BMVs comprise of four agonist adjuvants including MPLA for TLR4, recombinant flagellin (rFljB) for TLR5, oligodeoxynucleotides containing CpG motifs (CpG-ODN) for TLR9 and mifamurtide (MFT) for NOD2. 1,2-dipalmitoyl-*sn*-glycero-3-phosphocholine (DPPC) is selected as the liposomal scaffold. Lipophilic MPLA and MFT are intercalated into the phospholipid bilayer to mimic the bacterial cell wall. rFljB is conjugated through the polyethylene glycol to the surface of the liposomes to mimic flagellum. DNA nanoparticles containing CpG motifs are encapsulated into the hydrophilic core of liposomes to mimic the bacterial nucleoid (Fig. 7a). The synthetic BMVs activate both proinflammatory NF- κ B pathway and IRF pathway to produce various kinds of proinflammatory cytokines and type I interferons and subsequently lead to the comprehensive activation of immune system (Fig. 7b).

By incorporating the model antigen ovalbumin (OVA), cancer vaccines based on BMVs display superior anti-tumor therapeutic and prophylactic effects in treating melanoma to either the reported synthetic glucopyranosyl lipid adjuvant-stable emulsion (GLA-SE) or bacterium-derived Freund's adjuvant. The prominent anti-cancer efficacy is induced by establishing strong and durable OVA specific T cell immunity as well as T help 1 related humoral immune responses (Fig. 8).

3 **Combinatorial Immuno and Photothermal Therapy**

Recently, photothermal therapy combined with immunotherapy has been found to achieve synergistic efficacy in cancer treatment which promotes cancer regression and prevents relapse and metastasis. Photothermal therapy based on gold or copper sulfide nanoparticles can effectively ablate the tumor cells by generating

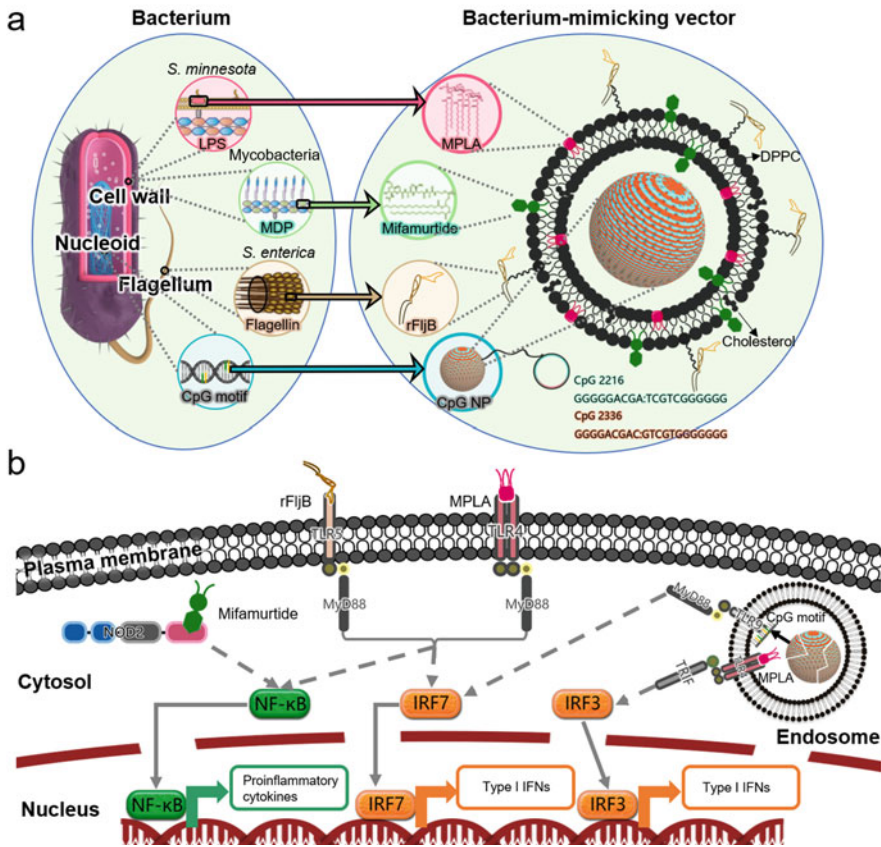


Fig. 7 Scheme of bacterium-mimicking vectors (BMVs) (a) and BMVs-mediated signaling pathways (b). (Adapted with permission [38]. Copyright 2019, Wiley-VCH)

localized heat. By carefully adjusting the power, frequency and position of laser beam, such therapy using materials with high photothermal conversion efficiency can precisely ablate the palpable primary tumors with minimized injury to the surrounding normal cells. However, PTT is not effective in controlling cancer relapse or metastasis. Tumor antigens diverse from patient to patient and are weak immunogenic. Considering the release of tumor antigens from the dying cells during PTT, immunotherapy especially adjuvant therapy is suitable to utilize these antigen sources as an auto-vaccine. By inducing the immune cells to recognize and kill tumor cells, cancer vaccine is able to enhance the anti-cancer efficacy and establish the durable immune responses against the relapse or metastasis of tumors.

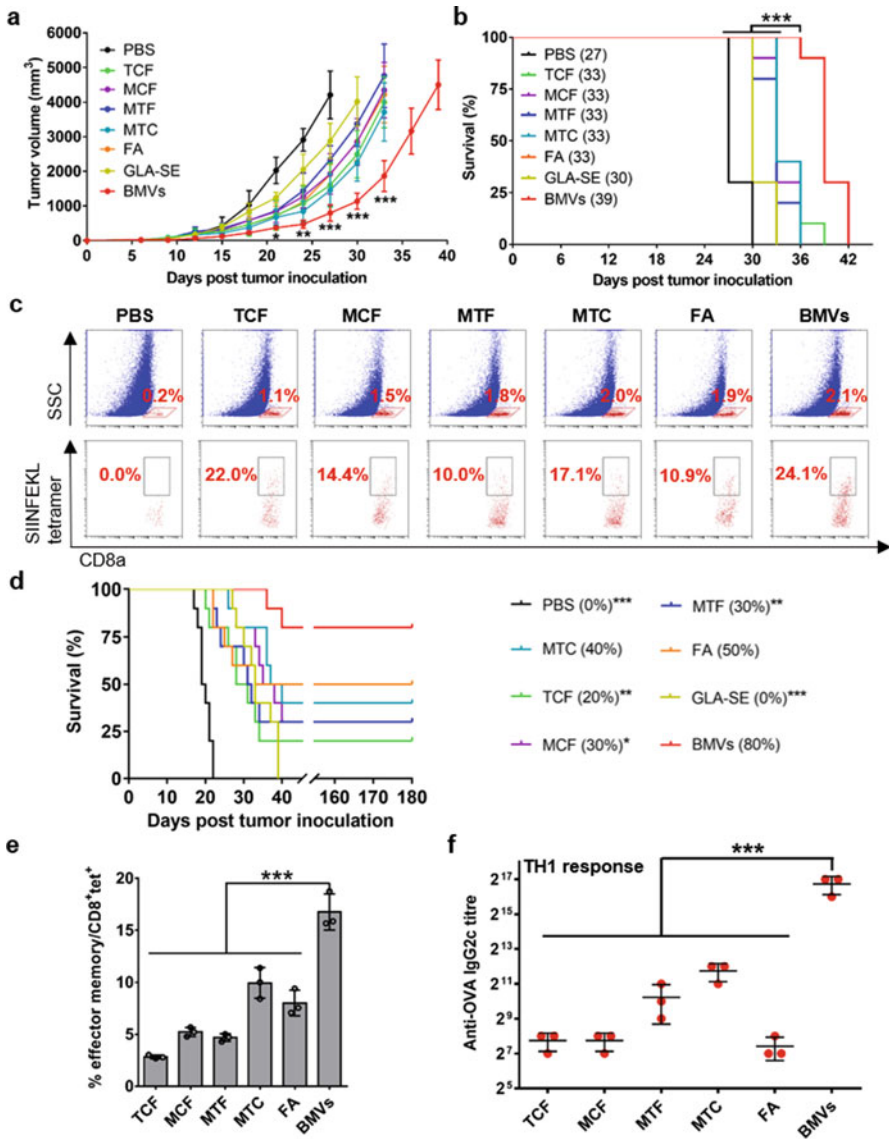


Fig. 8 Enhanced anti-tumor effect of BMVs as both the therapeutic and prophylactic adjuvants. Tumor growth curves (a) and survival curves (b) over time of mice in the therapeutic regimen. Median survival time of each group was listed in the brackets of (b), (c) Representative dot plots of OVA specific CD8⁺ T cells in tumors receiving therapeutic treatments. SSC, side scatter, (d) Survival curves over time of mice in the prophylactic regimen. Tumor-free rate after observation for 180 d of each group was listed in brackets, (e) Ratio of effector memory T cells (CD62L⁻CD44⁺) among OVA specific CD8⁺ cells in draining lymph nodes, (f) Anti-OVA IgG2c (TH1-related response) antibody titers in the sera. The acronym of TCF, MCF, MTF, or MTC represents the control liposomes comprising three adjuvants from concatenated single initials M (MPLA), T (Mifamurtide), C (CpG NPs), or F (rFljB). FA, Freund's adjuvants. Data are presented as mean ± s.d. **P* < 0.05, ***P* < 0.01, and ****P* < 0.001 compared to BMVs group by one-(e, f) or two-(a) way ANOVA with Dunnett's *post hoc* test or log-rank (Mantel–Cox) test (b, d) (Adapted with permission [38]. Copyright 2019, Wiley-VCH)

3.1 Immunogenic Cell Death Induced by PTT

The original purpose of PTT is to ablate the tumors as a local therapeutic modality. It is now recognized that a more important phenomenon termed immunogenic cell death (ICD) arises from PTT [18]. The generated heat kills the tumor cells and results in the release of huge amounts of DAMPs, which increases the immunogenicity of the tumor microenvironment. Despite that the intricate details of ICD mechanism remains to be elucidated, three key factors including calreticulin (CRT) cell surface translocation, and release of high mobility group protein 1 (HMGB1) and adenosine triphosphate (ATP) are characterized to promote phagocytosis of tumor cells, antigen presentation, cytokines secretion and activation of CD8⁺ cytotoxic T lymphocytes [39]. The released DAMPs as well as tumor related antigens from the irradiated tumor cells trigger the maturation of dendritic cells and stimulate the downstream effector T cells to recognize and destroy tumor cells not only at the primary but also at distant sites, thus exhibiting the *in situ* vaccination effects [40]. It is expected that agonist adjuvants based on TLRs or NLRs as typical PAMPs can improve the therapeutic effects of the ICD.

3.2 Immuno Adjuvant Therapy Synergizes PTT in Cancer Treatment

We have designed an NIR light-induced transformative nanoparticle platform that combines PTT with immunotherapy [27]. The delivery systems are based on chitosan-coated HCuSNPs that assemble the immunoadjuvants CpG motifs (HCuSNP-CpG) (Fig. 9a). Upon excitation at 900 nm, the nanoparticles break down into the small CuSNPs (SCuSNPs) and chitosan-CpG nanocomplexes (Chi-CpG-NPs). The CuSNPs generate heat to destroy tumor cells at the primary site to release tumor specific antigens. In the meantime, the released Chi-CpG-NPs can be phagocytized by dendritic cells, leading to the increased secretion of various proinflammatory cytokines and the activation of the immune cells (Fig. 9b, c). Then the activated dendritic cells capture the released tumor antigens and cross prime the T cells into antigen specific CD8⁺ cytotoxic T cells, tailoring the adaptive anti-cancer immunity. In the mice bearing EMT6 tumor, such therapeutic strategy has effectively relieved the primary tumor burden and significantly delayed the growth of untreated tumors at distant contralateral sites, indicating the success in eliciting systemic immunity not only against primary treated tumors but also against subsequent untreated tumors (Fig. 9d).

In another study using B16-OVA models, we have treated the melanoma-bearing mice with PTT in combination with BMVs without loading the tumor antigens. Due to the light absorption of melanin granules of the melanoma, the NIR light has been applied to the tumor to generate sufficient heat without the administration of any photothermal coupling agents. Particularly, the treatment has not been performed

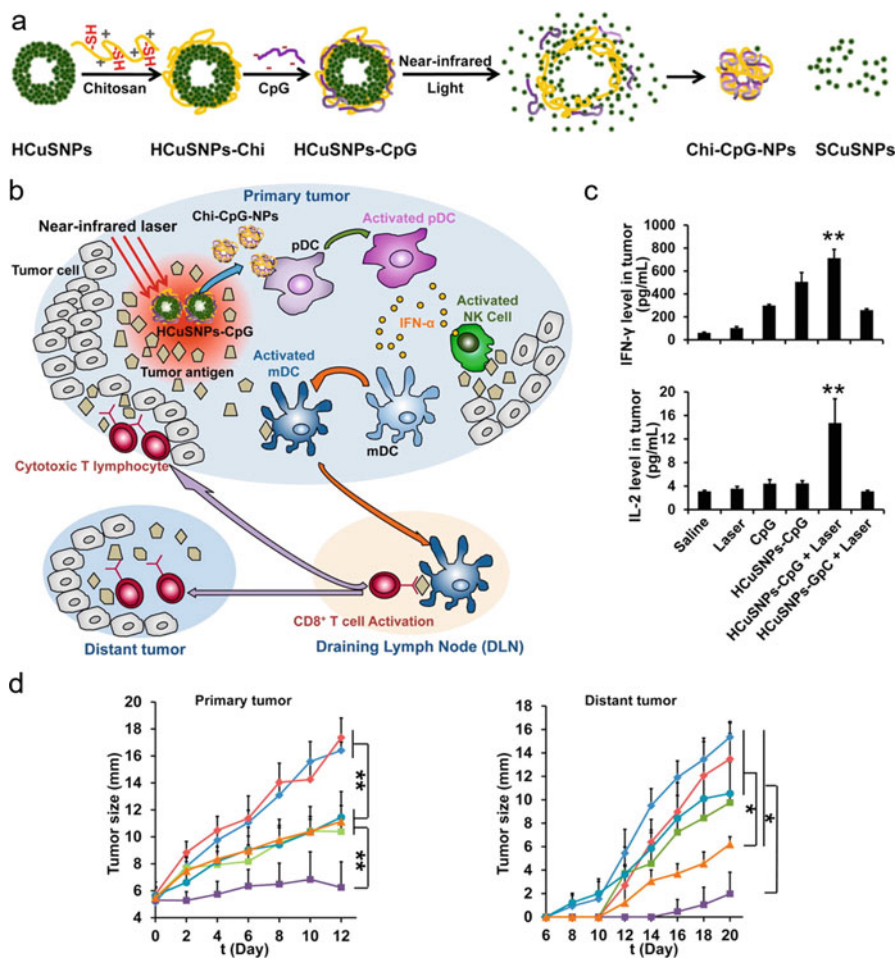


Fig. 9 Photothermal immunotherapy using HCuSNPs-CpG. (a) Scheme of the assembly of HCuSNPs-CpG and the disintegration triggered by NIR laser, (b) A diagram of the mechanism of HCuSNPs-CpG to treat primary and distant tumor, (c) IFN- γ and IL-12 levels in tumor of mice receiving different treatments, (d) Tumor growth curves of primary and distant tumor in EMT6 tumor-bearing mice following various treatments. Data are presented as mean \pm s.d. * $P < 0.05$ and ** $P < 0.01$ compared between “HCuSNPs-CpG + Laser” group and other groups (c) or between the compared groups (d) (Adapted with permission [27]). Copyright 2014, American Chemical Society)

until the large tumor established (200–300 mm³). BMVs adjuvant treatment alone does not produce prominent growth delay on the large tumor. In the laser treatment group, although the first dose of laser irradiation has reduced the tumor sizes, the residual tumor has quickly relapsed within 1 week and does not respond to the second PTT treatment. In the combinatorial treatment of PTT and BMVs, tumor slightly recurs 7 days post the first laser treatment. After the second irradiation, the

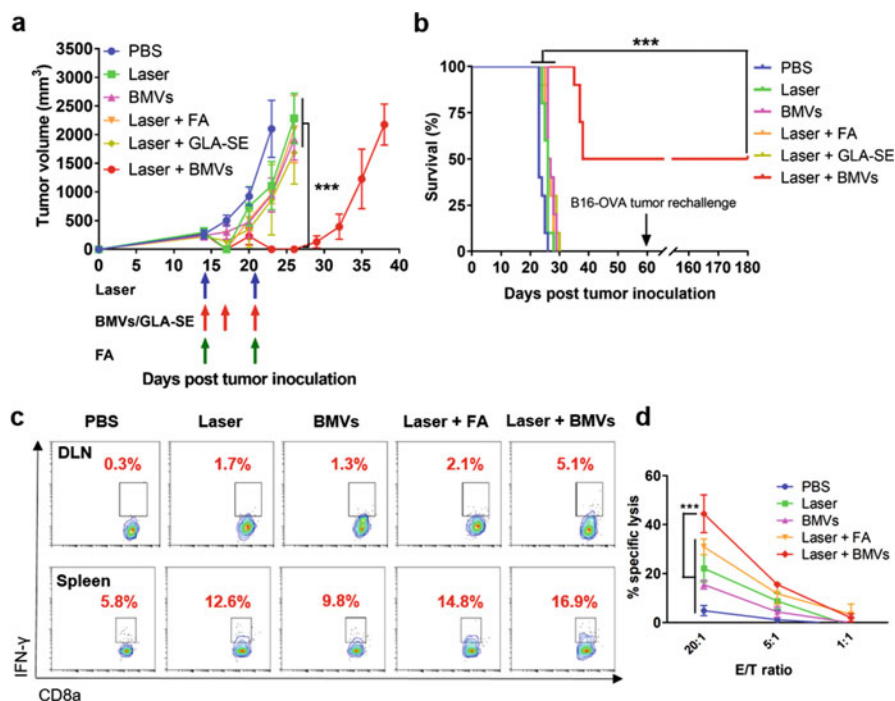


Fig. 10 PTT synergized with BMVs against large tumors. Tumor growth curves (a) and survival curves (b) over time of mice with various treatments. FA, Freund's adjuvant. (c) Representative contour plots of IFN- γ ⁺CD8⁺ lymphocytes isolated from the draining lymph node (DLN) or spleen of mice, (d) Cytolytic activity of the splenocytes. "E/T ratio" represents effector/target cell ratio. Data are expressed as mean \pm s.d. *** $P < 0.001$ compared to Laser + BMVs group by two-way ANOVA with Bonferroni's *post hoc* test (a, d) or log-rank (Mantel-Cox) test (b) (Adapted with permission [17]. Copyright 2019, Wiley-VCH)

tumor shrinks again with growth significantly delayed. Encouragingly, 5 out of 10 large tumors have been eradicated. The survivors have been completely protected against the second tumor challenge on the contralateral flank (Fig. 10a, b). In comparison, administration of Freund's adjuvant or GLA-SE does not produce the combined effect on the PTT-induced tumor growth delay. Both the flow cytometry and tumor cell specific lytic assay have demonstrated that the mice receiving laser plus BMVs treatment engender the most pronounced cytotoxic T lymphocytes against B16-OVA tumor cells (Fig. 10c, d).

4 Summary

Anti-cancer vaccines have shown some clinical efficacy as monotherapy. However, limitations exist including the weak potency to eradicate primary tumors and

difficulty to identify the tumor antigens. One feasible choice to overcome the pitfalls is to develop an optimal combination of adjuvants to enhance the immunogenicity of the vaccine. The bacterium-mimicking engineering strategy provides a rational approach to select pathogen-associated molecular patterns, which effectively induce the anti-tumor immune response. Photothermal therapy is a modality to complement immunotherapy. By significantly relieving the primary tumor burden, providing the source of tumor antigens and inducing ICD effects, PTT has strongly enhanced the therapeutic efficacy of immunotherapy at both primary and distant tumors, offering the possibility of a complete cure of cancer.

Acknowledgements This work was partially supported by grants from the National Natural Science Foundation of China (81991493 and 91859110).

References

1. Zou, L., Wang, H., He, B., Zeng, L., Tan, T., Cao, H., et al.: Current approaches of photothermal therapy in treating cancer metastasis with nanotherapeutics. *Theranostics*. **6**(6), 762–772 (2016)
2. Liu, Y., Crawford, B.M., Vo-Dinh, T.: Gold nanoparticles-mediated photothermal therapy and immunotherapy. *Immunotherapy*. **10**(13), 1175–1188 (2018)
3. Liu, Y., Bhattarai, P., Dai, Z., Chen, X.: Photothermal therapy and photoacoustic imaging via nanotheranostics in fighting cancer. *Chem. Soc. Rev.* **48**(7), 2053–2108 (2019)
4. Liu, Y., Ji, M., Wang, P.: Recent advances in small copper sulfide nanoparticles for molecular imaging and tumor therapy. *Mol. Pharm.* **16**(8), 3322–3332 (2019)
5. Ashikbayeva, Z., Tosi, D., Balmassov, D., Schena, E., Saccomandi, P., Inglezakis, V.: Application of nanoparticles and nanomaterials in thermal ablation therapy of cancer. *Nanomaterials* **9**(9), 1195 (2019)
6. Mitchell, T.C., Casella, C.R.: No pain no gain? Adjuvant effects of alum and monophosphoryl lipid a in pertussis and HPV vaccines. *Curr. Opin. Immunol.* **47**, 17–25 (2017)
7. Mahipal, A., Ejadi, S., Gnjjatic, S., Kim-Schulze, S., Lu, H., ter Meulen, J.H., et al.: First-in-human phase I dose-escalating trial of G305 in patients with advanced solid tumors expressing NY-ESO-1. *Cancer Immunol. Immunother.* **68**(7), 12111–11222 (2019)
8. Kager, L., Pötschger, U., Bielack, S.: Review of mifamurtide in the treatment of patients with osteosarcoma. *Ther. Clin. Risk Manag.* **6**, 279–286 (2010)
9. Moy, A.J., Tunnell, J.W.: Combinatorial immunotherapy and nanoparticle mediated hyperthermia. *Adv. Drug Deliv. Rev.* **114**, 175–183 (2017)
10. Jain, P.K., El-Sayed, I.H., El-Sayed, M.A.: Au nanoparticles target cancer. *Nano Today*. **2**(1), 18–29 (2007)
11. Guo, L., Panderi, I., Yan, D.D., Szulak, K., Li, Y., Chen, Y.T., et al.: A comparative study of hollow copper sulfide nanoparticles and hollow gold nanospheres on degradability and toxicity. *ACS Nano*. **7**(10), 8780–8793 (2013)
12. Li, Y., Lu, W., Huang, Q., Li, C., Chen, W.: Copper sulfide nanoparticles for photothermal ablation of tumor cells. *Nanomedicine*. **5**(8), 1161–1171 (2010)
13. Otelaja, O.O., Ha, D., Ly, T., Zhang, H., Robinson, R.D.: Highly conductive Cu_{2-x}S nanoparticle films through room-temperature processing and an order of magnitude enhancement of conductivity via electrophoretic deposition. *ACS Appl. Mater. Interfaces*. **6**(21), 18911–18920 (2014)
14. Samy, R., Liangran, G., Yajuan, L., Bingfang, Y., Wei, L.: Hollow copper sulfide nanoparticle-mediated transdermal drug delivery. *Small*. **8**(20), 3143–3150 (2012)

15. Zhang, Y., Qiao, T., Hu, X.: A simple hydrothermal route to nanocrystalline CuS. *J. Cryst. Growth*. **268**(1–2), 64–70 (2004)
16. Zhou, M., Zhang, R., Huang, M., Lu, W., Song, S., Melancon, M.P., et al.: A chelator-free multifunctional [64Cu] CuS nanoparticle platform for simultaneous micro-PET/CT imaging and photothermal ablation therapy. *J. Am. Chem. Soc.* **132**(43), 15351–15358 (2010)
17. Thongtem, T., Phuruangrat, A., Thongtem, S.: Synthesis and analysis of CuS with different morphologies using cyclic microwave irradiation. *J. Mater. Sci.* **42**(22), 9316–9323 (2007)
18. Saldanha, P.L., Brescia, R., Prato, M., Li, H., Povia, M., Manna, L., et al.: Generalized one-pot synthesis of copper sulfide, selenide-sulfide, and telluride-sulfide nanoparticles. *Chem. Mater.* **26**(3), 1442–1449 (2014)
19. Li, Y., Scott, J., Chen, Y., Guo, L., Zhao, M., Wang, X., et al.: Direct dry-grinding synthesis of monodisperse lipophilic CuS nanoparticles. *Mater. Chem. Phys.* **162**, 671–676 (2015)
20. Xu, H., Wang, W., Zhu, W.: Sonochemical synthesis of crystalline CuS nanoplates via an in situ template route. *Mater. Lett.* **60**(17–18), 2203–2206 (2006)
21. Khiew, P., Radiman, S., Huang, N., Ahamd, M.S.: Synthesis and characterization of copper sulfide nanoparticles in hexagonal phase lyotropic liquid crystal. *J. Cryst. Growth*. **268**(1–2), 227–237 (2004)
22. Kim, Y., Walsh, D.: Metal sulfide nanoparticles synthesized via enzyme treatment of biopolymer stabilized nanosuspensions. *Nanoscale*. **2**(2), 240–247 (2010)
23. Zhu, H., Wang, J., Wu, D.: Fast synthesis, formation mechanism, and control of shell thickness of CuS hollow spheres. *Inorg. Chem.* **48**(15), 7099–7104 (2009)
24. Goel, S., Chen, F., Cai, W.: Synthesis and biomedical applications of copper sulfide nanoparticles: from sensors to theranostics. *Small*. **10**(4), 631–645 (2014)
25. Wang, S., Riedinger, A., Li, H., Fu, C., Liu, H., Li, L., et al.: Plasmonic copper sulfide nanocrystals exhibiting near-infrared photothermal and photodynamic therapeutic effects. *ACS Nano*. **9**(2), 1788–1800 (2015)
26. Liu, J., Liang, H., Li, M., Luo, Z., Zhang, J., Guo, X., et al.: Tumor acidity activating multifunctional nanoplatform for NIR-mediated multiple enhanced photodynamic and photothermal tumor therapy. *Biomaterials*. **157**, 107–124 (2018)
27. Guo, L., Yan, D.D., Yang, D., Li, Y., Wang, X., Zalewski, O., et al.: Combinatorial photothermal and immuno cancer therapy using chitosan-coated hollow copper sulfide nanoparticles. *ACS Nano*. **8**(6), 5670–5681 (2014)
28. Shi, H., Yan, R., Wu, L., Sun, Y., Liu, S., Zhou, Z., et al.: Tumor-targeting CuS nanoparticles for multimodal imaging and guided photothermal therapy of lymph node metastasis. *Acta Biomater.* **72**, 256–265 (2018)
29. Han, L., Zhang, Y., Chen, X., Shu, Y., Wang, J.: Protein-modified hollow copper sulfide nanoparticles carrying indocyanine green for photothermal and photodynamic therapy. *J. Mater. Chem. B*. **4**(1), 105–112 (2016)
30. Ho, N.I., Huisin't Veld, L.G., Raaijmakers, T.K., Adema, G.J.: Adjuvants enhancing cross-presentation by dendritic cells: the key to more effective vaccines? *Front. Immunol.* **9**, 2874 (2018)
31. O'Neill, L.A., Golenbock, D., Bowie, A.G.: The history of toll-like receptors—redefining innate immunity. *Nat. Rev. Immunol.* **13**(6), 453–460 (2013)
32. Heim, V.J., Stafford, C.A., Nachbur, U.: The NOD signaling pathway: activation, regulation and outcomes. *Front. Cell Dev. Biol.* **7**, 208 (2019)
33. Wu, J., Chen, Z.J.: Innate immune sensing and signaling of cytosolic nucleic acids. *Annu. Rev. Immunol.* **32**, 461–488 (2014)
34. Casella, C.R., Mitchell, T.C.: Putting endotoxin to work for us: monophosphoryl lipid A as a safe and effective vaccine adjuvant. *Cell. Mol. Life Sci.* **65**(20), 3231 (2008)
35. Jimmy, R., Stern, C., Lisy, K., White, S.: Effectiveness of mifamurtide in addition to standard chemotherapy for high-grade osteosarcoma: a systematic review. *JBIS Database System Rev. Implement. Rep.* **15**(8), 2113–2152 (2017)

36. Haining, W.N., Davies, J., Kanzler, H., Linda, D., Thomas, B., John, E., et al.: CpG oligodeoxynucleotides alter lymphocyte and dendritic cell trafficking in humans. *Clin. Cancer Res.* **14**(17), 5626–5634 (2008)
37. Marchand, M., Punt, C., Aamdal, S., Escudier, B., Kruit, W., Keilholz, U., et al.: Immunisation of metastatic cancer patients with MAGE-3 protein combined with adjuvant SBAS-2: a clinical report. *Eur. J. Cancer.* **39**(1), 70–77 (2003)
38. Zheng, B., Xu, J., Chen, G., Zhang, S., Xiao, Z., Lu, W.: Bacterium-mimicking vector with enhanced adjuvanticity for cancer immunotherapy and minimized toxicity. *Adv. Funct. Mater.* **29**(33), 1901437 (2019)
39. Golden, E.B., Apetoh, L.: Radiotherapy and immunogenic cell death. *Semin. Radiat. Oncol.* **25**(1), 11–17 (2015)
40. Ng, C.W., Li, J., Pu, K.: Recent progresses in phototherapy-synergized cancer immunotherapy. *Adv. Funct. Mater.* **28**(46), 1804688 (2018)

Nanoparticle-Based Phototherapy in Combination with Checkpoint Blockade for Cancer Immunotherapy



Qian Chen and Zhuang Liu

1 Introduction

Phototherapy, an emerging cancer therapeutic strategy, usually utilizes phototherapeutic agents to selectively kill tumor cells under appropriate light irradiation. It generally falls into two categories, photothermal therapy (PTT) and photodynamic therapy (PDT) [1, 2]. PTT usually leverages optical absorbing agents to generate heat under appropriate light irradiation to burn cancer cells. Ideal photothermal agents should have high absorbance in the near-infrared (NIR) region (760–1000 nm), a transparency window for biological tissues, and should be able to efficiently convert the absorbed optical energy into heat. Various types of nanomaterials with high NIR absorbance have been exploited as PTT agents, exhibiting promising therapeutic efficacy in many preclinical animal studies. Examples include inorganic nanomaterials, such as gold nanostructures [3, 4], carbon-based nanomaterials [5], copper sulfide (CuS) nanoparticles [6, 7], palladium nanosheets [8], and other transition metal dichalcogenides [9, 10], and organic nanomaterials, such as NIR-light absorbing conjugated polymers [11, 12], porphyrins [13], and NIR dye-encapsulated polymeric nanoparticles [14], have been explored as effective PTT agents both in vitro and in vivo.

On the other hand, PDT relies on photosensitizers that can transfer the surrounding oxygen molecules to reactive oxygen species (ROS) or cytotoxic singlet oxygen ($^1\text{O}_2$) to kill the cancer cells under certain light irradiation [15]. PDT is an externally activatable treatment modality, which has been approved in clinic for cancer treatment. A wide range of photosensitizers, most of them containing porphyrin structures, have been applied for PDT. However, inefficient tumor accumulation

Q. Chen · Z. Liu (✉)

Institute of Functional Nano & Soft Materials (FUNSOM), Jiangsu Key Laboratory for Carbon-Based Functional Materials & Devices, Soochow University, Suzhou, Jiangsu, China
e-mail: liu@suda.edu.cn

and cell uptake of photosensitizers largely limit the application of PDT. Various nanomaterials, including liposomes [16], polymeric nanoparticles [17], quantum dots [18], magnetic nanoparticles [18], mesoporous silica nanoparticles [19], and carbon-based nanomaterials [20], have been developed to delivery photosensitizers, aiming to enhance their tumor accumulation and therapeutic efficacy. Moreover, most of the recently used photosensitizers are excited by visible light, which usually has limited the tissue penetration depth. To overcome this limitation, a unique type of nanomaterials, upconversion nanoparticles (UCNPs), which could emit visible light under NIR light excitation, has been explored to realize NIR-mediated PDT with improved tissue penetration [21].

In addition to directly killing cancer cells, phototherapy is also useful to trigger and/or improve other therapeutic treatments, achieving synergistic therapeutic effects. Furthermore, it has now been well-established that the dying tumor cells after phototherapy could release tumor-associated antigens and self-antigens, which could attract a large number of antigen-presenting cells (APCs) [22]. APCs, particularly dendritic cells (DCs), are able to capture these antigens and present these antigens to adaptive immune cells, eliciting strong antigen-specific immune responses [23]. Various immunogenic factors, including the exposure of calreticulin (CAR) on the cell surface, release of pro-inflammatory cytokines and factors (IL-6, TNF- α , and IL-1 β), and post-apoptotic exodus of high mobility groups, have been identified during the dying of tumor cells after phototherapy [24–26]. Thus, similar to cancer vaccines using cancer cell lysates, the tumor-associated antigens released after phototherapy in the presence of adjuvant nanoparticles could act as “tumor vaccines” [27]. To further promote the antitumor immune responses induced by phototherapy, immune checkpoint blockade could be selected to block the regulatory pathways that express on immune cells, enhancing immune stimulatory or subverting immune suppressive effects for the tumor infiltration, activation, and proliferation of T cells [28]. In this chapter, well-designed nanoparticle platforms used for phototherapy in combination with checkpoint blockade for cancer immunotherapy will be discussed.

2 Photothermal Therapy

In situ photothermal immunotherapy (ISPI) which combines local PTT and immunological stimulation with immunoadjuvant was first raised in 1997 [29]. It utilized 805 nm diode laser to increase the temperature in the target tumor which was pretreated with the glycosylated chitosan gel containing indocyanine green (ICG), directly killing the tumor cells and releasing a large number of tumor-associated antigens, self-antigens, and heat shock proteins (HSPs). Concomitantly, the immunological defense system was stimulated to against residual and metastatic tumor cells, significantly inhibiting the tumor recurrence and metastasis. These findings indicated that PTT of the primary tumor indeed triggered the specific immunological response in tumor-bearing rats. To facilitate the antitumor immunological response induced by ISPI,

additional immunological stimulations are required to activate the immune system, achieving the effective and continuable antitumor immune responses. In 2010, Chen and co-workers conducted a preliminary clinical study to evaluate the therapeutic efficacy of ISPI together with an immunological stimulator, imiquimod, a food and drug administration (FDA) approved Toll-like receptor 7 (TLR7) agonist, in late-stage melanoma patients [30]. Eleven patients with multiple cutaneous metastases received ISPI in one or multiple 6-week treatment cycles. During the ISPI treatment, three main components were applied directly in the cutaneous tumors: local injection of ICG and imiquimod, and local irradiation with 805 nm laser. Five patients were still alive at the time of their last follow-up and the 12-month overall survival was 70%. Thus, ISPI with imiquimod has clinical benefits for patients with advanced and late-stage melanoma.

Various inorganic nano-agents such as gold nanostructures [31], carbon nanotubes [32], graphene oxide [33], CuS nanoparticles [34] and MoS₂ nanosheets [35] with strong NIR absorbance have been explored for ISPI. Yata et al. modified gold nanoparticles with CpG oligodeoxynucleotides, and mixed them with hexapod-like structured DNA, obtaining the composite immunostimulatory gold–DNA hydrogel [31]. EG7-OVA tumors after injection of DNA hydrogel were irradiated with 780 nm laser, the local increased temperature could directly kill the cancer cells, consequently increasing the level of HSPs, improving the levels of tumor-associated antigen-specific IgG in the serum, and promoting the production of (IFN- γ) in the splenocytes. Thus, the DNA hydrogel-based PTT significantly inhibit the growth of tumor and prolong the survival of mice (Fig. 1a). Yata et al. reported the photothermally enhanced intracellular delivery of nanocarriers for CpG delivery [33]. In this work, they successfully used polyethylene glycol modified graphene oxide to load immune adjuvant CpG for photothermally enhanced immune response. The NIR optical absorbance of graphene oxide was further applied to promote the immunostimulatory activity of CpG, showing remarkably enhanced immune stimulation responses under laser irradiation, owing to the photothermally induced local heating that accelerated intracellular trafficking of CPG coated nanoparticles (Fig. 1b). In a following work, Lu and colleagues designed light-induced transformative CuS-based CpG systems for combined photothermal ablation and immunotherapy (Fig. 1c) [34]. After laser irradiation, the structures of nanoparticles break down, reassemble, and transform into polymer complexes that improve CpG tumor uptake and retention by plasmacytoid dendritic cells. Compared with immunotherapy or photothermal therapy alone, such CuS nanoparticles-mediated photothermal immunotherapy, exhibited more potent innate and adaptive immune responses, resulting in combined anticancer effects against primary treated and distant untreated tumors (Fig. 1d).

Besides the use of inorganic nano-agents, some small molecule dyes with high NIR absorbance have also been co-encapsulated with immunological stimulations into polymeric nanoparticles or liposomes for effective combination of PTT and immunotherapy. Li et al. developed an endogenous vaccine based on fluorophore-loaded liposomes (IR-7-lipo) coated with a multivalent immunoadjuvant (HA-CpG). Upon irradiation with 808 nm laser, IR-7-lipo induced cancer cell necrosis

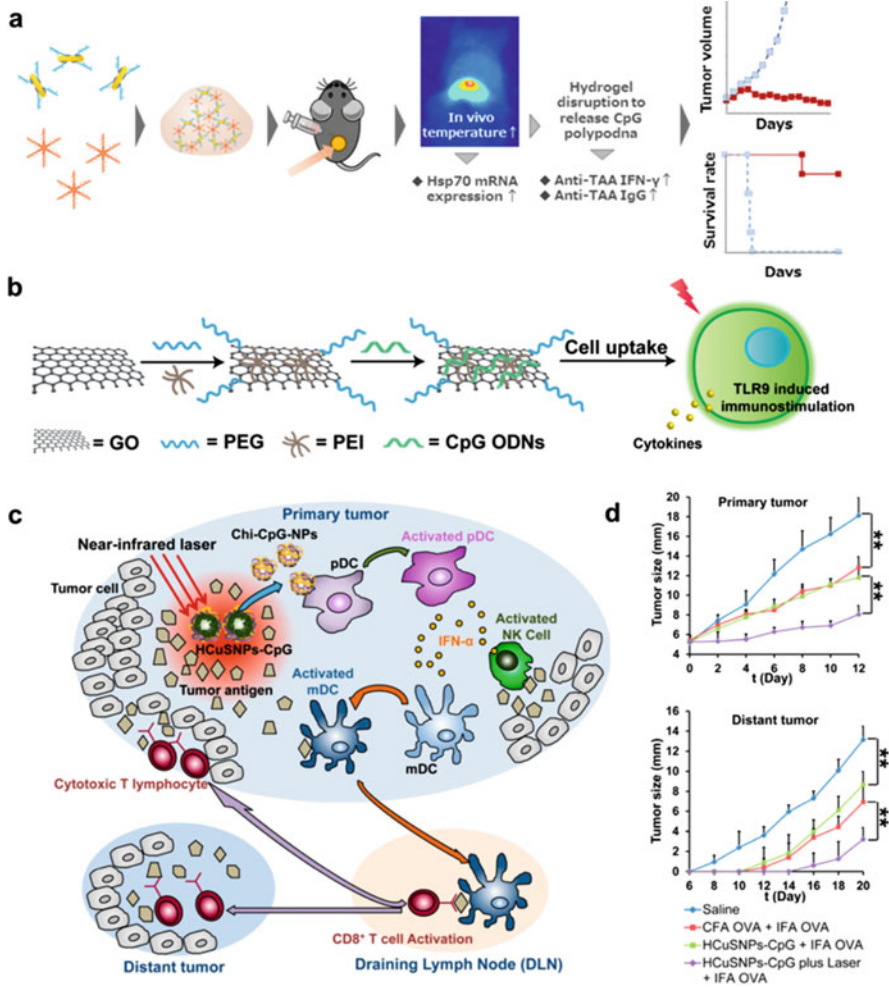


Fig. 1 Inorganic nano-agents based PTT mediated immunotherapy. **(a)** DNA hydrogel consisting of a hexapod-like structured DNA with CpG sequences and gold nanoparticles for photothermal immunotherapy. **(b)** Graphene oxide loaded immunostimulator CpG for photothermally enhanced cancer immunotherapy. **(c, d)** Chitosan-coated hollow copper sulfide nanoparticles for combined photothermal and immune cancer therapy, inhibiting the growth of primary treated and distant untreated tumors. Copyright from Elsevier, 2017 [31], Elsevier, 2014 [33], ACS, 2014 [34]

and released tumor-associated antigens, while the immunoadjuvant improved the expression of co-stimulatory molecules on DCs and promoted antigen presentation. The combination therapy of PTT and immunotherapy regulated the tumor micro-environment, enhanced antitumor immune response, eradicated tumors in mice and inhibited cancer metastasis [36]. Kumar et al. developed biodegradable and biocompatible poloxamer/glycated chitosan/polycaprolactone based nanoparticles

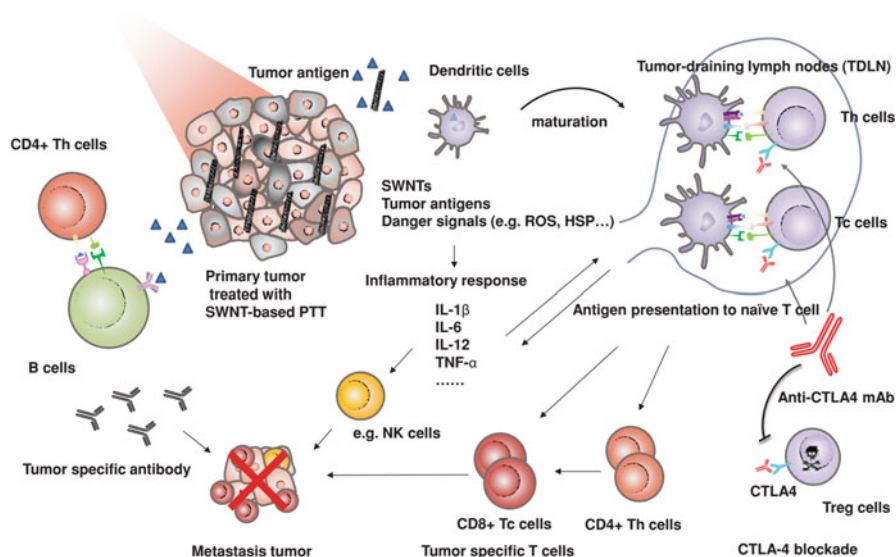


Fig. 2 Immunological responses triggered by carbon nanotubes-based photothermal therapy in combination with anti-CTLA-4 therapy to inhibit cancer metastasis. Copyright from Wiley-VCH, 2014 [38]

encapsulated with IR 820 for fluorescence imaging guided photo-immunotherapy [37]. Excitingly, glycol chitosan used here could work as the immunostimulatory agent and the IR 820 as the photothermal agent for PPT, both of them working together to kill drug and TNF- α dual-resistant breast cancer cells.

As an effective stimulator of the immune system, PTT also exhibits synergistic effects with immune checkpoint blockade to enhance immune stimulatory or reverse immune suppressive effects for T cell activation and proliferation. Liu and co-workers demonstrated the combination of anti-CTLA-4 with PTT using PEGylated single-wall carbon nanotubes (SWNTs) [38]. They found that polymer-coated SWNTs not only was used for photothermal tumor destruction, but also act as an immunological adjuvant to greatly promote maturation of DCs and production of anti-tumor cytokines. Moreover, CTLA-4 blockade applied after SWNT-based PTT of primary tumors would promote the infiltration of effective T cells and greatly abrogate regulatory T cells at distant tumors. Thus, such combined SWNT-based PTT and anti-CTLA-4 treatment was able to inhibit the growth of remaining cancer cells in both subcutaneous tumor model and lung metastasis model, promising for the treatment of cancer metastasis, the major cause of cancer death (Fig. 2). In a following work [39], they used three FDA-approved agents approved agents, PLGA as the encapsulating polymer, R837 as the immune adjuvant, and indocyanine green (ICG) as the near-infrared dye to enable PTT (Fig. 3). Upon photothermal ablation of primary tumors injected with PLGA-ICG-R837, the released tumor-associated antigens together with adjuvant (R837), could act as cancer vaccine,

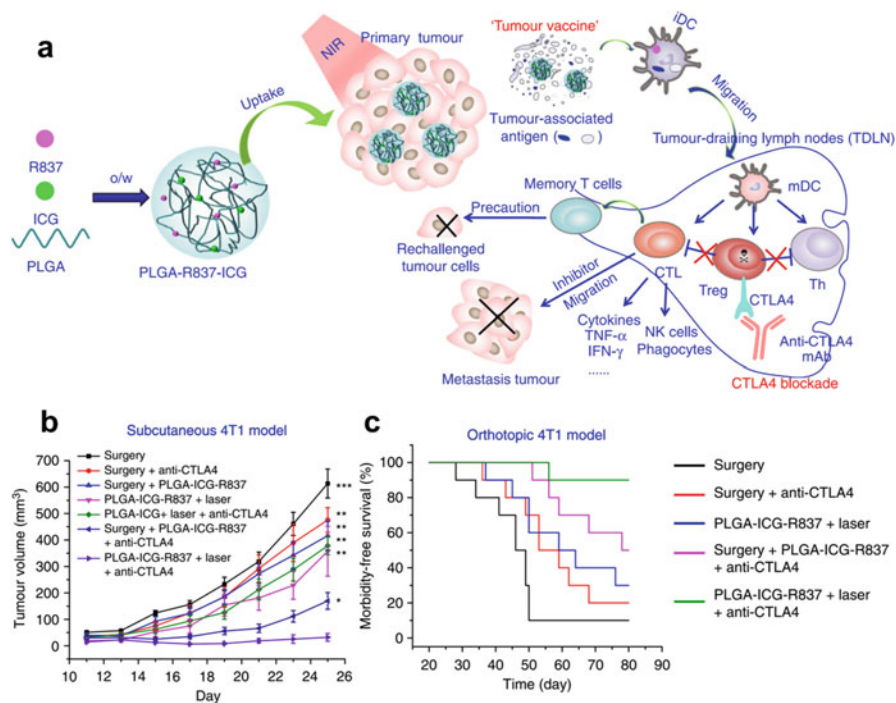


Fig. 3 Photothermal therapy with immune-adjuvant nanoparticles in combination with checkpoint blockade for effective cancer immunotherapy. **(a)** Scheme showing the mechanism of antitumor immune responses induced by PLGA-ICG-R837-based PTT together with checkpoint-blockade. **(b)** Tumor growth curves of mice after different treatment on subcutaneous 4T1 tumor model. **(c)** Morbidity-free survival of different groups of mice-bearing orthotopic 4T1 tumors with spontaneous metastases after various treatments. Copyright from Springer Nature, 2017 [39]

activating strong immunological responses. With the help of anti-CTLA4, which was able to inhibit the activities of Tregs, this strategy appeared to be particularly effective in inhibiting tumor metastasis. More importantly, such strategy exhibited strong immune-memory effect to protect mice from cancer recurrence.

3 Photodynamic Therapy

PDT is a clinically approved, minimally invasive therapeutic modality, depending on $^1\text{O}_2$ or ROS generated by photosensitizers under the appropriate light irradiation. Apart from destroying local tumor tissue and increasing the expression of several stress proteins, PDT could increase the tumor immunogenicity by increasing the expression of CAR and releasing tumor-associated antigens [40]. Moreover, PDT is able to cause acute local inflammation, which could attract different immune

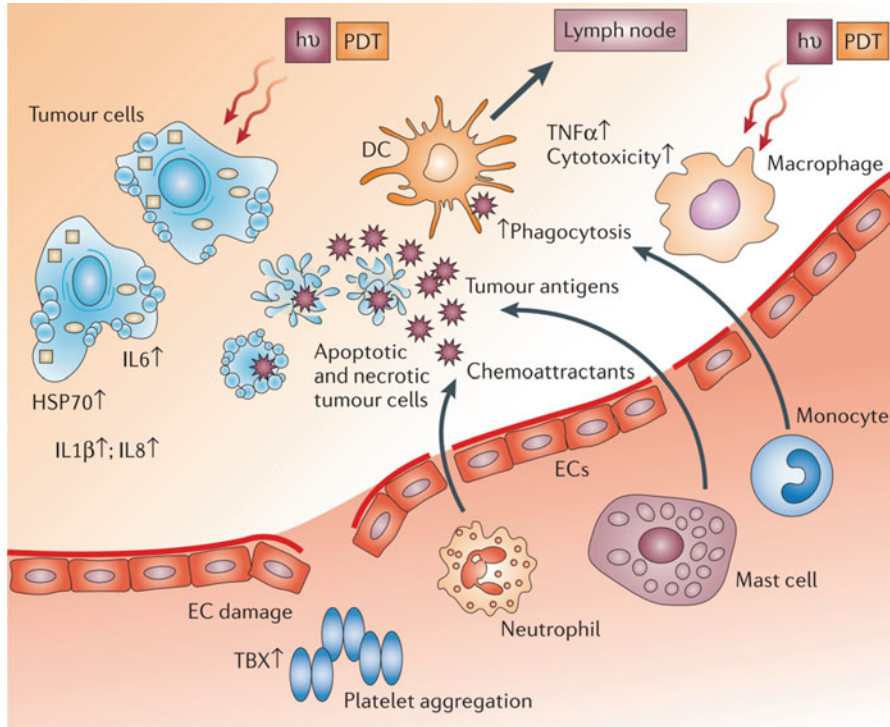


Fig. 4 Scheme showing the inflammation and immune responses induced by photodynamic therapy. The damage of endothelial cells after photodynamic therapy activates a case of events that lead to local inflammation, releasing different cytokines including interleukin 1 β (IL1 β), IL6 and IL8, the production of tumor-necrosis factor- α (TNF α), and infiltration of immune cells in the treated tumor. Necrotic and apoptotic tumor cells express heat-shock proteins (HSPs) and release tumor-associated antigens to DCs that migrate to lymph nodes to activate immune system. Copyright from Springer Nature, 2006 [40]

cells especially activated neutrophils into the tumor, activating both innate and adaptive immune systems (Fig. 4). Korbek group investigated the impact of PDT on the systemic and local kinetics of neutrophil trafficking and activity in different tumor models in mice. This study demonstrated that treatment of solid tumors by PDT indeed induced strong and protracted increase in systemic neutrophil numbers mediated by complement activation especially in the tumor [41]. In another work, Gollnick et al. also investigated the immunogenicity induced by PDT [42]. They found that the PDT-generated tumor cell lysates were potent vaccines, which was more effective than other modes of creating whole tumor vaccines, such as UV or ionizing irradiation. PDT-generated lysates could activate DCs to express IL-12, which is critical to the development of cellular immune responses.

Despite the immune responses induced by PDT alone, combination of PDT with immunological stimulators can further promote the immune responses. Posakony

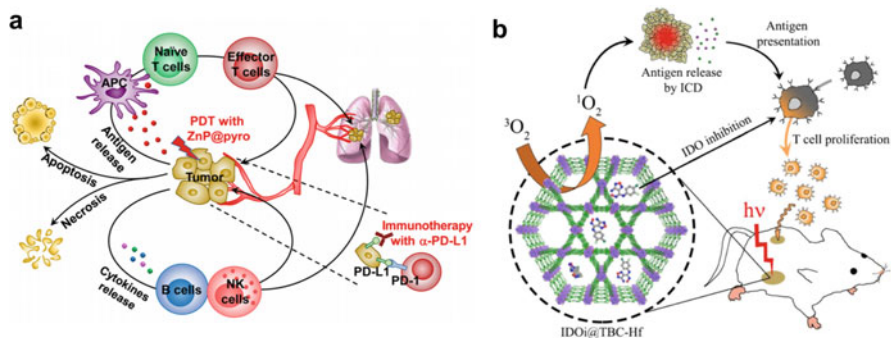


Fig. 5 Immunological responses triggered by nanoparticles-based photodynamic therapy in combination with immune checkpoint blockade. **(a)** The core–shell ZnP@pyro-based PDT treatment sensitizes tumors to anti-PD-L1 antibody, not only eradicating the primary 4 T1 breast tumor but also significantly preventing metastasis to the lung. **(b)** Chlorin-based nanoscale metal–organic framework (nMOF) loaded with a small-molecule IDO inhibitor for synergistic photodynamic and immunotherapy. Copyright from ACS, 2016 [46], ACS, 2016 [45]

and colleagues characterized and elucidated the nature of the interaction of optimized protocols of adjuvant Bacillus Calmette–Gue’rin (BCG) immunotherapy with PDT [43]. They found that BCG does not improve the efficiency of PDT during the early phase of tumor ablation, but significantly enhance the efficiency in preventing tumor recurrence by activating the T cells. Marrach et al. encapsulated ZnPc which is a long-wavelength absorbing PS within poly(D,L-lactic-co-glycolic acid)-b-poly(ethylene glycol) (PLGA-b-PEG). Then, coated the outside of the polymeric core with gold NPs (AuNPs) and modified with CpG-ODN. The hybrid nanoparticles containing both ZnPc and CpG-ODN after irradiation with a 660 nm light showed obvious photocytotoxicity to 4T1 metastatic mouse breast carcinoma cells. It was found that the combination of PDT with a synergistic immunostimulant in a single NP system resulted in significant immune response, which could be used for the treatment of metastatic cancer [44].

Considering the immunosuppression, immune checkpoint blockade also can be used enhance the immune responses induced by PDT. Lin and colleagues reported a treatment strategy that combined PDT based on a new chlorin-based nanoscale metal–organic framework (nMOF), TBC-Hf, and a small-molecule immunotherapy agent that inhibited IDO, encapsulated in the nMOF channels to induce systemic antitumor immunity. They detected increased T cell infiltration in the tumor microenvironment after activation of the immune system with the combination of IDO inhibition by the small-molecule immunotherapy agent and immunogenic cell death induced by PDT (Fig. 5a) [45]. Thus, the *in situ* vaccination induced by PDT working together with IDO inhibitors effectively trigger strong antitumor immune responses. In their a following work, they developed Zn-pyrophosphate (ZnP) nanoparticles loaded with photosensitizer pyrolipid (ZnP@pyro), which could cause the apoptosis and necrosis of tumor cells under the light irradiation, thus improving

the tumor immunogenicity (Fig. 5b). Moreover, the immunogenic ZnP@pyro-based PDT, particularly sensitizing tumor to anti-PD-L1 blockade, not only significantly eradicated the primary tumor but also prevented the tumor metastasis [46]. In another work, Wang et al. demonstrated that PDT-mediated cancer immunotherapy can be augmented by PD-L1 knockdown in cancer cells. They designed a versatile micelleplex by integrating an acid-activatable cationic micelle, photosensitizer (PS), and small interfering RNA (siRNA). Compared with PDT alone, the combination of PDT and PD-L1 KD showed significantly enhanced efficacy to inhibit tumor growth and metastasis in a B16-F10 melanoma tumor model [47].

The conventional photosensitizers for PDT are usually excited by visible light, which usually hampers the wide application of PDT owing to the limited tissue penetration depth. Many groups explored PDT using UCNPs, which are able to emit visible light under NIR light irradiation, showing much deeper tissue penetration compared to traditional visible light mediated PDT [21, 48]. Xu et al. utilized UCNPs to load chlorin e6 (Ce6), a photosensitizer, and R837, a Toll-like-receptor-7 agonist (UCNP-Ce6-R837) simultaneously for NIR-laser triggered PDT (Fig. 6). Similarly, UCNP-Ce6-R837 based PDT would enable effective photodynamic destruction of tumors to generate tumor-associated antigens, which

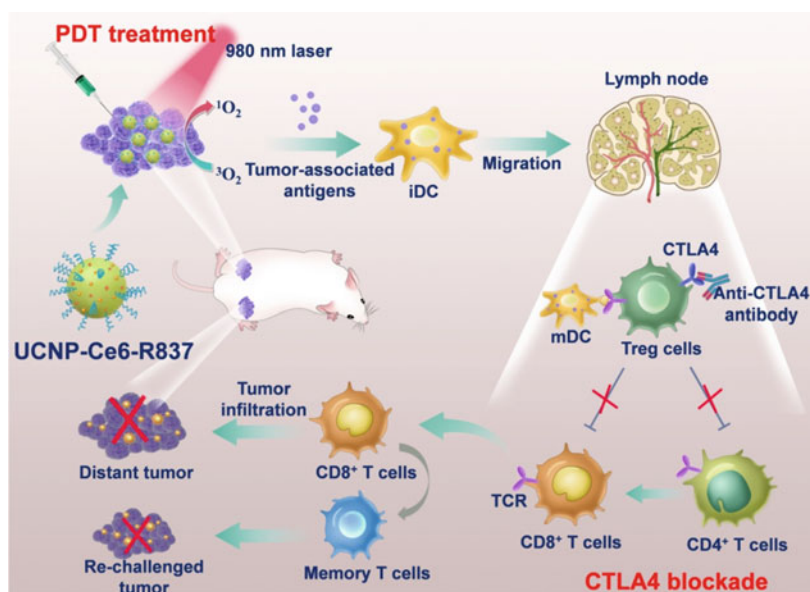


Fig. 6 Scheme showing the mechanism of combining NIR-mediated PDT with CTLA-4 checkpoint blockade for cancer immunotherapy. UCNP-Ce6-R837 nanoparticles under NIR light could enable effective photodynamic destruction of tumors and release tumor-associated antigens, which working together with adjuvant nanoparticles, inducing strong antitumor immune responses. With the help of a CTLA-4 checkpoint blockade, this strategy could effectively inhibit the tumor metastasis and recurrence. Copyright from ACS, 2017 [49]

in the presence of R837 were able to promote strong antitumor immune responses. More importantly, in combination with CTLA-4 checkpoint blockade, this strategy not only showed excellent efficacy in eliminating the primary tumors with treatment, but also resulted in strong antitumor immunities to inhibit the growth of distant tumors without treatment. Furthermore, such strategy also could provide a strong immune memory function to prevent cancer recurrence [49].

In addition to the limited penetration depth of the irradiation light, hypoxia (low oxygenation) in the tumor sites is another important barrier of PDT, as oxygen is required to generate ROS to kill cancer cells [50]. Moreover, the hypoxic tumor microenvironment usually limits the effective functions of T cells and promotes immunosuppression by multiple immunosuppressive cells including Tregs, M2 tumor-associated macrophages (TAM), and myeloid-derived suppressor cells (MDSC) [51]. To overcome the hypoxia in the solid tumor, Yang et al. fabricated hollow mesoporous MnO₂ nanoshells with PEG coating and photodynamic agent Ce6 and a chemotherapy drug doxorubicin (DOX) loading (H-MnO₂-PEG/C&D), as a multifunctional theranostic platform that was responsive to tumor microenvironment and was able to modulate TME, for enhanced cancer combination chemo-PDT therapy [52]. The relieved tumor hypoxia by MnO₂-triggered decomposition of endogenous H₂O₂ provided remarkable benefits not only for improving the efficacy of chemo-PDT, but also for reversing the immunosuppressive TME such as the polarization of tumor-associated macrophage to M1-phenotype to favor antitumor immunities post treatment. Further combination of with PD-L1 checkpoint blockade, such strategy offered an abscopal effect to inhibit the growth of not only primary tumors but also distant tumors without treatment owing to cytotoxic T cells (Fig. 7). Using a similar strategy, Lan et al. synthesized a nanoscale metal–organic framework (nMOF), consisting of Fe₃O clusters and photosensitizer 5,10,15,20-tetra(p-benzoato)porphyrin (TBP) ligands. Under the light irradiation in hypoxic

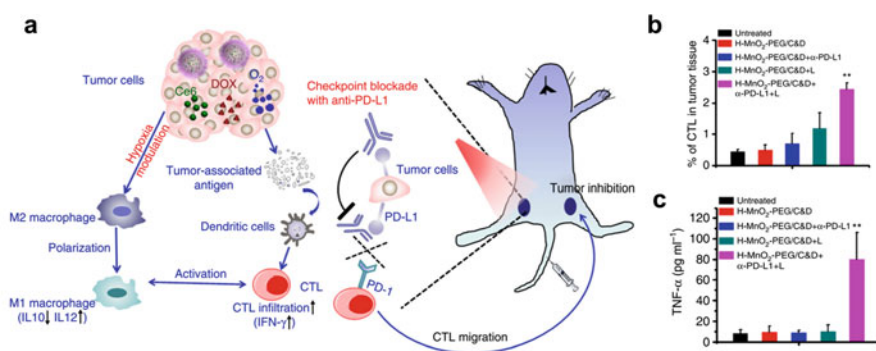


Fig. 7 Hollow MnO₂ as a tumor-microenvironment responsive nano-platform for combination therapy favoring antitumor immune responses. (a) scheme showing the mechanism of anti-tumor immune responses induced by H-MnO₂ complex in combination with anti-PD-L1 therapy. (b) The percentage of cytotoxic T lymphocytes (CTL) infiltrated in distant tumors. (c) The concentration of TNF-α in sera of mice after different treatments. Copyright from Springer Nature, 2017 [52]

tumors, Fe₃O clusters could induce the decomposition of endogenous H₂O₂ to produce O₂ via the Fenton-like reaction. nMOF-based PDT induced anti-tumor immune responses, achieving synergistic therapeutic effect with PD-L1 checkpoint blockade [53].

4 Conclusion and Future Perspectives

Photo-immunotherapy has exhibited promising pre-clinical responses on different tumor models due to its unique superiorities including specific antitumor immunity and long-term immunological memory responses. As shown in this chapter, novel nanoparticles-enabled phototherapy could induce apoptotic and necrotic tumor cell death, which is different from most traditional cytotoxic agents that usually induce apoptotic tumor cell death. In case of necrosis, also called immunogenic cell death, cytoplasmic components spill over into extracellular space via the damaged plasma membrane and induce strong inflammatory responses, and the debris of tumor cells after phototherapy could act as tumor-associated antigens. The acute inflammation caused by phototherapy could further potentiate immune responses by attracting various immune cells and promoting the tumor-associated antigen presentation to the active cellular immune system. The immune responses induced by phototherapy can work synergistically with immune checkpoint blockade to improve the therapeutic outcomes with limited side effects.

Despite the progress achieved, more work is still needed to investigate the dynamic immune response and understand how phototherapy impacts the specific cellular aspects of antitumor immunity, with the aim of providing basic principles or guidance for combination of phototherapy and immunotherapy for an individual patient. Specifically, one point to be considered is to optimize phototherapy for inducing local tumor cures and producing inflammation to stimulate the immune system. Furthermore, it is also important to design suitable nanoparticle mediated phototherapy that is suitable to in combination with immune adjuvant or immune checkpoint blockade. The timing and dosing frequency of immune checkpoint blockade also are very important to the therapeutic efficacy and should be explored in more details.

References

1. Cheng, L., Wang, C., Feng, L., Yang, K., Liu, Z.: Functional nanomaterials for phototherapies of cancer. *Chem. Rev.* **114**, 10869–10939 (2014)
2. Bown, S.: Phototherapy of tumors. *World J. Surg.* **7**, 700–709 (1983)
3. Xia, Y., et al.: Gold nanocages: from synthesis to theranostic applications. *Acc. Chem. Res.* **44**, 914–924 (2011)
4. Nikoobakht, B., El-Sayed, M.A.: Preparation and growth mechanism of gold nanorods (NRs) using seed-mediated growth method. *Chem. Mater.* **15**, 1957–1962 (2003)

5. Yang, K., Feng, L., Shi, X., Liu, Z.: Nano-graphene in biomedicine: theranostic applications. *Chem. Soc. Rev.* **42**, 530–547 (2013)
6. Tian, Q., et al.: Hydrophilic flower-like CuS superstructures as an efficient 980 nm laser-driven photothermal agent for ablation of cancer cells. *Adv. Mater.* **23**, 3542–3547 (2011)
7. Zhou, M., et al.: A chelator-free multifunctional [64Cu] CuS nanoparticle platform for simultaneous micro-PET/CT imaging and photothermal ablation therapy. *J. Am. Chem. Soc.* **132**, 15351–15358 (2010)
8. Huang, X., et al.: Freestanding palladium nanosheets with plasmonic and catalytic properties. *Nat. Nanotechnol.* **6**, 28 (2011)
9. Cheng, L., et al.: PEGylated WS₂ nanosheets as a multifunctional theranostic agent for in vivo dual-modal CT/photoacoustic imaging guided photothermal therapy. *Adv. Mater.* **26**, 1886–1893 (2014)
10. Liu, T., et al.: Drug delivery with PEGylated MoS₂ nano-sheets for combined photothermal and chemotherapy of cancer. *Adv. Mater.* **26**, 3433–3440 (2014)
11. Cheng, L., Yang, K., Chen, Q., Liu, Z.: Organic stealth nanoparticles for highly effective in vivo near-infrared photothermal therapy of cancer. *ACS Nano.* **6**, 5605–5613 (2012)
12. Yang, K., et al.: In vitro and in vivo near-infrared photothermal therapy of cancer using polypyrrole organic nanoparticles. *Adv. Mater.* **24**, 5586–5592 (2012)
13. Lovell, J.F., et al.: Porphysome nanovesicles generated by porphyrin bilayers for use as multimodal biophotonic contrast agents. *Nat. Mater.* **10**, 324 (2011)
14. Cheng, L., et al.: PEGylated micelle nanoparticles encapsulating a non-fluorescent near-infrared organic dye as a safe and highly-effective photothermal agent for in vivo cancer therapy. *Adv. Funct. Mater.* **23**, 5893–5902 (2013)
15. Nie, S.: Understanding and overcoming major barriers in cancer nanomedicine. *Nanomedicine.* **5**, 523–528 (2010)
16. Jiang, F., et al.: Photodynamic therapy of U87 human glioma in nude rat using liposome-delivered photofrin. *Lasers Surg. Med.* **22**, 74–80 (1998)
17. Son, K.J., et al.: Photosensitizing hollow nanocapsules for combination cancer therapy. *Angew. Chem.* **123**, 12174–12177 (2011)
18. Banerjee, R., et al.: Nanomedicine: magnetic nanoparticles and their biomedical applications. *Curr. Med. Chem.* **17**, 3120–3141 (2010)
19. Tu, H.L., et al.: In vitro studies of functionalized mesoporous silica nanoparticles for photodynamic therapy. *Adv. Mater.* **21**, 172–177 (2009)
20. Gandra, N., et al.: Photosensitized singlet oxygen production upon two-photon excitation of single-walled carbon nanotubes and their functionalized analogues. *J. Phys. Chem. C.* **113**, 5182–5185 (2009)
21. Wang, C., Tao, H., Cheng, L., Liu, Z.: Near-infrared light induced in vivo photodynamic therapy of cancer based on upconversion nanoparticles. *Biomaterials.* **32**, 6145–6154 (2011)
22. Duan, X., Chan, C., Lin, W.: Nanoparticle-mediated immunogenic cell death enables and potentiates cancer immunotherapy. *Angew. Chem. Int. Ed.* **58**, 670–680 (2019)
23. Joffre, O., Nolte, M.A., Spörri, R., Sousa, C.R.E.: Inflammatory signals in dendritic cell activation and the induction of adaptive immunity. *Immunol. Rev.* **227**, 234–247 (2009)
24. Kono, H., Rock, K.L.: How dying cells alert the immune system to danger. *Nat. Rev. Immunol.* **8**, 279 (2008)
25. Scaffidi, P., Misteli, T., Bianchi, M.E.: Release of chromatin protein HMGB1 by necrotic cells triggers inflammation. *Nature.* **418**, 191 (2002)
26. Obeid, M., et al.: Calreticulin exposure dictates the immunogenicity of cancer cell death. *Nat. Med.* **13**, 54 (2007)
27. Nestle, F.O., et al.: Vaccination of melanoma patients with peptide-or tumorlysate-pulsed dendritic cells. *Nat. Med.* **4**, 328 (1998)
28. Pardoll, D.M.: The blockade of immune checkpoints in cancer immunotherapy. *Nat. Rev. Cancer.* **12**, 252 (2012)
29. Chen, W.R., Adams, R.L., Carubelli, R., Nordquist, R.E.: Laser-photosensitizer assisted immunotherapy: a novel modality for cancer treatment. *Cancer Lett.* **115**, 25–30 (1997)

30. Li, X., et al.: Clinical effects of in situ photoimmunotherapy on late-stage melanoma patients: a preliminary study. *Cancer Biol. Ther.* **10**, 1081–1087 (2010)
31. Yata, T., et al.: DNA nanotechnology-based composite-type gold nanoparticle-immunostimulatory DNA hydrogel for tumor photothermal immunotherapy. *Biomaterials.* **146**, 136–145 (2017)
32. Zhou, F., et al.: Antitumor immunologically modified carbon nanotubes for photothermal therapy. *Biomaterials.* **33**, 3235–3242 (2012)
33. Tao, Y., Ju, E., Ren, J., Qu, X.: Immunostimulatory oligonucleotides-loaded cationic graphene oxide with photothermally enhanced immunogenicity for photothermal/immune cancer therapy. *Biomaterials.* **35**, 9963–9971 (2014)
34. Guo, L., et al.: Combinatorial photothermal and immuno cancer therapy using chitosan-coated hollow copper sulfide nanoparticles. *ACS Nano.* **8**, 5670–5681 (2014)
35. Han, Q., et al.: CpG loaded MoS₂ nanosheets as multifunctional agents for photothermal enhanced cancer immunotherapy. *Nanoscale.* **9**, 5927–5934 (2017)
36. Li, L., et al.: An endogenous vaccine based on fluorophores and multivalent immunoadjuvants regulates tumor micro-environment for synergistic photothermal and immunotherapy. *Theranostics.* **8**, 860 (2018)
37. Kumar, P., Srivastava, R.: IR 820 dye encapsulated in polycaprolactone glycol chitosan: Poloxamer blend nanoparticles for photo immunotherapy for breast cancer. *Mater. Sci. Eng. C.* **57**, 321–327 (2015)
38. Wang, C., et al.: Immunological responses triggered by photothermal therapy with carbon nanotubes in combination with anti-CTLA-4 therapy to inhibit cancer metastasis. *Adv. Mater.* **26**, 8154–8162 (2014)
39. Chen, Q., et al.: Photothermal therapy with immune-adjuvant nanoparticles together with checkpoint blockade for effective cancer immunotherapy. *Nat. Commun.* **7**, 13193 (2016)
40. Castano, A.P., Mroz, P., Hamblin, M.R.: Photodynamic therapy and anti-tumour immunity. *Nat. Rev. Cancer.* **6**, 535 (2006)
41. Ceccic, I., Parkins, C.S., Korbelik, M.: Induction of systemic neutrophil response in mice by photodynamic therapy of solid tumors. *Photochem. Photobiol.* **74**, 712–720 (2001)
42. Gollnick, S.O., Vaughan, L., Henderson, B.W.: Generation of effective antitumor vaccines using photodynamic therapy. *Cancer Res.* **62**, 1604–1608 (2002)
43. Korbelik, M., Sun, J., Posakony, J.J.: Interaction between photodynamic therapy and BCG immunotherapy responsible for the reduced recurrence of treated mouse tumors. *Photochem. Photobiol.* **73**, 403–409 (2001)
44. Marrache, S., et al.: Immune stimulating photoactive hybrid nanoparticles for metastatic breast cancer. *Integr. Biol.* **5**, 215–223 (2012)
45. Lu, K., et al.: Chlorin-based nanoscale metal–organic framework systemically rejects colorectal cancers via synergistic photodynamic therapy and checkpoint blockade immunotherapy. *J. Am. Chem. Soc.* **138**, 12502–12510 (2016)
46. Duan, X., et al.: Photodynamic therapy mediated by nontoxic core–shell nanoparticles synergizes with immune checkpoint blockade to elicit antitumor immunity and antimetastatic effect on breast cancer. *J. Am. Chem. Soc.* **138**, 16686–16695 (2016)
47. Wang, D., et al.: Acid-activatable versatile micelleplexes for PD-L1 blockade-enhanced cancer photodynamic immunotherapy. *Nano Lett.* **16**, 5503–5513 (2016)
48. Idris, N.M., et al.: In vivo photodynamic therapy using upconversion nanoparticles as remote-controlled nanotransducers. *Nat. Med.* **18**, 1580 (2012)
49. Xu, J., et al.: Near-infrared-triggered photodynamic therapy with multitasking upconversion nanoparticles in combination with checkpoint blockade for immunotherapy of colorectal cancer. *ACS Nano.* **11**, 4463–4474 (2017)
50. Chen, Q., et al.: Intelligent albumin–MnO₂ nanoparticles as pH-/H₂O₂-responsive dissociable nanocarriers to modulate tumor hypoxia for effective combination therapy. *Adv. Mater.* **28**, 7129–7136 (2016)

51. Huang, Y., et al.: Vascular normalizing doses of antiangiogenic treatment reprogram the immunosuppressive tumor microenvironment and enhance immunotherapy. *Proc. Natl. Acad. Sci.* **109**, 17561–17566 (2012)
52. Yang, G., et al.: Hollow MnO₂ as a tumor-microenvironment-responsive biodegradable nano-platform for combination therapy favoring antitumor immune responses. *Nat. Commun.* **8**, 902 (2017)
53. Lan, G., et al.: Nanoscale metal–organic framework overcomes hypoxia for photodynamic therapy primed cancer immunotherapy. *J. Am. Chem. Soc.* **140**, 5670–5673 (2018)

Development of Nanoparticles as a Vaccine Platform



Kenichi Niikura

1 Cellular Uptake of Nanoparticles and their Biodistribution

1.1 Effects of Size and Shape In Vitro

Nanoparticles and nanoparticle assemblies of different size and shape with various surface molecules have been synthesized in an effort to achieve efficient cellular uptake and/or induce immune responses (Fig. 1). In developing vaccines using nanoparticles, the first issue is how to set the particle size. The effect of nanoparticle size on their interactions with cells has been explored using quantum dots. Quantum dots are small particles, often with size of 10 nm or less, the localization of which can be detected in cells by their size-dependent fluorescence. With regard to interactions between cells and fluorescent quantum dots (CdTe), it has been reported that their distribution in cells differs in a size-dependent manner. Nabiev et al. reported that green QDs (2.1 nm in diameter) accumulated in the nuclei of THP-1 cells while the larger red QDs (3.4 nm in diameter) were retained in the cytoplasm [1]. When two particles of different size were added to cells at the same time, the green QDs were specifically deposited in the nuclei, suggesting that only smaller particles can be transported to the nucleus through the pores in the nuclear membrane. Chan and colleagues reported the size dependence of gold nanoparticles on incorporation efficiency into cells [2]. Gold nanoparticles have an advantage in that the particle size and shape can be easily controlled and that the number of gold particles in cells can be quantified by inductively coupled plasma atomic emission spectroscopy. In their experiments using gold nanoparticles in the range of 14–100 nm, those of 50 nm in diameter showed the most efficient incorporation

K. Niikura (✉)

Department of Applied Chemistry, Nippon Institute of Technology, Miyashiro, Saitama, Japan
e-mail: niikura.kenichi@nit.ac.jp

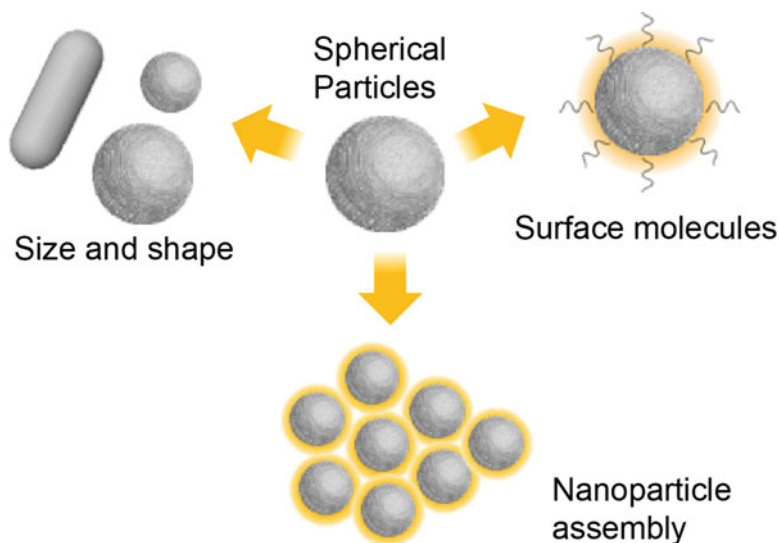


Fig. 1 Various factors associated with nanoparticles that affect cellular uptake and immune responses

into HeLa cells. Further, they investigated the effects of nanoparticle shape using gold nanorods and spherical gold nanoparticles. When the aspect ratio of the gold nanorods was increased, the uptake was lower than that of spherical particles. These reports suggest that both the size and shape of the nanoparticles are important factors in the development of nanoparticle vaccines.

Recently, we compared the uptake of triangular gold nanoplates with that of spherical particles [3]. Triangular plates with planar portions may be able to deliver more antigenic protein into cells than spherical particles of the same volume. The method of synthesizing triangular gold nanoplates was reported by Liz-Marzañ et al. [4]. The particle surface was coated with a ligand possessing a carboxylic acid, and the number of particles taken into HeLa cells and RAW264.7 cells was estimated after incubation for 24 hrs in cell culture medium (DMEM with 10% FBS). Four types of triangular plates having a side length of 46 to 94 nm were synthesized. For comparison, spherical particles (22, 39, and 66 nm in diameter) with a surface area or volume close to those of the triangular plates were also synthesized. Interestingly, in the case of the triangular plates, the uptake increased with increase in side length, whereas the uptake of the spheres decreased with increase in diameter. This reversed trend was similar in two types of cells. This probably indicates that nanoparticle shape and size affect their interactions with receptors on the cell membrane, or with the cell membrane itself, and the subsequent endocytosis process. The uptake mechanism in our study has not been elucidated yet, but these data suggest that the shape and size of nanoparticles have an impact on their interactions with cells and the subsequent uptake efficacy.

Lin et al. reported the cellular uptake and uptake mechanism of methylpolyethylene glycol (mPEG) -coated triangular gold plates, nanorods, and star-shaped gold particles [5]. Of these three, the uptake of the triangular plates by RAW 264.7 cells was the most efficient. Interestingly, it was shown that while the clathrin-mediated endocytic pathway is a common mechanism in endocytosis, there are other different uptake pathways that are dependent on particle shape. For the uptake of such non-specific particles, various factors, such as surface ligand density and type of serum proteins bound, can contribute to particle uptake. It is, therefore, difficult to compare particle shapes to identify which is the best for cellular uptake. However, different uptake mechanisms are more important for vaccine applications as the immune pathway may be controlled by changing the nanoparticle shape and size. In addition, the effects of shape and size are related to each other in a complex way (including other factors), thus, systematic studies dependent on the administration pathway will be essential to future research on nanoparticle vaccines.

It has long been known that polymer particles themselves act as adjuvants [6]. In recent years, the effects of the size and shape of soft materials such as polymers, rather than hard materials such as metals, have been investigated. Particles made of biocompatible molecules have great potential for vaccine applications. Caruso et al. have successfully controlled the size and shape of polyethylene glycol (PEG) capsules by coating the surface of silica with PEG and then removing the silica core [7]. The surface of the capsules was covered with antibodies that bind specifically to the cell surface. The degree of cellular uptake of these soft materials with controlled shapes (spherical and rod-like) and sizes were then compared. Furthermore, in order to eliminate the effect of particle sedimentation, incubation of cells was performed under two conditions: dynamic (with medium stirring) and static. The degree of their uptake was in the following order; small rods < large spheres < small spheres < large rods, for both incubation methods. Thus, even in the case of soft materials, the effect of size is also dependent on shape, and the combined effect of shape and size effect on cellular uptake remains complicated.

The effect of the shape of particles has been discussed not only in terms of the number taken up by cells but also in terms of their function as part of a drug transport system. Xu et al. used polycation-functionalized gold nanoparticles to investigate the effect of shape on gene transfection [8]. The binding of DNA to Au particles with an arrow-headed rod-like shape (~44 nm in length, ~12 nm in diameter) was shown to be the most efficient for gene expression in cells, whereas a spherical shape of about 40 nm in diameter showed low efficiency. Higher uptake into cells is one reason for the excellent gene transfection of the arrow-headed Au particles. Thus, research linking the shape and function of nanoparticles will become more important and receive more attention.

1.2 Design of Surface Ligand Molecules for Cytosolic Delivery

When delivering nanoparticles into a cell, the location within the cell is important to the subsequent immune responses. In particular, transportation into the cytosol from the lysosome enables activation of MHC class I cell-mediated immunity through antigen presentation [9]. Moreover, since some toll-like receptors are located in the cytosol, the specific immune pathway can be activated by the targeting these receptors. In this section, we will introduce the method of transporting nanoparticles into the cytosol by through surface modification. Rottelo et al. reported an interesting approach to the cytosolic delivery of proteins using nanoparticle-stabilized capsules [10]. Nanoparticle-stabilized capsules, which are constructed through the self-assembly of gold nanoparticles, have been reported to act as carriers for the cytosolic delivery of proteins through direct membrane fusion. By displaying guanidine and imidazole residues on the nanoparticle surface, proteins weakly bound to the capsule surface were released into the cytosol.

A supramolecular approach affords a powerful tool even for the transportation of nanoparticles. The multivalent display of molecules on a single nanoparticle induces dynamic changes to the surface character depending on the molecular conformation. We designed a molecule with a branched structure consisting of hydrophilic oligoethylene glycol (OEG) and a short-chain alkyl group (C8) to cover gold nanoparticles (Fig. 2) [11]. The OEG site and the alkyl chain site of this molecule are immobilized by a flexible ether bond so that the molecule can move according to the environment. In a hydrophobic environment, in particular, exposure of the alkyl chain site to the outermost surface can be expected to promote penetration of the particles into a biological membrane. The branched molecules were presented on the surface of gold nanoparticles with quaternary cation molecules for the attachment of siRNAs. Only when the branched molecules were displayed, the suppression of luciferase expression in HeLa cells was confirmed, suggesting that the siRNAs were delivered into the cytosol. Electron microscopic observation of cell sections suggested that a majority of the particles were trapped in the endosomes, but a portion of the particles taken up had migrated to the cytoplasm. This study suggests that approaches using supramolecules on a particle surface would be useful for the delivery of antigenic proteins and adjuvant molecules.

1.3 Effects of Size and Shape on Biodistributions In Vivo

The shape and size of nanoparticles affect not only their interactions with cells but also their biodistribution *in vivo*. The PRINT method developed by DeSimone et al. is known to be a powerful method capable of controlling the size and shape of polymers [12]. The biodistribution of PEG-coated 80×320 nm rod-like hydrogel particles and 55×60 nm sphere-like hydrogel particles prepared by the PRINT method was reported in tumor-bearing mice. The sphere-like particles showed a

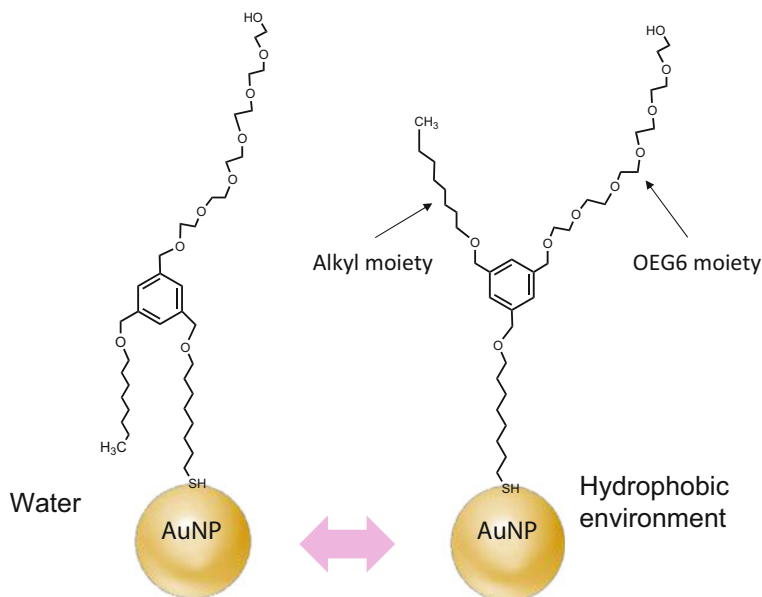


Fig. 2 Branched molecule for the cytosolic delivery of nanoparticle [11]

two-fold larger accumulation in the liver, while the rod-like particles tended to accumulate in the spleen in comparison with the sphere-like particles, meaning that shape is an important factor in the organ-specific delivery of nanomaterials. The effects of shape and size effect nanomaterials on biodistribution were also explored using fluorescent mesoporous silica nanoparticles [13]. In these studies, short rods (185 nm) were trapped in the liver in the early stage of uptake and long rods (720 nm) tended to accumulate in the spleen. These data indicate that the shape of nanomaterials impacts their biodistribution.

Biodistribution has also been studied using PEGylated gold nanoparticles doped with radioactive gold atoms (Radioactive Au-doped gold nanoparticles) without fluorescent dyes [14]. Interestingly, spherical gold nanoparticles showed much longer blood circulation compared to nanorods, nanodisks and nanocages of a similar size (~ 50 nm). Mitragotri et al. clarified the effect of shape from a physico-chemical approach [15]. They prepared antibodies-coated polystyrene nanospheres and nanorods with the same volume and the interaction with the antigens immobilized in the microfluidic system was examined under flow conditions. They found that nanorods showed higher adhesion in a specific manner than did the nanospheres and applied the shape-specific effect of the particles to endothelial targeting.

2 Effects of Particle Shape and Size on Immune Response

2.1 Merits of Using Nanoparticles for Vaccines

This section focuses on vaccine development using nanoparticles. Antigens and adjuvants play important roles in vaccines. Adjuvant is the general term for substances used to enhance the immunogenicity of an antigen. In many cases, sufficient immunogenicity cannot be obtained with antigen proteins alone, and adjuvants may be added to enhance antigenicity, which reduces the number of inoculations and the amount of expensive antigens required for protection. There are several benefits to using nanoparticles as a vaccine: (1) The use of particles can prevent the rapid degradation of encapsulated or immobilized antigens. (2) They can deliver antigens in a manner similar to the structure of the original virus. B cells that recognize viral antigens on the cell surface are known to strongly recognize and respond to the repetitive structure of viral proteins that are characteristic of viruses [16]. In fact, it is known that virus-like capsules can be effective vaccines. (3) Multiple molecules such as adjuvants and antigens can simultaneously sent to immune cells. (4) The particles themselves can act as adjuvants.

If particles themselves can alter the immune response, particles could elicit a response qualitatively different from that of the antigen alone. Natural viruses vary in size and shape and there are many hints in their shape and size to design nanomaterials [17]. The immune responses are also expected to be sensitive to the size and shape of the virus. Nanoparticles have various physicochemical factors such as shape, size, surface charge, hydrophobicity, and rigidity. Adjusting these factors allows control of the adjuvant and vaccine activity.

2.2 Effects of Nanoparticle Size on Vaccine Activity

This section summarizes the effects of size and shape of nanoparticles on immunization. The effects of polymer particle size on immune response were reported by Plebanski et al. [18]. Polymer nanoparticles with different diameters (20–123 nm in diameter) were coated with ovalbumin protein (OVA) and the coated particles were administered intradermally to the hind footpads of mice. They found that immobilization on the particles increased the amount of antibody produced against OVA compared to when the mice were inoculated with OVA in solution and, interestingly, the type of cytokine response in spleen cell samples from the mice differed according to particles size. Particles about 40 nm induced IFN- γ responses associated with the Th1 route, while particles of about 100 nm induced IL-4 responses associated with the Th2 route. This indicates that the Th1 and Th2 immune reactions; that is, the immune activation pathways, differ depending on particle size.

Akashi et al. reported vaccine studies using hydrophobic poly (γ -glutamic acid) (γ -PGA) nanoparticles, which are highly biocompatible polymers. They synthesized antigen-loaded polymer nanoparticles using modified γ -PGA with hydrophobic amino acids and immunized mice subcutaneously [19, 20]. Interestingly, the polymer particles strongly induced antigen-specific cellular immunity in addition to humoral immunity. For antigen-specific cellular immunity, antigen presentation by the MHC-class I pathway is necessary. Thus, they speculated that the polymer particles can cause antigen leakage from the endosomes into the cytosol in immune cells. Akashi et al. also found that the addition of polymer particles (mean diameter: 460 nm) to dendritic cells promotes the expression of genes associated with phagocytosis and protective immune response [21]. This indicates that the nanoparticles themselves have an adjuvant effect.

There are several reports on the use of nanoparticles to activate the cellular immune pathway. Jewell et al. proposed a nanoparticle vaccine in which both antigen peptides and adjuvant poly ICs are assembled on the surface of gold nanoparticles through a layer-by-layer (LbL) method [22]. A major feature of their LbL approach is the simultaneous immobilization of adjuvant and antigen molecules on the nanoparticle without the use of other synthetic polymers, thereby preventing the unexpected activation of immune responses. The LbL-coated gold nanoparticles induced antigen-specific T cell responses, which is a key process in cell-mediated immunity, in both dendritic cell experiments and *in vivo* experiments in mice. No effect was seen with a mixed solution of the antigen and the adjuvant molecule, indicating the importance of their co-display on the same particle [22].

The mucosal immune response is important for protection against viral and bacterial infections. The effects of particle size on intranasal immunization have also been reported [23]. OVA, as an antigen model, was immobilized on 30 or 200 nm polypropylene sulfide nanoparticles for intranasal administration in mice. Even when the amount of the injected antigen was the same, they found that using 200 nm particles was more effective for the induction of both systemic IgG and mucosal IgA in serum.

2.3 Effects of Nanoparticle Shape on Vaccine Activity

Gold nanoparticles have commonly been used for biomedical applications [24–26], such as nanoparticle-based vaccines and adjuvants. Maysinger et al. found that the type of cytokines secreted in immune cells, called microglia, when treated with gold nanoparticles was dependent on the shape of the nanoparticles (spherical, sea urchin-like or rod-shaped nanoparticles) [27]. Furthermore, when administered intranasally to mice, microglial activation was found to be the highest for rod-shaped particles. This report indicates the possibility of eliciting different immune cell responses depending on the shape of the nanomaterials at the cellular and *in vivo* levels.

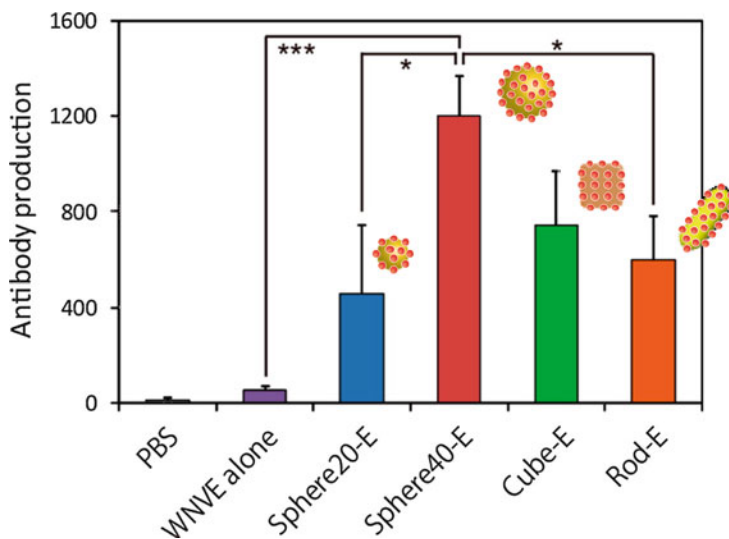


Fig. 3 West Nile virus envelope (WNVE) protein-specific IgG ELISA end-point titers in mice immunized twice with 100 ng WNVE/animal. Significant differences: * $p < 0.05$; *** $p < 0.001$ (means \pm SEM, $n = 10$). Sphere40-E provided the highest level of antibody induction among the four different AuNPs. WNVE protein alone induced only low-level anti-WNVE IgG antibody production. Adapted with permission from reference 28 (*ACS Nano* 2013, 7, 5, 3926–3938). Copyright (2013) American Chemical Society

We prepared gold nano-sized spheres, rods, and cubes that were coated with West Nile virus antigen and investigated which shape induced the greatest antibody production when intraperitoneally administered to mice [28]. Cationic particles were coated with an anionic polymer, and antigen proteins were immobilized on the polymer by electrostatic interactions. In this experiment, as the surface area differed depending on the shape, the number of particles administered was adjusted so that the amount of antigen was the same. It was found that spherical particles of 40 nm induced the highest level of antibody production (Fig. 3). The rod-shaped particles also induced a lower level of antibody production than did spherical particles of 40 nm in diameter. Exploring the reasons for this at the cellular level revealed that the types of cytokines differed between 40 nm spheres and rod particles, while 20 nm spheres induced much lower cytokine production. The difference could not be explained by the number of particles taken up into the cells. Although it is not possible to immediately link the results of the cell and animal experiments, these suggest that the potential exists to control vaccine activity by optimization of the size and shape of the particles.

Chan et al. reported the effects of particle size on antibody production in terms of the underlying mechanism [29]. OVA-attached gold nanoparticles of 50 and 100 nm in size induced larger humoral immune responses compared to small particles (5–15 nm) when administered to the intradermal footpad of mice, as the large particles

bound to the surface of follicle dendritic cells in the lymph node follicles, enabling efficient display of the antigens on the nanoparticles to B cells. On the other hand, the smaller particles tended to be internalized into the cells.

Recently, we reported gold nanoparticle-based SARS vaccines [30]. The spike (S) proteins of coronavirus were electrostatically conjugated with gold nanoparticles (40 nm in size) and S-AuNP conjugates were subcutaneously immunized to mice. A strong induction of IgG against the S protein was observed in a manner similar to the results of the West Nile virus experiment. However, the conjugation induced highly allergic inflammatory responses and failed to induce any protective immune responses against the virus. This indicates that, for practical vaccine development, a simple increase in IgG production against antigens is not sufficient. Rather, we need to consider how the antigens are displayed on the nanoparticle surface to produce protective antibodies and how to suppress allergic inflammatory responses. Particle shape and size may affect cell uptake efficiency, tissue localization, adjuvant activity, and the ability of cells to bind to receptors. In the future, further elucidation of the mechanisms underlying the effects of the shape and size on vaccine activity will lead to the development of new vaccines that can suppress side reactions and appropriately activate the desired immune pathway.

We fabricated short poly (I:C) adjuvant molecules conjugated with gold nanoparticles of various sizes and shapes and investigated how the shape and size of the particles affected intranasal and subcutaneous administration [31]. In this experiment, 100 ng of hemagglutinin (HA), antigen HA protein, was administered. In the case of subcutaneous administration, there was no significant difference in IgG production among the different shapes and sizes. Interestingly, in the case of nasal administration, the IgA production level for 40 nm spherical particles was lower than those for the other particles. Further, the effect of shape on nasal administration was marked by a reduction in the amount of antigen from 100 to 10 ng. Immobilization of poly (I:C) on rod-shaped particles was more effective in lowering the virus titer remaining in the nasal cavity than was that of spherical particles (Fig. 4). In this study, adjuvant molecules were immobilized on gold nanoparticles instead of antigens, but it has been shown that immobilization of adjuvants can also improve the effectiveness of vaccines in a shape-dependent manner.

3 Summary

This chapter summarized recent studies on the cellular uptake of nanoparticles and their effects on immune response *in vivo*. Although they are of nanoscale, there are a wide variety of factors that need to be addressed when considering nanoparticles: size, shape, surface molecules (hydrophobicity and charge), and so on. In fact, surface molecules on particles also have a large impact on immune responses [32]. Many studies have shown that these physico-chemical factors strongly influence the efficiency of cellular uptake, distribution *in vivo*, and immune

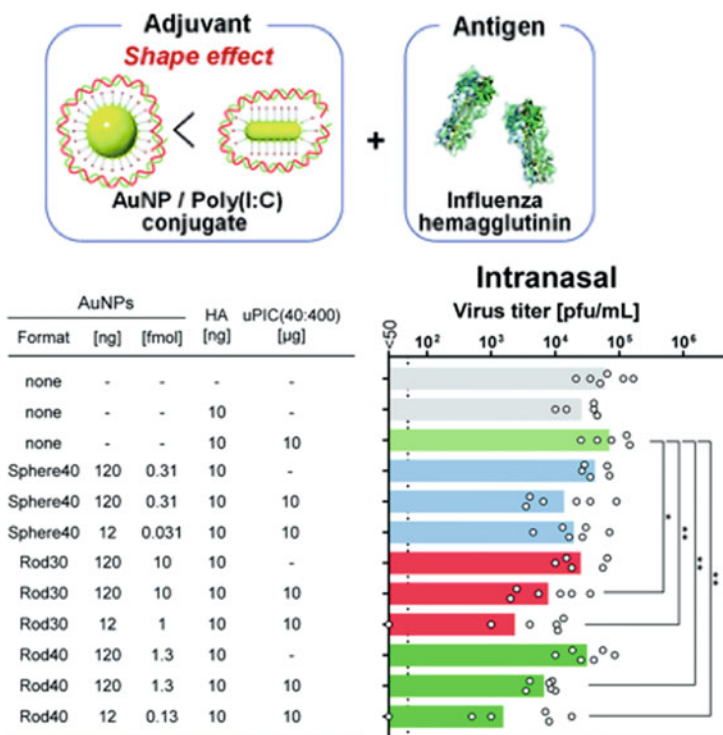


Fig. 4 The reduction in the viral load in nasal wash obtained from mice immunized intranasally with 10 ng of antigen HA protein. Sphere 40: spherical gold nanoparticles with a diameter of ca. 40 nm. Rod30 and rod40: gold nanorods with a length of ca. 30 and 40 nm, respectively. Gold nanoparticles and nanorods were complexed with poly(I:C) adjuvant and administered with influenza HA antigens. The graph indicates that rod30 and rod40 were more effective than was sphere40 as a carrier of poly(I:C) to reduce viral load. Adapted from reference 31 (*RSC Adv.* **2018**, 16,527–16,536). Copyright (2018) Royal Society of Chemistry

responses. Based on these phenomena, it is necessary to study the mechanisms of how nanoparticles interact with biomolecules and circulate in the living body to give rise to those phenomena. The application of nanoparticles to vaccines is an important and attractive field in which nanotechnology can contribute to life sciences from multiple perspectives including materials science, physics, biology, and pharmaceuticals. These interdisciplinary studies are expected to aid in the development of effective and safe nanoparticle-based vaccines.

Acknowledgments The author acknowledges support from a JSPS Grant-in-Aid for Scientific Research Grant Number 19 K05217 and 16H0822.

References

1. Nabiev, I., Mitchell, S., Davies, A., Williams, Y., Kelleher, D., Moore, R., Gun'ko, Y.K., Byrne, S., Rakovich, Y.P., Donegan, J.F., Sukhanova, A., Conroy, J., Cottell, D., Gaponik, N., Rogach, A., Volkov, Y.: Nonfunctionalized nanocrystals can exploit a cell's active transport machinery delivering them to specific nuclear and cytoplasmic compartments. *Nano Lett.* **7**, 3452–3461 (2007). <https://doi.org/10.1021/nl0719832>
2. Chithrani, B.D., Ghazani, A.A., Chan, W.C.W.: Determining the size and shape dependence of gold nanoparticle uptake into mammalian cells. *Nano Lett.* **6**, 662–668 (2006). <https://doi.org/10.1021/nl052396o>
3. Nambara, K., Niikura, K., Mitomo, H., Ninomiya, T., Takeuchi, C., Wei, J., Matsuo, Y., Ijiro, K.: Reverse size dependences of the cellular uptake of triangular and spherical gold nanoparticles. *Langmuir*. **32**, 12559–12567 (2016). <https://doi.org/10.1021/acs.langmuir.6b02064>
4. Scarabelli, L., Coronado-Puchau, M., Giner-Casares, J.J., Langer, J., Liz-Marzán, L.M.: Monodisperse gold nanotriangles: size control, large-scale self-assembly, and performance in surface-enhanced Raman scattering. *ACS Nano*. **8**, 5833–5842 (2014). <https://doi.org/10.1021/nl500727w>
5. Xie, X., Liao, J., Shao, X., Li, Q., Lin, Y.: The effect of shape on cellular uptake of gold nanoparticles in the forms of stars, rods, and triangles. *Sci. Rep.* **7**, 3827 (2017). <https://doi.org/10.1038/s41598-017-04229-z>
6. Kreuter, J., Speiser, P.P.: New adjuvants on a polymethylmethacrylate base. *Infect. Immun.* **13**, 204–210 (1976)
7. Song, D., Cui, J., Ju, Y., Faria, M., Sun, H., Howard, C.B., Thurecht, K.J., Caruso, F.: Cellular targeting of biospecific antibody-functionalized poly(ethylene glycol) capsules: do shape and size matter? *ACS Appl. Mater. Interfaces*. **11**, 28720–28731 (2019). <https://doi.org/10.1021/acscami.9b10304>
8. Yan, P., Wang, R., Zhao, N., Zhao, H., Chen, D.-F., Xu, F.-J.: Polycation-functionalized gold nanoparticles with different morphologies for superior gene transfection. *Nanoscale*. **7**, 5281–5291 (2015). <https://doi.org/10.1039/C5NR00481K>
9. Zhu, M., Wang, R., Nie, G.: Applications of nanomaterials as vaccine adjuvants. *Hum. Vaccin. Immunother.* **10**, 2761–2774 (2014). <https://doi.org/10.4161/hv.29589>
10. Tang, R., Jiang, Z., Ray, M., Houa, S., Rotello, V.M.: Cytosolic delivery of large proteins using nanoparticle-stabilized nanocapsules. *Nanoscale*. **8**, 18038–18041 (2016). <https://doi.org/10.1039/C6NR07162G>
11. Niikura, K., Kobayashi, K., Takeuchi, C., Fujitani, N., Takahara, S., Ninomiya, T., Hagiwara, K., Mitomo, H., Ito, Y., Osada, Y., Ijiro, K.: Amphiphilic gold nanoparticles displaying flexible bifurcated ligands as a carrier for siRNA delivery into the cell cytosol. *ACS Appl. Mater. Interfaces*. **6**, 22146–22154 (2014). <https://doi.org/10.1021/am505577j>
12. Reuter, K.G., Perry, J.L., Kim, D., Luft, J.C., Liu, R., DeSimone, J.M.: Targeted PRINT hydrogels: the role of nanoparticle size and ligand density on cell association, biodistribution, and tumor accumulation. *Nano Lett.* **15**, 6371–6378 (2015). <https://doi.org/10.1021/acs.nanolett.5b01362>
13. Huang, X., Li, L., Liu, T., Hao, N., Liu, H., Chen, D., Tang, F.: The shape effect of mesoporous silica nanoparticles on biodistribution, clearance, and biocompatibility in vivo. *ACS Nano*. **5**, 5390–5399 (2011). <https://doi.org/10.1021/nl200365a>
14. Black, K.C.L., Wang, Y., Luehmann, H.P., Cai, X., Xing, W., Pang, B., Zhao, Y., Cutler, C.S., Wang, L.V., Liu, Y., Xia, Y.: Radioactive ¹⁹⁸Au-doped nanostructures with different shapes for in vivo analyses of their biodistribution, tumor uptake, and intratumoral distribution. *ACS Nano*. **8**, 4385–4394 (2014). <https://doi.org/10.1021/nl406258m>
15. Kolhar, P., Anselmo, A.C., Gupta, V., Pant, K., Prabhakar Pandian, B., Ruoslahti, E., Mitragotri, S.: Using shape effects to target antibody-coated nanoparticles to lung and brain endothelium. *Proc. Natl. Acad. Sci. U. S. A.* **110**, 10753–10758 (2013). <https://doi.org/10.1073/pnas.1308345110>

16. Bachmann, M.F., Rohrer, U.H., Kundig, T.M., Burki, K., Hengartner, H., Zinkernagel, R.M.: The influence of antigen organization on B cell responsiveness. *Science*. **262**, 1448–1451 (1993). <https://doi.org/10.1126/science.8248784>
17. Kinnear, C., Moore, T.L., Rodriguez-Lorenzo, L., Rothen-Rutishauser, B., Petri-Fink, A.: Form follows function: nanoparticle shape and its implications for nanomedicine. *Chem. Rev.* **117**, 11476–11521 (2017). <https://doi.org/10.1021/acs.chemrev.7b00194>
18. Mottram, P.L., Leong, D., Crimeen-Irwin, B., Gloster, S., Xiang, S.D., Meanger, J., Ghildyal, R., Vardaxis, N., Plebanski, M.: Type 1 and 2 immunity following vaccination is influenced by nanoparticle size: formulation of a model vaccine for respiratory syncytial virus. *Mol. Pharm.* **4**, 73–84 (2007). <https://doi.org/10.1021/mp060096p>
19. Akagi, T., Zhu, Y., Shima, F., Akashi, M.: Biodegradable nanoparticles composed of enantiomeric poly(γ -glutamic acid)-graft-poly(lactide) copolymers as vaccine carriers for dominant induction of cellular immunity. *Biomater. Sci.* **2**, 530–537 (2014). <https://doi.org/10.1039/C3BM60279F>
20. Shima, F., Akagi, T., Akashi, M.: Effect of hydrophobic side chains in the induction of immune responses by nanoparticle adjuvants consisting of amphiphilic poly(γ -glutamic acid). *Bioconjug. Chem.* **26**, 890–898 (2015). <https://doi.org/10.1021/acs.bioconjchem.5b00106>
21. Matsusaki, M., Larsson, K., Akagi, T., Lindstedt, M., Akashi, M., Borrebaeck, C.A.K.: Nanosphere induced gene expression in human dendritic cells. *Nano Lett.* **5**, 2168–2173 (2005). <https://doi.org/10.1021/nl050541s>
22. Zhang, P., Chiu, Y.-C., Tostanoski, L.H., Jewell, C.M.: Polyelectrolyte multilayers assembled entirely from immune signals on gold nanoparticle templates promote antigen-specific T cell response. *ACS Nano*. **9**, 6465–6477 (2015). <https://doi.org/10.1021/acsnano.5b02153>
23. Stano, A., Nembrini, C., Swartz, M.A., Hubbell, J.A., Simeoni, E.: Nanoparticle size influences the magnitude and quality of mucosal immune responses after intranasal immunization. *Vaccine*. **30**, 7541–7546 (2012). <https://doi.org/10.1016/j.vaccine.2012.10.050>
24. Dykman, L.A., Khlebtsov, N.G.: Immunological properties of gold nanoparticles. *Chem. Sci.* **8**, 1719–1735 (2017). <https://doi.org/10.1039/C6SC03631G>
25. Yang, X., Yang, M., Pang, B., Vara, M., Xia, Y.: Gold nanomaterials at work in biomedicine. *Chem. Rev.* **115**, 10410–10488 (2015). <https://doi.org/10.1021/acs.chemrev.5b00193>
26. Giljohann, D.A., Seferos, D.S., Daniel, W.L., Massich, M.D., Patel, P.C., Mirkin, C.A.: Gold nanoparticles for biology and medicine. *Angew. Chem. Int. Ed.* **49**, 3280–3294 (2010). <https://doi.org/10.1002/anie.200904359>
27. Hutter, E., Boridy, S., Labrecque, S., Lalancette-Hébert, M., Kriz, J., Winnik, F.M., Maysinger, D.: Microglial response to gold nanoparticles. *ACS Nano*. **4**, 2595–2606 (2010). <https://doi.org/10.1021/nn901869f>
28. Niikura, K., Matsunaga, T., Suzuki, T., Kobayashi, S., Yamaguchi, H., Orba, Y., Kawaguchi, A., Hasegawa, H., Kajino, K., Ninomiya, T., Ijio, K., Sawa, H.: Gold nanoparticles as a vaccine platform: influence of size and shape on immunological responses in vitro and in vivo. *ACS Nano*. **7**, 3926–3938 (2013). <https://doi.org/10.1021/nn3057005>
29. Zhang, Y.-N., Lazarovits, J., Poon, W., Ouyang, B., Nguyen, L.N.M., Kingston, B.R., Chan, W.C.W.: Nanoparticle size influences antigen retention and presentation in lymph node follicles for humoral immunity. *Nano Lett.* **19**, 7226–7235 (2019). <https://doi.org/10.1021/acs.nanolett.9b02834>
30. Sekimukai, H., Iwata-Yoshikawa, N., Fukushi, S., Tani, H., Kataoka, M., Suzuki, T., Hasegawa, H., Niikura, K., Arai, K., Nagata, N.: Gold nanoparticle-adjuvanted S protein induces a strong antigen-specific IgG response against severe acute respiratory syndrome-related coronavirus infection, but fails to induce protective antibodies and limit eosinophilic infiltration in lungs. *Microbiol. Immunol.* **64**, 33–51 (2020). <https://doi.org/10.1111/1348-0421.12754>
31. Tazaki, T., Tabata, K., Aina, A., Ohara, Y., Kobayashi, S., Ninomiya, T., Orba, Y., Mitomo, H., Nakano, T., Hasegawa, H., Ijio, K., Sawa, H., Suzuki, T., Niikura, K.: Shape-dependent adjuvanticity of nanoparticle-conjugated RNA adjuvants for intranasal inactivated influenza vaccines. *RSC Adv.* **8**, 16527–16536 (2018). <https://doi.org/10.1039/C8RA01690A>
32. Moyano, D.F., Goldsmith, M., Solfiell, D.J., Landesman-Milo, D., Miranda, O.R., Peer, D., Rotello, V.M.: Nanoparticle hydrophobicity dictates immune response. *J. Am. Chem. Soc.* **134**(9), 3965–3967 (2012). <https://doi.org/10.1021/ja2108905>

Multifunctional Gold Nanostars for Sensitive Detection, Photothermal Treatment and Immunotherapy of Brain Tumor



Yang Liu, Pakawat Chongsathidkiet, Ren Odion, Peter E. Fecci, and Tuan Vo-Dinh 

1 Introduction

Intracranial tumor is a major public health issue and the morbidity associated with intracranial tumor growth is substantial [1, 2]. Of different brain tumors, glioblastoma (GBM) is the most common and aggressive one with more than 10,000 newly diagnosed patients in the United States each year [3, 4]. Even with the highest first year cost (> \$120,000), the prognosis for GBM patients is dismal and the median survival is only 15 months after aggressive standard of care treatments including surgical resection, chemotherapy and radiation therapy [5, 6]. Less than 5% of the patients survives for more than 3 years [7]. Cancer vaccine has been

Y. Liu · T. Vo-Dinh (✉)

Fitzpatrick Institute for Photonics, Duke University, Durham, NC, USA

Department of Biomedical Engineering, Duke University, Durham, NC, USA

Department of Chemistry, Duke University, Durham, NC, USA

e-mail: tuan.vodinh@duke.edu

P. Chongsathidkiet

Department of Neurosurgery, Duke University School of Medicine, Durham, NC, USA

Brain Tumor Immunotherapy Program, Duke University Medical Center, Durham, NC, USA

R. Odion

Department of Biomedical Engineering, Duke University, Durham, NC, USA

Department of Chemistry, Duke University, Durham, NC, USA

P. E. Fecci

Department of Neurosurgery, Duke University School of Medicine, Durham, NC, USA

Brain Tumor Immunotherapy Program, Duke University Medical Center, Durham, NC, USA

Department of Pathology, Duke University Graduate School, Durham, NC, USA

Department of Immunology, Duke University Graduate School, Durham, NC, USA

considered as a promising approach to improve GBM patients' outcomes but several phase II and phase III trials did not show significant survival difference from controls [8–10]. Although oncolytic virus therapy demonstrated promising results in Phase I and Phase II trials, larger Phase III trials are required to demonstrate that their benefits outweigh the risks [11–14]. Even for the state-of-the-art checkpoint inhibitor immunotherapy, the clinical trial results are disappointing and a recent Phase 3 clinical trial of PD-1 inhibitor (nivolumab) failed to demonstrate survival improvement compared to the current treatment [15–17]. CAR-T cell therapy is another interesting approach leveraging genetically modified T cells, but the overall survival of patients was not improved in a clinical trial potentially due to the tumor immunosuppressive microenvironment [18, 19]. Despite decades of efforts, GBM is still a deadly disease without effective treatment options. It is thus clear that radically new therapeutic approaches are urgently needed for patients with GBM.

We have developed a novel toxic surfactant-free method to synthesize star-shaped gold nanoparticles, named as gold nanostars (GNS), for GBM detection and treatment [20]. GNS nanoparticles have a tunable plasmonic peak in the near infrared (NIR) tissue optical window, making it suitable for *in vivo* biomedical applications. Furthermore, GNS nanoparticles have unique tip-enhanced plasmonics, which enables superior electromagnetic field enhancement near their sharp spikes. GNS has extremely high two-photon luminescence (TPL) cross-section (more than 4.0×10^6 Göppert–Mayer unit), which is 100 times higher than gold nanorod and 8000 times higher than gold nanocube [21]. The GNS has also been found to have higher photon-to-heat conversion efficiency than gold nanoshell (94% compared to 61%) [22]. This chapter provides an overview of the application of GNS as versatile and biocompatible nanoplatform for detection and photoimmunotherapy in murine models of GBM.

2 Theoretical Consideration of Laser Excitation Energy into a Brain Tissue Phantom

The thermal response of laser-irradiated tissue is highly dependent on the unique optical properties of the tissue. Photons propagating in the tissue go through a series of scattering and absorption events wherein the photon's energy is randomly scattered off in a different direction or absorbed. The behavior of the photon in tissue is thus highly dependent on the molecular composition and geometrical configuration of the tissue. For example, visible light readily passes through air and glass without being absorbed, yet most objects such as our skin will block this light. On the other hand, high energy photons such as X-rays will readily pass through most of our body's soft tissue.

To achieve optimal photothermal efficiency of the GNS-mediated LITT treatment, several factors should be considered: (1) the optical properties of the tissue, (2) the laser excitation wavelength, (3) the absorption efficiency of the GNS

platform, and (4) the photon-to-heat conversion of GNS are especially important factors in thermal therapies that utilize laser irradiation such as the LITT modality. Applications that use lasers utilizing wavelengths below infrared must contend with limited penetration depth along with off-target absorption and heating. Tissue such as the skin and blood vessels will absorb much of the laser energy before reaching a tumor tissue target for example. Different strategies must be employed to circumvent this limited penetration to deliver enough energy to the tumor site to induce ablation or hyperthermia. Laser delivery by optical fiber is the most common strategy in which the fiber head is invasively placed near the target area to deliver the laser light directly. Another option is to optical sources of specific wavelengths of light that are the tissue “optical window”, a narrow wavelength band between 700 and 1100 nm where there is little tissue absorption. The use of the 1064-nm laser in this study is suitable to excite within this optical window, where tissue components absorb the least and photon can travel deeper in tissue. The GNSs have a tunable plasmonic absorption band in the near infrared region around 1000 nm, where there is low tissue absorption, and therefore they are most suitable for LITT-based photothermal treatment. Gold nanostars have a very high photon to heat conversion, and paired with its ability to target tumors via the Enhanced-Permeation and Retention (EPR) effect, the nanoplatform can be used to greatly enhance photothermal therapy.

In this study we investigate the optical response of tissue to analyze the resulting heating after laser irradiation via an optical fiber onto a tissue phantom. The spatio-temporal evolution of the aggregate photons’ energy in a layer can be modelled using a second order differential equation shown below.

$$\frac{1}{c} \frac{\partial \varphi(r, t)}{\partial t} + \mu_a \varphi(r, t) - \frac{1}{3(\mu_a + \mu_s')} \frac{\partial^2 \varphi(r, t)}{\partial r \partial t} = S(r, t) \quad (1)$$

$$\delta = \sqrt{\frac{1}{3\mu_a(\mu_a + \mu_s')}} \quad (2)$$

In short, this diffusion equation models the concentration of photon energy in a volume as captured by the term φ (it is also known as the fluence rate). This equation describes the position and movement of the photon concentration through time and is dictated mainly by three terms: the absorption coefficient μ_a , the scattering coefficient μ_s , and the light source S . These properties are either intrinsic to the material or dependent on the light source geometry. The second equation is known as the penetration depth and is roughly the inverse of the sum of the absorption and scattering coefficient of the material. It is the depth at which the magnitude of the energy decays to $1/e$ of its value. One can see that the penetration of a laser is thus inversely proportional to the optical absorption and scattering of the material. A steady-state solution of this diffusion equation can also be simplified to the well-known Beer-Lambert Law with some unit conversion with the optical properties.

From there, the optical properties can be measured experimentally using absorption spectroscopy.

The diffusion equation is a simple model and relies on the assumption that the scattering of the material is much greater than the absorption (the material must be turbid). Additionally, the equation breaks down for distances below the mean free path length between interactions $l_t < 1/(\mu_a + \mu_s')$. The Monte Carlo Modeling of Photon Transport is a numerical method that uses utilizes a stochastic model to estimate ensemble-averaged quantities [23]. In this context, the ensemble of simulated randomly scattered and absorbed photons is simply the photon energy concentration in space and time (the same as the diffusion equation from earlier). The algorithm consists of randomly sampling variables from probability density functions. These include the photon step size, scattering angle, absorption, etc. A specified number of photons are individually launched and tracked, each depositing energy in different voxel coordinates. The final output consists of a photon fluence map that can be converted to an absorption map.

Monte Carlo Simulations of Laser Irradiation of Gold Nanostars in Optically Scattering Tissue. A key goal is modelling the interaction light with tissue once there is a volume of highly absorbing gold nanostars embedded within. This can show the effective use of gold nanostars as a localized heat zone for more specific thermal therapy. The model depicts a homogenous layer of a specified optical property at 1064-nm excitation. Gray matter of brain tissue is chosen as the model tissue as there is a clinical need for more effective treatment of glioblastoma that minimizes off target heating and damage. Taken from existing literature, the absorption and scattering coefficients are 0.56 and 56.8 cm^{-1} respectively with an anisotropy value g of 0.9 [24].

The optical properties of the gold nanostar was experimentally determined using absorption spectroscopy. Since nanoparticles including GNSs have the tendency to accumulate preferentially in tumors due to the EPR effect, we use the tumor model as an area that contains concentration of GNS. Our studies using mouse model have determined that the GNS concentration in tumors is approximately 20 $\mu\text{g/g}$ (0.1 nM) using inductively coupled plasma mass spectrometry (ICP-MS) and nanoparticle tracking analysis. To match the typical amount of gold nanostar found accumulated in tumors, the concentration of the GNS particles was set to 0.1 nM, which corresponds to an absorption coefficient of about 1.154 cm^{-1} . This absorption was added to baseline optical property of the surrounding tissue. A collimated beam with a radius of 1 cm and an isotropic point source placed 3 cm within the volume were chosen as sources. These correspond to typical laser irradiation configurations with a standoff beam and a fiber delivered source. A spherical volume containing only the gold nanostar was embedded within the tissue near the source. Each simulation was set to run for 30 minutes, roughly corresponding to about 20 million photons. The point source simulation depicts the typical penetration depth of light through brain tissue, while the collimated beam simulation models the immuno photothermal setup used in further experiments showing increased absorption in regions with high GNS concentrations such as in tumors.

Fig. 1 Monte Carlo simulation of absorbed photon energy in gray matter from a laser point source laser

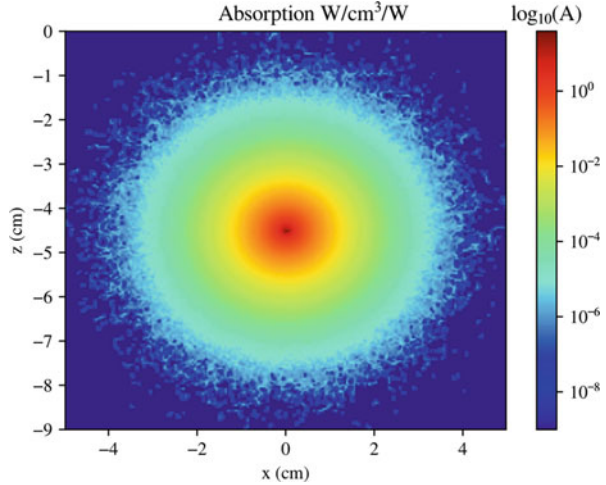


Figure 1 depicts the logarithmic absorption of energy through the gray matter tissue. Most of the energy was deposited in a localized region close to the laser source and quickly drops off after a few millimeters. This corresponds to the calculated penetration depth of 0.31 cm, a value that reinforces the notion that light inside tissue does not travel very far before losing much of its energy. The results of this simulation also points to a more limited kill radius as less of the overall target tissue is ultimately heated.

Figure 2a shows the log scale energy absorption simulation that corresponds to a collimated laser beam (initially in the air) toward the tissue mimicking the optical response of gray matter brain tissue. Figures 2b shows the energy absorption map of tissue having a simulated tumor (the spherical volume of gold nanostars) near the laser excitation location. The Monte Carlo theoretical simulation results show markedly higher absorption of the tumor area relative to the surrounding tissue. The results of these simulations point to higher specificity in photon absorption where there are gold nanostars. With gold nanostars' high photon-to-heat conversion, heating is much more efficient as well. This demonstrates the feasibility of gold nanostars as a nanoplatform for selective and efficient heating of targeted photothermal therapy. From the point of view of clinical treatment of brain tumors, the current LITT technology is limited by ablation volume or a distribution that does not adequately conform to tumor margins, resulting in either incomplete penetration across the tumor or collateral damage to healthy tissues beyond its margins. Our theoretical study demonstrates combining LITT with gold nanoparticles that act as “lightning rods” can expand laser treatment coverages by conducting heat more efficiently than normal tissue. Furthermore, GNS selectively accumulate within intracranial tumors and both expand coverage and protect surrounding healthy tissue structures.

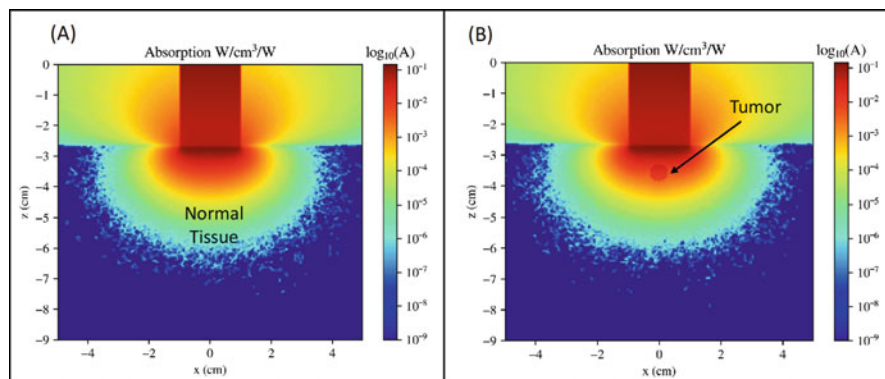


Fig. 2 (a) Energy absorption simulation that correspond to a collimated laser beam (initially in the air) toward the tissue; (b) Energy absorption simulation that correspond to a collimated laser beam (initially in the air) toward the tissue having a tumor containing gold nanostars. The Monte Carlo theoretical simulation results show markedly higher absorption of the tumor area relative to the surrounding normal tissue

3 Sensitive Brain Cancer Detection with Gold Nanostars

Sensitive brain cancer imaging may result in earlier detection, improved ability to determine extent of disease, and better treatment planning, which could improve patients' outcome as tumor size has been found to be an important prognostic factor [25]. Magnetic resonance imaging (MRI) is an imaging modality effective for soft tissue examination and has been widely used as the clinical diagnostic method for a suspected brain tumor [26, 27]. The smallest detectable tumor size for MRI modality is approximately 3 mm [28–31]. Positron emission tomography (PET) is a quantitative and highly sensitive imaging modality with a detection threshold as low as 10^{-12} M for positron emitters [32, 33]. However, traditional ^{18}F -FDG PET is not ideal for brain tumor detection because brain tumors tend to be isometabolic or even hypometabolic compared to normal brain tissue [34, 35]. Therefore, it is of great significance to develop novel methods for sensitive brain tumor imaging aimed to improve early detection, treatment guidance and therapeutic response monitoring.

We have developed a GNS nanoprobe radiolabeled with ^{124}I for sensitive brain tumor detection using PET imaging [36]. GNS nanoparticles were labeled with ^{124}I through strong I-Au chemical bonding with $>98\%$ labeling efficiency after 30 minutes incubation at room temperature. The stability of radiolabeled GNS was examined in both phosphate-buffered saline (PBS) and plasma with anti-clotting heparin. Experimental results showed that $97.2 \pm 0.2\%$ (PBS) and $97.7 \pm 0.4\%$ (plasma) of ^{124}I remained on the GNS after 7-day incubation at 37°C . The developed GNS nanoprobe accumulates selectively in brain tumor through compromised blood-brain barrier (BBB) (Fig. 3) after injection via tail vein into two different orthotopic glioma models, intracranial injection of U87MG GBM

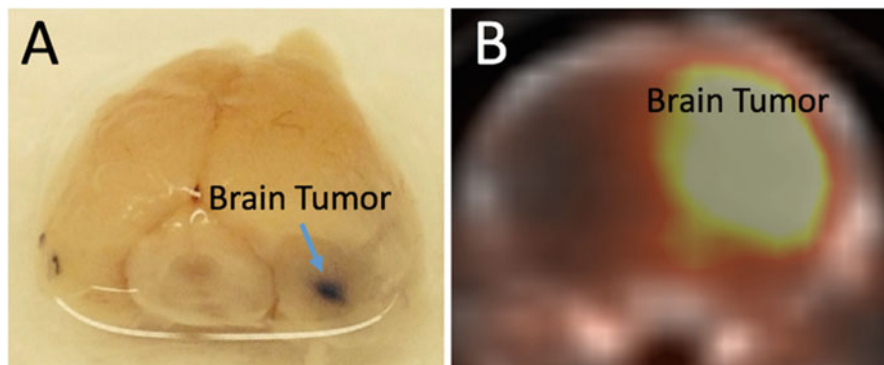


Fig. 3 GNS accumulation in intracranial murine models of GBM (a) Gross specimen of mouse brain with brain tumor shown in black color due to the uptake of light-absorbing GNS nanoparticles. The specimen was collected at 24 h after IV injection of GNS. (b) PET/CT scan of brain-tumor bearing mouse 48 h after ^{124}I labeled GNS IV injection. The average tumor uptake is 7.2% ID/g. (Adapted from Ref [36])

cells (Fig. 3a) and neural stems cells with IDH-1, p53 and PDGFB gene mutations (Fig. 3b). With high-resolution two-photon microscopy, we confirmed that GNS nanoparticles accumulate only within brain tumor boundary but not surrounding healthy brain tissue after systemic administration (Fig. 4). Figure 5 shows PET/CT scans for brain at various time points after intravenous (IV) administration of radiolabeled GNS nanoprobe. At 10 min, there was no discernable uptake difference between tumor and normal brain; however, beginning at 4 hours, the tumor uptake of GNS was higher than normal brain with the contrast ratio between tumor and normal brain increasing over time. The T/N ratio was 1.0, 2.5, 3.8, 7 and 7.8 at 10 min, 4 h, 24 h, 48 h and 120 h, respectively. The increased T/N ratios at 48 and 120 h compared to 24 h were consistent with the decreased normal brain background signal due to GNS clearance from the blood.

The detection size limit of ^{124}I -GNS for brain tumor with PET/CT scan was also explored. (Fig. 6a) shows a small focal area of increased intensity in the PET/CT scan obtained 48 hours after ^{124}I -GNS systemic injection. ^{124}I -GNS accumulated more in the tumor than the surrounding normal brain tissue resulting in a T/N of 4.7. Histopathology showed a tumor size less than 0.5 mm in all three dimensions (Fig. 6b). Further TPL imaging confirmed the presence of GNS inside this sub-millimeter brain tumor (Fig. 4c). Some GNS nanoparticles were found to be close to tumor cell nuclei, indicating GNS nanoparticles can accumulate inside tumor cells. Here we demonstrate the feasibility of GNS nanoprobe for sub-millimeter brain tumor detection with sensitive PET imaging.

To identify the subcellular location of the GNS at nanometer resolution, TEM imaging was performed on both tumor and non-tumor regions of the brain harvested at 48 hours after GNS injection. A coronal section was prepared and processed for TEM imaging. Cerebral vessels were compared between the tumor region and

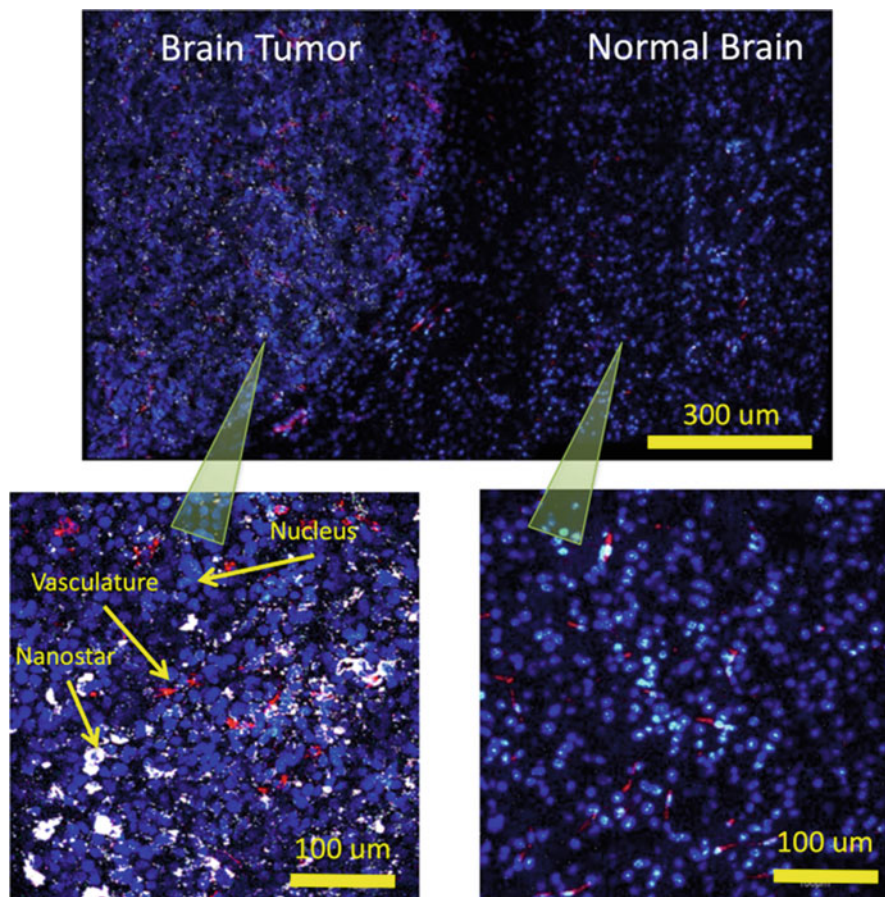


Fig. 4 GNS nanoprobe selectively accumulate in the brain tumor after IV injection. GNS (bright spots) only appear in tumor part but not in normal brain tissue. There is clear boundary for GNS distribution between tumor and normal brain tissue. Red (vasculature); Blue (cell nucleus) and white spots (GNS). GNS nanoprobe have extremely high two-photon luminescence (TPL) cross-section (50,000 times higher than gold nanospheres) due to tip-enhanced plasmonics

contralateral normal brain. The brain tumor vasculature was disrupted and became permeable to GNS. As shown in Fig. 7a, b, GNS were found in both the tumor interstitial space and blood vessel suggesting GNS penetrate through the vessel formed inside the tumor. Figure 7c, d shows that the GNS diffused through the extracellular space and were localized in intracellular vesicles within brain tumor cells. In contrast, the vasculature in the normal brain part appeared intact and GNS nanoparticles remained inside the blood vessel (Fig. 8). Therefore, GNS nanoparticles can permeate through disrupted tumor BBB but not intact normal BBB. After permeation, GNS nanoparticles could enter tumor cells by endocytosis.

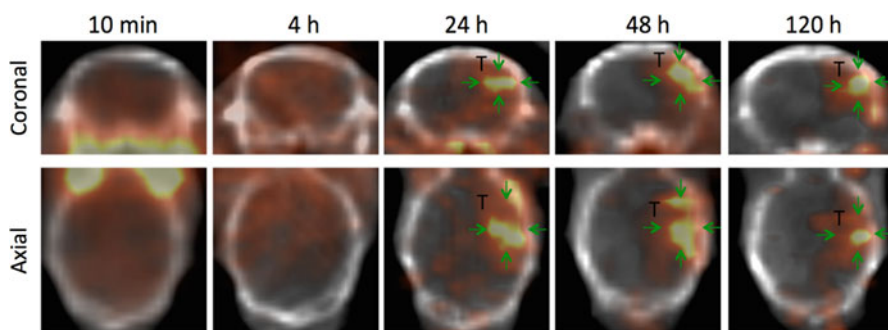


Fig. 5 PET/CT imaging of brain tumor with ^{124}I -GNS nanoprobes. Top and bottom rows show coronal and axial image, respectively. (Adapted from Ref [36])

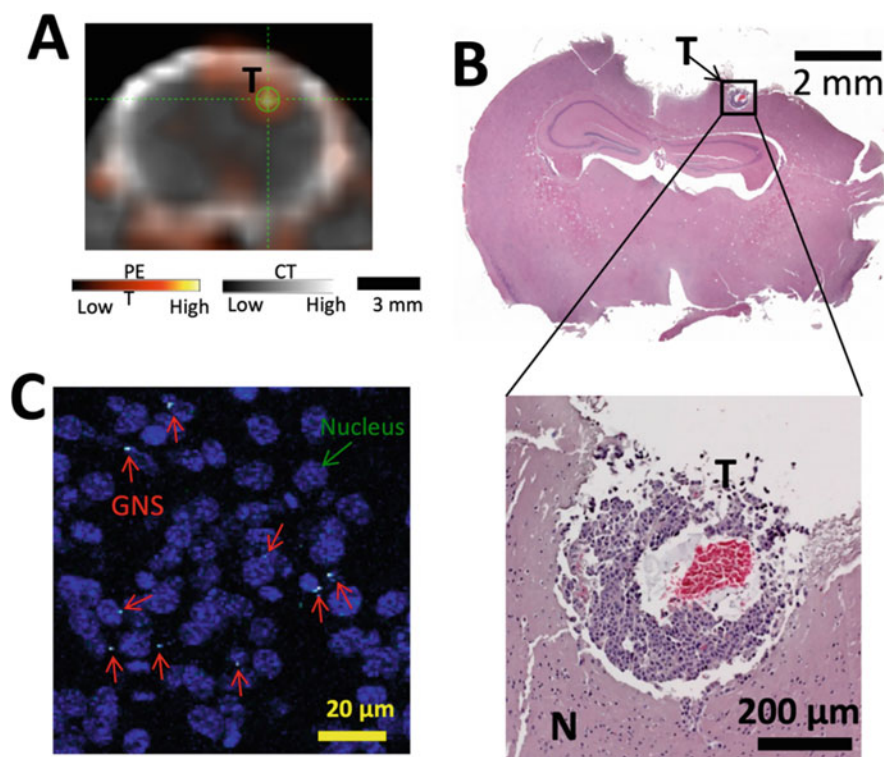


Fig. 6 Sensitive brain tumor detection with ^{124}I -GNS. (a) a small brain tumor identified using PET/CT image with ^{124}I -GNS nanoprobes. (b) H&E histopathology examination confirmed the identified brain tumor region from PET/CT imaging. (c) TPL imaging showed that the GNS (white spots) were identified inside the tumor. The tumor cell nuclei were stained with DAPI (blue). (T), tumor; (N) normal brain. (Adapted from Ref [36])

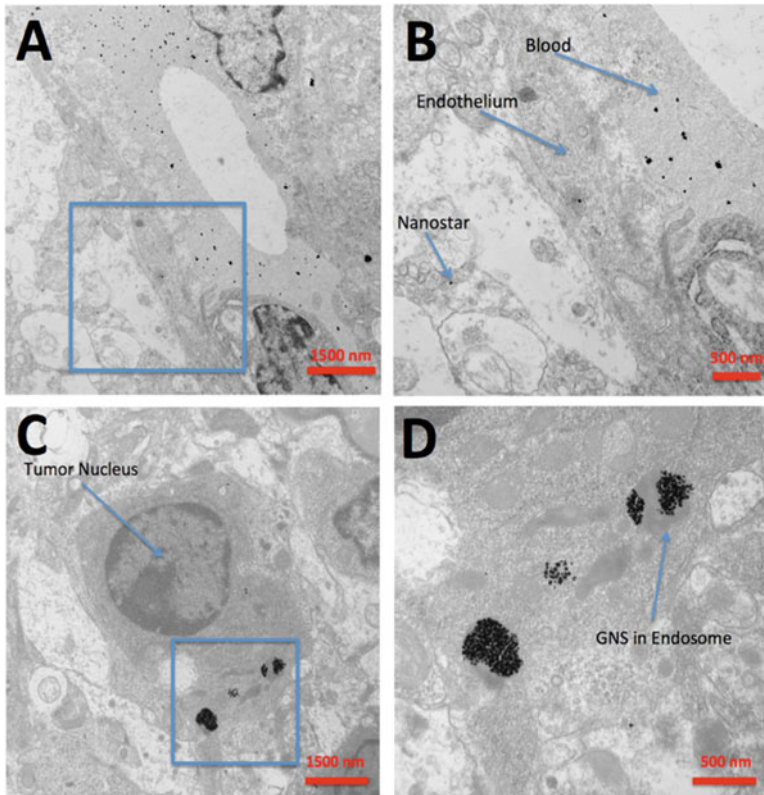


Fig. 7 (a, b) TEM imaging of GNS in the brain tumor after intravenous injection. (c, d) TEM imaging of GNS nanoparticles in endosomes inside brain tumor cells after intravenous injection. (Adapted from Ref [36])

4 Synergistic Photoimmunotherapy of Brain Tumor with GNS

Laser interstitial thermal therapy (LITT), a minimally invasive technique employed clinically that uses a stereotactically-guided laser to apply heat to lesions, resulting in cell death has emerged as a novel treatment modality for brain pathologies including brain tumors [37]. LITT employs the principle of hyperthermia (HT) aiming to increase temperature above physiologic body temperature with the goal of directly inducing cellular damage, as well as promote local and systemic antitumor immune effects. While high temperature HT ($>55\text{ }^{\circ}\text{C}$) can actually induce immediate thermal death of targeted tumors, it is now clear that mild fever-range HT ($<43\text{ }^{\circ}\text{C}$) can be used to (1) improve drug delivery to tumors, (2) improve cancer cell sensitivity to other therapies, and (3) trigger potent systemic anti-cancer immune responses [38–40]. When a tumor is heated, several important vascular

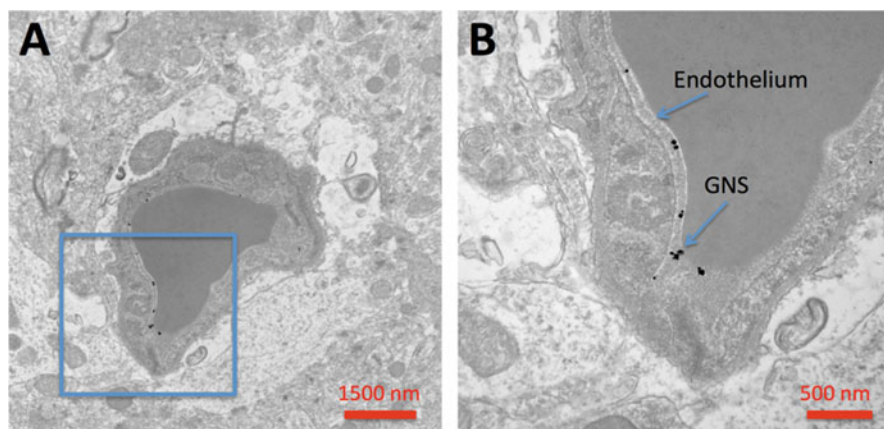


Fig. 8 (a, b) TEM imaging of GNS identified inside the normal brain vasculature after intravenous injection. GNS nanoprobe were found to be blocked by the intact blood-brain-barrier and near the inner endothelium wall. (Adapted from Ref [36])

physiological effects occur, including vasodilation, which increases blood flow to the tumor and adjacent tissues [41]. In the case of brain tumors, even a mild increase of local temperature dramatically enhances BBB permeability allowing the passage of large therapeutic molecules, including large monoclonal antibodies such as immune checkpoint inhibitors [42]. However, this novel technology has several limitations, with the most prominent being the size of treatable lesions (roughly 3 cm through a single trajectory) and the lack of specific conformity to tumor margins. Significant pitfalls thus include either incomplete treatment or collateral damage to healthy tissues beyond tumor margins, because of limited light penetration and non-uniform thermal properties in intracranial tissues. Here we show that nanotechnology can be used to overcome these limitations.

Gold-nanostars (GNS) provide LITT with superior coverage and immunogenic cancer cell ablation. The sharp GNS branches are plasmonic-active (i.e., exhibit enhanced electromagnetic properties), acting like “lightning rods” to convert laser light into heat [43]. The enhanced permeability and retention (EPR) effect in tumors cause preferential accumulation of intravenously injected GNS within even intracranial tumors, allowing us to take advantage of the GNS superior photon-to-heat conversion [44]. As an ideal photothermal transducer for cancer therapy at the nanoscale level, GNS can be exploited for activation by near-infrared (NIR) light in deep tissue. Finally, GNS-mediated photothermal therapy induces a highly immunogenic mode of cancer cell death, bolstering both the primary immune response and eliciting immunologic memory [45].

Provided access, checkpoint blockade remains a promising immunotherapeutic approach to brain tumors [46]. Thermal tumor ablation results in highly immunogenic cell death coupled with a temporary BBB disruption [40, 42]. The two concomitant effects offer a novel therapeutic window for immunotherapies

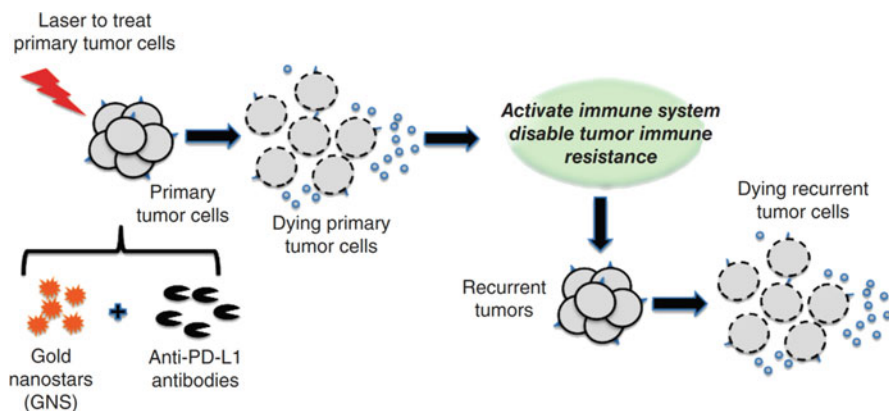
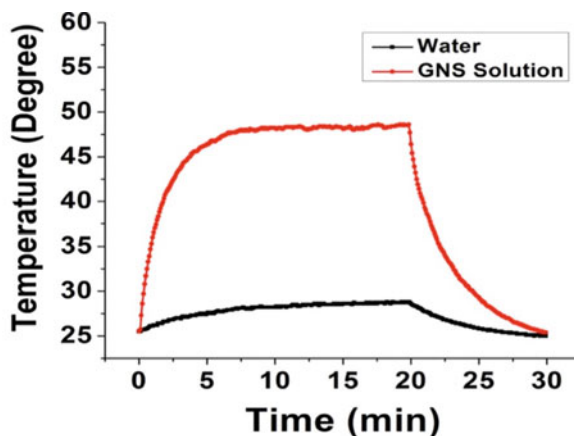


Fig. 9 Scheme for the Synergistic Immuno-Photothermal Nanotherapy (SYMPHONY). The SYMPHONYOY therapy can not only treat primary tumor with thermal ablation but also trigger a powerful anti-cancer immune response to prevent cancer recurrences. (Adapted from REF [51])

otherwise limited by tumor-driven immune suppression. Some of promising efforts have aimed to reverse dysfunction within the T cell compartment [47], as this is the cell population most directly responsible for antitumor activity. Tumor-driven dysregulation of immune checkpoint pathways toward T cell deactivation is a major mechanism of immunosuppression in numerous cancers [48]. Cancer cells frequently upregulate PD-L1 (Programmed Death Ligand-1) on their surface, which binds to PD-1, the immune checkpoint receptor on T cells to curtail their response [49]. Blockage of the interaction between PD-1 and its ligand has been extensively investigated [50].

We have merged GNS-enhanced photothermal treatment with checkpoint immunotherapy to demonstrate a novel therapeutic platform, for which we coined the term: SYMPHONY (SYnergistic iMmuno PHotothermal Nanotherapy), for brain cancer treatment [45]. As shown in Fig. 9, our SYMPHONY therapy contains two treatment arms. The first treatment arm is GNS-mediated photothermal therapy. After systemic administration, GNS nanoparticles accumulate preferentially in the tumor due to the EPR effect. Upon laser irradiation, GNS nanoparticles accumulated in tumors convert light to heat and kill cancer cells with increased temperature. The second treatment arm involves anti-PD-L1 antibody administration, which benefits both from improved access and T cell enabling in the setting of laser-induced hyperthermia to elicit synergistic and effective anti-tumor immunity. In a murine GBM animal model, SYMPHONY proved uniquely capable of producing long-term survivors that reject re-challenge with cancer cells injection, heralding the successful emergence of immunologic memory. To the best of our knowledge, this study is the first to demonstrate the novel combination of GNS-mediated photothermal therapy and checkpoint immunotherapy for GBM treatment with a murine model.

Fig. 10 Temperature profile of water and GNS solution with 0.8 W/cm^2 laser irradiation. The solution temperature was monitored using a near-infrared camera. GNS solution has significantly higher temperature increase than that of water solution. (Adapted from REF [51])



Due to tip-enhanced plasmonics, GNS with multiple sharp branches can exhibit enhanced electromagnetic properties, acting like “lightning rods” to convert and amplify stereotactically-delivered laser light into heat efficiently, which makes GNS a superior photon-to-heat transducer. As shown in Fig. 10, with 0.8 W/cm^2 808 nm laser irradiation, $50 \mu\text{g/ml}$ GNS solution showed a temperature increase of $23.5 \text{ }^\circ\text{C}$, while pure water (0.8 ml) showed a temperature increase of only $2.6 \text{ }^\circ\text{C}$ with the same laser irradiation.

For the *in vivo* study of SYMPHONY therapy on brain cancer, CT2A murine glioma cells (5×10^5) were implanted within the right flank of C57BL/6 mice. When the average tumor size reached 5–6 mm, mice were randomly divided into six groups for various combinations of treatments involving laser irradiation, GNS injection and anti-PD-L1 immunotherapy. Six groups were included in this study with each group having 10 mice: (1) Anti-PD-L1 + GNS + Laser (SYMPHONY); (2) Anti-PD-L1 alone; (3) GNS alone; (4) Laser alone; (5) GNS + Laser; (6) Untreated control. Following randomization, 2 mg GNS were IV injected via tail vein. One day following the GNS injection, extracorporeal laser application (808 nm, 10 min) was performed on tumors. The first intraperitoneal administration of anti-PD-L1 was performed 30 min following laser treatment. Anti-PD-L1 antibody was administrated every 3 days until the end of the experiment, and tumor volumes were assessed every 3 days as well. Figure 11 shows the increase of tumor volumes of the different mouse groups over time. The SYMPHONY group reflects the most effective therapeutic effect as it exhibited the greatest restriction to tumor growth. It is noteworthy that the therapeutic response for GNS + laser groups resulted in smaller tumor growth as compared to anti-PD-L1 therapy alone. This result demonstrates the effectiveness of GNS-mediated photothermal therapy in treating primary tumors. The SYMPHONY group and the Laser + GNS group produced the two most effective results showing the smallest tumor growth. Furthermore, only these two groups (SYMPHONY group and Laser + GNS group) resulted in long-term tumor-free survival in subsets of mice.

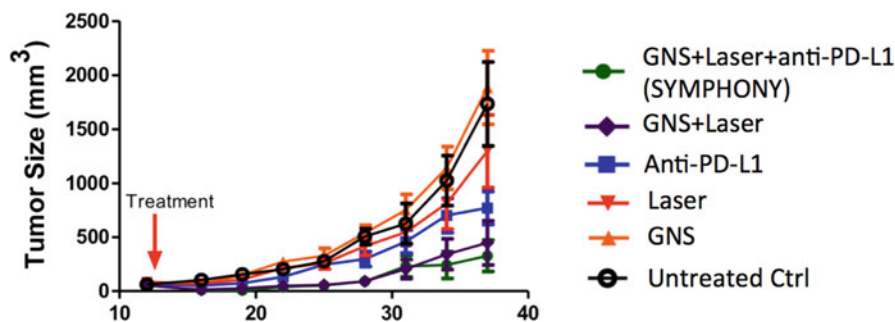


Fig. 11 Plot of tumor volumes over time after treatment. Only the GNS + Laser and GNS + Laser + anti-PD-L1 (SYMPHONY) groups had tumor-free long-term survival. These two groups also had the smallest average tumor size at the conclusion of the experiment. Tumor volume data are shown as mean \pm s.e.m. (Adapted from REF [51])

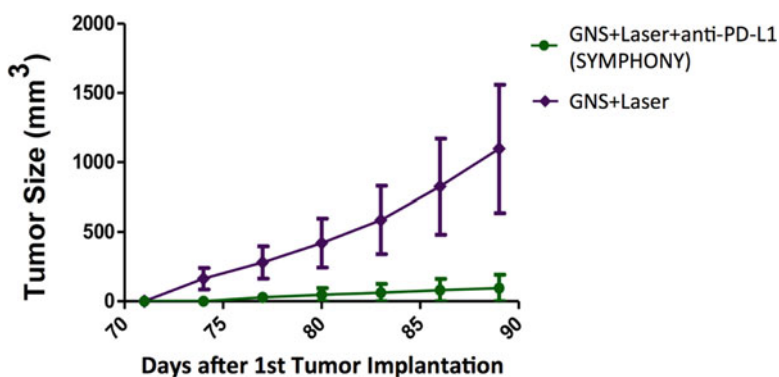


Fig. 12 Rechallenge study for tumor-free mice after treatment. Tumor-free survivors from the GNS + Laser and GNS + Laser + anti-PD-L1 groups were rechallenged in the contralateral flank with glioma cells. The tumor-free mice in the SYMPHONY group were more effective in rejecting the rechallenge when compared to the mice in the GNS + Laser group. (Adapted from REF [51])

For the long-term tumor-free mice from the photothermal therapy (GNS + Laser; $n = 5$) and the SYMPHONY (combined photothermal therapy and anti-PD-L1 immunotherapy; $n = 3$) groups, we performed rechallenge by injecting 5×10^5 CT2A glioma cells in the contralateral flank on Day 50. Two out of three mice (67%) from the group receiving SYMPHONY rejected the re-challenge while this was true for two out of five mice (40%) from the group receiving GNS-mediated photothermal therapy (Fig. 12). This result demonstrates that SYMPHONY therapy can generate memorized anti-cancer immune responses to prevent cancer recurrence.

5 *In Vivo* Toxicity of GNS

GNS toxicity study evaluating biocompatibility is crucial for their biomedical applications and future clinical translation. Previous studies with various animal models including mice, rats and dogs have demonstrated that gold nanoparticles with a spherical shape are biocompatible [52, 53]. However, there are a few studies have reported toxicity evaluation of nonspherical gold nanoparticles (like star-shape). We have performed a comprehensive *in vivo* study including mice behavior observation, body weight monitoring, blood chemistry test and H&E histopathology examination to assess the potential toxicity of PEGylated GNS nanoparticles 6 months after IV administration [36]. Statistical analysis on body weight was performed with a mixed-model ANOVA to assess the effect of gold nanoparticle dosage on body weight over time. One-way ANOVA statistical analysis was performed to compare the effect of GNS dosage (PBS, 20 mg/kg, and 80 mg/kg) on different aspects of blood chemistry test items including BUN, creatinine, calcium, protein, albumin, globulin, glucose, cholesterol, ALT (GPT), AST (GOT), ALP and bilirubin. For all comparisons, the data was considered statistically significant for $P < 0.05$.

During the 6-month toxicity study, all mice were carefully monitored and found to not exhibit stress or any other abnormal behavior. Body weight was used as a guideline for assessing mice's general health condition and was monitored weekly. Experimental results (Fig. 13) show no difference with statistical significance on body weight between the control group and groups receiving GNS doses up to 80 mg/kg by mixed-model ANOVA analysis (criteria $P = 0.05$). Mice were sacrificed 6 months after GNS IV injection and plasma was harvested for blood chemistry test. ANOVA statistical analyses were performed and no statistically significant difference on blood chemistry test results between the control group and study groups receiving 20 or 80 mg/kg GNS dose was observed (Fig. 14). Blood chemistry test results showed preservation of liver and kidney function after GNS IV injection. H&E histopathology examination of brain, heart, liver, kidney and spleen was also performed (Fig. 15). No remarkable tissue structure changes indicating GNS-related toxicity up to 80 mg/kg dose were identified by a veterinary pathologist. After *in vivo* long-term toxicity, we also performed a short-term study with high dose (500 mg/kg), 10–100 folds higher than typically *in vivo* used dosage, to investigate potential acute toxicity. None of 5 mice died 1 week after IV injection. In conclusion, our newly developed GNS showed no deleterious adverse effects in both short-term and long-term preclinical studies. The biocompatible GNS warrants further evaluation for future clinical translation.

6 Conclusion and Future Perspective

GBM is the most common primary malignant brain tumor with one of the poorest prognosis known to mankind. We have used GNS nanoparticles for brain cancer sensitive detection and effective photoimmunotherapy in murine models. The developed GNS nanoprobes can accumulate selectively in brain tumor by the EPR

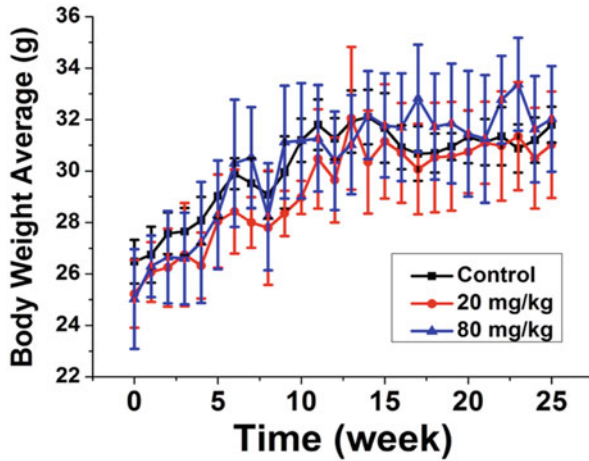


Fig. 13 Toxicity study of GNS nanoparticles using murine animal model. Body weight was monitored once per week after GNS intravenous injection for 6 months. Mixed-model ANOVA was used to perform statistical analysis and results show that there is no difference between control group and groups with 20 and 80 mg/kg dose. The result is considered statistically significant for $P < 0.05$ (95% confidence interval). Each group contained 4 mice and error bar was shown as the standard deviation. (Adapted from REF [36])

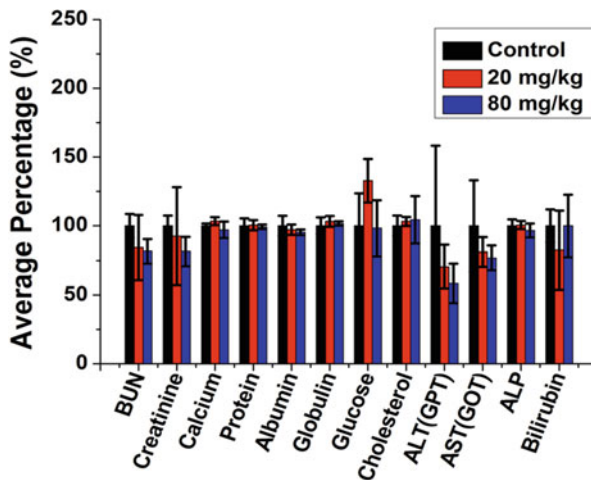


Fig. 14 Mice were sacrificed 6 months after GNS intravenous injection and blood was harvested for blood chemistry test. One-way ANOVA was used to perform statistical analysis and results show that there is no difference between control group and groups with 20 mg/kg and 80 mg/kg dose. The result is considered statistically significant for $P < 0.05$. Each group contained 4 mice and error bar was shown as the standard deviation. (Adapted from REF [36])

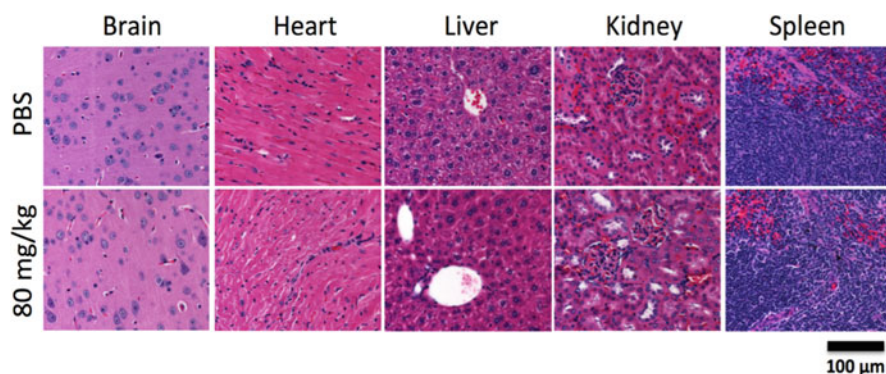


Fig. 15 H&E histopathology examination of various organs of mice 6 months after 80 mg/kg GNS intravenous injection through tail vein. No tissue structure changes related with GNS toxicity were identified. Scale bar, 100 μm . (Adapted from ref. [36])

effect. The radiolabeled GNS nanoprobe shows the potential to detect brain tumor as small as 0.5 mm, which is superior to any currently available non-invasive imaging modality. In addition, we also demonstrated that the SYMPHONY therapy combining GNS-mediated photothermal therapy and checkpoint immunotherapy can improve the therapeutic effect against aggressive GBM cancer in a murine animal model. The tumor-bearing mice that were cured by the SYMPHONY treatment successfully rejected rechallenge with anti-tumor immune response memory. Additional studies will achieve better understanding and optimal exploitation of the mechanisms underlying these novel synergistic treatment modalities in order to enhance and broaden the anti-cancer immune response. As a result, biocompatible GNS nanoparticles have great potential in future translational medicine studies for brain cancer diagnostics and therapeutics.

Acknowledgements This work was supported by National Institutes of Health (1R01EB028078-01A1).

References

1. Omuro, A., DeAngelis, L.M.: Glioblastoma and other malignant gliomas: a clinical review. *JAMA—J. Am. Med. Assoc.* **310**(17), 1842–1850 (2013)
2. Ostrom, Q.T., Bauchet, L., Davis, F.G., Deltour, I., Fisher, J.L., Langer, C.E., Pekmezci, M., Schwartzbaum, J.A., Turner, M.C., Walsh, K.M., Wrensch, M.R., Barnholtz-Sloan, J.S.: The epidemiology of glioma in adults: a “state of the science” review. *Neuro. Oncol.* **16**(7), 896–913 (2014)
3. Ostrom, Q.T., Gittleman, H., Fulop, J., Liu, M., Blanda, R., Kromer, C., Wolinsky, Y., Kruchko, C., Barnholtz-Sloan, J.S.: CBTRUS statistical report: primary brain and central nervous system tumors diagnosed in the United States in 2008–2012. *Neuro-Oncology.* **17**(4), 1–62 (2015)

4. Davis, M.E.: Glioblastoma: overview of disease and treatment. *Clin. J. Oncol. Nurs.* **20**(5), 2–8 (2016)
5. Mariotto, A.B., Yabroff, K.B., Shao, Y., Feuer, E.J., Brown, M.L.: Projections of the cost of cancer care in the United States: 2010–2020. *J. Natl. Cancer Inst.* **103**, 117–2128 (2011)
6. Stupp, R., Mason, W.P., Van Den Bent, M.J., Weller, M., Fisher, B., Taphoorn, M.J.B., Belanger, K., Brandes, A.A., Marosi, C., Bogdahn, U., Curschmann, J., Janzer, R.C., Ludwin, S.K., Gorlia, T., Allgeier, A., Lacombe, D., Cairncross, G., Eisenhauer, E., Mirimanoff, R.O.: Radiotherapy plus concomitant and adjuvant temozolomide for glioblastoma. *N. Engl. J. Med.* **352**(10), 987–996 (2005)
7. Krex, D., Klink, B., Hartmann, C., Deimling, A.V., Pietsch, T., Simon, M., Sabel, M., Steinbach, J.P., Heese, O., Reifenberger, G., Weller, M., Schackert, G.: Long-term survival with glioblastoma multiforme. *Brain.* **130**, 2596–2606 (2007)
8. Weller, M., Butowski, N., Tran, D.D., Recht, L.D., Lim, M., Hirte, H., Ashby, L., Mechtler, L., Goldlust, S.A., Iwamoto, F., Drappatz, J., O'Rourke, D.M., Wong, M., Hamilton, M.G., Finocchiaro, G., Perry, J., Wick, W., Green, J., He, Y., Turner, C.D., Yellin, M.J., Keler, T., Davis, T.A., Stupp, R., Sampson, J.H.: Rindopepimut with temozolomide for patients with newly diagnosed EGFRvIII-expressing glioblastoma (ACT IV): a randomized, double-blind, international phase 3 trial. *Lancet Oncol.* **18**(10), 1373–1385 (2017)
9. Inogés, S., Tejada, S., de Cerio, A.L., Pérez-Larraya, J.G., Espinós, J., Idoate, M.A., Domínguez, P.D., de Eulate, R.G., Aristu, J., Bendandi, M., Pastor, F., Alonso, M., Andreu, E., Cardoso, F.P., Valle, R.D.: A phase II trial of autologous dendritic cell vaccination and radiochemotherapy following fluorescence-guided surgery in newly diagnosed glioblastoma patients. *J. Transl. Med.* **15**(1), 104 (2017)
10. Bloch, O., Lim, M., Sughrue, M.E., Komotar, R.J., Abrahams, J.M., O'Rourke, D.M., D'Ambrosio, A., Bruce, J.N., Parsa, A.T.: Autologous heat shock protein peptide vaccination for newly diagnosed glioblastoma: impact of peripheral PD-L1 expression on response to therapy. *Clin. Cancer Res.* **23**(14), 3575–3584 (2017)
11. Desjardins, A., Gromeier, M., Herndon, J.E., Beaubier, N., Bolognesi, D.P., Friedman, A.H., Friedman, H.S., McSherry, F., Muscat, A.M., Nair, S., Peters, K.B., Randazzo, D., Sampson, J.H., Vlahovic, G., Harrison, W.T., McLendon, R.E., Ashley, D., Bigner, D.: Recurrent glioblastoma treated with recombinant poliovirus. *N. Engl. J. Med.* **279**, 150–161 (2018)
12. Chiocca, E.A., Abbed, K.M., Tatter, S., Louis, D.N., Hochberg, F.H., Barker, F., Kracher, J., Grossman, S.A., Fisher, J.D., Carson, K., Rosenblum, M., Mikkelsen, T., Olson, J., Markert, J., Rosenfeld, S., Nabors, L.B., Brem, S., Phuphanich, S., Freeman, S., Kaplan, R., Zwiebel, J.: A phase I open-label, dose escalation, multi-institutional trial of injection with an E1B-attenuated adenovirus, ONYX-015, into the peritumoral region of recurrent malignant gliomas, in the adjuvant setting. *Mol. Ther.* **10**(5), 958–966 (2004)
13. Wheeler, L.A., Manzanera, A.G., Bell, S.D., Cavaliere, R., McGregor, J.M., Grecula, J.C., Newton, H.B., Lo, S.S., Badie, B., Portnow, J., Teh, B.S., Trask, T.W., Baskin, D.S., New, P.Z., Aguilar, L.K., Aguilar-Cordova, E., Chiocca, E.A.: Phase II multicenter study of gene-mediated cytotoxic immunotherapy as adjuvant to surgical resection for newly diagnosed malignant glioma. *Neuro-Oncology.* **18**(8), 1137–1145 (2016)
14. Ji, N., Weng, D., Liu, C., Gu, Z., Chen, S., Guo, Y., Fan, Z., Wang, X., Chen, J., Zhao, Y., Zhou, J., Wang, J., Ma, D., Li, N.: Adenovirus-mediated delivery of herpes simplex virus thymidine kinase administration improves outcome of recurrent high-grade glioma. *Oncotarget.* **7**(4), 4369–4378 (2016)
15. Reardon, D.A., Omuro, A., Brandes, A.A., Rieger, J., Wick, A., Sepulveda, J., Phuphanich, S., de Souza, P., Ahluwalia, M.S., Lim, M., Vlahovic, G., Sampson, J.: Randomized phase 3 study evaluating the efficacy and safety of nivolumab vs bevacizumab in patients with recurrent glioblastoma: CheckMate 143. *Neuro. Oncol.* **19**(3), 21 (2017)

16. Weller, M., van den Bent, M., Tonn, J.C., Stupp, R., Preusser, M., Cohen-Jonathan-Moyal, E., Henriksson, R., Rhun, E.L., Balana, C., Chinot, O., Bendszus, M., Reijneveld, J.C., Dhermain, F., French, P., Marosi, C., Watts, C., Oberg, I., Pilkington, G., Baumert, B.G., Taphoorn, M.J.B., Hegi, M., Westphal, M., Reifenberger, G., Soffiatti, R., Wick, W.: European Association for Neuro-Oncology (EANO) guideline on the diagnosis and treatment of adult astrocytic and oligodendroglial gliomas. *Lancet Oncol.* **18**(6), 315–329 (2017)
17. Omuro, A., Vlahovic, G., Lim, M., Sahebjam, S., Baehring, J., Cloughesy, T., Voloschin, A., Ramkissoon, S.H., Ligon, K.L., Latek, R., Zwirter, R., Strauss, L., Paliwal, P., Harbison, C.T., Reardon, D.A., Sampson, J.H.: Nivolumab with or without ipilimumab in patients with recurrent glioblastoma: results from exploratory phase I cohorts of CheckMate 143. *Neuro-Oncology.* **20**(5), 674–686 (2018)
18. O'Rourke, D.M., Nasrallah, M.P., Desai, A., Melenhorst, J.J., Mansfield, K., Morrissette, J.J.D., Martinez-Lage, M., Brem, S., Maloney, E., Shen, A., Isaacs, R., Mohan, S., Plesa, G., Lacey, S.F., Navenot, J.M., Zheng, Z., Levine, B.L., Okada, H., June, C.H., Brogdon, J.L., Maus, M.V.: A single dose of peripherally infused EGFRvIII-directed CAR T cells mediates antigen loss and induces adaptive resistance in patients with recurrent glioblastoma. *Sci. Transl. Med.* **19**(9), 399 (2017)
19. Fesnak, A.D., June, C.H., Levine, B.L.: Engineered T cells: the promise and challenges of cancer immunotherapy. *Nat. Rev. Cancer.* **16**(9), 566–581 (2016)
20. Yuan, H., Khoury, C.G., Hwang, H., Wilson, C.M., Grant, G.A., Vo-Dinh, T.: Gold nanostars: surfactant-free synthesis, 3D modelling, and two-photon photoluminescence imaging. *Nanotechnology.* **23**(7), 075102 (2012)
21. Gao, N.Y., Chen, Y., Li, L., Guan, Z., Zhao, T., Zhou, N., Yuan, P., Yao, S.Q., Xu, Q.H.: Shape-dependent two-photon luminescence of single gold nanoparticles. *J. Phys. Chem. C.* **118**(25), 13904–13911 (2012)
22. Liu, Y., Ashton, J.R., Moding, E.J., Yuan, H., Register, J.K., Fales, A.M., Choi, J., Whitley, M.J., Zhao, X., Qi, Y., Ma, Y., Vaidyanathan, G., Zalutsky, M.R., Kirsch, D.G., Badea, C.T., Vo-Dinh, T.: A plasmonic gold nanostar theranostic probe for in vivo tumor imaging and photothermal therapy. *Theranostics.* **5**(9), 946–960 (2015)
23. Wang, L., Jacques, S.L., Zheng, L.: MCML-Monte Carlo Modeling of light transport in multi-layered tissues. *Comput. Methods. Programs. Biomed.* **47**(2), 131–146 (1995)
24. Yaroslavsky, A.N., Schulze, P.C., Yaroslavsky, I.V., Schober, R., Ulrich, F., Schwarzmaier, H.-J.: Optical properties of selected native and coagulated human brain tissues in vitro in the visible and near infrared spectral range. *Phys. Med. Biol.* **47**(12), 2059 (2002)
25. Mohammadi, A., Schroeder, J.L., Angelov, L., Chao, S.T., Murphy, E.S., Yu, J.S., Neyman, G., Jia, X., Suh, J.H., Barnett, G.H.: Vogelbaum: impact of the radiosurgery prescription dose on the local control of small (2 cm or smaller) brain metastases. *J. Neurosurg.* **126**(3), 735–743 (2017)
26. Omuro, A., DeAngelis, L.M.: Glioblastoma and other malignant gliomas: a clinical review. *J. Am. Med. Assoc.* **310**(17), 1842–1850 (2013)
27. Huang, Q.L., Cao, X., Chai, X., Wang, X., Xiao, C., Wang, J.: The radiological imaging features of easily misdiagnosed epithelioid glioblastoma in seven patients. *World Neurosurg.* **124**, 527–532 (2019)
28. Sze, G., Milano, E., Johnson, C., Heier, L.: Detection of brain metastases: comparison of contrast-enhanced MR with unenhanced MR and enhanced CT. *Am. J. Neuroradiol.* **11**, 785–791 (1990)
29. Schellinger, P.D., Meinck, H.M., Thron, A.: Diagnostic accuracy of MRI compared to CCT in patients with brain metastases. *J. Neuro-Oncol.* **44**(3), 275–281 (1999)
30. Erdi, Y.E.: Limits of tumor detectability in nuclear medicine and PET. *Mol. Imaging Radionucl. Ther.* **21**, 23–28 (2012)
31. Yuh, W.T., Tali, E.T., Nguyen, H.D., Simonson, T.M., Mayr, N.A., Fisher, D.J.: The effect of contrast dose, imaging time, and lesion size in the MR detection of intracerebral metastasis. *Am. J. Neuroradiol.* **16**(2), 373–380 (1995)

32. Gambhir, S.S., Herschman, H.R., Cherry, S.R., Barrio, J.R., Satyamurthy, N., Toyokuni, T., Phelps, M.E., Larson, S.M., Balatoni, J., Finn, R., Sadelain, M., Tjuvajev, J., Blasberg, R.: Imaging transgene expression with radionuclide imaging technologies. *Neoplasia*. **2**, 118–138 (2000)
33. Gambhir, S.S.: Molecular imaging of cancer with positron emission tomography. *Nat. Rev. Cancer*. **2**(9), 683–693 (2002)
34. Karunanithi, S., Sharma, P., Kumar, A.: 18F-FDOPA PET/CT for detection of recurrence in patients with glioma: prospective comparison with 18F-FDG PET/CT. *Eur. J. Nucl. Med. Mol. Imaging*. **40**(7), 1025–1035 (2013)
35. Venneti, S., Dunphy, M.P., Zhang, H., Pitter, K.L., Zanzonico, P., Campos, C., Carlin, S.D., Rocca, G.L., Lyashchenko, S., Ploessl, K., Rohle, D., Omuro, A.M., Cross, J.R., Brennan, C.W., Weber, W.A., Holland, E.C., Mellingshoff, I.K., Kung, H.F., Lewis, J.S., Thompson, C.B.: Glutamine-based PET imaging facilitates enhanced metabolic evaluation of gliomas in vivo. *Sci. Transl. Med.* **7**(274), 217 (2015)
36. Liu, Y., Carpenter, A.B., Pirozzi, C.J., Yuan, H., Waitkus, M.S., Zhou, Z., Hansen, L., Seywald, M., Odion, R., Greer, P.K., Hawk, T., Chin, B.B., Vaidyanathan, G., Zalutsky, M.R., Yan, H., Vo-Dinh, T.: Non-invasive sensitive brain tumor detection using dual-modality bioimaging nanoprobe. *Nanotechnology*. **30**(27), 275101 (2019)
37. Belykh, E., Yagmurlu, K., Martirosyan, N.L., Lei, T., Izadyyazanabadi, M., Malik, K.M., Byvaltsev, V.A., Nakaji, P., Preul, M.C.: Laser application in neurosurgery. *Surg. Neurol. Int.* **8**, 274–274 (2017)
38. Kennedy, L.C., Bickford, L.R., Lewinski, N.A., Coughlin, A.J., Hu, Y., Day, E.S., West, J.L., Drezek, R.A.: A new era for cancer treatment: gold-nanoparticle-mediated thermal therapies. *Small*. **7**(2), 169–183 (2011)
39. Frey, B., Weiss, E.M., Rubner, Y., Wunderlich, R., Ott, O.J., Sauer, R., Fietkau, R., Gaipl, U.S.: Old and new facts about hyperthermia-induced modulations of the immune system. *Int. J. Hyperth.* **28**(6), 528–542 (2012)
40. Evans, S.S., Repasky, E.A., Fisher, D.T.: Fever and the thermal regulation of immunity: the immune system feels the heat. *Nat. Rev. Immunol.* **15**(6), 335–349 (2015)
41. Jordan, B.F., Sonveaux, P.: Targeting tumor perfusion and oxygenation to improve the outcome of anticancer therapy. *Front. Pharmacol.* **3**, 94–94 (2012)
42. Li, J.B., Li, C.S., Yuan, W., Wu, J., Li, J., Li, Z., Zhao, Y.: Mild hypothermia alleviates brain oedema and blood-brain barrier disruption by attenuating tight junction and adherens junction breakdown in a swine model of cardiopulmonary resuscitation. *PLoS One*. **12**(3), 20 (2017)
43. Yuan, H., Fales, A.M., Vo-Dinh, T.: TAT peptide-functionalized gold nanostars: enhanced intracellular delivery and efficient NIR photothermal therapy using ultralow irradiance. *J. Am. Chem. Soc.* **134**(28), 11358–11361 (2012)
44. Maeda, H., Tsukigawa, K., Fang, J.: A retrospective 30 years after discovery of the enhanced permeability and retention effect of solid tumors: next-generation chemotherapeutics and photodynamic therapy-problems, solution, and prospects. *Microcirculation*. **23**, 173–182 (2016)
45. Liu, Y., Maccarini, P., Palmer, G.M., Etienne, W., Zhao, Y., Lee, C.T., Ma, X., Inman, B.A., Vo-Dinh, T.: Synergistic immune photothermal nanotherapy (SYMPHONY) for the treatment of unresectable and metastatic cancers. *Sci. Rep.* **7**, 8606 (2017)
46. Sampson, J.H., Gunn, M.D., Fecci, P.E., Ashley, D.M.: Brain immunology and immunotherapy in brain tumours. *Nat. Rev. Cancer*. **20**(1), 12–25 (2020)
47. Waldman, A.D., Fritz, J.M., Lenardo, M.J.: A guide to cancer immunotherapy: from T cell basic science to clinical practice. *Nat. Rev. Immunol.* (2020). <https://doi.org/10.1038/s41577-020-0306-5>
48. Topalian, S.L., Drake, C.G., Pardoll, D.M.: Targeting the PD-1/B7-H1(PD-L1) pathway to activate anti-tumor immunity. *Curr. Opin. Immunol.* **24**(2), 207–212 (2012)
49. Okazaki, T., Honjo, T.: PD-1 and PD1 ligands: from discovery to clinical application. *Int. Immunol.* **19**, 813–824 (2007)

50. Pardoll, D.M.: The blockade of immune checkpoints in cancer immunotherapy. *Nat. Rev. Cancer.* **12**(4), 252–264 (2012)
51. Liu, Y., Chongsathidkiet, P., Crawford, B.M., Odion, R., Dechant, C.A., Kemeny, H.R., Cui, X., Maccarini, P.F., Lascola, C.D., Fecci, P.E., Vo-Dinh, T.: Plasmonic gold nanostar-mediated photothermal immunotherapy for brain tumor ablation and immunologic memory. *Immunotherapy.* **11**(15), 1293–1302 (2019)
52. Thakor, A.S., Luong, R., Paulmurugan, R., Lin, F.I., Kempen, P., Zavaleta, C., Chu, P., Massoud, T.F., Sinclair, R., Gambhir, S.S.: The fate and toxicity of Raman-active silica-gold nanoparticles in mice. *Sci. Transl. Med.* **3**(79), 79ra33 (2011)
53. Gad, S.C., Sharp, K.L., Montgomery, C., Payne, J.D., Goodrich, G.P.: Evaluation of the toxicity of intravenous delivery of Auroshell particles (Gold-Silica Nanoshells). *Int. J. Toxicol.* **31**(6), 584–594 (2012)

Index

A

- Abscopal effects, 20, 186, 218
- Acquired immune system, 5, 55, 124
- Adjuvants
 - antigenic proteins, 226
 - BMVs treatment, 204
 - cancer vaccines, 30
 - immune adjuvants, 52–53
 - MPLA, 198
 - nanoparticle-delivered adjuvants, 15
 - NOD2, 198
 - payload delivery, 120–121
 - prophylactic, 202
 - TLR-based vaccine, 198
- Adoptive-cell therapy, 120
- Adoptive lymphocyte transfer (ALT), 32–34, 38–39, 249
- Antigen-presenting cells (APCs), 7, 15, 20, 120, 144, 158, 210
 - antigen-loaded NPs, 14
 - innate immune system, 52
 - and neutrophils, 6
 - Sipuleucel-T, 53
- Artificial APCs (aAPCs), 120

B

- Bacillus Calmette–Guerin (BCG)
 - immunotherapy, 19, 53, 216
- Bacterium-mimicking liposomes
 - engineering, 200
 - immunotherapy, 196
 - TLRs and NLRs, 197
- Bessel function, 95

- Biodistribution, 7, 9, 151, 163, 223–227
- Biomaterials, 42, 118, 120
- Brightfield microscopy, 71, 74

C

- Cancer immunoediting, 12, 13, 68
- Cancer immunosurveillance, 12–13, 68
- Cancer immunotherapy, 13, 117
 - ALT (*see* Adoptive lymphocyte transfer (ALT))
 - autoimmune disease, 148
 - challenges
 - immune access, 36–37
 - immune suppression, 37
 - chemokines, 145
 - cold tumours, 148
 - cytokines, 145
 - early, 144–145
 - emergence, 144
 - enzymes, 145
 - ICB, 35–36
 - immune suppressive cells, 145
 - immune system, 147
 - killing tumour cells, 145
 - nanostructures, 148
 - nanotechnology (*see* Nanotechnologies)
 - strategies, 29, 30
 - vaccines, 30–32
 - viral-based strategies, 34–35
 - See also* Immunotherapy
- Cancer vaccine, 144–145
- CAR-T cell therapy, 236
- Cationic dextran (C-dextran), 151

- Cellular imaging, 77–80
- Cellular uptake
 gold nanorods, 9
 surface properties, 10
- Chemo-immunotherapy
 antibody immunotherapy, 134
 antitumor effect, 132
 antitumor efficiency, 134
 chemotherapeutic drugs, 134
 chitosan nanoparticles, 134
 cisplatin, 131
 2,3-dimethylmaleic anhydride coating, 133
 drug screening models, 131
 heat shock protein, 132–133
 immunogenic cell death, 131, 132, 134
 immunophenotyping, 134
 indoleamine 2,3-dioxygenase 1 (IDO), 134
 innate immune system, 135
 lymph nodes, 135
 magnetite nanoparticles, 132
 methotrexate, 131
 multifunctional nanostars, 132
 nanoparticle-based therapeutics, 132
 nanoparticles, 132
 plasmonic nanomaterials, 132
 smart nanomaterials, 133
 synergistic tumor treatments, 133
 tumor tissue, 131
- Chemokine ligand 12 (CXCL12), 159, 167
- Chemokines, 52, 144–146
- Chemotherapy, 118, 143
- Chimeric antigen receptor (CAR) T cell therapy, 33–34, 39, 69, 236
- Clinical trial design, *see* Drug development
- Colony stimulating factor 1 receptor (CSF-1R), 153, 154
- Copper sulfide nanoparticles (CuSNPs), 191
 absorption wavelength, 192
 anti-tumor therapeutic effects, 192
 biomedical applications
 drug delivery systems, 195–196
 photothermal therapy, 195
 direct dry-grinding synthesis, 194
 hydrothermal/solvothermal methods, 193–194
 material and production cost, 192
 microwave irradiation, 194
 PTT, 192
 solid, 194
 synthesis, 193
 treatment, 193
- Cyclooxygenase 2 (COX-2), 157–158
- Cytokines, 52, 144, 146
- Cytotoxic T lymphocyte-associated antigen 4 (CTLA-4), 13, 36, 53, 128, 129, 147, 149, 161–163, 182–183, 213, 217
- Cytotoxic T lymphocytes (CTLs), 135, 144, 150
- D**
- Damage-associated molecular patterns (DAMPs), 6, 20, 35, 124, 126, 183, 184, 197, 203
- Dendritic cells (DCs), 136, 158
 vaccines, 31
- Drug development
 attrition rate, 56
 challenges, immunotherapy trials
 biomarkers, 60, 61
 combination therapies, 61
 dosing, 58–59
 imaging, 59–60
 trends in trial design, 62–63
 clinical phase, 57–58
 pembrolizumab, 56
 phases, 55
 preclinical phase, 56–57
- E**
- Electromagnetic (EM) radiation, 123
- Endocytosis, 6
- Engineered metallic nanoparticles, 8, 9
- Enhanced permeability and retention (EPR), 7, 12, 17, 90, 118, 136, 180, 181, 195, 237, 238, 245, 246, 249
- Enzymes, 144–147, 155, 157, 162
- External energy sources, 17, 18
- F**
- FDA Safety and Innovation Act (FDASIA), 56
- Finite-element model (FEM), 177, 178
- Fluorescence imaging, 70
- Fluorescence microscopy, 70
- Fluorescence reporter, 75, 76, 78, 79
- Folate receptor (FR), 128
- Food and Drug Administration (FDA), 16, 31, 35–37, 55, 56, 58, 62, 63, 120, 129, 177, 211, 230
- Functional imaging, 60, 77–80

G

- Glucocorticoid-induced TNFR-related receptor (GITR), 149–150
- GNS, *see* Gold nanostars (GNSs)
- Gold nanoparticles (GNPs), 120, 121, 123–125, 181
- advantages, 8–9
 - cylindrical GNPs, 10
 - effect of size and shape, 9
 - effect of surface modifications, 9–10
 - in filter organs, 9
 - nanoshells, 18
 - rod-shaped GNPs, 10
- Gold nanostars (GNSs), 89, 174, 241
- absorption spectrum, 177
 - diffusion equation models, 237
 - EPR effect, 181
 - GBM detection, 236
 - laser-irradiated tissue, 236
 - lightning rod effect, 177–178
 - LITT modality, 237
 - Monte Carlo Modeling, 238
 - nanoparticles, 242
 - nanoprobe, 240
 - optical absorption properties, 176
 - optical properties, 238
 - optical tunability, 175
 - PET/CT imaging, 243
 - photoimmunotherapy, 236
 - photothermal studies, 182
 - sensitive brain tumor detection, 240–245
 - sizes, 179
 - structure, 175
 - surfactant-free synthesis, 176
 - toxicity study, 249–251
- Granulocytes, 6, 10, 31, 37
- Green's function, 94, 95, 98, 109–110

H

- Heat flow equation, 91, 92, 95–97, 100, 102
- Heat shock proteins (HSPs), 17, 20, 126, 155, 183, 184, 210, 211, 215
- Hemagglutinin (HA), 231, 232
- Hemoglobin oxygen saturation, 74, 78
- Hollow CuSNPs (HCuSNPs), 196
- Hydrothermal/solvothermal methods, 193–194
- Hydroxy ethyl starch-poly lactide (HES-PLA), 158
- Hyperthermia (HT), 123, 174
- benefits, 175
 - external energy sources, 18
 - HSPs, 17

- immune-mediated anti-tumor nanotechnology, 17
- NP-mediated thermal techniques, 17–18
- traditional HT modalities, 17

I

- IL-1 β -mediated inflammatory responses, 124
- Immune cell reporter, 75–76
- Immune checkpoint, 19, 21, 34–36, 43–44, 147
- Immune checkpoint blockade (ICB) agents, 128
- Immune checkpoint blockade therapy (ICBT), 147, 156
- cancer immunotherapy, 161
- α CTLA-4, 162–163
- α PD-1, 162
- α PD-L1, 161–162
- Immune RECISt (iRECISt), 60
- Immune response, 37
- activation, 43
 - anti-tumor, 39
 - and tumor cells, 36
- Immune system
- acquired immune system, 5
 - adaptive immunity, 5
 - effect of nanoparticles, 5
 - immunostimulation, 4
 - immunosuppression, 4
 - innate immune system, 5–6
 - innate immunity, 5
 - nanoparticle system, 4
 - role, 51
 - tissue-specific cell types, 6
- Immuno adjuvant therapy
- BMVs, 204
 - B16-OVA models, 203
 - B16-OVA tumor cells, 205
 - HCuSNPs, 203
- Immunofluorescence labeling, 77
- Immunogenic cell death (ICD), 131, 155, 156, 203, 206
- Immunomodulatory molecule delivery system (iMods), 155
- Immuno-oncology, 51, 52, 56, 59, 60
- body's defense system, 67–68
 - carcinogenesis, 68
 - elimination phase, 68
 - equilibrium phase, 68
 - escape phase, 68
 - immune system, 68–69
 - immunoediting, 68
 - immuno-evasion, 68

- Immunostimulation, 4, 39
 Immunosuppression, 4, 13, 14, 19, 34, 37, 39,
 134, 135, 148, 157, 182, 216, 218
 Immunotherapeutics, 13, 29, 30, 33, 34, 37, 44,
 118, 123, 152, 163
 Immunotherapy
 bladder cancer cells, 184
 cancer, 182–183
 CD4 (helper) T-cells, 52
 drug development (*see* Drug development)
 immune system, 51–52
 nano-immunotherapy, 183
 nonspecific immunity
 checkpoint inhibitors, 53, 54
 chemokines, 52
 cytokines, 52
 immune adjuvants, 52–53
 NP-mediated hyperthermia, 18
 specific immunity
 ACT, 53
 antibodies and antibody-drug
 conjugates, 55
 OVs (*see* Oncolytic viruses (OVs))
 vaccines, 54–55
 strategies, 18–19
 synergistic dual-modality, 19–21
 use of nanoparticles, 69
 using checkpoint inhibitors, 19
 viral-based strategies, 34–35
 Indocyanine green (ICG), 21, 195, 210, 211,
 213
 Indoleamine 2,3-dioxygenases (IDO), 43, 134,
 135, 155–157, 216
 Inflammatory cytokines, 125
 Innate immune system, 5–6, 52
In situ photoimmunotherapy (ISPI), 210–211
 Interleukin-10 (IL-10), 145, 146, 150, 151,
 153, 159–160
 Intravital microscopy
 advantages, 69–70
 brightfield microscopy, 71, 74
 confocal imaging and structured
 illumination, 71–72
 conventional wide field fluorescence
 microscope, 70–71
 functional imaging, 77–80
 genetic reporter models, immune cells,
 75–76
 hemoglobin absorption contrast, 78, 79
 immune function, 67
 immunofluorescence labeling, 77
 immuno-oncology (*see* Immuno-oncology)
 multiphoton microscopy, 72–73
 OCT (*see* Optical coherence tomography
 (OCT))
 photoacoustic microscopy, 73
 use of nanoparticles, 69
 window chamber models, 74–75
 Investigational New Drug (IND), 55–57, 156

L
 Laser interstitial thermal therapy (LITT), 236,
 237, 239, 244, 245
 Layer-by-layer (LbL) method, 229
 Lighting-rod effect, 178, 179
 Lipid calcium phosphate (LCP), 150, 159
 Liposomal muramyl tripeptide phosphatidyl
 ethanolamine (L-MTP-PE), 198,
 199
 Liposomes, 129
 Lung metastases, 125

M
 Macrophage colony stimulating factor
 (MCSF), 153
 Matrix metalloprotease (MMP), 153
 Mesoporous silica nanoparticles (MSNP), 156
 Methylene blue (MB), 128
 Modern medicine, 22
 Molecular imaging, 69, 73, 74
 Monte Carlo theoretical simulation, 239
 Mucosal immune response, 229
 Multidrug resistance (MDR), 69, 160
 Multiphoton microscopy, 72–73
 Multiple drug resistance (MDR), 69, 160
 Myeloid derived suppressor cells (MDSCs),
 35, 37, 125, 145–147, 150–152, 155,
 157, 160, 218

N
 Nanometer, 3, 4, 241
 Nanoparticle-mediated heating
 analytical solutions, 91
 antitumor immune effects, 89
 finite-element based methods, 91
 GNS, 89
 Green's function, 109–110
 heat flow equation, 92
 heat generation
 planewave source, 94
 point source, 93
 heat production, 90
 homogeneous medium, 91

- immune system, 89
- immunologic memory, 90
- light absorption, 90
- near-infrared (NIR), 90
- optical energy, 90, 91
- optical heat sources, 92–93
- optical power (*see* Optical power)
- particles, 90
- photo immunotherapy hyperthermia (HT), 89
- photothermal therapy (PTT), 90
- physiologic body temperature, 89
- plasmon resonances, 90, 91
- stead-state temperature, 91
- targeted tumors, 89
- temperature elevation, 90, 91, 111–112
- Nanoparticles (NPs)
 - adjuvant activity, 15–16
 - adjuvants, 225
 - cancer immunosurveillance and TME, 12–13
 - cellular uptake, 225
 - cytosolic delivery, 227
 - effect of NPs sizes, 6–8
 - electron microscopic observation, 226
 - gold, 229
 - HeLa cells, 224
 - on immune system, 5
 - with innate immune system, 5–6
 - ligand molecules, 226
 - nanosystems with tumor antigens, 13–14
 - NP-mediated hyperthermia, 17–18 (*see also* Hyperthermia (HT))
 - phototherapy, 209
 - physicochemical properties, 6
 - QDs, 223
 - shape and size dependency
 - cellular immune pathway, 229
 - immune response, 228
 - mucosal immune response, 229
 - OVA, 228
 - vaccine development, 228
 - shape, structure and surface effect, 8–12
 - size and shape, 223, 226
 - size of gold nanostars, 8
 - titanium dioxide NPs, 10
 - VLPs and cancer immunotherapy, 16
 - WNVE, 230
 - See also* NPs systems
- Nanostructure materials
 - cancer therapy, 143–144
 - immune suppressive factors, 163–167
- Nanotechnologies, 120
 - ALT improvement, 38–39
 - cancer vaccines, 39–42
 - ICBT, 43–44
 - and immune system, 4–6
 - nanometers, 3–4
 - NPs (*see* Nanoparticles (NPs))
 - in tumor immune therapy strategies, 69
 - virial-based immunotherapy, 42
- Natural killer (NK) cells, 6
- Near-infrared (NIR), 90, 124, 136
- Near-infrared photoimmunotherapy (NIR-PIT), 149
- Nonsteroidal anti-inflammatory drugs (NSAIDs), 157
- NPs systems
 - adjuvant delivery, 120
 - adoptive-cell therapy, 120
 - bioengineering, 118
 - biomaterial carrier, 120
 - biomaterials, 118
 - cancer immunotherapy, 117
 - CpG molecules, 121
 - development, 117
 - drug delivery, 118, 122
 - efficacy and toxicity, 118
 - gold nanovaccine (AuNV), 122
 - immune cells, 119, 120
 - immunomodulation, 119
 - immunotherapy-loaded particles, 118
 - innate and adaptive immune system, 118
 - intratumoral/peritumoral injections, 119
 - lipids, 122
 - lymph nodes, 122
 - nanorods, 118
 - nanotechnology, 118, 122
 - nucleic acid, 122
 - photodynamic immunotherapy (*see* Photodynamic immunotherapy)
 - photothermal immunotherapy (*see* Photothermal immunotherapy)
 - physicochemical properties, 118
 - technologies, 117
 - TNF- α , 121
 - tumor parenchyma and tumor-draining lymph nodes, 120
- Nuclear targeting peptide (NTP), 12
- O**
- Oligoethylene glycol (OEG), 226
- Oncolytic viruses (OVs), 16, 30, 34–36, 42, 55
 - therapy, 236
- Optical coherence tomography (OCT), 73, 78
- Optical imaging, 71–73, 78–80
 - See also* Intravital microscopy

- Optical power
 cooling, 96–97
 heat flow equation, 97
 heat production, 94
 steady-state temperatures, 96, 100–101
 thermal boundary conditions, 97–98
 time-dependent temperature, 94–96,
 98–100
- Ovalbumin protein (OVA), 228
- P**
- Pathogen-associated molecular patterns
 (PAMPs), 6
- Pattern recognition receptors (PRRs), 6
- PEG-modified single-walled carbon nanotubes
 (PEG-SWCNTs), 150
- Pembrolizumab, 33, 53, 56, 58
- Peptide/antigenic vaccines, 31–32
- Photoacoustic microscopy, 73
- Photodynamic immunotherapy
 antitumor immunity, 129
 cancer cells, 129
 cancer immunotherapy, 128
 CD8+ T cells, 129
 cell receptors, 129
 chlorin, 129
 luminescence, 128
 metformin, 129, 130
 nanomaterials, 127–129
 N-dihydrogalactochitosan (GC), 131
 organic nanomaterials, 129
 particles, 128
 photosensitizers, 127
 polymeric/inorganic nanocarriers, 128
 SERS, 127, 128
 tumor cells, 126
- Photodynamic therapy (PDT), 118, 209
 application, 210
 BCG, 216
 CTLA-4 checkpoint, 217
 immunosuppression, 216
 lysates, 215
 MnO₂-triggered decomposition, 218
 nMOF-base, 219
 PD-L1 knockdown, 217
 photosensitizers, 217
 tumor immunogenicity, 214
- Photon transport, 238
- Photothermal immunotherapy
 cancer immune memory response, 126
 cancer vaccine effect, 126
 citrate reduction method, 123
 cytokines, 124
 doxorubicin, 125
 GNP, 123
 HT, 123
 human T cells, 125
 immune cells, 125
 immune modulatory agents, 125
 immune system, 124
 lightning rod effect, 124
 macrophages, 125
 metallic nanostructures, 123
 systemic effects, 125
 tumor cell necrosis, 124–125
- Photothermal therapy (PTT), 118
 cancer treatment, 17
 combination therapy, 212
 DNA hydrogel-based, 211
 gold nanoshells, 18
 immune-adjuvant nanoparticles, 214
 immuno adjuvant therapy, 203–205
 immunogenic cell death, 203
 immunological defense system, 210
 and immunotherapy, 191
 adjuvant therapy, 201
 gold/copper, 200
 inorganic nano-agents, 211–212
 and ISPI, 210
 and PD-L1 treatment, 185, 186
 and PDT, 209
 photothermal agent, 213
- Plasmonic-active metallic nanoparticles, 136
- Plasmonics
 GNS, 174
 nanomedicine, 173
- Poly(ethylene glycol) (PEG), 129, 153
- Poly(ethylene oxide) (PEO), 10
- Poly(lactic-co-glycolic acid) (PLGA), 21, 38,
 43, 151, 153, 213
- Polyethyleneimine (PEI), 15, 151, 195
- Positron emission tomography (PET), 240
- PRINT method, 226
- Programmed death ligand 1 (PD-L1), 19, 43,
 60, 161, 162, 183, 186, 218, 246
- Prostatic Acid Phosphatase (PAP), 53
- R**
- Radiolabeling, 7
- Radiotherapy, 143
- Raman spectroscopy, 174
- Reactive oxygen species (ROS), 144
- Red fluorescent protein (RFP), 122
- Regulatory T cells (Treg cells), 145, 148–150
- Response Evaluation Criteria in Solid Tumors
 (RECIST) criteria, 59

Reticuloendothelial system (RES), 129
RNA-lipoplexes (RNA-LPX), 122

S

Simulations

- efficiencies, 101
- nanoparticle, 101
- planewave illumination
 - steady-state temperature elevation, 104–107
 - temperature-elevation profiles, 104, 105, 108
- plasmonic particles, 101
- point source illumination
 - radial profiles, 102
 - steady-state temperature elevation, 102–104
- temperature elevations, 101

Single-wall carbon nanotubes (SWNTs)

- CTLA-4 blockade, 213
- PTT and anti-CTLA-4 treatment, 213

Sipuleucel-T, 53, 60, 69, 145

Small-interfering RNA (siRNA), 15, 39, 123, 153, 160, 217, 226

Structured illumination, 71–72

Surface-enhanced Raman scattering (SERS), 11, 12

- characteristic, 180
- monitoring, 181

Surface-enhanced resonance Raman scattering (SERRS), 127, 128

SYMPHONY procedure, 185, 246

- anti-cancer immune responses, 248
- in vivo* study, 247

Synergistic immuno photo nanotherapy (SYMPHONY), 19, 20, 90, 126, 127, 174

T

Talimogene laherparepvec (T-VEC), 35, 37, 55

T cell receptor (TCR), 120

Titanium dioxide NPs, 10

Toll like receptor (TLR), 121

- receptor-7 (TLR-7), 135
- receptor 9 (TLR9), 124

Transforming growth factor beta (TGF- β), 148, 158–159

Triethylene glycol (TEG), 121

Tumor-infiltrating lymphocytes (TILs), 32, 120

Tumor microenvironment (TME), 12–13, 35, 37, 42, 44, 52, 77–80, 155–163

Tumor necrosis factor alpha (TNF- α), 125

Tumor-specific antigens, 126

Tumour-associated macrophages (TAMs), 145–147, 153–154, 218

Tumour microenvironment (TME)

- chemokines, 146
- COX-2, 157–158
- cytokines, 146
- IDO, 155–157
- IL-10, 159–160
- immune response, 145
- immune suppressive cells, 145–146
- MDSC, 150–152
- organized interaction, 147
- TAM, 153–154
- TGF- β , 158–159
- Treg cells, 148–150
- VEGF, 160

V

Vaccine, 14

- and adjuvants, 229
- DC vaccines, 31
- goal, 30
- gold nanovaccine (AuNV), 122
- nanotechnologies, 39–42
- neoantigen, 54
- peptide/antigenic vaccines, 31–32
- prevention, 54
- SARS, 231
- therapeutic cancer, 54
- use, 54

Vascular endothelial growth factor (VEGF), 37, 145, 146, 153, 160

Virus-like particles (VLPs), 16

W

Window chamber, 67, 74–75, 77, 78, 180